HELLENIC REPUBLIC

UNIVERSITY OF IOANNINA

SCHOOL OF ENGINEERING

DEPARTMENT OF MATERIALS SCIENCE AND ENGINEERING

Development of Physiological Metabolic Models in Diabetes Based on Data Mining Techniques

Eleni I. Georga

PhD Thesis

IOANNINA 2018

ΕΛΛΗΝΙΚΗ ΔΗΜΟΚΡΑΤΙΑ

ΠΑΝΕΠΙΣΤΗΜΙΟ ΙΩΑΝΝΙΝΩΝ

ΠΟΛΥΤΕΧΝΙΚΗ ΣΧΟΛΗ

ΤΜΗΜΑ ΜΗΧΑΝΙΚΩΝ ΕΠΙΣΤΗΜΗΣ ΥΛΙΚΩΝ

Ανάπτυξη Μοντέλων Φυσιολογίας / Μεταβολισμού Διαβητικών Ασθενών με χρήση Τεχνικών Εξόρυξης Δεδομένων

Ελένη Ι. Γεώργα

ΔΙΔΑΚΤΟΡΙΚΗ ΔΙΑΤΡΙΒΗ

ΙΩΑΝΝΙΝΑ 2018

«Η έγκριση της διδακτορικής διατριβής από το Τμήμα Μηχανικών Επιστήμης Υλικών της Πολυτεχνικής Σχολής του Πανεπιστημίου Ιωαννίνων δεν υποδηλώνει αποδοχή των γνωμών του συγγραφέα Ν. 5343/32, άρθρο 202, παράγραφος 2».

Date of Application of Ms. Eleni Georga: 29-08-2008

Date of Appointment of PhD Advisory Committee: 06-04-2009

Members of the 3 Member Advisory Committee:

Thesis Advisor

Dimitrios Fotiadis, Professor, Department of Materials Science and Engineering, School of Engineering, University of Ioannina

Members

Aristidis Likas, Professor, Department of Computer Science and Engineering, School of Engineering, University of Ioannina

Antonios Charalambopoulos, Professor, School of Applied Mathematics and Physics, National Technical University of Athens

Date of Thesis Subject Definition: 06-04-2009

PhD Thesis Title: Development of Physiological Metabolic Models in Diabetes Based on Data Mining Techniques

Date of Appointment of the 7 member Examination Committee: 20-02-2017

Dimitrios Fotiadis	Professor, Department of Materials Science and Engineering, School of Engineering, University of Ioannina
Aristidis Likas	Professor, Department of Computer Science and Engineering, School of Engineering, University of Ioannina
Antonios Charalambopoulos	Professor, School of Applied Mathematics and Physics, National Technical University of Athens
Stelios Tigas	Associate Professor of Endocrinology, Faculty of Medicine, School of Health Sciences, University of Ioannina
Leonidas Gergidis	Associate Professor, Department of Materials Science and Engineering, School of Engineering, University of Ioannina
José Carlos Príncipe	Distinguished Professor, Department of Electrical and Computer Engineering, University of Florida, USA
Metin Akay	John S Dunn Endowed Chair Professor, Department of Biomedical Engineering, University of Houston, USA

The PhD thesis is approved, with **«Excellent»** on **26-11-2018**

The Chairman of the Department **The Secretary of the Department**

Alkiviadis Paipetis
Professor

Maria Kontou

Ημερομηνία Αίτησης της κας Ελένης Γεώργα: 29-08-2008

Ημερομηνία Ορισμού Τριμελούς Συμβουλευτικής Επιτροπής: 06-04-2009

Μέλη Τριμελούς Συμβουλευτικής Επιτροπής:

Επιβλέπων

Δημήτριος Φωτιάδης, Καθηγητής, Τμήμα Μηχανικών Επιστήμης Υλικών, Πολυτεχνική Σχολή, Πανεπιστήμιο Ιωαννίνων

Μέλη

Αριστείδης Λύκας, Καθηγητής, Τμήμα Μηχανικών Η/Υ και Πληροφορικής, Πολυτεχνική Σχολή, Πανεπιστήμιο Ιωαννίνων

Αντώνιος Χαραλαμπόπουλος, Καθηγητής, Σχολή Εφαρμοσμένων Μαθηματικών και Φυσικών Επιστημών, Εθνικό Μετσόβιο Πολυτεχνείο

Ημερομηνία Ορισμού Θέματος: 06-04-2009

Θέμα Διατριβής: Ανάπτυξη Μοντέλων Φυσιολογίας / Μεταβολισμού Διαβητικών Ασθενών με χρήση Τεχνικών Εξόρυξης Δεδομένων

Διορισμός Επταμελούς Εξεταστικής Επιτροπής: 20-02-2017

Δημήτριος Φωτιάδης	Καθηγητής, Τμήμα Μηχανικών Επιστήμης Υλικών, Πολυτεχνική Σχολή, Πανεπιστήμιο Ιωαννίνων
Αριστείδης Λύκας	Καθηγητής, Τμήμα Μηχανικών Η/Υ και Πληροφορικής, Πολυτεχνική Σχολή, Πανεπιστήμιο Ιωαννίνων
Αντώνιος Χαραλαμπόπουλος	Καθηγητής, Σχολή Εφαρμοσμένων Μαθηματικών και Φυσικών Επιστημών, Εθνικό Μετσόβιο Πολυτεχνείο
Στυλιανός Τίγκας	Επίκουρος Καθηγητής Ενδοκρινολογίας, Τμήμα Ιατρικής, Σχολή Επιστημών Υγείας, Πανεπιστήμιο Ιωαννίνων
Λεωνίδας Γεργίδης	Επίκουρος Καθηγητής, Τμήμα Μηχανικών Επιστήμης Υλικών, Πολυτεχνική Σχολή, Πανεπιστήμιο Ιωαννίνων
José Carlos Príncipe	Distinguished Professor, Department of Electrical and Computer Engineering, University of Florida, USA
Metin Akay	John S Dunn Endowed Chair Professor, Department of Biomedical Engineering, University of Houston, USA

Έγκριση Διδακτορικής Διατριβής με βαθμό **«ΑΡΙΣΤΑ»** στις **26-11-2018**

Ο Πρόεδρος του Τμήματος

Αλκιβιάδης Παϊπέτης
Καθηγητής

Η Γραμματέας του Τμήματος

Μαρία Κόντου

DEDICATION

To my parents, my sister and my brother

ACKNOWLEDGEMENTS

First of all, I would like to cordially thank and express my sincere gratitude to my supervisor, Professor Dimitrios I. Fotiadis, for all his support and guidance he has given to me throughout my PhD studies. His mentoring inspired me to advance and widen my research interests, and allowed me to grow as a data scientist. I would also like to thank the members of my advisory committee, Professor Aristidis Likas and Professor Antonios Charalampopoulos, for their continuous support and inspiration to advancing my background in machine learning and applied mathematics.

I would like to express my sincere thanks to the Distinguished Professor José Carlos Príncipe for his excellent guidance in conducting the final research step in this PhD thesis. I would also like to express my sincere appreciation to the Associate Professor Stelios Tigas, the Associate Professor Leonidas Gergidis, and the John S Dunn Endowed Chair Professor Metin Akay for their participation in my examination committee.

I would like to cordially thank Dr. Vasilios Protopappas for his great assistance and the excellent collaboration we had throughout these years. I would also like to warmly thank all my colleagues and friends from the Unit of Medical Technology and Intelligent Information Systems for the harmonious cooperation we had, their great support and invaluable advices.

Last but not least, I would like to express my deepest gratitude and thanks to my parents and family for their constant unending support and encouragement throughout my PhD journey, and all of my friends who helped me in order to complete this thesis.

This research was part funded by the European Commission as well as through the National Strategic Reference Framework.

TABLE OF CONTENTS

LIST OF FIGURES

LIST OF TABLES

LIST OF SYMBOLS

t	Time
y	Model output (i.e. subcutaneous glucose concentration)
$x \in R^d$	Input vector
p	Prediction step
T	Sampling interval of subcutaneous glucose concentration
l	Prediction horizon ($l = pT$)
v_i	The i^{th} input variable
n_{v_i}	Embedding dimension of variable v_i
Δt_{v_i}	Sampling period of variable v_i
gl	Subcutaneous glucose concentration
SEE	Cumulative amount of the energy expended during physical activities or exercise
h	Hour of day (1-24)
I_{ex}	Exogenous insulin flow
B_d	Dimeric insulin absorption rate constant
c_d	Dimeric insulin concentration in the subcutaneous tissue
V_{sc}	Subcutaneous insulin distribution volume
r	Distance from the insulin injection site
I_p	Plasma insulin concentration
I_h	Insulin concentration in the liver
I_i	Insulin concentration in the interstitial fluid
V_d	Plasma insulin distribution volume
k_1, k_2 and k_3	Rate constants of plasma, hepatic and interstitial insulin elimination, respectively

D	Amount of meal carbohydrate content
q_{gut}	The amount of glucose in the gut
k_{abs}	Intestinal glucose absorption rate constant
G_{empt}	Rate of gastric emptying
Ra	Rate of appearance of exogenous glucose into the systemic circulation
SRa	Cumulative amount of exogenous glucose that appeared in the systemic circulation
$Z = \left\{\left(x^i, y_i\right)\right\}_{i=1}^{N}$	Dataset where $\left(x^i, y_i\right) \in Z = X \times Y,\ X \subseteq R^d, Y \subseteq R$ and $\left(x^i, y_i\right) \equiv \left(x\left(t_i - pT\right), y\left(t_i\right)\right)$
$\theta \in R^m$	Model parameters' vector
$E\left(\theta\right)$	Loss function
$\hat{y}\left(t\middle\vert\theta\right)$	p -step ahead of $y\left(t\right)$ by the parametric function $f : R^d \to R$ and $\hat{\theta} = \arg\min_{\theta \in R^m} E\left(\theta\right)$
$\kappa : X \times X \to R$	Kernel function
φ	Feature space
H	Reproducing kernel Hilbert space associated with the feature space $\varphi : X \to H, \varphi\left(x\right) = \kappa\left(x, \cdot\right)$
$w \in R^m$	Parameters' vector of a generalized linear regression model
b	Bias parameter
a_i, a_i^*	Lagrange multipliers in the SVR function
ξ_i, ξ_i^*	Slack variables in the SVR function
ε	Error in the ε-insensitive error function in the SVR algorithm
C	Regularization parameter in the SVR algorithm
γ	Gaussian kernel parameter
σ	Gaussian kernel bandwidth
$F = \left\{F_j\right\}_{j=1}^{d}$	Feature set
ω_j	Importance score assigned to feature F_j

J	The set of indices of F i.e. $J = [1, \ldots, d]$
R	Ranked list of features $\left[F_{j'_1}, \ldots, F_{j'_d}\right]$, where $J' = \left[j'_1, \ldots, j'_d\right]$, $j'_j \in J$ and $W_{j'_j} \geq W_{j'_{j+1}}$
ntree	Number of trees in the Random Forests algorithm
mtry	Number of randomly selected features in the Random Forests algorithm
T_k	The k^{th} tree in the Random Forests algorithm, $k = 1, \ldots, ntree$
K	Number of nearest neighbours in the RReliefF algorithm
σ'	Hyperparameter of the RReliefF algorithm
$\alpha_{m,k}$	Term accounting for the distance between instances u_m and v_k in the RReliefF algorithm
$\mu, \boldsymbol{\sigma}^2$	Mean and covariance of a Gaussian distribution
K_C	$N \times N$ covariance matrix
$\mathbf{y}$	The target vector $[y_1, \ldots, y_N]^T$
β	Constant variance of Gaussian distributed noise with zero mean
$\mathbf{k}$	Kernel vector $\mathbf{k} = \left[\kappa(x, x_1), \ldots, \kappa(x, x_N)\right]^T$ or $\mathbf{k} = \left[\kappa(x_i, c_1), \ldots, \kappa(x_i, c_{m_{i-1}})\right]^T$ in time-invariant or adaptive kernel-based models
$\mathbf{M}$	Parametric model $\mathbf{M}(\theta)$
$Q \subseteq X$	Dictionary such that $Q(i) = \left\{q^j(i)\right\}_{j=1}^{m_i}$: the dictionary at iteration i, and m_i: size of the dictionary at iteration i
$a(i) \in R^{m_i}$	Coefficient vector of kernel adaptive filter at iteration i
$\mathbf{K} \in R^{N \times N}$	Gram matrix
$\tilde{\mathbf{K}} \in R^{m_i \times m_i}$	Gram matrix defined on $C(i)$
e	Prediction error $e = y - \hat{y}$
ε_x	Quantization parameter in QKLMS-FB algorithm
M	Maximum dictionary size

$E_k(i)$	Significance of centre q_k at iteration i
η	Step size parameter in QKLMS-FB algorithm
$p(X)$	Probability density function over X
$\lambda_j(i)$	Function $\lambda_j(i)$ quantifies the number of input vectors being quantized to centre q^j
β	Forgetting factor in QKLMS-FB algorithm
δ_i	ALD criterion at iteration i
ν	Sparsification parameter in KRLS-ALD algorithm
$c(i)$	Parameter vector of ALD at iteration i

LIST OF ABBREVIATIONS

ALD	Approximate Linear Dependency
AR	Autoregressive
ARMA	Autoregressive Moving Average
ARMAX	Autoregressive Moving Average with Extra Inputs
ARX	Autoregressive with Extra Inputs
AUC	Area under the Receiver Operating Characteristic Curve
CG-EGA	Continuous Glucose Error Grid Analysis
CGM	Continuous Glucose Monitoring
CSII	Continuous Subcutaneous Insulin Infusion
ECG	Electrocardiogram
EE	Energy Expenditure
EEG	Electroencephalogram
EGA	Error Grid Analysis
EKF	Extended Kalman Filter
ESOD	Energy of the Second Order Differences
FFNN	Feed-Forward Neural Network
FPG	Fasting Plasma Glucose
GP	Gaussian Processes
GSR	Galvanic Skin Response
GTFM	Generalized Transfer Function Model
HAAF	Hypoglycaemia-Associated Autonomic Failure
HbA1c	Glycated Haemoglobin
HRV	Heart Rate Variability
ICR	Insulin-to-Carbohydrate-Ratio
IFG	Impaired Fasting Glucose
IGT	Impaired Glucose Tolerance
IIT	Intensive Insulin Therapy

KAF	Kernel Adaptive Filtering
KLMS	Kernel Least Mean Square
KRLS	Kernel Recursive Least Squares
KRLS-ALD	Approximate Linear Dependency Kernel Recursive Least Squares
LV	Latent Variable
LVX	Latent Variable with Extra Inputs
MAPE	Mean Absolute Percentage Error
MARD	Mean Absolute Relative Difference
MDI	Multiple Daily Insulin Injections
MSE	Mean Squared Error
OGTT	Oral Glucose Tolerance Test
OOB	Out-of-Bag
PRED-EGA	Prediction-Error Grid Analysis
PSD	Power Spectral Density
QKLMS-FB	Fixed Budget Quantized Kernel Least Mean Square
RAD	Relative Absolute Deviation
RBF	Radial Basis Function
RF	Random Forests
RKHS	Reproducing Kernel Hilbert Space
RMSE	Root Mean Squared Error
RNN	Recurrent Neural Network
ROC	Receiver Operating Characteristic
SAP	Sensor-Augmented Pump
SMBG	Self-Monitoring of Blood Glucose
SOM	Self-Organizing Map
SSGPE	Sum of Squares of the Glucose Prediction Error
SVR	Support Vector Regression
TG	Temporal Gain
TL	Time Lag
WFNN	Wavelet Fuzzy Neural Network

ABSTRACT

In this thesis, we address the problem of the short-term prediction of glucose concentration in the interstitial fluid in people with type 1 diabetes under free-living conditions. This thesis consists of three main parts. In the first part, we approached the specified problem via a time-invariant support vector regression function of multiple input variables, concerning the recent subcutaneous glucose profile, the effect of food and insulin intake, the energy expenditure due to physical activities and the time of the day, which was evaluated individually for each patient. By utilizing different input cases, the effect of each input to the model's prediction error was quantified and, it was demonstrated that the effective combination of multivariable data can significantly improve the prediction error. The subsequent study on the evaluation of the proposed model with respect to the prediction of single hypoglycaemic events, drove us to introduce new input variables accounting for recurrent nocturnal hypoglycaemia, due to antecedent hypoglycaemia, exercise, and sleep, which resulted in a considerably higher sensitivity and precision values. In the second part of this thesis, we proceeded to feature ranking for assessing, separately for each patient, the importance of the defined feature set with respect to subcutaneous glucose concentration prediction, aiming at the customization of the input of the regression function. To this end, the random forests and RReliefF algorithms were employed, and through a forward sequential feature selection procedure, we investigated the effectiveness of highly-ranked features on the prediction error by kernel-based regression models (support vector regression and Gaussian processes). In the third part of this thesis, we demonstrated the capability of sparse kernel adaptive filtering algorithms (i.e. fixed budget quantized kernel least mean square algorithm, and approximate linear dependency kernel recursive least squares algorithm) to learn online and predict the short-term course of the subcutaneous glucose concentration in type 1 diabetes. In parallel, we verified that multivariate data improve systematically both the regularity and the time lag of the predictions, reducing the errors in critical glucose value regions.

ΠΕΡΙΛΗΨΗ

Η παρούσα διδακτορική διατριβή πραγματεύεται το πρόβλημα της βραχυπρόθεσμης πρόβλεψης της συγκέντρωσης της γλυκόζης στον υποδόριο χώρο σε άτομα με σακχαρώδη διαβήτη τύπου 1 και υπό κανονικές συνθήκες διαβίωσης. Η διδακτορική διατριβή αποτελείται από τρία μέρη. Στο πρώτο μέρος, προσεγγίσαμε το συγκεκριμένο πρόβλημα μέσω μίας χρονικά-αμετάβλητης συνάρτησης παλινδρόμησης διανυσμάτων υποστήριξης, η αξιολόγηση (εκπαίδευση και έλεγχος) της οποίας πραγματοποιήθηκε ξεχωριστά για τον κάθε ασθενή. Η είσοδος του μοντέλου περιγράφει το πρόσφατο ιστορικό της υποδόριας γλυκόζης, την επίδραση του φαγητού και της θεραπείας ινσουλίνης, την κατανάλωση ενέργειας κατά τις φυσικές δραστηριότητες, και χρονική πληροφορία αναφορικά με την ώρα της ημέρας κατά την οποία πραγματοποιείται η πρόβλεψη. Εξετάζοντας διαφορετικές περιπτώσεις εισόδου, ποσοτικοποιήσαμε την επίδραση κάθε μεταβλητής στο σφάλμα πρόβλεψης της συγκέντρωσης της γλυκόζης, και δείξαμε ότι ο συνδυασμός πολύ-μεταβλητών δεδομένων βελτιώνει σημαντικά το σφάλμα πρόβλεψης. Εν συνεχεία, εξετάσαμε τη συμπεριφορά του προτεινομένου μοντέλου ως προς την πρόβλεψη των μεμονωμένων υπογλυκαιμικών επεισοδίων. Η μελέτη αυτή μας οδήγησε στην εισαγωγή νέων μεταβλητών εισόδου οι οποίες στοχεύουν να περιγράψουν την επίδραση της προηγηθείσας υπογλυκαιμίας, της άσκησης και του νυχτερινού ύπνου στην εκδήλωση ενός υπογλυκαιμικού επεισοδίου, οι οποίες και βελτίωσαν την ευαισθησία και τη θετική προγνωστική αξία του μοντέλου. Στο δεύτερο μέρος της παρούσας διδακτορικής διατριβής προχωρήσαμε σε τεχνικές κατάταξης χαρακτηριστικών για την αξιολόγηση της προβλεπτικής αξίας του συνόλου των χαρακτηριστικών, με απώτερο στόχο την εξατομίκευση της εισόδου της συνάρτησης παλινδρόμησης της συγκέντρωσης της γλυκόζης στον υποδόριο χώρο. Ειδικότερα, χρησιμοποιήσαμε τον αλγόριθμο τυχαίων δασών και τον αλγόριθμο RReliefF, και μέσω μιας διαδικασίας εμπρόσθιας διαδοχικής επιλογής χαρακτηριστικών, διερευνήσαμε την επίδραση των πιο σημαντικών χαρακτηριστικών στο σφάλμα πρόβλεψης των βασιζόμενων σε συναρτήσεις πυρήνα μοντέλων παλινδρόμησης (παλινδρόμηση διανυσμάτων υποστήριξης και Gaussian διαδικασίες). Στο τρίτο μέρος της παρούσας διδακτορικής διατριβής, προτείναμε την προσαρμοστική εκμάθηση και πρόβλεψης

της βραχυπρόθεσμη πορείας την υποδόριας συγκέντρωσης της γλυκόζης στον διαβήτη τύπου 1 μέσω αραιών αναπαραστάσεων προσαρμοστικών φίλτρων πυρήνα. Ειδικότερα, οι αλγόριθμοι που εξετάσαμε αποτελούν αναπαραστάσεις της μεθόδου ελαχίστων μέσων τετραγώνων και επαναληπτικών ελαχίστων τετραγώνων στον χώρο συναρτήσεων Hilbert με αναπαραγωγικό πυρήνα. Παράλληλα, επαληθεύσαμε ότι, όταν λαμβάνονται υπόψιν οι εξωγενείς είσοδοι, υπάρχει συστηματική βελτίωση της ποιότητας των προβλέψεων, ως προς την ομαλότητα και τη χρονική υστέρηση, καθώς και μείωση του σφάλματος στις κρίσιμες περιοχές της υπογλυκαιμίας και υπεργλυκαιμίας.

CHAPTER 1. INTRODUCTION

1.1 Background and Thesis Motivation

Diabetes is a group of metabolic disorders characterized by hyperglycaemia resulting from defects in insulin secretion, insulin action or both [1]. Type 1 diabetes results from a cellular-mediated autoimmune destruction of the β-cells in the pancreas leading to absolute insulin deficiency. On the other hand, type 2 diabetes is characterized by a progressive loss of insulin secretion on the background of insulin resistance [2]. According to the International Diabetes Federation, the number of people (adults 20-79 years) with diabetes worldwide is estimated to rise from 415 million in 2015 to 642 million in 2040, while the incidence of type 1 diabetes among children and adolescents is increasing by around 3% annually. Moreover, the long-term microvascular and macrovascular complications related to chronic hyperglycaemia render diabetes a major cause of early death in most countries.

The most vital and challenging issue for people with type 1 or advanced type 2 diabetes is the achievement and maintenance of euglycaemia overtime in a safe manner. Intensive insulin therapy (IIT), implemented by either multiple daily insulin injections (MDI) or continuous subcutaneous insulin infusion (CSII), could be the remedy to hyperglycaemia in type 1 diabetes should it did not increase the risk of hypoglycaemia [3]. The effective integration of continuous glucose monitoring (CGM) and CSII technologies into one system, i.e. sensor-augmented pump (SAP), allows for improvements in glycaemic control of type 1 diabetes when compared with MDI therapy or the individual components alone [1, 4, 5]; however, the problem of severe hypoglycaemia and, in particular, nocturnal hypoglycaemia is not solved. CGM enabled a high time-resolution description of the short-term glucose dynamics in the subcutaneous space, the awareness of which by both patients and physicians

has been shown to improve the long-term glycaemic control [i.e. glycated haemoglobin (HbA1c) levels] in type 1 diabetes and facilitate the evaluation of the response to therapy, as compared to self-monitoring of the blood glucose concentration (SMBG). The continuously improved accuracy of CGM effected its approval for making therapeutic decisions in Europe [6, 7]. However, there is still room for improvement in the hypoglycaemic range which, in conjunction with the lag time of interstitial fluid glucose concentration relative to blood glucose concentration, hinders the precise detection of hypoglycaemia based merely on CGM data. In addition, only the combined use of CGM, CSII and blood glucose predictive algorithms has been shown to reduce the incidence and duration of hypoglycaemia, though it may come at a price of an increase in hyperglycaemia [8, 9]. More specifically, the integration of low-glucose predictive alerts into today open- or hybrid closed loop systems of glycaemic control in diabetes is imperative towards minimizing the risk of hypoglycaemic events or hyperglycaemic excursions [10, 11].

Medical care in diabetes can be enhanced by the development of computational models of blood glucose metabolism able to predict the blood glucose response to various stimuli. In particular, short-term predictive modelling of blood glucose concentration has the potential to further advance insulin-treated diabetes management either: (i) in open loop conditions by providing advanced knowledge of abnormal glycaemic variations and facilitating the appropriate patient reaction in crucial situations, such as asymptomatic hypoglycaemia, or (ii) in closed loop conditions as an integral component of the control algorithm of an artificial pancreas system [12-15]. To this end, more dynamic and sensitive to overall patient's context predictive algorithms may result in tighter glycaemic control minimizing the risk of hypoglycaemia and setting the appropriate conditions for closing the loop during the day.

Motivated by the need for a more precise daily care of type 1 diabetes, this thesis's primary objective is the development of a personalized, adaptive, real-time, data driven computational solution to the short-term predictive modelling of subcutaneous glycaemic dynamics in type 1 diabetes, which shall be highly accurate as well as computationally efficient. In particular, we aim at establishing a multivariate nonlinear prediction model of subcutaneous glucose concentration course in type 1 diabetes capable of learning the short-term effect of insulin therapy, carbohydrate content of meals and physical activity on the subsequent glycaemic dynamics under free-living conditions. We place special emphasis on the assessment of its predictive capacity in critical glucose value regions (i.e. hypoglycaemia and hyperglycaemia) and, especially, as regards the prediction of hypoglycaemic events

overnight. In this direction, a subsequent objective became to assess the significance of the defined feature set and to define the minimum feature set maximizing the generalization capability of the predictive model. Considering the intrinsic nonlinearity and non-stationarity of the blood glucose regulatory system, we opted for nonlinear dynamical machine learning models aiming at establishing an adaptive solution which may explain the intra-patient and inter-patient variability. Mathematical models of the kinetics of exogenous materials (i.e. subcutaneously administered insulin, carbohydrates ingestion) in the glucose-insulin system are also employed at the input level of the data-driven models. Throughout the doctoral research, a multivariate dataset aggregating daily self-monitoring health, behavioural, and physiological data and characterized by a high-level of input excitation is exploited, which supported learning the different modes the glucose-insulin regulatory system.

1.2 Overview of the Thesis

The thesis is organized as follows:

The second chapter presents the medical background of the normal physiology of blood glucose metabolism and the pathophysiology of diabetes. Special focus is given on the glucose counterregulatory mechanisms which are responsible for the prevention or correction of the hypoglycaemia. In addition, existing approaches to the assessment of glycaemic control and the principles of insulin therapy are discussed. The clinical impact of more advanced medical technologies for monitoring and controlling blood glucose levels (i.e. CGM, CSII) in type 1 diabetes is also pointed out, as well as of current paradigms of closed-loop blood glucose control systems.

The third chapter presents the current status of the literature in the field of identification and short term prediction of the subcutaneous glucose concentration in type 1 diabetes. The existing modelling approaches were stratified with respect to the type of the learning method (batch vs. online learning), and, the type of the regression function (i.e. linear or nonlinear function of the input), whereas specific details are provided as regards the dataset, the defined feature set, the training/testing procedure, and the estimation of the generalization error. A separate section is devoted to the sub problem of hypoglycaemic events prediction, which is formulated either as a regression or a classification function. In this chapter, the contribution of the thesis along with the novelties that it introduces are clearly stated.

In the fourth chapter, we present our first approach to short-term predictive modelling of the subcutaneous glucose concentration in type 1 diabetes. The chapter is divided into two main parts. In the first part, we describe the formulation of the respective multivariate regression problem, the determination of the input, as well as, the individual modules of the proposed method [i.e. support vector regression (SVR), physiological models of the kinetics of subcutaneously administered insulin and glucose ingestion]. In addition, we provide a systematic evaluation of the effect of the exogenous inputs [i.e. plasma insulin concentration, appearance of meal-derived glucose in the systemic circulation, energy expenditure (EE) during physical activities] on the daily glucose prediction both in normal and critical glucose value regions, by employing established goodness-of-fit metrics and procedures. The second part presents a thorough evaluation of the performance of the SVR-based glucose prediction model with respect to the prediction of individual hypoglycaemic events, emphasizing on the definition of a hypoglycaemic event and, subsequently, a true positive prediction.

In the fifth chapter, we present our study on the individualized evaluation of the short term predictors of subcutaneous glucose concentration and the subsequent refinement of the model's input. In particular, we propose feature ranking as a pre-processing step in the construction of patient-specific glucose predictive models. The results derived from two feature evaluation algorithms suitable for regression problems [i.e. random forests (RF), RReliefF] are discussed, and their generality and effectiveness is demonstrated with respect to the performance of kernel-based regression modelling [i.e. SVR, Gaussian processes (GP)] by employing a forward feature selection procedure.

In the sixth chapter, we approach the problem of subcutaneous glucose concentration prediction in type 1 diabetes from the point of view of nonlinear adaptive models for regression. Kernel adaptive filtering (KAF) is proposed as a learning scheme for the nonlinear dynamical system of glucose and, particularly, we analyse KAF methods which generalize least mean square or recursive least squares algorithms in a reproducing kernel Hilbert space (RKHS) yielding, in parallel, a sparse regularized solution. Similarly to our previous studies, the influence of the multivariate feature set on the generalization capability of the model, especially in the regions of hypoglycaemia and hyperglycaemia, is systematically investigated.

Finally, in the seventh chapter, the conclusions of this thesis are highlighted, based on the results and limitations as they result from the previous chapters. Directions and trends for future research in the field are also discussed.

CHAPTER 2. BLOOD GLUCOSE METABOLISM AND TYPE 1 DIABETES

2.1 Physiology of the Blood Glucose Metabolism

2.1.1 Blood Glucose Metabolism

Blood glucose is derived from three sources: (i) the intestinal absorption of glucose following the ingestion of a meal, (ii) the breakdown of glycogen in liver and muscles (i.e. glycogenolysis), and (iii) the synthesis of glucose in liver and kidney from other substrates (i.e. gluconeogenesis); lactate, alanine and glycerol are the major gluconeogenic precursors. Glucose transported into tissues is either metabolized via glycolysis to pyruvate, which in turn is either completely oxidized or converted to lactate, or is directly stored as glycogen into the liver and muscles [16].

Blood glucose diffuses down the concentration gradient, from the capillaries, via the interstitial fluid, into tissue cells. Glucose transport across cell membranes is facilitated by specific proteins, embedded in the membrane, which are called glucose transporters, with the GLUT family of passive glucose transporters allowing the movement of glucose across a cell membrane down a concentration gradient. Assuming Michaelis-Menten kinetics, each member GLUTn of the GLUT family is characterized by a Michaelis-Menten constant K_m. Tissues requiring a constant glucose uptake (e.g. the brain), independently of the extracellular glucose

concentration over the normal range, express GLUT with a low K_m value. The sodium-glucose cotransporter (SGLT) family consists of active glucose transporters which allow the movement of glucose across a cell membrane up a concentration gradient.

The liver plays a significant role in carbohydrate metabolism. The nutrients absorbed from the small intestine into the blood are first transported, via the hepatic portal vein, into the hepatocytes, before they reach the systemic circulation. The key glucoregulatory hormones insulin and glucagon, which are secreted by the pancreas, are also first transferred to the liver via the hepatic portal vein. Glucose transport into hepatocytes is facilitated by the GLUT2 transporter which is characterized by a relatively high K_m value ($K_m = 7-20$ mmol·L^{-1}), which, in turn, implies that the glucose uptake rate by hepatocytes is determined by the concentration gradient across the hepatocyte membrane. Glucose is phosphorylated intracellularly by the enzyme glucokinase to form glucose 6-phosphate, which is either stored as glycogen or is glycolyzed. Hepatic glycogen synthesis is stimulated postprandially by insulin, which brings about the activation of the main regulatory enzyme of glycogen synthesis, i.e. glycogen synthase. Concurrently, insulin inhibits glycogen breakdown by inactivating the key enzyme, i.e. glycogen phosphorylase. The pathway of glycolysis is also stimulated by insulin. A decrease in insulin to glucagon ratio (e.g. during overnight fasted conditions) will bring about the activation of glycogen phosphorylase and, concurrently, the inactivation of glycogen synthase, favouring glycogen breakdown and the formation of glucose 6-phosphate. Glucose 6-phosphate is converted to glucose by glucose-6-phosphatase and, then it is released into the circulation via the GLUT2 transporter. Besides glucagon, epinephrine also regulates the activation of glycogen phosphorylase. The synthesis of glucose 6-phosphate from other substrates, gluconeogenesis, takes also place in the liver, and similarly to glycogenolysis, it is stimulated by glucagon and inhibited by insulin. Hepatic gluconeogenesis is additionally regulated by the rate of supply of gluconeogenic precursors from other tissues.

The energy demands of the brain are entirely covered by glucose oxidation (except in the case of prolonged starvation), accounting for 20% of whole body daily EE (120 g of glucose). The presence, predominantly, of GLUT3 ($K_m = 1.6$ mmol·L^{-1}) as well as GLUT1 ($K_m = 5-7$ mmol·L^{-1}) transporters accomplishes a constant glucose utilization rate by brain cells. Other tissues, such as the skeletal and cardiac muscle and the adipose tissue, use either glucose or free fatty acids as a metabolic fuel depending on their blood availability. Glucose

uptake by these tissues is mainly facilitated by the insulin-sensitive GLUT4 glucose transporters ($K_m = 5$ mmol·L^{-1}); when insulin binds to its receptors, GLUT4 glucose transporters move from the cell interior, where they are stored in membrane vesicles, to the cell membrane increasing thus the glucose uptake rate. It should be mentioned that glucose within the skeletal muscle cell enters either the glycolytic pathway or is stored as glycogen; however, muscle glycogen cannot contribute directly to blood glucose due to the lack of the glucose-6-phosphatase enzyme.

2.1.2 Blood Glucose Regulation

Blood glucose homeostasis is precisely coordinated by: (i) hormones and neurotransmitters regulating intermediary metabolism (i.e. glucose, fatty acid, and amino acid metabolism), (ii) proteins, enzymes and other small molecules involved in glucose metabolism pathways within cells, and (iii) gluconeogenic substrates [17, 18]. Insulin, which is secreted from the β-cells of the pancreatic islets, is the main regulatory hormone of blood glucose. Insulin binding to its receptor proteins embedded in the cell surface: (i) stimulates glucose uptake by insulin-sensitive tissues (i.e. skeletal and cardiac muscle, adipose tissue), (ii) suppresses hepatic glucose production, and (iii) stimulates both uptake and storage of fatty acids as triacylglycerol within adipocytes and, in parallel, suppresses lipolysis (i.e. the breakdown of triacylglycerol into free fatty acids and glycerol in the adipose tissue); together resulting in a decrease in blood glucose concentration.

The rate of insulin secretion is itself primarily regulated by the circulating glucose which enters β-cells via the GLUT2 transporters ($K_m = 7 - 20$ mmol·L^{-1}); adenosine-5'-triphosphate (ATP) production by glycolysis within the β-cell leads to the exocytosis of insulin. As it shown in Figure 2.1, the insulin secretion rate vs. blood glucose concentration curve resembles a sigmoid function, with insulin secretion increasing as the blood glucose concentration rises above its normal value of 90 mg·dL^{-1} [19, 20]. Gastrointestinal inhibitory polypeptide (GIP) and glucagon-like peptide-1 (GLP-1) incretin hormones, which are secreted from the intestine in response to glucose ingestion, amplify glucose-stimulated insulin secretion, which explains the greater increase in plasma insulin levels in response to an oral glucose load compared with an isoglycaemic amount of intravenously infused glucose. In addition, the GLP-1 suppresses gastric emptying.

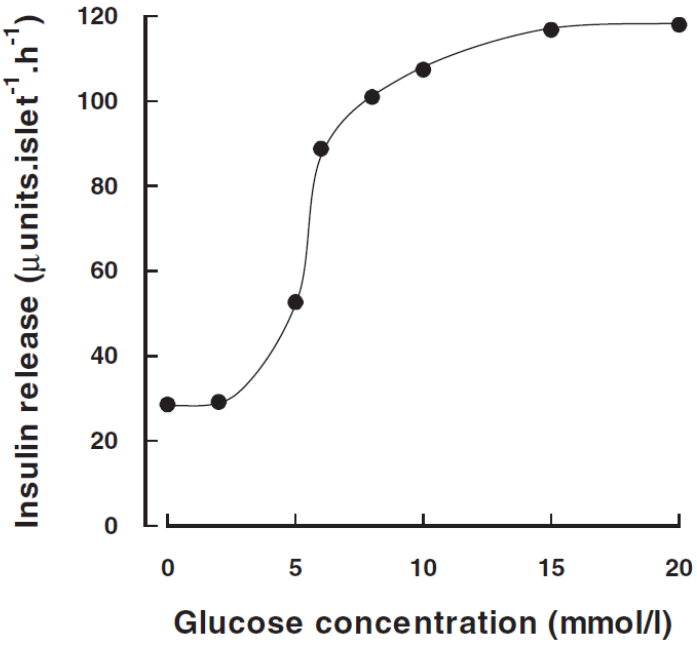

Figure 2.1 Dose–response curve for the effect of glucose concentration on the rate of insulin secretion by isolated human islets of Langerhans, studied in vitro. [21]

2.1.3 Blood Glucose Counterregulation

Blood glucose counterregulation encompasses all those processes which prevent or rapidly correct hypoglycaemia, i.e. a blood glucose concentration value below 70 mg·dL^{-1} [22]. Firstly, the suppression of endogenous insulin secretion, as blood glucose concentration declines below 80-85 mg·dL^{-1}, stimulates hepatic glucose production and inhibits insulin-stimulated glucose uptake. Secondly, a further reduction of blood glucose concentration marginally below the 65-70 mg·dL^{-1} induces the activation of counter-regulatory hormones:

1. Glucagon, which is secreted from the α-cells of the pancreatic islets, constitutes the primary defence against hypoglycaemia by increasing hepatic glucose synthesis (i.e. glycogenolysis and gluconeogenesis).
2. Epinephrine, which is secreted from the chromaffin cells of the adrenal medulla, increases hepatic as well as renal glucose production, and increases plasma gluconeogenic precursor and free fatty acid (via lipolysis) concentrations. Its response to hypoglycaemia becomes critical in the case of glucagon deficiency.
3. Growth hormone and cortisol act synergistically in prolonged hypoglycaemia by increasing the synthesis of gluconeogenic enzymes, inhibiting glucose uptake by tissues and increasing the breakdown of muscle protein.

2.1.4 The Postabsorptive Phase

In the postabsorptive state (i.e. the period between meals when all of the last meal has been absorbed from the intestinal tract), blood glucose and plasma insulin concentrations are typically around 90 $mg \cdot dL^{-1}$ and 60 $pmol \cdot L^{-1}$, respectively. Moreover, the rate of hepatic glucose production equals that of glucose utilization by tissues (2.2 $mg \cdot kg^{-1} \cdot min^{-1}$ on average) [18, 22]. Figure 2.2 illustrates glucose metabolism after an overnight fast. Glycogenolysis and gluconeogenesis, which both take place in the liver, contribute almost equally (~50%) in endogenous glucose production [17, 23, 24]. The stimulus for both processes is a decreased insulin to glucagon ratio. The disposal of glucose into cells follows primarily the glycolytic pathway, where a significant proportion of glucose is converted to lactate, the main gluconeogenic substrate [17, 25]. Insulin-independent glucose utilization in the brain, the splanchnic tissues, the kidney and the blood cells accounts for approximately 50%, 10%, 10% and 5%, respectively, of basal glucose uptake, whereas insulin-dependent glucose utilization, primarily in the skeletal muscle and secondarily in the adipose tissue, accounts for the remaining 25% [17]. As the insulin to glucagon ratio decreases, glucose uptake by most tissues is progressively reduced and their energy supply increasingly derives from lipolysis, fatty acid oxidation and ketogenesis (i.e. the breakdown of fatty acids and ketogenic amino acids into ketone bodies). In addition, the hepatic glycogen content is gradually reduced and gluconeogenesis becomes the predominant source of glucose production. Under prolonged fasting conditions, renal gluconeogenesis is substantially stimulated.

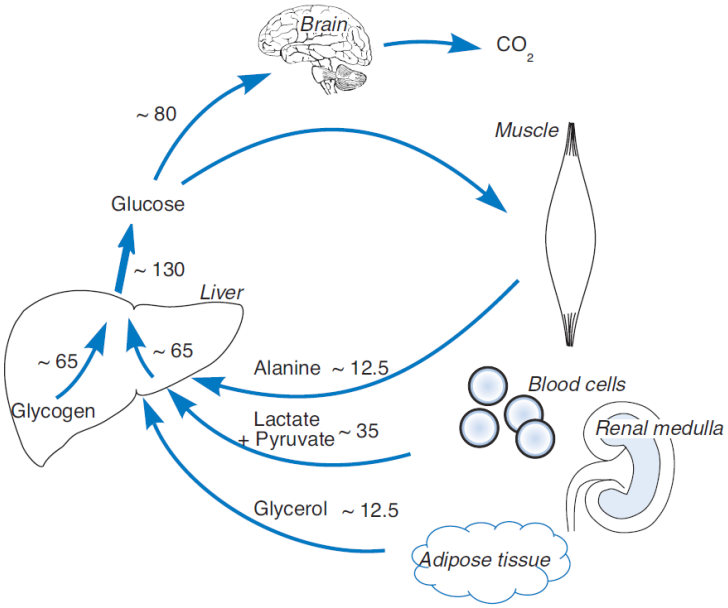

Figure 2.2 The pattern of glucose metabolism after an overnight fast. The numbers are approximations only, in mg per min, for a typical person of 65 kg body weight. [21]

2.1.5 The Postprandial Phase

In the postprandial state, the increase of blood glucose concentration and the subsequent increase of insulin secretion from the pancreatic β-cells result in: (i) the suppression of endogenous glucose production and, (ii) the stimulation of glucose uptake. Plasma concentration of non-esterified fatty acids is also reduced postprandially, due to the insulin-stimulated suppression of fat mobilization in the adipose tissue, which further enhances blood glucose utilization by the skeletal muscle. Figure 2.3 portrays the direct (i.e. glucose from the small intestine to liver glycogen) and the indirect (i.e. glucose forming lactate in peripheral tissues which is then converted to glucose-6-phosphate and glycogen in the liver) pathways of glycogen deposition. Skeletal muscle glycogen synthesis is also stimulated by the rise of plasma insulin concentration.

Figure 2.4 illustrates the time course of blood concentration of glucose, insulin and glucagon following the ingestion of 75g of glucose in healthy subjects [17]. Blood glucose concentration increases within ~15 min, reaches its peak in 30-60 min and returns to its postabsorptive levels within 3-4 h. Plasma insulin concentration exhibits a similar behaviour to that of blood glucose being three to fourfold higher than its basal levels, whereas blood glucagon concentration is suppressed by ~50%. As it is shown in Figure 2.5, the rate of exogenous (ingested) glucose appearance into the systemic circulation reaches its peak in 60-80 min and gradually declines thereafter [17]. In parallel, the hepatic glucose release is markedly suppressed by 80% within 1-2 h after the oral glucose load.

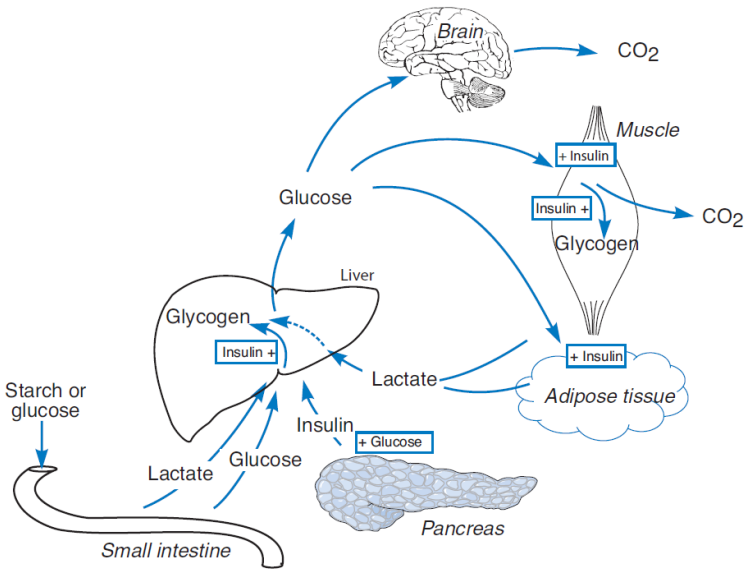

Figure 2.3 The pattern of glucose metabolism after a carbohydrate breakfast. [21]

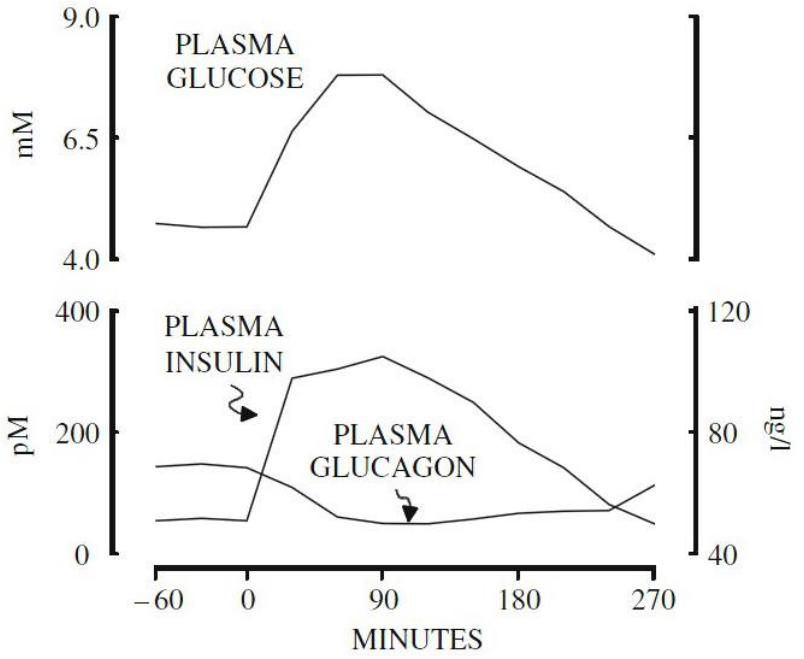

Figure 2.4 Changes in plasma glucose, insulin, and glucagon after ingestion of a 75 g oral glucose load in normal volunteers. "Principles of Diabetes Mellitus, Normal Glucose Homeostasis, 2004, 39-56, John E. Gerich, Steven D. Wittlin, Christian Meyer, (©Springer Science+Business Media New York 2004) With permission of Springer".

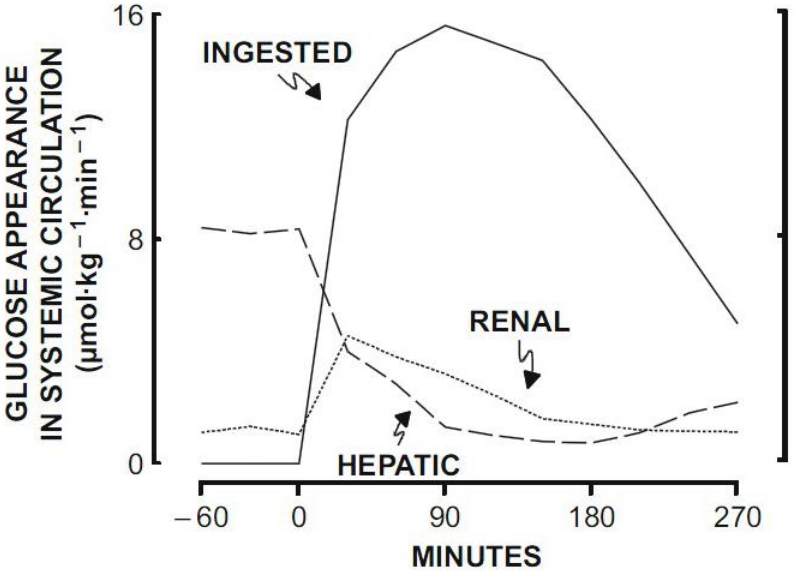

Figure 2.5 Changes in rates of entry of glucose into the circulation from ingested glucose, liver, and kidney. "Principles of Diabetes Mellitus, Normal Glucose Homeostasis, 2004, 39-56, John E. Gerich, Steven D. Wittlin, Christian Meyer, (©Springer Science+Business Media New York 2004) With permission of Springer".

2.2 Diagnosis and Classification of Diabetes

2.2.1 Diagnosis of Diabetes

Diabetes is a group of metabolic diseases characterized by hyperglycaemia resulting from defects in insulin secretion, insulin action or both [1]. The diagnosis of diabetes is based on plasma glucose criteria, either the fasting plasma glucose (FPG) or the 2-h plasma glucose after a 75-g oral glucose tolerance test (OGTT), or the HbA1c criterion [1]. Additionally, a random plasma glucose concentration value of ≥200 $mg \cdot dL^{-1}$, accompanied with classic hyperglycaemic symptoms or a hyperglycaemic crisis, suffices to diagnose diabetes. The current diagnostic criteria for diabetes are summarized in *Table 2.1* [1]. The concordance between FPG and OGTT as well as between HbA1c and either plasma glucose criterion is imperfect, with the HbA1c designated cut point presenting the lower sensitivity. More specifically, the HbA1c cut point of ≥6.5% has been found to identify one third fewer cases of undiagnosed diabetes than an FPG cut point of ≥126 $mg \cdot dL^{-1}$, which is partially offset by the HbA1c test's greater convenience (since fasting is not required), lower inter-day variability during periods of stress and illness and greater preanalytical stability as compared with FPG and OGTT. However, the effect of age, race/ethnicity and anaemia/hemoglobinopathies on average HbA1c should be considered.

Table 2.1 Criteria for the Diagnosis of Diabetes [1]

FPG ≥126 $mg \cdot dL^{-1}$ (7.0 $mmol \cdot L^{-1}$). Fasting is defined as no caloric intake for at least 8 h.*
Two-hour plasma glucose ≥200 $mg \cdot dL^{-1}$ (11.1 $mmol \cdot L^{-1}$) during an OGTT. The test should be performed as described by the World Health Organization, using a glucose load containing the equivalent of 75 g anhydrous glucose dissolved in water.*
HbA1C ≥6.5%(48 $mmol \cdot mol^{-1}$). The test should be performed in a laboratory using a method that is NGSP certified and standardized to the Diabetes Control and Complications Trial (DCCT).*
In a patient with classic symptoms of hyperglycaemia or hyperglycaemic crisis, a random plasma glucose ≥200 $mgdL^{-1}$ (11.1 $mmolL^{-1}$).

*In the absence of unequivocal hyperglycaemia, criteria 1-3 should be confirmed by repeat testing.

All three tests can be also applied for the identification of people with prediabetes, an

intermediate stage associated with at increased risk for developing diabetes as well as cardiovascular disease. Prediabetes is formally defined as: (i) impaired fasting glucose (IFG), i.e. 100 mg·dL^{-1} ≤ FPG ≤ 125 mg·dL^{-1}, or (ii) impaired glucose tolerance (IGT), i.e. 140 mg·dL^{-1} ≤ 2-hour plasma glucose during an OGTT ≤ 199 mg·dL^{-1}, or (iii) an HbA1c range of 5.7 - 6.4%.

2.2.2 Classification of Diabetes

Diabetes can be classified into the following general categories: (i) type 1 diabetes due to an autoimmune destruction of the pancreatic β-cells usually leading to an absolute deficiency of insulin secretion, (ii) type 2 diabetes due to a progressive loss of β-cell insulin secretion frequently on the background of resistance to insulin action, (iii) gestational diabetes mellitus which is defined as diabetes diagnosed in the second or third trimester of pregnancy which is not clearly either pre-existing type 1 or type 2 diabetes, and similar to type 2 diabetes its main underlying pathophysiological abnormality is insulin resistance, and (iv) other specific types of diabetes which are mainly associated with monogenetic defects in β-cell function [e.g. neonatal diabetes, maturity-onset diabetes of the young (MODY)], diseases of the exocrine pancreas (e.g. cystic fibrosis-related diabetes), and drug- or chemical-induced diabetes [e.g. glucocorticoid-induced, new-onset diabetes after transplantation (NODAT)] [26]. The vast majority of people with diabetes suffer from either type 1 or type 2 diabetes.

2.2.2.1 Type 1 Diabetes

Type 1 diabetes accounts for 5-10% of all patients with diabetes and results from a cellular-mediated autoimmune destruction of the β-cells in the pancreatic islets. Type 1 diabetes is defined by the presence of at least one of the following autoimmune markers: (i) islet cell autoantibodies, (ii) autoantibodies to insulin, (iii) autoantibodies to glutamic acid decarboxylase (GAD65) and, (iv) autoantibodies to the tyrosine phosphatases IA-2, IA-2β and ZnT8 [1, 26]. In addition, autoimmune type 1 diabetes has strong, either predisposing or protective, human leukocyte antigen (HLA) associations with linkage to the DQA and DQB genes. The development of the disease encompasses three distinct stages (*Table 2.2*). Its rate of progression is dependent on the age at first detection of antibodies, number of antibodies, antibody specificity, and antibody titer. C-peptide concentration, which decreases with the loss of insulin secretory capacity, can provide insight into disease progression. Moreover,

individuals with a low first-phase insulin secretory response (<100 uU·mL^{-1}), assessed by the intravenous glucose tolerance test, who concurrently express pancreatic autoantibodies are at high risk of developing immune-mediated type 1 diabetes. Type 1 diabetes has multiple genetic predispositions; the expression of two or more autoantibodies in first degree relatives of patients with immune-mediated type 1 diabetes indicates an increased risk (>90%) over the next 10 years [27].

Idiopathic type 1 diabetes, which constitutes a rare form of type 1 diabetes, is characterized by episodic ketoacidosis and varying degrees of insulin deficiency between episodes [1, 26]. Idiopathic type 1 diabetes is strongly inherited, lacks immunological evidence of β-cell deficiency and is not HLA associated.

Table 2.2 Staging of Type 1 Diabetes [1]

	Stage 1	**Stage 2**	**Stage 3**
Characteristics	Autoimmunity Normoglycaemia Pre-symptomatic	Autoimmunity Dysglycaemia Pre-symptomatic	New-onset hyperglycaemia Symptomatic
Diagnostic criteria	Multiple autoantibodies No IGT or IFG	Multiple autoantibodies Dysglycaemia: IFG and/or IGT FPG 100–125 mgdL^{-1} 2-h PG 140–199 mgdL^{-1} A1C 5.7–6.4% (39–47 mmol mol^{-1}) or ≥10% increase in A1C	Clinical symptoms Diabetes by standard criteria

2.2.2.2 Type 2 Diabetes

Type 2 diabetes, which accounts for ~90-95% of those with diabetes, is characterized by a combination of inadequate insulin secretion and resistance to insulin action [1, 26]. The β-cell demise and dysfunction often worsen in the long-run and absolute insulin replacement therapy is needed. In contrast to immune-mediated type 1 diabetes, the aetiology of type 2 diabetes is unidentified. The risk of developing this form of diabetes increases with age, obesity, particularly intra-abdominal obesity, and lack of physical activity. It is more prevalent in women with prior gestational diabetes mellitus, in individuals with hypertension or

dyslipidaemia, and in certain racial/ethnic subgroups. Types 2 diabetes is also associated with a greater genetic predisposition as compared to the autoimmune form of type 1 diabetes, although its genetics are not well defined.

2.3 Assessment of Glycaemic Control

2.3.1 HbA1c Testing

Chronic hyperglycaemia in diabetes is associated with long-term microvascular (peripheral neuropathy, nephropathy and retinopathy) and macrovascular (coronary heart disease, peripheral arterial disease, and stroke) complications. HbA1c, a biomarker of average plasma glucose concentration over the preceding ~3 months ($r = 0.92$ [28]), carries a strong prognostic significance with respect to long-term microvascular and macrovascular complications in both type 1 and type 2 diabetes [29-31]. Glycaemic recommendations for non-pregnant adults with diabetes encompass an HbA1c of less than 7% (53 mmol mol^{-1}) accompanied by preprandial capillary plasma glucose in the range of 80-130 $mg \cdot dL^{-1}$, and peak postprandial capillary plasma glucose (measured 1-2 h after the beginning of the meal) of less than 180 $mg \cdot dL^{-1}$. However, the American Diabetes Association (ADA) stresses that glycaemic targets should be individualized based on duration of diabetes, age/life expectancy, comorbid conditions, advanced microvascular or cardiovascular complications, hypoglycaemia unawareness, and individual patient preferences [32].

2.3.2 Self-monitoring of Blood Glucose

SMBG constitutes an integral component of each effective diabetes management plan allowing patients to assess their instant glycaemic status and their individual response to therapy. Increased daily frequency of SMBG in type 1 diabetes management has been associated with lower HbA1c levels (-0.2% per additional test per day) and fewer acute complications [33, 34]. The ADA recommends that most patients on intensive insulin regimen (multiple-dose insulin or insulin pump therapy) should consider SMBG prior to meals and snacks, occasionally postprandially, at bedtime, prior to exercise, when they suspect low blood glucose, after treating low blood glucose until they are normoglycemic, and prior to critical tasks such as driving, which corresponds to 6-10 (or more) measurements daily [32]. Optimal use of SMBG

requires the proper integration of SMBG results into lifestyle management and pharmacologic therapy of type 1 diabetes.

2.3.3 Continuous Glucose Monitoring

CGM technologies, relying on a subcutaneously implantable sensor, report the glucose concentration in the interstitial fluid at intervals of 1-5 min. CGM systems intended for real-time use (e.g. Medtronic Minimed® 530G, 640G; DexcomG4®, G5™; Freestyle® Navigator II) display the level and rate of change of subcutaneous glucose concentration, with recent systems providing also customizable predictive alerts for hypo- and hyperglycaemic excursions [6]. On the other hand, professional (operating in a "blind" mode) CGM systems (e.g. Medtronic iPro®2) target at the retrospective evaluation of CGM data by healthcare professionals in order to assess the quality of glycaemic control and magnitude of glycaemic variability, detect crucial glycaemic patterns (e.g. dawn phenomenon, postprandial hyperglycaemia, asymptomatic and nocturnal hypoglycaemia) and evaluate the effect of treatment interventions [6, 35]. Standardization of the presentation and analysis of CGM data is considered crucial to optimizing decision making in both clinical and self-monitoring conditions [36, 37]. Figure 2.6 portrays the ambulatory glucose profile report of a typical subject during two weeks of monitoring.

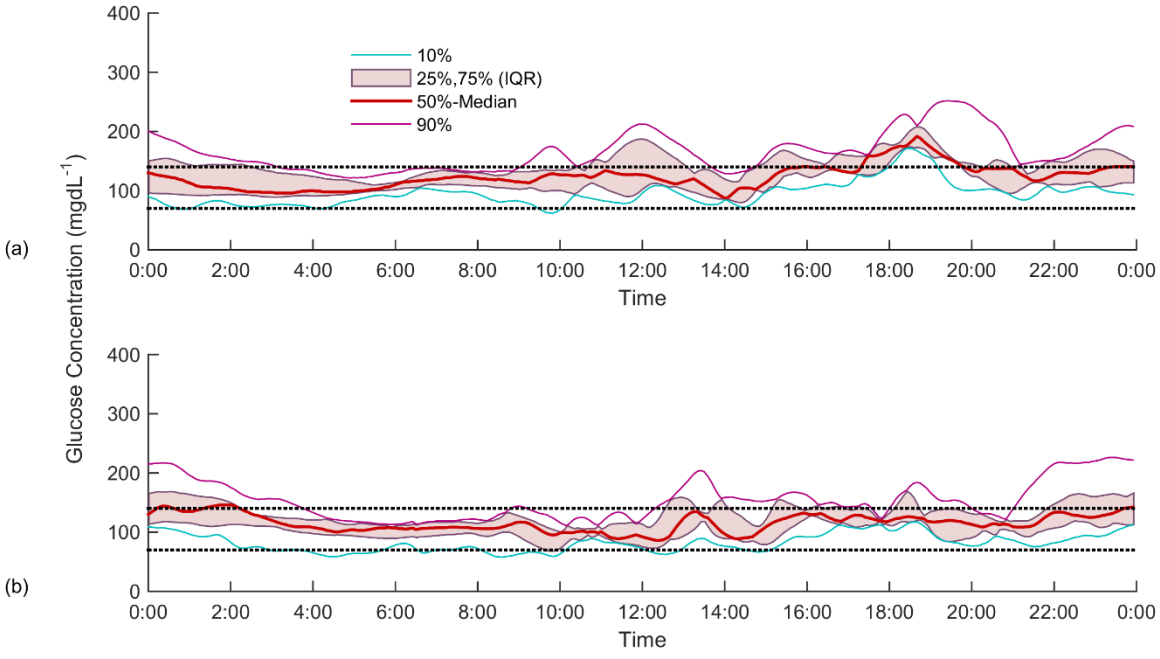

Figure 2.6 Ambulatory glucose profile of a person with type 1 diabetes during (a) the first and (b) second week of the observational period.

Proper calibration of CGM systems based on capillary blood glucose measurements highly affects the accuracy and time lag (TL) of the estimated interstitial fluid glucose concentration relative to blood glucose concentration. A comparative effectiveness analysis of three CGM systems (FreeStyle Navigator, Abbott Diabetes Care; G4 Platinum, Dexcom; Enlite, Medtronic) in adults and adolescents with type 1 diabetes under closed-loop blood-glucose control showed that the G4 Platinum and FreeStyle Navigator outperform in terms of accuracy the Enlite sensor, with the aggregate mean absolute relative difference (MARD) of all paired subcutaneous-venous plasma glucose points being 10.8±9.9%, 12.3±12.1% and 17.9±15.8%, respectively [38]. The accuracy and reliability of contemporary CGM systems have been substantially improved, effecting their approval for making therapeutic decisions without confirmation with a blood glucose test [6, 7].

The findings of numerous clinical trials confirm that CGM results in lower HbA1c in type 1 diabetes as compared to SMBG [35, 39-42]; however, they have not shown consistent reductions in severe hypoglycaemia [43-45]. Baseline glycaemic control and frequency of CGM sensor use are determinants of its HbA1c-lowering effect on type 1 diabetes for all age groups, while age (≥25 years) correlates with frequency of CGM use [39]. A meta-analysis of randomized control trials in adults with type 1 diabetes demonstrated that (i) CGM results in lower HbA1c levels by 0.30% on average as compared to SMBG, (ii) every one day increase of sensor usage per week increased the effect of CGM on HbA1 by 0.15% and (iii) every 1% increase in baseline HbA1c increased the effect by 0.126% [40]. It has been also demonstrated that CGM can be of considerable benefit to individuals with type 1 diabetes with HbA1c <7.0-7.5%, reducing the frequency of hypoglycaemia (≤70 $mg \cdot dL^{-1}$) and maintaining tight glucose control [46, 47].

2.3.4 Hypoglycaemia in Diabetes

2.3.4.1 Definition and Classification of Hypoglycaemia

Hypoglycaemia is defined as a blood glucose concentration value ≤70 $mg \cdot dL^{-1}$ and is typically accompanied by a number of neurogenic (e.g. palpitation, tremor, anxiety, sweating, hunger and paresthesia) or neuroglycopenic symptoms (e.g. cognitive impairment, behavioural changes, confusion, seizure, coma or, if untreated, death) [17]. *Table 2.3* presents the

classification of hypoglycaemia in diabetes according to the American Diabetes Association and Endocrine Society Workgroup [17]. Recently, the International Hypoglycaemia Study Group recommended that a plasma glucose concentration of <54 mg·dL^{-1}, detected by self-monitoring of plasma glucose, CGM (for at least 20 minutes), or a laboratory measurement of plasma glucose, should be used to define "clinically significant biochemical hypoglycaemia" and should be reported in relevant clinical studies [18].

Table 2.3 The American Diabetes Association and Endocrine Society Classification of Hypoglycaemia in Diabetes [17]

Severe hypoglycaemia	An event requiring assistance of another person to actively administer carbohydrates, glucagon, or take other corrective actions. Plasma glucose concentrations may not be available during an event, but neurological recovery following the return of plasma glucose to normal is considered sufficient evidence that the event was induced by a low plasma glucose concentration.
Documented symptomatic hypoglycaemia	An event during which typical symptoms of hypoglycaemia are accompanied by a measured plasma glucose concentration ≤70 mgdL^{-1}.
Asymptomatic hypoglycaemia	An event not accompanied by typical symptoms of hypoglycaemia but with a measured plasma glucose concentration ≤70 mgdL^{-1}.
Probable symptomatic hypoglycaemia	An event during which symptoms typical of hypoglycaemia are not accompanied by a plasma glucose determination but that was presumably caused by a plasma glucose concentration ≤70 mgdL^{-1}.
Pseudo-hypoglycaemia	An event during which the person with diabetes reports any of the typical symptoms of hypoglycaemia with a measured plasma glucose concentration >70 mgdL^{-1} but approaching that level.

2.3.4.2 Glucose Counterregulation in Diabetes

Hypoglycaemia in individuals with type 1 or advanced type 2 diabetes is the result of therapeutic hyperinsulinemia and an attenuated physiological response to falling plasma glucose concentrations [2, 19-21]. Therapeutic hyperinsulinemia is primarily related to patient's actions leading to relative, with respect to the rates of glucose influx and efflux out of the circulation, or absolute excess of circulating insulin (e.g. incorrect insulin dosing, type or timing, missed meal, exercise, overnight fast, alcohol consumption). On the other hand, both defective glucose counterregulation and hypoglycaemia unawareness are linked to the pathophysiology of diabetes *per se*. In type 1 diabetes or insulin-treated type 2 diabetes, the

counterregulatory system cannot prevent or restore hypoglycaemia: (i) plasma insulin concentration, as a function of the clearance of administered insulin, is not reduced, (ii) the primary defence against hypoglycaemia, i.e. stimulation of glucagon secretion, is lacking, and (iii) the epinephrine response to hypoglycaemia is attenuated. In addition, the diminished response of the sympathetic nervous system to hypoglycaemia in people with type 1 diabetes leads to hypoglycaemia unawareness. According to the concept of hypoglycaemia-associated autonomic failure (HAAF) in diabetes, recent hypoglycaemic events (even asymptomatic ones), exercise and sleep intensify both defective glucose counterregulation and hypoglycaemia unawareness by further suppressing epinephrine response to a subsequent hypoglycaemic event as well as neurogenic symptoms [2, 22].

2.4 Insulin Therapy

2.4.1 Insulin Analogues

Available insulin products include regular human insulin as well as analogues of human insulin with specific pharmacokinetic/pharmacodynamic properties, which, as it is shown in *Table 2.4*, are classified as rapid-acting, short-acting, intermediate-acting and long-acting insulins [27, 48, 49]. The gradual dissociation of regular insulin hexamers into dimers and monomers, which are the forms of insulin which are absorbed into the bloodstream, results in a delayed onset (30-60 min) and duration of action. Rapid-acting insulin analogues are produced by altering one (i.e. Aspart) or two (i.e. Lispro, Glulisine) amino acids in the sequence of regular insulin such that their rate of absorption, following subcutaneous administration, increases. Neutral protamine hagedorn (NPH) insulin exhibits an intermediate-acting profile with an onset of action of 2-4 h, peak action from 6 to 10 h and duration of action up to 16 h. Long-acting insulin analogues (i.e. Glargine, Detemir, Degludec) show no pronounced peak metabolic effect and provide 24-h of basal insulin supply. The pharmacodynamics of regular and NPH insulin are dose-dependent with larger doses causing a delay in the peak and increasing their duration of action. The absorption of subcutaneously injected insulin into the bloodstream shows substantial intra-patient and inter-patient variability, which is significantly associated with blood flow differences in the subcutaneous tissue attributed to the site of injection *per se* or other exogenous factors (e.g. exercise, heat application or local massage)

[48, 49]. The increase of blood flow at the injection site is translated to a higher rate of absorption. In addition, smaller insulin concentrations result in more rapid pharmacokinetics.

Table 2.4 Pharmacodynamics of Regular Insulin and Insulin Analogues [49]

		Onset of Action (h)	Peak Action (h)	Effective Duration of Action (h)	Maximum Duration (h)
Rapid-Acting Insulin Analogues	Lispo	0.25 - 0.5	0.5-1.5	3-4	4-6
	Aspart	0.25 - 0.5	0.5 -1.25	3-4	4-6
	Glulisine	0.25 - 0.5	0.5 -1.25	3-4	4-6
Short-Acting Insulin	Regular	0.5 - 1	2-3	3-6	6-8
Intermediate-Acting Insulin Analogues	NPH	2-4	6-10	10-16	14-16
Long-Acting Insulin Analogues	Glargine	0.5-1.5	8-16	18-20	20-24
	Detemir	0.5-1.5	6-8	14	~20
	Degludec	0.5-1.5	none	24	40

2.4.2 Principles of Intensive Insulin Therapy

Intensive insulin therapy, defined as MDI of prandial (bolus) and basal insulin or CSII, attempts to replicate the pattern of physiologic insulin secretion such that individualized glycaemic targets are achieved. The prevailing scheme to MDI therapy uses long-acting insulin at bedtime to provide a basal insulin supply throughout the day, and rapid-acting insulin before each meal to control postprandial glucose excursions. The ADA recommends optimizing the timing and dose of prandial insulin based on the type of insulin used, measured blood glucose concentration, carbohydrate intake and timing of the meal and anticipated activity. In the case of CSII therapy, rapid-acting insulin is delivered subcutaneously by an insulin pump at a customizable basal insulin infusion rate (in 25/1000-unit increments) with bolus doses being manually administered using a built-in bolus calculator (in 1/10-unit increments). CSII therapy provides greater flexibility and more precise insulin administration than MDI therapy. A key safety issue of CSII is the risk of insulin under-delivery due to the gradually altered absorption of insulin at the subcutaneous site.

Despite the continuous improvements in rapid- and long-acting insulin analogues, hypoglycaemia remains the main side effect of intensive insulin therapy (IIT). A systematic meta-analysis concluded that there are minimal differences in HbA1c and rates of severe hypoglycaemia between CSII and MDI in type 1 adults and children [45, 50]. More integrative solutions, such as SAP effectively combining CGM and CSII into one system, have been shown

to significantly improve HbA1c, when compared with MDI or CSSI, without reducing severe hypoglycaemia [4, 5]. Substantial reductions of overall hypoglycaemic ($\leq$70 mg·dL^{-1}) exposure as well severe hypoglycaemia in type 1 diabetes, without increasing HbA1c levels, come from SAP interrupting insulin delivery when existing or predicted subcutaneous glucose concentration reaches a pre-set low-glucose threshold value [9-11, 51-54].

2.4.3 Closed-Loop Control of Blood Glucose in Type 1 Diabetes

An artificial pancreas should ideally emulate the physiologic feedback glucose-responsive functionality of β-cells [8]. Artificial pancreas systems consist of a CGM sensor, an insulin pump and a control algorithm which adjusts the insulin infusion rate in response to recent CGM measurements such that glycaemic targets are safely achieved and maintained. The main algorithmic approaches to closed-loop control of blood glucose in type 1 diabetes are proportional-integral-derivative control, model predictive control and fuzzy logic [55]. The functionality of the controller may be supported by hypoglycaemia risk minimizing modules, i.e. threshold-based or predictive low-glucose insulin suspension [56, 57]. At present, hybrid closed-loop systems combine automatic inter-prandial insulin delivery with manual administration of prandial insulin boluses [58]. Finally, bihormonal artificial pancreas systems adopt a more holistic approach, regulating blood glucose by subcutaneously delivering both insulin and glucagon hormones aiming at hypoglycaemia prevention or counterregulation [8, 59, 60].

The safety and efficacy of overnight closed-loop delivery of insulin in type 1 diabetes has been well-demonstrated in numerous, mainly randomised controlled, clinical trials, with all studies consistently concluding that artificial pancreas approaches can reduce nocturnal hypoglycaemia and improve overall nocturnal glycaemic control both in an inpatient and an outpatient setting [56, 61-66]. In addition, there is now considerable evidence that 24h closed-loop blood glucose control in outpatient settings can lead to an increase in the percentage of time in the target range reducing, in parallel, the time in hypoglycaemia as compared with conventional CSII therapy or SAP therapy, with dual-hormone artificial pancreas systems being associated with a greater improvement in time in target range compared with single-hormone systems [8, 54, 59, 67-69].

CHAPTER 3. LITERATURE OVERVIEW

3.1 Introduction

The prediction of the short-term course of subcutaneous glucose concentration in individuals with type 1 diabetes is a research problem that has been widely studied, particularly, since the adoption of CGM and CSII in the daily management of the disease. From a data-driven perspective, the dynamic system of blood glucose metabolism is approximated by a parameterized model relying on linear system identification or generalized linear (with respect to the parameters) regression approaches.

The p-step-ahead prediction of subcutaneous glucose concentration at time t is described as a function $\hat{y}(t|\theta) = f\left(Z^{t-pT}, \theta\right)$ of previous input-output observations up to time $t - pT$ (denoted by Z^{t-pT}), with T being the sampling interval of subcutaneous glucose concentration and $\theta \in R^m$ the parameters of the model. The function f might be linear or nonlinear with respect to the input Z^{t-pT} and the parameter vector $\theta \in R^m$ is learnt on a training set Z by (regularized) least squares such that $\hat{\theta} = \arg\min_{\theta \in R^m} E(\theta)$, where $E(\theta)$ is the error function. The class of the model, the parameter estimation method, the formulation of the input along with the quality of the observed data determine the generalization error of the derived predictive model.

3.2 Linear Time Series Models of Glucose Concentration in the Interstitial Fluid

3.2.1 Autoregressive and Moving Average Models

Linear system identification techniques have been applied to subcutaneous glucose predictive modelling by assuming that the underlying system of blood glucose metabolism is linear and time-invariant. Literature suggests that autoregressive (AR) models of high order can effectively explain the variance of the subcutaneous glucose concentration signal in the case where its high frequency components are not modelled [70-72]. In addition, should the frequency content of the glucose signal is adequately captured, then AR model portability among patients is feasible [71, 73]. Nevertheless, the existent inter-patient variability in response to exogenous inputs indicates training and testing of multivariate glucose models need to be applied individually, as is the case in the undermentioned studies. *Table 3.1* presents the main studies proposing AR models of the subcutaneous glucose concentration in people with diabetes, which were identified by prediction error methods and were evaluated by different statistical measures and for different values of prediction horizon.

Gani et al. proposed an AR model of order 30, AR(30), which parameters were obtained through regularized least squares on smoothed CGM data [70]. The Tikhonov approach was applied both for smoothing the raw CGM data as well as for regularizing the parameter estimates. The stationarity of the CGM time series was verified before the analysis. The dataset comprised nine subjects with type 1 diabetes who were monitored over 5 days. The training and test set were each comprised of 2000 samples, with the sampling interval of CGM measurements being equal to $T = 1\text{min}$. Both the root mean squared error (RMSE) and the TL corresponding to the maximum of the cross-correlation function were evaluated with respect to the smoothed glucose signal. The estimated AR coefficients reflected the temporal behaviour of the autocorrelation function of the glucose signal, leading to stable accurate 30-min predictions with negligible RMSE (0.1 ± 0.02 mmol·L^{-1}) and TL (0.2 ± 0.4 min). The prediction accuracy decreased with increasing prediction horizon, with prediction horizons of 60 min and 90 min being associated with higher errors (0.7 ± 0.1 mmol·L^{-1} and 1.6 ± 0.2 mmol·L^{-1}, respectively) and clinically acceptable TLs (12.3 ± 2.8 min and 38.4 ± 5.2 min, respectively).

Lu et al. showed that the frequency content of the subcutaneous glucose concentration signal in people with type 1 diabetes resembles that of the blood glucose signal, retaining the four frequency bands (Band I: 5-15 min, Band II: 60-120 min, Band III: 150-500 min, Band

IV: ≥700 min as they are characterized by the periodicity of blood glucose signal's oscillations), despite the time delay and signal attenuation from the blood-to-interstitial transport [72, 74]. In particular, Bands III and IV accounted for the majority of the subcutaneous glucose signal's power spectral density (PSD), whereas ~1.5 % and ~0.6% of PSD fall into Band II and Band I, respectively. Lu et al., by applying the same training and testing AR configuration as in [70], compared the predictive capacity of bands II-IV and of their pairwise combinations for prediction horizons of 0-50 min. A reference AR model was also developed using the overall spectrum of the glucose signal except Band I. The high-frequency band, i.e. Band I was treated as noise considering that it is associated with rapid pulsatile insulin secretion by pancreatic β-cells in healthy individuals [75, 76]. They showed that: (i) the reference AR model yields the smallest RMSE for all horizons, (ii) the AR models concerning the medium-frequency dynamics (Band II or Band III) exhibit comparable performance to the reference model for prediction horizons <25 min yielding negligible RMSEs (<3 $mg \cdot dL^{-1}$), (iii) Band III models outperform Band II models for longer prediction horizons (25-50 min), (iv) Band IV model, which had systematically inferior performance for horizons <40 min, outperform Band II and III models for prediction horizons >45 min, and (v) models combining Band II, with either Band III or Band IV, compare well with the reference model over the 0-50 prediction horizon range, and outperform each of the single-band models. The latter confirms the importance of Band II which represents the glucose dynamics in response to meal intake and insulin injections.

In a subsequent study by Gani et al. [71], the PSD analysis of the subcutaneous glucose concentration signals of people with type 1 or type 2 diabetes, coming from three different studies, provided corroborating evidence on the preservation of the four frequency bands I-IV across different individuals. Therefore, the invariance of the AR parameters on a periodic signal's amplitude and phase and their sole dependency on its frequency led to regularized AR(30) models of comparable short-term (≤30 min) predictive capacity. Nevertheless, the need for filtering out the high-frequency glucose dynamics (with periods <60 min) and regularizing the AR fitting method was stressed for obtaining physiologically plausible AR parameters and robust models.

3.2.2 Autoregressive and Moving Average Models with Extra Inputs

Table 3.1 presents the state-of-the-art studies which employ linear time-invariant models with

extra inputs to predict short-term subcutaneous glucose dynamics.

In Stahl et al. [77], a number of linear system identification models [i.e. autoregressive moving average model (ARMA), autoregressive moving average model with extra inputs (ARMAX), and generalized transfer function model (GTFM)] were evaluated on interpolated blood glucose concentration values aiming at providing reasonably accurate 2-h-ahead predictions. Data were collected from one subject with type 1 diabetes in ambulatory conditions, with the first week of data comprising the training set and the second week of data comprising the test set. The insulin (Input 1) and carbohydrate (Input 2) fluxes, computed via compartmental modelling, formed the exogenous inputs to the system. The separation of system dynamics by a GTFM of order $n_a = 5$, $n_{b1} = 2$, $n_{b2} = 3$, $n_{f1} = 1$, $n_{f2} = 1$, $n_c = 3$ and $n_d = 2$ (GTFM(5,2,3,1,1,3,2)) resulted in less correlated residuals as compared with an ARMAX model of order $n_a = 6$, $n_{b1} = 2$, $n_{b2} = 1$ and $n_c = 1$ (ARMAX(6,2,1,1)), and yielded a slight increase in the FIT% concerning the 2-h-ahead (eight-step-ahead) predictions from 59.11% to 60.83%. Stahl et al. pointed out that the accuracy of blood glucose concentration predictions is affected by: (i) potentially unrepresented inputs and unmeasured disturbances, and (ii) the almost concurrent and, more importantly, in a specified ratio delivery of insulin and carbohydrates [insulin-to-carbohydrate ratio (ICR)]. In addition, the spectral coherence between the input and output variables supported the presence of nonlinear system dynamics.

Cescon et al. [78] carried out a detailed evaluation of ARMAX models of interpolated blood glucose concentration, which were fed with interpolated plasma insulin concentration measurements and the simulated rate of appearance of glucose into plasma following carbohydrate intestinal absorption [79]. In particular, ARMAX models of order in the range $1 \le n_a \le 10$, $1 \le n_{bi} \le 10$, $1 \le n_c \le 10$, and $1 \le n_{u_i} \le 3$, with $i = 1, 2$, which were identified using data collected in a clinical setting (equally split into training and test set) [80], satisfied the criteria of stability, uncorrelated (white noise) residuals and physiologically sensible responses to 1 IU of insulin and 10 g of carbohydrates. In addition, 30 min-ahead predictions were associated with a FIT% 68.19% and a VAF% 89.27. As regards 60 min-ahead predictions, a VAF≥50% was achieved in the majority of patients; nevertheless, the requirement of FIT≥50% was not achieved.

A simulation study relying on the physiological model of Hovorka et al. linked the generalization capability of autoregressive with extra inputs (ARX), ARMAX and Box-Jenkins

models with the linear dependence between the bolus insulin dose (u_1) and the meal carbohydrate content (u_2) vectors as assessed by the condition number of the input matrix $[u_1, u_2]$ [81, 82]. Models' input comprised the simulated profiles of plasma insulin concentration and exogenous glucose appearance rate [82]. The median FIT% of ARMAX and Box-Jenkins models (77% and 73%, respectively) in the case of 1-h ahead predictions was negatively correlated with the condition number ($r = -0.86$ and $r = -0.88$, respectively), whereas these correlations were weaker for 2-h ahead predictions ($r = -0.64$ and $r = -0.82$, respectively). On the other hand, the median FIT% of ARX models was correlated to a significantly lesser extent with the condition number, with $r = -0.43$ (FIT% 51%) and $r = -0.39$ (FIT% 25%) for 1-h and 2-h ahead predictions, respectively.

An attempt to address input collinearity was made by Zhao et al. via latent variables [83]. The proposed scheme combined partial least squares regression and canonical correlation analysis. The effect of carbohydrates and subcutaneously administered insulin was described by the corresponding finite impulse response functions [84]. The method was evaluated on 10 *in silico* subjects from the University of Virginia/Padova type 1 diabetes simulator [85] and under three different simulation scenarios (Case I: ideal ICR, Case II: 30% increase in ICR and Case III: 30% decrease in ICR). Both univariate and multivariate L models (LV and LVX, respectively) were compared and contrasted with the respective AR and ARX models for a maximum prediction horizon of 60 min. Regarding the *in silico* subjects, LVX and ARX models performed equally well in Case I clearly outperforming AR and LV models for prediction horizons ≥30 min. In addition, the LVX model, unlike the ARX model, maintained its accuracy in Cases II and III. A complementary retrospective evaluation on 7 subjects with type 1 diabetes, monitored in ambulatory conditions, revealed the predominance of LVX models for prediction horizons ≥30 min.

Zhao et al. proposed additionally a methodology for rapid identification of ARX models of subcutaneous glucose concentration in type 1 diabetes [86]. In particular, (i) a base ARX model, with the same input configuration as in [83], was first estimated by least squares using data from one subject, and (ii) for each new subject, the parameters concerning the exogenous inputs of insulin and carbohydrate responses (i.e. $B_1(q)$ and $B_2(q)$, respectively) were iteratively updated (increment or decrement by a predefined step) according to the sign of the difference $mean(\hat{y}) - mean(y)$ using a small amount of data. A proof-of-concept study

including 30 *in-silico* subjects from the University of Virginia/Padova type 1 diabetes simulator [85], demonstrated a slightly better performance as compared with individualized ARX models for prediction horizons ≥30 min in the case where training and test data come from different simulation scenarios (Case I: ideal ICR, Case II: 30% increase in ICR, Case III: 30% decrease in ICR, and Case IV: Case I with bolus insulin being injected 30 min later after the respective meal).

The problem of multi-step-ahead prediction of subcutaneous glucose concentration in type 1 diabetes was also formulated as a subspace-based multiple-input multiple-output system of the inputs $u \in R^m$, the outputs $y \in R^l$, the state $x \in R^n$, and, an uncorrelated with u, zero-mean white noise process $\varepsilon \in R^l$ [87]. The input $u \in R^2$ (i.e. $m = 2$) described the rate of appearance of ingested glucose into plasma and the plasma insulin concentration [79]. Predictions of future subcutaneous glucose concentration from time t up to time $t + f - 1$ were expressed as a linear combination, $\hat{y}^f = \hat{\Gamma} z^p + \hat{\Lambda} u^f$, of the past joint input-output data $z^p = \begin{bmatrix} u^p & y^p \end{bmatrix}^T \in R^{(m+l)p}$ and the future input $u^f \in R^{mf}$ within the time intervals $[t-p, t-1]$ and $[t, t+f-1]$, respectively. The optimization of $\hat{\Gamma} \in R^{lp \times (l+m)p}$ and $\hat{\Lambda} \in R^{lp \times mf}$ was formulated as a least-squares problem assuming that: (i) the input signals are persistently exciting of order at least mf, (ii) the intersection of the spans of the Hankel matrices Z^p and U^f is zero [88]. Given a sampling interval of $T = 10\,\text{min}$, two different model configurations were examined, i.e. Case A with $f = 3$ and Case B with $f = 12$. The assessment of the model using as reference the blood glucose signal and, in parallel, the comparison with a Kalman-based third-order ARMAX model demonstrated the competitiveness of their approach.

Table 3.1 Linear System Models of Short-Term Prediction of Subcutaneous Glucose Concentration in Diabetes

Study	Model	Input	Dataset		Prediction Performance		
Gani et al. [70]	Regularized AR(30)	CGM data	*Subjects:* Nine people with type 1 diabetes [89] *CGM Device:* iSense, iSense Corp. *Sampling Interval:* 1 min *Monitoring Period:* 5 days		*RMSE* 30 min: 0.1±0.02 mmol·L^{-1} 60 min: 0.7±0.1 mmol·L^{-1} 90 min: 1.6±0.2 mmol·L^{-1}	*TL* 30 min: 0.2±0.4 min 60 min: 12.3±2.8 min 90 min: 38.4±5.2 min	
Gani et al. [71]	Regularized AR(30)	CGM data	Study 1	*Monitoring Period:* 5 days *Sampling Interval:* 1 min *Subjects:* Nine people with type 1 diabetes [89] *CGM Device:* iSense, iSense Corp.	Same-Subject *RMSE* 30 min: 0.17±0.02 mmol·L^{-1} *TL* 30 min: 0.6±1.7 min *Clarke EGA - Zone A:* 30 min: 99.0%	Cross-Subject *RMSE* 30 min: 0.18±0.03 mmol·L^{-1} *TL* 30 min: 0.3±1.2 min	Cross-Study *RMSE* 30 min: 0.17±0.03 mmol·L^{-1} *TL* 30 min: 0.4±1.4 min
			Study 2	*Subjects:* 18 children with type 1 diabetes *CGM Device:* Guardian RT, Medronic Inc. *Sampling Interval:* 5 min *Monitoring Period:* 6 days	Same-Subject *RMSE* 30 min: 0.21±0.06 mmol·L^{-1} *TL* 30 min: 0.0±0.0 min *Clarke EGA - Zone A:* 30 min: 99.3%	Cross-Subject *RMSE* 30 min: 0.21±0.07 mmol·L^{-1} *TL* 30 min: 0.1±0.8 min	Cross-Study *RMSE* 30 min: 0.22±0.08 mmol·L^{-1} *TL* 30 min: 0.2±1.0 min
			Study 3	*Subjects:* 7 people with type 2 diabetes *CGM Device:* Dexcom, Dexcom Inc. *Sampling Interval:* 5 min *Monitoring Period:* 56 days	Same-Subject *RMSE* 30 min: 0.16±0.03 mmol·L^{-1} *TL* 30 min: 0.0±0.0 min *Clarke EGA - Zone A:* 30 min: 99.5%	Cross-Subject *RMSE* 30 min: 0.16±0.03 mmol·L^{-1} *TL* 30 min: 0.0±0.0 min	Cross-Study *RMSE* 30 min: 0.17±0.03 mmol·L^{-1} *TL* 30 min: 0.0±0.0 min
Finan et al. [81]	ARMAX models	Blood glucose concentration Insulin and carbohydrate compartmental modelling [82]	In-silico type 1 diabetes data		*FIT%* 1-h: 77% 2-h: 65%	*RAD:* 1-h: 4.7% 2-h: 6.3%	*Clarke EGA - Zone A:* 1-h: 99% 2-h: 94%
Cescon &	ARMAX models	Linearly interpolated blood	*Subjects:* Nine people with type 1		*FIT%*		*VAF%*

Study	Model	Input	Dataset	Prediction Performance	
Johansson [78]		glucose and insulin concentration Insulin and carbohydrate compartmental modelling [79]	diabetes [80] *Monitoring Period:* 3 days *Sampling Interval:* 1 min	30 min: 68.19±8.83 60 min: 41.15±15.81 90 min: 23.42±20.71 120 min: 12.67±25.02	30 min: 89.27±5.82 60 min: 63.75±20.85 90 min: 39.15±37.54 120 min: 21.12±53.47
Cescon et al. [87]	Subspace-based multi-step models	CGM data Insulin and carbohydrate compartmental modelling	*Subjects:* Nine people with type 1 diabetes [80] *CGM Device:* Abbot Freestyle Navigator *Sampling Interval:* 10 min *Monitoring Period:* 3 days	Case A *Prediction error standard deviation* 10 min: 3.66±0.99 mg·dL^{-1} 20 min: 9.44±2.63 mg·dL^{-1} 30 min: 15.58±4.87 mg·dL^{-1}	Case B *Prediction error standard deviation* 30 min: 19.77±7.46 mg·dL^{-1} 60 min: 39.44±16.11 mg·dL^{-1} 90 min: 52.28±21.04 mg·dL^{-1} 120 min: 59.56±24.44 mg·dL^{-1}
Zhao et al [83]	Latent variable – based model without or with extra inputs (i.e. LV, LVX)	CGM data Second-order transfer function models of insulin and meal intake [84]	*Subjects:* Seven people with type 1 diabetes *CGM Device:* DexCom 7 Plus, DexCom *Monitoring Period:* - *Sampling Interval:* 5 min	LV *RMSE* 15 min: 11.3±2.4 mg·dL^{-1} 30 min: 19.7±3.3 mg·dL^{-1} 45 min: 26.0±3.8 mg·dL^{-1} 60 min: 31.2±4.0 mg·dL^{-1} *Clarke EGA - Zone A:* 15 min: 96.4±2.0 % 30 min: 84.9±7.6 % 45 min: 76.3±10.2 % 60 min: 68.4±9.6 %	LVX *RMSE* 15 min: 11.1±2.4 mg·dL^{-1} 30 min: 18.7±3.7 mg·dL^{-1} 45 min: 24.4±4.7 mg·dL^{-1} 60 min: 29.2±5.5 mg·dL^{-1} *Clarke EGA - Zone A:* 15 min: 96.8±1.8 % 30 min: 86.1±7.5 % 45 min: 78.8±9.9 % 60 min: 72.1±10.6 %
Zhao et al [73, 86]	ARX, Model migration	CGM data Second-order transfer function models of insulin and meal intake [84]	In-silico data / University of Virginia / University of Padova Simulator	*RMSE* Adolescents:14.85±4.94 mg·dL^{-1} Adults: 10.98±2.10 mg·dL^{-1} Children: 18.56±10.29 mg·dL^{-1}	*CG-rEGA - Zone A* Adolescents:70.76±1.31 % Adults: 70.50±0.57 % Children: 66.87±5.71 %

RAD: Relative absolute deviation; EGA: Error grid analysis.

3.3 Non-Linear Models of Glucose Concentration in the Interstitial Fluid

Linear regression models, which comprise linear combinations of adaptive non-linear basis functions, have been effectively applied to the identification and prediction of the subcutaneous glucose concentration in type 1 diabetes. Literature suggests that nonlinear modelling of the subcutaneous glucose concentration yields significantly more accurate short-term (≤30 min) and mostly long-term (>30min) predictions as compared with linear, with respect to the input, models and, in addition, benefit from the utilization of particularly configured multivariate features sets. *Table 3.2* presents the state-of-the-art studies treating the short-term prediction of subcutaneous glucose concentration as a nonlinear regression problem.

3.3.1 Neural Network-based Regression Models

Nonlinearity in the blood glucose system has been addressed via black-box parameterizations and, particularly, neural network-based regression models. A two-layer feed-forward neural network (FFNN) fed with subcutaneous glucose concentration measurements during the preceding 20 min produced considerably lower RMSEs for prediction horizons of 30 min and 45 min when compared with a first-order AR model identified by weighted recursive least-squares; though, FFNN-based predictions were associated with a higher temporal delay [90]. Multivariate nonlinear regression models of subcutaneous glucose concentration are expected to exhibit a better predictive performance than univariate solutions considering the short-term auto-correlation of the subcutaneous glucose concentration, which becomes zero at about 30 min [91], as well as the immediate effect of exogenous inputs on blood glucose regulation. Similarly to linear time series models, quantitative information on carbohydrates intake or subcutaneous insulin administration is incorporated through compartmental modelling of their respective kinetics and dynamics. In particular, Mougiakakou et al was the first to combine a recurrent neural network (RNN) with compartmental models of plasma insulin concentration and carbohydrates absorption [92, 93].

Zecchin et al. proposed a hybrid predictive scheme combining a FFNN with a linear model of short-term (30 min ahead) subcutaneous glucose system dynamics [94]. The p -step-ahead prediction of subcutaneous glucose concentration at time t was expressed as the sum of the linear model's output $\hat{y}_l(t)$ and the estimation of the associated error $\hat{e}(t) = y(t) - \hat{y}_l(t)$, i.e. $\hat{y}(t) = \hat{y}_l(t) + \hat{e}(t)$. The linear model was postulated as a first-order polynomial which

parameters were learnt recursively by weighted least squares [95]. The error $\hat{e}(t)$ was estimated by a FFNN function of: (i) the error $e(t-pT)=y(t-pT)-\hat{y}_l(t-pT)$ relating to the glucose concentration value at time $t-pT$, (ii) the trend $(1-z^{-T_m})e(t-pT)$ over the last $T_m=15\,\text{min}$, (iii) the value of $y(t-pT)$, (iv) the trend $(1-z^{-T_m})y(t-pT)$ over the last $T_m=15\,\text{min}$, (v) the glucose rate of appearance at time t, i.e. $Ra(t)$ computed according to [79], and (vi) the difference vector $\left[(1-z^{T_a}),(z^{T_a}-z^{2T_a}),(z^{2T_a}-z^{3T_a})\right]^T Ra(t)$ with $T_a=10\,\text{min}$, which entails the announcement of each meal at least pT minutes in advance. The FFNN was comprised of one hidden layer with 8 neurons having a tangent sigmoid activation function, and one output layer with one neuron having a linear function. The weights and bias parameters of the FNNN were trained based on the Levenberg-Marquardt back-propagation algorithm applied in a batch mode and with early-stopping (i.e. validation set). In addition, both network structure and inputs were determined by 10-fold cross-validation over the training set. The method was evaluated on 20 *in silico* subjects from the University of Virginia/Padova type 1 diabetes simulator [85] as well as on 15 subjects with type 1 diabetes monitored in free-living conditions [80]. The data of all patients were merged and, subsequently, properly divided into training and test sets aiming at deriving a non-personalized predictive solution. The comparison with two state-of-the-art univariate glucose models, having a linear time-varying AR(1) [95] and a non-linear FFNN [90] structure, respectively, with regard to the real data and for a 30-min prediction horizon, demonstrated a RMSE almost identical to that of the FFNN (14.0±4.1 vs. 14.2±4.5 vs. 19.6±7.2 mg·dL^{-1}) accompanied by improved, comparable to those of the recursive AR(1) model, temporal gain (TG) (16.2±3.7 vs. 12.8±1.6 vs. 16.7±4.2 min) and regularity indices ($ESOD_{norm}$ 2.7±1.6 vs. 105.3±52.8 vs. 3.9±0.8).

Zecchin et al., in a subsequent study, substituted a jump neural network for the abovementioned hybrid scheme and, in parallel, reduced the input complexity [96]. A jump neural network resembles a FFNN which inputs are connected to the first hidden layer and the output layer as well. The p-step-ahead prediction of subcutaneous glucose concentration at time t was based on: (i) the glucose concentration value at time $t-pT$, i.e. $y(t-pT)$, (ii) the difference $\Delta y(t-pT)$, (ii) the rate of glucose appearance into plasma at time $t-pT$, i.e. $Ra(t-pT)$, and (iv) the difference $\Delta Ra(t-pT)$. The connection of the input to the output

layer introduced the term $w_{IO}^{T}\left[y(t-pT),\Delta y(t-pT),Ra(t-pT),\Delta Ra(t-pT),1\right]^{T}$, where w_{IO} is the corresponding weight vector, whose first two terms account for the linear glycaemic dynamics and the last two capture the linear short-term effect of Ra on the subcutaneous glucose concentration. The jump neural network comprises 1 hidden layer of 5 neurons with a tangent sigmoid activation function, and one output neuron with a linear function. As in the preceding study of Zecchin et al. [94], the model's parameters were optimized by the Levenberg-Marquardt back-propagation algorithm over the training set via cross-validation. The method was evaluated on 20 subjects with type 1 diabetes, who were monitored over a 2-3 day period in real-life conditions; with the datasets of 10 patients forming the training and validation sets, and the remaining 10 datasets forming the test set. An average RMSE of 16.6±3.1 mg·dL^{-1} and an average TG of 18.5±3.4 min were obtained, whereas the predicted profile was characterized by limited spurious oscillations ($ESOD_{norm}$: 9.6±1.6). In addition, the jump neural network had on average a statistically comparable generalization performance to the reference model proposed in [94].

Three different types of artificial neural networks (ANNs), i.e. a self-organizing map (SOM), a neuro-fuzzy network with wavelets as activation functions [wavelet fuzzy neural network (WFNN)], and a FFNN, were compared with respect to the prediction of the subcutaneous glucose concentration in type 1 diabetes over a 30-, 60-, and 120-min horizon [97]. Two input cases, i.e. Case 1 and Case 2, were defined aiming to examine the contribution of EE to the prediction performance. The univariate input case, Case 1, consisted of $y(t-pT)$ and $\Delta y(t-pT)$, whereas in Case 2, the sum of EE within the 30-min interval $\left[t-pT-150,t-pT-120\right]$ was additionally introduced. The dataset was comprised of 10 patients with type 1 diabetes who were observed for 6 days. All models were evaluated individually for each patient by 10-fold cross-validation, and their hyper-parameters were either preselected or determined though 10-fold cross-validation over each training set. In Case 1, SOM was found statistically more accurate than FFNN and WFNN for all horizons. Moreover, the continuous glucose error grid analysis (CG-EGA) revealed its better performance over hypoglycaemic and hyperglycaemic ranges. Case 2 yielded a substantial improvement in average predictive performance over all prediction horizons (RMSE: -7%, -3%, -10%; MARD: -6%, -5% , -11%; r: +0.2%, -0.1%, +1%, for SOM, WFNN and FFNN, respectively) and, primarily, in the hypoglycaemic range.

3.3.2 Ensemble Models

Ensemble learning have been shown to improve the generalization error of glucose prediction methods. Stahl et al. proposed a sliding window Bayesian model averaging approach to combining multiple predictive models of subcutaneous glucose concentration [98]. A probabilistic mixture of the form:

$$p\left(y_i \middle| x^i\right) = \sum_j p\left(M_j \middle| x^i\right) p\left(y_i \middle| x^i, M_j\right), \tag{3.1}$$

was produced, in which $p\left(y_i \middle| x^i, M_j\right)$ is the conditional probability of y_i at time t_i given the input x^i received until $t_i - pT$ and model M_j, and $p\left(M_j \mid x^i\right)$ represent the input-dependent mixing coefficients. In particular, the input space was partitioned into different regions (clusters), and an one-to-one correspondence was assumed between them and the latent variable z_i, such that:

$$p\left(M_j \middle| x^i\right) = \sum_{z_i} p\left(M_j \middle| z_i, x^i\right) p\left(z_i \middle| x^i\right), \tag{3.2}$$

under the constraint $\sum_j p\left(M_j \middle| x^i\right) = 1$. By assuming that each instant t_i is associated with only one z_i and $p\left(z_i \middle| x^i\right)$ is equal for all z_i (3.2) was condensed to $p\left(M_j \middle| x^i\right) = p\left(M_j \middle| z_i, x^i\right)$. A window-based constrained optimization problem was formulated using an asymmetric cost function, which consider the absolute glucose value and the sign of the prediction error. The efficacy of the ensemble model was shown using: (i) simulated data which consisted of two dynamic modes and were generated by the University of Virginia/Padova type 1 diabetes simulator (20 datasets of 8 days each), as well as, (ii) data from 6 type 1 diabetes subjects monitored over 3 days in a clinical trial setting (the DAQ trial and the DIAdvisor I B and C trials, conducted within the DIAdvisor project [80]). Three linear state space models with 2 extra inputs, the plasma insulin concentration and the exogenous glucose appearance rate, were identified on one simulated dataset (Model I: trained on mode A data, Model II: trained on mode B data, Model III: trained on the entire dataset). Subsequently, a p-step-ahead prediction model was inferred using a Kalman filter, and the ensemble model was tested on the remaining 19 datasets. On the other hand, a state-space-based model [99], a recursive ARX model [100] and a kernel-based model [101] were identified on the clinical trial dataset. Each

of the base models was trained on the first trial data (DAQ), whereas the ensemble prediction model was evaluated via cross-validation on B and C trial data. In both experiments, the RMSE of the ensemble model (for 60-min and 40-min prediction horizons, respectively) was found comparable to that of the best performing base model.

An adaptive weighted model averaging approach was proposed in [102], where, at each iteration i, the weighing coefficient of each model M_j, w_i^j, was adjusted according to the sum of squared prediction errors up to iteration i. A forgetting factor $\alpha \in (0,1)$ was introduced in order to control the contribution of past instances such that:

$$w_i^j = \frac{1}{SSE_i^j} \Big/ \sum_j \frac{1}{SSE_i^j}, \tag{3.3}$$

where

$$SSE_i^j = \sum_{n=1}^{i} \alpha^{i-n} \left(e_n^j\right)^2. \tag{3.4}$$

The p-step-ahead prediction of subcutaneous glucose concentration at time t_i was given by the weighted sum of the base model predictions. Three univariate models of subcutaneous glucose concentration, namely an AR(5) model, an extreme learning machine with 3 inputs (i.e. subcutaneous glucose concentration values over the last 15 min) and 25 hidden nodes, and a SVR model ($C = 50$, $\varepsilon = 0.5$ and local optimization of kernel type and parameters), were combined and evaluated on 10 subjects with type 1 diabetes randomly selected from a JDRF randomized clinical trial [99]. A ~58% of the dataset of each patient (which corresponds to the first 2500 min of CGM with a sampling interval $T = 5\,\text{min}$) was used as the training set, and the remaining ~42% (which corresponds to the last 1800 min) as the test set. The ensemble glucose prediction solution was systematically more accurate compared to the constituent models for prediction horizons ≤45 min, exhibiting a higher robustness to glucose dynamics variations and prediction horizon increase.

Table 3.2 Nonlinear Machine Learning Models of Short-Term Prediction of Subcutaneous Glucose Concentration in Diabetes

Study	Model	Input	Dataset	Prediction Performance	
Zecchin et al. [94]	FFNN & First-order recursive AR model Non-personalized model	CGM data Carbohydrate compartmental modelling [79]	*Subjects:* Fifteen people with type 1 diabetes *CGM Device:* Freestyle Navigator, Abbot Diabetes Care *Sampling Interval:* 1 min *Monitoring Period:* 7 days	30 min: *RMSE* 14.0±4.1 mg·dL^{-1} *Time Gain* 16.2±3.7 min $ESOD_{norm}$ 2.7±1.6 *J* 10.8±7.4	
Zecchin et al. [96, 103]	Jump neural networ Non-personalized model	CGM data Carbohydrate compartmental modelling [79]	*Subjects:* Twenty people with type 1 diabetes *CGM Device:* Dexcom Seven Plus, Dexcom *Sampling Interval:* 5 min *Monitoring Period:* 2-3 days	30 min: *RMSE* 16.6±3.1 mg·dL^{-1} *Time Gain* 18.5±3.4 min $ESOD_{norm}$ 9.6±1.6	
Zarkogianni et al. [97]	SOM	CGM data Physical activity: Energy expenditure	*Subjects:* Ten people with type 1 diabetes *CGM Device:* Guardian RT, Medronic Inc. *Sampling Interval:* 5 min *Monitoring Period:* 6 days	Case 1 *RMSE* 30 min: 12.29±2.27 mg·dL^{-1} 60 min: 21.06±3.20 mg·dL^{-1} 120 min: 33.68±5.26 mg·dL^{-1} r (%) 30 min: 97.92±0.70 60 min: 94.00±1.77 120 min: 84.22±4.87 *MARD* 30 min: 5.34±1.08 60 min: 9.36±1.95 120 min: 15.99±3.14 *CG-EGA (Accurate Readings)* 30 min: Hypo 91.11%, Hyper 88.59% 60 min: Hypo 78.47%, Hyper 86.96% 120 min: Hypo 56.40%, Hyper 84.73%	Case2 *RMSE* 30 min: 11.42±2.33 mg·dL^{-1} 60 min: 19.58.06±3.80 mg·dL^{-1} 120 min: 31.00±6.07 mg·dL^{-1} r (%) 30 min: 98.14±0.37 60 min: 94.26±1.27 120 min: 84.28±6.54 *MARD* 30 min: 5.19±1.48 60 min: 8.95±2.24 120 min: 14.56±3.46 *CG-EGA (Accurate Readings)* 30 min: Hypo 89.10%, Hyper 90.65% 60 min: Hypo 76.70%, Hyper 89.06% 120 min: Hypo 58.77%, Hyper 86.17%
Stahl et al.	Sliding	CGM data	*Subjects:* Six people with type 1	Trial B	Trial C

Study	Model	Input	Dataset	Prediction Performance	
[98]	window Bayesian model averaging Linear state-space models Recursive ARX model Kernel-based model	Carbohydrate and insulin compartmental modelling [79]	diabetes *CGM Device:* Freestyle Navigator, Abbot Diabetes Care, Dexcom Seven Plus, Dexcom *Sampling Interval:* - *Monitoring Period:* 3 days	$RMSE/RMSE_{best}$ 1.03 [0.75-1.04]* *CG-EGA - Zones A+B* 95.5% *Median [min-max]	$RMSE/RMSE_{best}$ 1.03 [0.94-1.05]* *CG-EGA - Zones A+B* 95.3% *Median [min-max]

$ESOD_{norm}$: Normalized energy of the second order differences

3.4 Adaptive Models of Glucose Concentration in the Interstitial Fluid

The analysis of the short-term subcutaneous glucose dynamics in type 1 diabetes has verified that a universal or global AR prediction model of subcutaneous glucose concentration is feasible in different frequency ranges, which characterize different physiological mechanisms exemplified by the periodicity of their oscillations [71, 73]. However, the high inter- and intra-patient variability of blood glucose dynamics in response to exogenous inputs supports the individualization of the predictive models and their continuous adaptation to both biological (e.g. variations in insulin sensitivity or body mass) and environmental changes (e.g. variations in the level of physical activity) as well. For instance, the slow decrease of the sample autocorrelation function of frequently-sampled blood glucose data from subjects with type 1 diabetes under ambulatory conditions over 2 days as well as their non-constant mean and variance evidenced a nonstationary process, which effect on AR modelling for each patient was ameliorated by taking the first difference of the glucose measurements [104]. The need for capturing the variations in the blood glucose system dynamics can be partially met by performing a periodic patient-specific re-estimation of model parameters (i.e. retraining). Nevertheless, sequential (or recursive) learning algorithms with the inherent ability to represent the time-varying behaviour of the underlying blood glucose regulatory system would allow for a better representation of the associated spatial and temporal input-output dependencies. *Table 3.3* reports the state-of-the-art studies employing dynamical models to the short-term prediction of the subcutaneous glucose concentration in diabetes.

3.4.1 Linear Adaptive Models

Sparacino et al. investigated the effect of the forgetting factor on the performance of an AR model of first-order, AR(1), which parameters were recursively identified by weighted least squares after applying low-pass filtering to CGM data [95]. A constant forgetting factor equal to 0.5 was shown to better balance the mean squared prediction error (MSE), the energy of the second-order differences of the predicted profile (ESOD), and the associated time delays between the predicted and the measured profile. In particular, the evaluation of the predictive model on 28 people with type 1 diabetes, whose subcutaneous glucose concentration was monitored with a sampling interval over 48 h in ambulatory conditions, demonstrated a median MSE of 353 $mg \cdot dL^{-1}$, a median ESOD of 35925, and average lag of 2.15±15.63 min and 2.35±13.03 min on positive (nadir-to-peak) and negative (peak-to-nadir) trends for a prediction horizon of 30 min. As expected, a time-invariant AR(1) model resulted in lags close to the

prediction horizon when applied to the same dataset, which could be attributed to the low order of the model. Finan et al. assessed the performance of a recursively identified (weighted least squares with a constant forgetting factor equal to 0.99) low-order ARX model of subcutaneous glucose concentration, which extra inputs comprised the insulin infusion rate and the meals' carbohydrate amount, in dynamic ambulatory conditions and for 3 prediction horizons of 30, 60, an 90 min. More specifically, Prednisone was administered to six people with type 1 diabetes over the last 3 days of the monitoring period inducing, thus, a decrease in insulin sensitivity. Nevertheless, the results did not reveal any noticeable contribution of the recursive estimation of ARX model's parameters on the prediction performance over ARX models trained in a batch mode.

The feasibility of a linear adaptive ARX solution to the prediction of the short-term subcutaneous glucose dynamics in type 2 diabetes has been demonstrated in [105, 106]. In particular, weighted recursive least squares with an adjustable forgetting factor, according to the variation of model parameters over a window of size $N_w = 5$ steps, was used to identify both ARMA and ARMAX models of the subcutaneous glucose concentration. The extra inputs concerned physiological signals related to a subject's physical activity and emotional condition [i.e. EE, average longitudinal acceleration, heat flux, galvanic skin response (GSR), and near-body temperature]. The Akaike information criterion was applied for selecting the order of the respective ARMA and ARMAX models with constant parameters over the entire dataset (ARMA $n_A = 2,\ n_C = 1$; ARMAX $n_A = 2,\ n_B = [1,1,2,2,2],\ n_C = 1$ and the delay $d = [4,4,5,7,5]$). It was shown that a multivariate ARMAX model outperforms a univariate model as applied to five people with type 2 diabetes under free-living conditions (23.8±2.4 days) [Sum of squares of the glucose prediction error (SSGPE):7.43 % vs. 8.81 %; Relative absolute deviation (RAD): 4.24±5.14 % vs 5.77±7.18 %)]. Similarly, constrained weighted recursive least squares, with a time-varying forgetting factor, provided a stable 30-min-ahead ARMAX prediction model of the subcutaneous glucose concentration in patients with type 1 diabetes fed with information on insulin on-board, EE, and GSR ($n_A = 1,\ n_B = [11,3,3]$, $n_C = 1$ and the delay $d = [1,2,2]$) [107]. Physiological constraints were imposed to the model's parameters related to the extra inputs (i.e. insulin on-board, EE, and GSR) and, additionally, the spectral radius of the state matrix of the respective state-space representation of the ARMAX model was set less than or equal to 1 to assure the stability of the model. It should be

mentioned that a Kalman filter provided real-time smoothing of the raw CGM data. This model was evaluated on 14 people with type 1 diabetes, who were monitored under free-living conditions, and achieved an average RMSE of 18.55 mg·dL^{-1} and an average SSGPE of 9.91 % for a prediction horizon of 30 min. Moreover, its incorporation into a generalized predictive insulin controller allowed the accurate prediction of hypoglycaemic events and led to the prevention of post-exercise hypoglycaemia [108].

3.4.2 Nonlinear Adaptive Models

A discrete-time state-space model with time-varying coefficients was used to describe the subcutaneous glucose concentration dynamics in response to insulin ($u_1(t)$) and carbohydrate intake ($u_2(t)$) [109]. The absorption of subcutaneously injected insulin and the absorption of carbohydrates in the small intestine were both modelled through truncated Gaussian finite impulse response filter functions considering a time span of N_1 and N_2, and a delay of d_1 and d_2 sampling intervals, respectively. The state variable (glucose concentration in the interstitial fluid) and the coefficients of the model (autoregression: $a_i(t),\ i=1,\ldots,p$; linear regression on $u_1(t)$: $\beta_i(t),\ i=1,\ldots,q$; linear regression on $u_2(t)$: $\gamma_i(t),\ i=1,\ldots,r$;) were estimated simultaneously by a second-order extended Kalman filter (EKF), constraining $\beta_i(t)$ and $\gamma_i(t)$ to negative and positive values, respectively. The model, with $p=2,\ q=6,\ r=6,\ \mathrm{N}_1=24,\ \mathrm{d}_1=6,\ \mu_1=18,\ \sigma_1=9,\ \mathrm{N}_2=18,\ \mathrm{d}_2=1,\ \mu_2=3,$ and $\sigma_2=6$ was evaluated on five insulin-pump treated people with type 1 diabetes who were monitored under normal daily life conditions for ≤3 days using a 5-min sampling interval. All performance metrics were computed using predictions starting from the second day of the observational period, whereas EKF hyper-parameter tuning was performed on data from the first day. The EKF-based state-space model was found to outperform a recursively-identified ARX model with a similar configuration ($n_A=2,$ and $n_B=[6,6]$, a forgetting factor of 0.95, and without imposing the constraints $\beta_i<0,\ \gamma_i>0,\ i=1,\ldots,6$) ($R^2$: 0.71±0.19 vs 0.64±0.24; RAD (%): 20.31±10.44 vs 22.20±11.83; Time gain: 12.00±10.37 vs 1.00±2.24). It was also demonstrated that the exploitation of meal information improves the temporal gain (TG) of predictions, though the goodness-of-fit was not affected (Time gain: 12.00±10.37 min vs 6.00±6.52 min). However,

EKF-identified state-space models provide a solution to nonlinear problems that is non-optimal [110, 111].

Two different real-time adaptive models, a RNN and an ARX model, were comparatively assessed with regard to the prediction of subcutaneous glucose concentration 15, 30 and 45 min ahead in people with type 1 diabetes under SAP therapy, as well as, their capability of forming an early warning system of hypoglycaemia [112, 113]. The insulin infusion rate constituted the extra input to ARX and RNN models. Both models were identified individually for each patient using half of his/her dataset as the training set and the remaining as the test set. The selection of the ARX model's orders and the estimation of its parameters relied on the minimum description length criterion and the recursive least squares method, respectively. During the evaluation process, the ARX model's output was corrected by the expected instantaneous prediction error (relating to time t for which the prediction is made); the instantaneous prediction error of the ARX model was estimated by a linear combination of the current (relating to time $t - pT$ at which the prediction is made) subcutaneous glucose concentration and its first and second derivatives ($T = 5\,\text{min}$), the parameters of which were identified via least squares on the training set corresponding to the specified prediction horizon. Similarly, a RNN with two feedback loops was trained based on teacher-forced, real-time, recurrent learning, with its architecture being selected via trial-and-error processing. The dataset was comprised of 23 people with type 1 diabetes who were monitored during everyday living conditions. It was shown that the output correction module contributes to a significant reduction of the TL of ARX-based predictions, inducing, though, an insignificant increase in the RMSE. The RNN model yielded less erroneous and less lagged predictions as compared with the corrected ARX model for all prediction horizons (30-min-predictions' RMSE: 18.9 vs 27.7 mg·dL^{-1}; 30-min-predictions' TL: 10 vs 15 min). In addition, their combination resulted in 100% correct alarms of hypoglycaemic events which is indicative of the complementary qualities of linear and non-linear models with respect to predictive modelling of subcutaneous glucose dynamics.

Naumova et al. proposed a novel approach to iteratively selecting/adjusting the hyper-parameters of a Tikhonov regularization learning algorithm (i.e. the regularization parameter and the parameters of the kernel generating the associated Reproducing Kernel Hilbert Space) to each new input, which was evaluated in the context of the blood glucose prediction problem [101]. Pairing each subcutaneous glucose concentration measurement g with the associated

sampling time t, a regularized function of time $f:\left(R_+^2\right)^m \to \left(R_+^2\right)^n$ is learnt on a training set $Z=\left\{\left(x_\mu, y_\mu\right), \mu=1,\ldots,M\right\}$ of size $|Z|=M$, where $x=\left[\left(t_{-m+1}^\mu, g_{-m+1}^\mu\right),\ldots,\left(t_0^\mu, g_0^\mu\right)\right]$, $y=\left[\left(t_1^\mu, g_1^\mu\right),\ldots,\left(t_n^\mu, g_n^\mu\right)\right]$, t_0 denotes the time at which a prediction is made, $t_{-m+1}<\cdots<t_{-1}<t_0<t_1<\cdots<t_n$ and $\left|t_i^\mu - t_i^{\mu+1}\right|>1$ h such that samples in Z are could be considered as linearly independent. In particular, $f\left(x\right)$ is the minimizer of:

$$1/|Z|\sum_{\mu=1}^{|Z|}\left\| f\left(x_\mu\right)-y_\mu\right\|_{\left(\mathbb{R}^2\right)^n}^2+\lambda\left\| f\right\|_{RKHS_K}^2, \tag{3.5}$$

which, according to the Representer Theorem, is given by:

$$f\left(x\right)=\sum_{\mu=1}^{|Z|}c_\mu^\lambda K\left(x,x_\mu\right), \tag{3.6}$$

where λ is the regularization parameter. The vector of coefficients $c^\lambda=\left(\lambda|Z|I+\mathrm{K}\right)^{-1}$ y $c^\lambda=\left(\lambda|Z|I+\mathrm{K}\right)^{-1}$ y with I the $|Z|\times|Z|$ unit matrix, $\mathrm{K}=\left\{K\left(x_i,x_j\right)\right\}_{i,j=1}^{|Z|}$ is the Gram matrix and y=$\left(y_1,\ldots,y_{|Z|}\right)^T$. The set of admissible kernels is parameterized in terms of $\omega=\left(\alpha,\beta,\gamma\right)$ such that:

$$K\left(x_1,x_2\right)=\left(x_1,x_2\right)^\alpha+\beta\exp\left[-\gamma\left(x_1-x_2\right)^2\right]. \tag{3.7}$$

The learning process of the hyper-parameters of f (meta-learning) was divided into 3 phases: (i) the optimum kernel K^μ (i.e. ω_μ^o) and regularization parameter λ_μ^o are learnt for each sample $\left(x_\mu, y_\mu\right)$ (formulated as M regularized learning problems defined on $Z^{(\mu)}=\left\{\left(t_i^\mu, g_i^\mu\right), i=-m+1,\ldots,n\right\}$, $\mu=1,\ldots,M$), (ii) a two-dimensional meta-feature vector u_μ is computed for each x_μ, comprising the coefficients of the linear least squares fit from $\left(t_{-m+1}^\mu,\ldots,t_0^\mu\right)$ to $\left(g_{-m+1}^\mu,\ldots,g_0^\mu\right)$ (iii) the optimum kernel K and regularization parameter λ of f are learnt as a function of the vector $\mathbb{u}$ (formulated as a regularized learning problem defined on $Z'=\left\{\left(u_\mu,\omega_\mu^o\right),\mu=1,\ldots,M\right\}$). The optimization of the hyper-parameters of the

$M+1$ regularized learning problems was performed by partitioning the respective datasets into two mutually exclusive sets (training and validation sets) and minimizing, via grid search over ω, a functional accounting for the regularized loss as well as the validation error. Moreover, the regularization parameter λ was taken as a functional of K (i..e. $\lambda = \lambda(K) \in [\lambda_{\min}, \lambda_{\max}]$). The performance of the overall scheme was assessed using data from 2 clinical trials executed within the framework of the DIAdvisor project (Trial I: CGM data ($T = 10\,\text{min}$) from 9 type 1 or type 2 diabetes patients monitored over ~10 days; Trial II: CGM ($T = 5\,\text{min}$) and frequently sampled blood glucose data from 6 type 1 or type 2 diabetes patients monitored over 3 days). It should be stressed the abovementioned meta-learning procedure was applied only once for one particular patient ($n = m = 6$, $M = 24$, $T = 5\,\text{min}$). Regarding Trial I, the Clarke error grid analysis (EGA) revealed significantly higher percentages of predictions in Zones A and B for 30-, 60-, and 75-min prediction horizons as compared with two state of the art methods (AR- and neural network-based glucose prediction approaches [89, 114]). In addition, the prediction-error grid analysis (PRED-EGA), with reference the Yellow Spring Instruments (YSI) analyser blood glucose measurements from Trial II, showed that it may provide more accurate estimations as well as 1-step-ahead predictions of blood glucose concentration in the hypoglycaemic and hyperglycaemic ranges as compared with the specified CGM system (DExCom® SEVEN® PLUS, 2011).

Table 3.3 Adaptive Models of Short-Term Prediction of Subcutaneous Glucose Concentration in Diabetes

Study	Model	Input	Dataset	Prediction Performance		
Sparacino et al. [95]	AR Weighted recursive least squares with a forgetting factor equal to 0.5	CGM data	*Subjects:* Twenty eight people with type 1 diabetes *CGM Device:* Glucoday *Sampling Interval:* 3 min *Monitoring Period:* 48 h	*MSPE (mg dL^{-1})* 30 min: 353 (146, 924) 45 min: 1200 (480, 3690) *Median(10%, 90% percentiles)	*ESOD* 30 min: 35925 (6675, 302364) 45 min: 90780 (14543, 917982) *Median(10%, 90% percentiles)	*TL* *Positive Trends* 30 min: 2.15±15.63 min 45 min: 8.09±19.37 min *Negative Trends* 30 min: 2.35±13.03 min 45 min: 7.42±15.27 min
Finan et al. [115]	ARX Weighted recursive least squares	CGM data Meal and insulin modelling	*Subjects:* Six people with type 1 diabetes monitored in normal daily life conditions. They were administered Prednisone for 3 days. *CGM Device:* CGMS®, Medtronic Minimed Inc. *Sampling Interval:* 5 min *Monitoring Period:* 2-8 days without the prednisone medication. 3 additional days with the prednisone medication	*FIT* 30 min: 65 % 60 min: 40 % 90 min: 19 %		*RMSE* 30 min: 27 mg dL^{-1} 60 min: 45 mg dL^{-1} 90 min: 61 mg dL^{-1}
Eren-Oruklu et al. [105]	ARMA Weighted recursive least squares with an adaptive forgetting factor	CGM data	*Subjects:* Fourteen people with type 2 diabetes monitored in normal daily life conditions *CGM Device:* System Gold™, Medtronic Inc. *Sampling Interval:* 5 min *Monitoring Period:* 48 h	*SSGPE* 30 min: 5.56±2.38 %		*RAD* 30 min: 3.83+1.63 %
				CG-EGA		
				Hypoglycaemia Accurate Readings 92.94% Benign Errors 5.29%	*Euglycaemia* Accurate Readings 91.50% Benign Errors 7.87%	*Hyperglycaemia* Accurate Readings 89.79% Benign Errors 8.70%
Eren-Oruklu et al. [106]	ARMAX Weighted recursive least squares with an adaptive forgetting factor	CGM data Physiological Data: Energy expenditure, average longitudinal acceleration, heat flux, GSR, near-body temperature	*Subjects:* Five people with type 2 diabetes monitored in normal daily life conditions *CGM Device:* MMT-7012, Medtronic Inc. *Sampling Interval:* 5 min *Monitoring Period:* 23.8±2.4 days	Univariate Model		Multivariate Model
				SSGPE 30 min: 8.81 %	*RAD* 30 min: 5.77±7.18 %	*SSGPE* 30 min:7.43 %	*RAD* 30 min: 4.24±5.14 %

Study	Model	Input	Dataset	Prediction Performance	
Turksoy et al. [107, 108, 116]	ARMAX in state-space form Constrained recursive least squares Real-time Kalman filtering	CGM data Insulin on board Energy expenditure and GSR	*Subjects:* Fourteen people with type 1 diabetes monitored in normal daily life conditions *CGM Device:* iPRO, Medtronic Inc. *Sampling Interval:* 5 min *Monitoring Period:* -	*RMSE* 15 min: 7.18 mg dL^{-1} 30 min: 18.55 mg dL^{-1} 60 min: 48.93 mg dL^{-1}	*SSGPE* 15 min: 3.84 % 30 min: 9.91 % 60 min: 26.08 %
Bayrak et al. [117]	AR Recursive partial least squares Real-time Savitzky-Golay filter	CGM data	*Subjects:* Seventeen people with type 1 diabetes *CGM Device:* Guardian RT, Medtronic Inc. *Sampling Interval:* 5 min *Monitoring Period:* -	*RMSE* 10 min: 1.78 mg dL^{-1} 20 min: 4.32 mg dL^{-1} 30 min: 7.79 mg dL^{-1} 40 min: 11.84 mg dL^{-1} 50 min: 15.92 mg dL^{-1}	*SSGPE* 10 min: 1.66 % 20 min: 4.06 % 30 min: 7.35 % 40 min: 11.22 % 50 min: 15.19 %
Daskalaki et al. [112, 113, 118]	Ensemble Modelling 1) ARX with output correction module (cARX) Recursive least squares 2) RNN with real-time recurrent learning	CGM data Insulin infusion rate data	*Subjects:* Twenty three people with type 1 diabetes under SAP therapy monitored in normal daily life conditions *CGM Device:* Minimed CGM, Medtronic Inc. *CGM Sampling Interval:* 5 min *Monitoring Period:* Training Set 5.30±1.40 days Evaluation Set 4.83±1.80 days	cARX	RNN
				RMSE 15 min: 16.8 mg dL^{-1} 30 min: 27.7 mg dL^{-1} 45 min: 37.0 mg dL^{-1}	*RMSE* 15 min: 11.9 mg dL^{-1} 30 min: 18.9 mg dL^{-1} 45 min: 26.1 mg dL^{-1}
				TL 15 min: 5 min 30 min: 15 min 45 min: 30 min	*TL* 15 min: 5 min 30 min: 10 min 45 min: 20 min
				Correlation Coefficient 15 min: 0.96 30 min: 0.90 45 min: 0.82	*Correlation Coefficient* 15 min: 0.98 30 min: 0.94 45 min: 0.90
Naumova et al. [101]	Regularized kernel learning Meta-learning approach to choosing a kernel and a regularization parameter	CGM data	Six people with type 1 diabetes under a hospitalized setting CGM Device: DexCom CGM Sampling Interval: 5 min Blood Glucose Device: Yellow Springs Instrument	*Clarke EGA*	
				Zone A (%) 30 min: 91.3 60 min: 75.14 75 min: 68.77	*Zone B (%)* 30 min: 8.51 60 min: 24.13 75 min: 29.97	*Zone D (%)* 30 min: 0.19 60 min: 0.54 75 min: 0.82
				PRED-EGA *(with reference to blood glucose measurements)*	

Study	Model	Input	Dataset	Prediction Performance			
				Hypoglycaemia Accurate Readings 10 min:90.82 % 20 min: 81.75 % Benign Errors 10 min:5.16 % 20 min: 5.16 %	*Euglycaemia*: Accurate Readings 10 min: 82.96 % 20 min: 82.11 % Benign Errors 10 min: 13.05 % 20 min: 16.08 %	*Hyperglycaemia* Accurate Readings 10 min:90.52 % 20 min: 90.81 % Benign Errors 10 min:4.14 % 20 min: 1.33 %	
Wang et al. [109]	Time-varying state-space model Extended Kalman Filter	CGM data FIR modelling of subcutaneous insulin absorption and meal absorption	*Subjects:* Five people with type 1 diabetes using insulin pump monitored in normal daily life conditions *CGM Device:* Minimed CGM MMT-7102, Medtronic Inc. *Sampling Interval:* 5 min *Monitoring Period:* 60.4±10.6 hours	R^2 0.71±0.19	*RAD* 20.31±10.44 %	*Time Gain (min)* 12.00±10.37 mn	*J* 377.93±644.32

RAD: Relative absolute deviation; EGA: Error grid analysis.

3.5 Prediction of Hypoglycaemia

The precise prediction of the short-term course of subcutaneous glucose concentration may contribute significantly to the prevention of hypoglycaemic events in the daily management of insulin-treated diabetes. The hypoglycaemia prediction problem has been addressed through linear system identification or machine learning regression or classification models, which exploit the recent CGM profile of the patient in conjunction with information on the insulin therapy or his/her behaviour (e.g. meals, physical activity). Physiological signals linked to autonomic and central nervous system activation in response to a hypoglycaemic excursion [i.e. GSR, electrocardiogram (ECG), electroencephalogram] have been also exploited towards hypoglycaemia detection or prediction [11, 119]. Nevertheless, the non-specificity of GSR- and ECG-related features to hypoglycaemia (e.g. increase in perspiration or heart rate) together with the effect of HAAF necessitate properly fusing them with blood or subcutaneous glucose concentration data, aiming at reducing the false positive predictions.

3.5.1 Hypoglycaemia Prediction as a Regression Problem

The assessment of the predictive capacity of a glucose prediction model in the hypoglycaemic region can be implemented either in a sample- or an event-based manner. *Table 3.4* reports regression models which were evaluated with respect to their ability to predict single hypoglycaemic concentration values. Both CG-EGA and PRED-EGA enable the classification of individual predictions of subcutaneous glucose concentration as accurate readings (AR), benign errors (BE) or erroneous reading (ER) separately for the hypoglycaemic ($\leq$70 mg dL^{-1}), the euglycaemic (71-180 mg dL^{-1}) and the hyperglycaemic (>180 mg dL^{-1}) glucose ranges, taking into account the result of the point-error and rate-error grid analyses as well as the clinical impact of the consequent treatment decisions. For instance, in Naumova et al. [101], PRED-EGA characterized 90.89%, 90.82%, and 81.75% of the predictions in the hypoglycaemic range as accurate for 0-, 10-, and 20-min prediction horizons, respectively, with reference to blood glucose samples by the YSI analyser. Each individual prediction can be also characterized as true positive (TP) with regard to the corresponding actual glucose concentration value if both fall in the hypoglycaemic region, which, in turn, allows the computation of classical metrics of the performance of a model (e.g. accuracy, sensitivity, specificity, false positive rate) [120]. On the other hand, the problem of hypoglycaemic event prediction concerns the early prediction of the onset of the event [121, 122]. We focus on

methods treating the problem of hypoglycaemia prediction as an event prediction problem, emphasising on the definition of a hypoglycaemic event, the inference of a predictive warning and the evaluation of a TP event (*Table 3.5*).

Weighted recursive least squares, with an adjustable forgetting factor, was used for the identification of ARMA models of subcutaneous glucose dynamics in diabetes [107, 123]. Eren-Orukle et al., having set the hypoglycaemic threshold to 60 mg·dL^{-1}, defined a hypoglycaemic event as at least two consecutive (i.e. ≥10 min) blood glucose concentration measurements ≤60 mg·dL^{-1}, and denoted its end by a blood glucose value >65 mg·dL^{-1} [123]. In this context, three different approaches to hypoglycaemic alarm generation were proposed: (i) Absolute Predicted Value: A hypoglycaemic alarm was issued at time t_i if the *p*-step-ahead prediction of subcutaneous glucose concentration $\hat{y}\left(t_i + pT \middle| \theta\right)$ was <60 mg·dL^{-1}, (ii) Cumulative Sum Control Chart (CUSUM): A hypoglycaemic alarm was issued at time t_i if the lower control limit of the CUSUM, $C_i^- = \max\left[0, \left(\mu_0 - K\right) - \hat{y}\left(t_i + pT \middle| \theta\right) + C_{i-1}^-\right]$, exceeded a certain threshold value $\approx 5\sigma$, where $C_0^- = 0$, $K = \left|\mu_1 - \mu_0\right|/2$, $\mu_0 = 65\ \text{mg}\cdot\text{dL}^{-1}$ and $\mu_1 = 60\ \text{mg}\cdot\text{dL}^{-1}$ are the target mean glucose concentration value and the out-of-control mean glucose concentration values, respectively, and $\sigma = 1\ \text{mg}\cdot\text{dL}^{-1}$ is the standard deviation of the glucose signal, and (iii) Exponentially Weighted Moving-Average (EWMA) Control Chart: A hypoglycaemic alarm was issued at time t_i if $z_i = \lambda\hat{y}\left(t_i + pT \middle| \theta\right) + \left(1-\lambda\right)z_{i-1}$, with $z_0 = \mu_0 = 65\ \text{mg}\cdot\text{dL}^{-1}$ and centreline equal to μ_0, crosses the lower control limit $LCL_i = \mu_0 - L\sigma\sqrt{\lambda/\left(2-\lambda\right)\left[1-\left(1-\lambda\right)^{2i}\right]}$, where the parameter $L = 5$ determines the width of control limits and $\lambda = 0.8$ ($0 \le \lambda \le 1$). The method was assessed on 54 subjects with type 1 diabetes who underwent an insulin-induced hypoglycaemia test (≤55 mg·dL^{-1}) during their short-term (24 hours) inpatient stay. Besides CGM, the blood glucose concentration was also measured at regular intervals, i.e. every 60 min during the day, every 30 min during the night and every 5 min during the hypoglycaemic event. A TP prediction was considered when the alarm had been issued 45 min at most before a true hypoglycaemic event, as assessed by the reference blood glucose measurements, and an FP prediction was considered when an alarm had been incorrectly issued during a non-hypoglycaemic period or it had been issued >45 min before the event. A sensitivity 89%, a false positive rate 11% and a detection time (the time

interval between the start of the alarm and the start of the hypoglycaemic event) 27.7±5.32 min were reported for the EWMA control chart method.

As it is described in 3.4.1, physiological signals related to a subject's physical activity or emotional condition (i.e. EE, GSR) as well as information on insulin regime (i.e. insulin on-board) complemented the input of a recursive ARMA model and, in conjunction with physiological constraints imposed to model parameters, led to stable accurate short-term (30-min ahead) predictions of the subcutaneous glucose concentration [107]. In particular, Turksoy et al. defined a hypoglycaemic event as successive subcutaneous glucose concentration values ≤70 mg·dL^{-1}, with sequences of hypoglycaemic values being separated by ≥2 non-hypoglycaemic values being considered two discrete events. An alarm was immediately issued when the current subcutaneous glucose concentration value or its 1-step-ahead (i.e. 5 min) prediction were below the defined hypoglycaemic threshold (70 mg·dL^{-1}). Otherwise, the algorithm examined if the $p>1$-step-ahead-predictions of subcutaneous glucose concentration cross the hypoglycaemic threshold and, accordingly, alerts the patient. The predictive alarm system became more sensitive to nocturnal or post exercise hypoglycaemic events by increasing the threshold to 80 mg·dL^{-1} based on information provided by the SenseWear® Armband (BodyMedia Inc.) physical activity monitor. Similarly to [123], an alarm followed by a true event in the next 60 min signified a TP prediction. On average, a sensitivity 0.815 accompanied with a false positive rate 0.343 and a detection time 29.06 min were obtained for a dataset of 12 subjects with type 1 diabetes who had been observed in real-life conditions.

Daskalaki et al. constructed an ensemble predictive modelling scheme of hypoglycaemia in type 1 diabetes by linearly combining the output of the two online adaptive models presented in 3.4.2, i.e. the ARX model with the output correction module and the RNN model; the output of the ensemble model was given as the linear combination of the outputs $\hat{y}^{(1)}$ and $\hat{y}^{(2)}$ of the individual models, $\hat{y}=a\hat{y}^{(1)}+(1-a)\hat{y}^{(2)}$, with $a\in[0,1]$ [112, 113, 118]. The definition of a hypoglycaemic event encompassed the occurrence of ≥2 (i.e. ≥10 min) consecutive subcutaneous glucose concentration measurements below 70 mg·dL^{-1}. A hypoglycaemic alarm was inferred if: (i) the current glucose value was within the euglycaemic range, (ii) the 15-min-ahead or at least one of the 30- or 45-min-ahead predictions were within the hypoglycaemic range, and (iii) the event was predicted for the first time. The maximum acceptable time distance between the issued alarm and the start of the event, which also defined

TP predictions, was set equal to the largest prediction horizon examined by the authors, i.e. 45 min. Both ARX and RNN models were individually trained and tested on data from 23 patients with type 1 diabetes under SAP and during everyday living conditions; the first half of the data was used in model identification and the second one in model testing. The selection of the parameter $a \in [0,1]$ was based on the maximization of a heuristic function of the TP predictions, the detection time and the false alarms over the training set. A perfect sensitivity [100.0% (100.0-100.0)] was achieved, which was complemented by a detection time of 16.7 min (10.0-25.0) and 0.8 daily false alarms (0.0 -1.2) (the median and the 5^{th} - 95^{th} percentiles were given for each metric).

3.5.2 Hypoglycaemia Prediction as a Classification Problem

A retrospective analysis of CGM data, relying on support vector machines classification, was proposed as a complementary procedure to CGM calibration algorithms–[124, 125]. In particular, Jensen et al. treated the problem of hypoglycaemia detection as a 2-class problem, with hypoglycaemia being defined as a plasma glucose ≤ 70 mg·dL^{-1} and non-hypoglycaemia as a plasma glucose >70 mg·dL^{-1}. A ≥30 min subsequent period with no plasma glucose ≤ 70 mg·dL^{-1} signified the end of the event. A candidate set of 2289 features, formed by using CGM measurements in the time interval $[t_i - 120, t_i + 120]$, was tested for its discriminative ability with respect to the classification of the subcutaneous glucose concentration at time t_i. A feature selection method based on principal component analysis was used to confine the input size, whereas SVR training was performed in parallel with a forward selection procedure in a leave-one-subject-out cross-validation mode. In total, seven features were retained: 1) the current subcutaneous glucose concentration value, 2) the linear regression of CGM values in the interval $[t_i - 60, t_i + 5]$, 3) the kurtosis of CGM values in the interval $[t_i - 5, t_i + 115]$, 4) the time since last insulin injection, 5) the kurtosis of CGM values in the interval $[t_i - 50, t_i + 15]$, 6) the kurtosis of CGM values in the interval $[t_i - 70, t_i]$, and 7) the skewness of CGM values in the interval $[t_i - 120, t_i - 60]$. A minimum of four consecutive subcutaneous glucose values being classified as hypoglycaemic define a detected event, whereas a TP prediction requires at least one of them be confirmed by a plasma glucose measurement ≤70 mgdL^{-1}. The study population consisted of 10 subjects with type 1 diabetes, who underwent an insulin induced

hypoglycaemia test during which capillary blood samples were drawn every 10 min; otherwise, every 30-60 min. Moreover, patients were equipped with a CGM system (Guardian® RT CGM, Medtronic). A 100% sensitivity with 1 FP showed a significant improvement over CGM alone (63% sensitivity with 0 FP) or an optimized calibration algorithm (89% sensitivity with 2 FP), which had been shown to improve the accuracy (i.e. MARD) of the Guardian® RT CGM system in all glycaemic ranges.

Cichosz et al. tested the hypothesis that the integration of ECG and CGM data could enhance the early detection of a hypoglycaemic event as compared to a CGM system [126, 127]. A two-class problem was defined, where each input vector x^i in the dataset $Z = \left\{\left(x^i, y_i\right)\right\}_{i=1}^{N}$ is classified as $y_i \in \left\{C_{non-hypo}, C_{hypo}\right\}$ based on the reference blood glucose measurement at time t_i. The RR intervals in the ECG signal were grouped in epochs of 5 min and the Heart Rate Variability (HRV) in each epoch was analysed using time domain, frequency domain and non-linear measures. A number of features were extracted by combining HRV measures of different epochs prior to t_i using a set of typical statistical operators i.e. differentiation, average, slope standard deviation, skewness, and ratio. In addition, a confined set of features was extracted from CGM measurements 0-30 min prior to t_i, i.e. the subcutaneous glucose concentration at $gl\left(t_i\right)$, the difference $gl\left(t_i\right) - gl\left(t_i - 30\right)$, the slope of all CGM measurements in the interval $\left[t_i - 30, t_i\right]$ and the slope relative to the current reading. The classification framework encompassed feature ranking, based on class separability criteria (i.e. receiver operating characteristic (ROC) curve) and their intercorrelation, followed by a forward selection procedure in conjunction with a binary linear logistic regression classifier. Frequent blood glucose measurements (every 10 min) were obtained during an insulin-induced hypoglycaemia test from ten patients with type 1 diabetes, who were continuously monitored (Guardian RT CGM, Medtronic Inc; ECG Lead II) in a hospital-setting for two days. A leave-one-patient-out cross-validation showed that single blood glucose values below 70 mg·dL^{-1} were predicted 1-step-ahead (i.e. 10 min) with a specificity comparable to that of the CGM (0.99 vs. 0.98), a considerably higher sensitivity than CGM (0.79 vs. 0.33) and a total area under the ROC curve (AUC) 0.98. In addition, hypoglycaemic events, being defined as ≥2 consecutive low (<70 mg·dL^{-1}) blood glucose concentration levels, were all correctly detected, compared to sensitivity 0.75 provided by CGM, without any FP predictions. Most importantly,

the time difference between the onset of the detected event and the nadir blood glucose of a TP event was improved from 0±11 to 22±11 min. In a subsequent study, Cichosz et al. studied the performance of the developed algorithm in the prediction of spontaneous hypoglycaemic events in free-living conditions, using a dataset of 21 patients with type 1 diabetes collected over a 3-day monitoring period [127]. Single vein plasma glucose and self-monitoring blood glucose (SMBG) measurements below 70 $mg \cdot dL^{-1}$ were used as reference hypoglycaemic values in order to locate hypoglycaemic events into CGM time series, which means that the precise start of the event is not known. Different prediction horizons were examined ranging from 0 to 30 min; for a prediction horizon of 20 min, the model yielded a ROC AUC 0.96 with sensitivity 100% and specificity 91%.

Table 3.4 Hypoglycaemia Prediction Methods evaluated in a Sample-based Mode

Study	Model	Input	Dataset	Prediction Performance	
Zarkogianni et al. [97]	Self-Organizing Map Hypoglycaemic Threshold: 70 mg dL^{-1}	CGM data Physical activity: Energy expenditure	*Subjects:* Ten people with type 1 diabetes monitored in normal daily life conditions *CGM Device:* Guardian RT, Medtronic Inc. *Sampling Interval:* 5 min *Monitoring Period:* 6 days	Case 1 *CG-EGA Hypoglycaemia* 30 min: AR 91.1 % BE 2.4 % ER 6.5 % 60 min: AR 78.5 % BE 2.5 % ER 19.0 % 120 min: AR 56.4 % BE 2.1 % ER 41.5 %	Case2 *CG-EGA Hypoglycaemia* 30 min: AR 89.1% BE 0.9 % ER 10.0 % 60 min: AR 76.7% BE 1.2 % ER 22.1 % 120 min: AR 58.8% BE 1.2 % ER 40.0 %
Eren-Oruklu et al. [105]	ARMA Weighted recursive least squares with an adaptive forgetting factor Hypoglycaemic Threshold: 70 mg dL^{-1}	CGM data	*Subjects:* Fourteen people with type 2 diabetes monitored in normal daily life conditions *CGM Device:* System Gold™, Medtronic Inc. *Sampling Interval:* 5 min *Monitoring Period:* 2 days	*CG-EGA Hypoglycaemia* 30 min: AR 92.94 % BE 5.29 % ER 1.77 %	
Eren-Oruklu et al. [106]	ARMAX Weighted recursive least squares with an adaptive forgetting factor Hypoglycaemic Threshold: 60 mg dL^{-1}	CGM data Physiological Data: Energy expenditure, average longitudinal acceleration, heat flux, GSR, near-body temperature	*Subjects:* Five people with type 2 diabetes monitored in normal daily life conditions *CGM Device:* MMT-7012, Medtronic Inc. *Sampling Interval:* 5 min *Monitoring Period:* 23.8±2.4 days	*Sensitivity* 30 min: 74 % *False Discovery Rate* 30 min: 31 %	
Wang et al. [102, 109]	Time-varying state-space model Extended Kalman Filter Hypoglycaemic Threshold: 70 mg dL^{-1}	CGM data FIR modelling of subcutaneous insulin absorption and meal absorption	*Subjects:* Five people with type 1 diabetes using insulin pump monitored in normal daily life conditions *CGM Device:* Minimed CGM MMT-7102, Medtronic Inc. *Sampling Interval:* 5 min *Monitoring Period:* 60.4±10.6 hours	*Sensitivity* 30 min: 78.71±7.26 % *False Discovery Rate* 30 min: 35.60±9.61 % *Detection Time* 30 min: 12.00±10.37 min	

Study	Model	Input	Dataset	Prediction Performance
Naumova et al. [101]	Regularized kernel learning Meta-learning approach to choosing a kernel and a regularization parameter Hypoglycaemic Threshold: 70 mg dL^{-1}	CGM data	*Subjects:* Six people with type 1 diabetes under a hospitalized setting *CGM Device:* DexCom *CGM Sampling Interval:* 5 min *Blood Glucose Device:* Yellow Springs Instrument *BG Sampling Interval:* 5-10 min for specific time periods resulting in 120 blood samples per patient *Monitoring Period:* 3 days	*PRED-EGA* (with reference to blood glucose measurements) 0 min: AR: 90.89 %, BE: 4.94 %, ER: 4.17 % 10 min: AR: 90.82 %, BE: 5.16 %, ER: 4.02 % 20 min: AR: 81.75 %, BE: 5.16 %, ER: 13.09 %

Table 3.5 Hypoglycaemia Prediction Methods evaluated in an Event-based Mode

Study	Model	Input	Dataset	Prediction Performance		
Zhao et al [73, 86]	ARX, Model migration Hypoglycaemic Threshold: 70 mg dL^{-1} Event Definition Start: ≥3 consecutive s.c. glucose concentration values below or equal to 70 mg dL^{-1}. End: ≥3 consecutive s.c. glucose concentration values above 65 mg dL^{-1}	CGM data Second-order transfer function models of insulin and meal intake [84]	In-silico data / University of Virginia / University of Padova Simulator Sampling Interval: 5 min	*Sensitivity* 30 min: Adolescents:60.96 % Adults: 58.84 % Children: 74.92 %	*Specificity* 30 min: Adolescents: 99.65 % Adults: 99.59 % Children: 97.34 %	*TL* 30 min: Adolescents: 4.71±2.21 samples Adults: 5.00±2.24 samples Children: 3.59±2.45 samples
Eren-Oruklu et al. [123]	ARMA Weighted recursive least squares with an adaptive forgetting factor Hypoglycaemic Threshold: 60 mg dL^{-1} Event Definition Start: ≥2 consecutive (10 minutes or more) blood glucose measurements below or equal to the threshold value. End: Blood glucose concentration rises above 65 mg dL^{-1}	CGM data	*Subjects:* 54 people with type 1 diabetes monitored in a hospital setting [128, 129] *CGM Device:* CGMS™, Medtronic Inc. *Sampling Interval:* 5 min *Monitoring Period:* 1 day	Absolute Predicted Value *Sensitivity* 30 min: 89.0 % *Specificity* 30 min: 67.0 % *False Positive Rate* 30 min: 33.0 % *False Discovery Rate* 30 min: 15.0 %	Cumulative-Sum *Sensitivity* 30 min: 87.5 % *Specificity* 30 min: 74.0 % *False Positive Rate* 30 min: 26.0 % *False Discovery Rate* 30 min: 12.5 %	Exponentially Weighted Moving-Average Control Chart *Sensitivity* 30 min: 89.0 % *Specificity* 30 min: 78.0 % *False Positive Rate* 30 min: 22.0 % *False Discovery Rate* 30 min: 11.0 %

Study	Model	Input	Dataset	Prediction Performance		
				Detection Time 30 min: 30.00±5.51 min	*Detection Time* 30 min: 25.80±6.46 min	*Detection Time* 30 min: 27.7±5.32 min
Turksoy et al. [107, 108, 116]	ARMAX in state-space form Constrained recursive least squares Real-time Kalman filtering Hypoglycaemic Threshold: 70 mg dL^{-1} Event Definition Start: ≥1 consecutive s.c. glucose concentration values below or equal to 70 mg dL^{-1}. End: ≥1 consecutive s.c. glucose concentration values above 70 mg dL^{-1}	CGM data Insulin on board Energy expenditure and GSR	*Subjects:* Fourteen people with type 1 diabetes monitored in normal daily life conditions *CGM Device:* iPRO, Medtronic Inc. *Sampling Interval:* 5 min *Monitoring Period:* -	*Sensitivity* 30 min: 0.78±0.16 *False Positive Rate* 30 min: 0.37±0.06 *Detection Time* 30 min: 32±3.34 min		
Bayrak et al. [117]	AR Recursive partial least squares Real-time Savitzky-Golay filter Event Definition Start: ≥1 consecutive s.c. glucose concentration values below or equal to 70 mg dL^{-1}. End: ≥1 consecutive s.c. glucose concentration values above 70 mg dL^{-1}	CGM data	*Subjects:* Seventeen people with type 1 diabetes *CGM Device:* Guardian RT, Medtronic Inc. *Sampling Interval:* 5 min *Monitoring Period:* -	*Sensitivity* 30 min: 0.86 *False Positives / Day* 30 min: 0.42 *Detection Time* 30 min: 25.25 min		
Daskalaki et al. [112, 113, 118]	Ensemble Modelling 1) ARX with output correction module; Recursive least squares 2) RNN with real-time recurrent learning Hypoglycaemic Threshold: 70 mg dL^{-1} Event Definition Start: ≥2 consecutive s.c. glucose concentration values below or equal to 70 mg dL^{-1}.	CGM data Insulin infusion rate data	*Subjects:* Twenty three people with type 1 diabetes under SAP therapy monitored in normal daily life conditions *CGM Device:* Minimed CGM, Medtronic Inc. *CGM Sampling Interval:* 5 min *Monitoring Period:* Training Set 5.30±1.40 days Evaluation Set 4.83±1.80 days	*Correct Warnings* 100.0 (100.0-100.0) %* *Detection Time* 16.7 (10.0-25.0) min* *Daily False Alarms* 0.8 (0.0-1.2)* *Values are Median (5^{th} – 95^{th} percentiles)		

3.6 Contribution of the Thesis

3.6.1 A Multivariate Kernel-based Regression Model of Subcutaneous Glucose Concentration in Type 1 Diabetes

3.6.1.1 Status of the Literature

Linear identification of the underlying blood glucose regulation system, with or without extra inputs, had been met in a number of studies. Different linear time-invariant model structures, ranging from AR to state-space ones, combined with physiological models of the kinetics of subcutaneously administered insulin and glucose ingestion, provided a linear predictive framework to the approximation of the dynamics of the glucose system in both type 1 and type 2 diabetes, which was associated with reasonably accurate short-term (≤30 min) predictions.

Moreover, multivariate nonlinear, with respect to the input, regression techniques of machine learning, and, particularly, neural network-based regression models (e.g. FFNN and RNN) had been effectively applied to the identification and prediction of the subcutaneous glucose concentration in type 1 diabetes, and the potential for improved performance over 30-min horizon, as compared to AR approaches, was demonstrated. However, the input of such models was limited to past continuous measurements of the subcutaneous glucose concentration combined with quantitative information concerning the carbohydrates intake and/or the exogenous insulin administration. The inclusion of real-time physical activity data into predictive models had just emerged, which was considered very important given the prominent effect of exercise on blood glucose concentration. In addition, the real contribution of exogenous inputs to a specific model predictions had not been quantified in a systematic way.

3.6.1.2 Contribution of the Thesis

In [130], the problem of subcutaneous glucose concentration prediction in patients with type 1 diabetes was addressed, for the first time in the literature, in the context of SVR taking advantage of a multivariate dataset acquired under free-living conditions. In particular, we proposed an individualized predictive model relying on SVR of multiple input variables

concerning the recent subcutaneous glucose profile, the effect of food and insulin intake, the EE due to physical activities and the time of the day (as a predictor of the 24-h variations of glucose). Physiological models of the subcutaneous insulin absorption and the glucose absorption following oral ingestion were combined with the patient-specific predictive model of the subcutaneous glucose concentration. By utilizing different input cases, the effect of each input to the model's prediction error was quantified and, it was demonstrated that the availability of multivariable data and their effective combination can significantly improve the error of both short-term (i.e. for 15 min and 30 min) and long-term (i.e. for 60 min and 120 min) predictions.

3.6.2 Prediction of Hypoglycaemic Events under Free-Living Conditions

3.6.2.1 Status of the Literature

The prevention of hypoglycaemic events is of paramount importance in the daily management of insulin-treated diabetes. The use of short-term prediction algorithms of the subcutaneous glucose concentration may contribute significantly towards this direction. This specific problem had been dealt with through linear, time-invariant or adaptive, ARMA models, which had their predictive capability validated by hypoglycaemic clamp studies. The literature suggests that, although the recent glucose profile is a prominent predictor of hypoglycaemia, the overall patient's context greatly impacts its accurate estimation. Moreover, the effect of HAAF necessitates properly fusing blood or subcutaneous glucose data with information on medication (insulin therapy), behaviour (e.g. meals, physical activity) or physiological signals linked to autonomic nervous system activation in response to a hypoglycaemic excursion, aiming at reducing false positive predictions.

3.6.2.2 Contribution of the Thesis

Machine-learning techniques may efficiently represent the linear or non-linear effect of patient's contextual information (e.g. meals, insulin, exercise, sleep) on the subcutaneous glucose concentration, without requiring any *a priori* knowledge about the underlying glucose regulation dynamics, whereas they exhibit a very good generalization performance.

In [131], we extended the SVR-based model, which was presented in [130], to predict

separately the nocturnal hypoglycaemic events during sleep and the non-nocturnal (i.e., diurnal) ones over 30-min and 60-min horizons based on real-life data. In particular, we introduced new input variables accounting for recurrent nocturnal hypoglycaemia due to antecedent hypoglycaemia, exercise, and sleep (i.e. HAAF). We showed that hypoglycaemia prediction using SVR can be accurate and performs better in most diurnal and nocturnal cases compared with other techniques applied to the same data and task. Results suggested that the prediction of nocturnal hypoglycaemic events becomes more accurate when HAAF-related factors are additionally considered.

3.6.3 Evaluation of Short-Term Predictors of Glucose Concentration in Type 1 Diabetes Combining Feature Ranking and Regression Models

3.6.3.1 Status of the Literature

Literature suggested that nonlinear modelling of the short-term (≤30 min) and mostly long-term (>30min) subcutaneous glucose concentration is significantly more accurate as compared with linear, with respect to the input, approaches and, in addition, benefits from the utilization of particularly configured multivariate features sets. The majority of glucose prediction methods found in the literature were trained individually for each patient, which renders them as personalized solutions. However, their feature space was equally defined for all patients (e.g. by explicitly defining the embedding dimension for each input in order to model the glucose dynamics). The latter entails the specification of a high-dimensional input with the aim of fully capturing the temporal relationships between the input and the output, which, in turn, may compromise the generalization capability of the model. Given that linear regression methods are suited for learning *a priori* defined and fixed memory mappings of input-output data in a stationary environment, we presumed that feature evaluation can be included within the model development pipeline.

3.6.3.2 Contribution of the Thesis

In [134], we proposed feature ranking as a pre-processing step in the construction of patient-specific predictive models of the short-term subcutaneous glucose concentration in type 1 diabetes. Two well-established feature ranking algorithms suitable for regression problems, i.e.

RF and RReliefF, were employed for assessing, separately for each patient, the set of features defined in [130]. The generality and effectiveness of the feature ranking were examined with respect to the predictive performance of a kernel-based regression model (SVR or GP) by employing a forward selection procedure. Both feature evaluation algorithms produced rational, robust results revealing, whose quality was further verified by their noticeable contribution in short-term kernel-based predictive modelling of the subcutaneous glucose concentration. More specifically, the convergence of the error curves for feature subsets about half the size of the original feature set did confirmed that both feature ranking algorithms properly locate high in hierarchy the most predictive features of glucose concentration. The consequent reduction of the input size is of particularly important for regression analysis. Our results suggested that RF and RReliefF can find the most informative features and can be successfully used to customize the input of glucose predictive models.

3.6.4 Short-term Prediction of Glucose in Type 1 Diabetes Using Kernel Adaptive Filters

3.6.4.1 Status of the Literature

The feasibility of linear AR and moving average models, based primarily on weighted recursive least squares, to predict the short-term subcutaneous glucose dynamics in type 1 and 2 diabetes has been demonstrated. On the other hand, nonlinear adaptive learning of the glucose system, as one of the most promising research directions for implementing precision medicine in the self-management of diabetes, has been attempted so far through suboptimal solutions (i.e. extended Kalman filters) or real-time RNNs. In this context, novel nonlinear recursive frameworks to the online identification and prediction of the dynamic glucose system in type 1 diabetes can be evaluated. Targeting at a real-time AR or multivariate model, special emphasis should be placed on their time and space complexity in combination with their convergence behaviour and generalization capacity.

3.6.4.2 Contribution of the Thesis

In [132], we proposed KAF as a learning scheme for the nonlinear dynamical system of glucose. KAF are capable of handling nonlinearities by expressing all operations in terms of inner products in the RKHS sparsifying, in parallel, the solution online to confine the structure

of the underlying radial basis function (RBF) network and, consequently, accomplish regularization. Nonlinear regression was performed in a reproducing kernel Hilbert space, by either the fixed budget quantized kernel least mean square (QKLMS-FB) or the approximate linear dependency kernel recursive least squares (KRLS-ALD) algorithm, such that a sparse model structure is accomplished. We showed not only the feasibility of KAF to predict the short-term course of subcutaneous glucose concentration, but also that multivariate data improve systematically both the regularity and the TL of the predictions, reducing the errors in critical glucose value regions for a prediction horizon ≥30 min.

CHAPTER 4. MULTIVARIATE PREDICTION OF SUBCUTANEOUS GLUCOSE CONCENTRATION IN TYPE 1 DIABETES PATIENTS BASED ON SUPPORT VECTOR REGRESSION

4.1 Modelling Subcutaneous Glucose Concentration as a Support Vector Regression Problem

4.1.1 Introduction

The homeostatic regulation of glucose concentration in the blood stream is primarily controlled by the action of two pancreatic hormones, insulin and glucagon. Type 1 diabetes is caused by a cellular-mediated autoimmune destruction of the β-cells in the pancreas leading to absolute deficiency of insulin secretion and, consequently, to elevated blood glucose concentration [1]. The chronic hyperglycaemia of diabetes is associated with long-term microvascular (diabetic neuropathy, nephropathy and retinopathy) and macrovascular complications (coronary artery disease, peripheral arterial disease and stroke), rendering diabetes as a leading cause of morbidity and mortality worldwide. The use of IIT for the management of type 1 diabetes, based on multiple-dose insulin injections (3-4 daily injections) or CSII, leads to tight glycaemic control, which has been shown to reduce the incidence of diabetic complications [133]. Patients on IIT are more likely to experience hypoglycaemia; however, this side effect can be mitigated

by self-monitoring their blood glucose frequently throughout the day.

Recent advances in glucose monitoring technologies allow patients to measure the glucose concentration in the subcutaneous interstitial space continuously and, thus, patients can evaluate their individual response to therapy in a more efficient way [134]. However, achieving and maintaining tight glycaemic control in diabetes, necessitates the proper consideration of additional factors having a direct impact on subsequent blood glucose concentrations, such as nutrition, physical activity, patient's psychological status and his overall lifestyle [132, 135, 136]. In addition, the endogenous processes involved in the regulation of glucose homeostasis, for which there is scientific evidence that exhibit circadian rhythms [137, 138], as well as the prominent intra- and inter-patient variability in response to therapy [139-141] render glucose control in type 1 diabetes a rather difficult procedure. To this end, medical care in diabetes can be enhanced by the development of computational models of glucose metabolism, which offer the potential to predict the blood glucose response to various stimuli. Such predictive models can provide advanced knowledge of abnormal glycaemic variations facilitating the appropriate patient reaction in crucial situations, such as asymptomatic hypoglycaemia.

Considerable research efforts have been reported towards the development of mathematical models suitable for simulating the physiology of healthy blood glucose metabolism as well as the pathophysiology of type 1 diabetes [142, 143]. In particular, linear compartmental models, which are a class of dynamic models based on mass conservation principles, have been mainly used for studying the underlying processes involved in the regulation of blood glucose. Despite the fact that new important quantitative knowledge has been gained on glucose metabolism and control by insulin [79, 144, 145], the predictive capability of compartmental models is still limited due to the inherent complexity of the glucose-insulin system. On the other hand, data-driven modelling techniques are able to predict the glucose concentration by utilizing only the information hidden in the input-output data, without needing a priori knowledge about the relationship between them. Neural network models for predicting the time course of the blood glucose concentration in subjects with type 1 diabetes, have been investigated in a number of studies [77, 146, 147]. In those studies, the predictive models were evaluated using discrete blood glucose measurements, which were recorded three or more times daily. Nevertheless, CGM provides significant insight into glycaemic control giving rise to more accurate predictions of glucose concentration in the blood as well as in the subcutaneous interstitial fluid. In the latter case, the existent effect of the TL between blood and subcutaneous glucose, which ranges from 5 to 15 min [148], can be

mitigated using predictive models of sufficient long-term prediction horizon.

The fact that glucose prediction could be enhanced by exploiting the recent history of the CGM measurements was initially suggested by Bremer and Gough [104]. This has been further supported by other studies [70, 71, 95, 105, 149], which demonstrated that AR and ARMA models can provide accurate, short-term (up to 30 min) predictions of the subcutaneous glucose concentration in both type 1 and type 2 diabetes. In order to address the nonlinear behaviour of the subcutaneous glucose time series, Pérez-Gandía et al. [90] developed a neural network model based on the CGM values during the preceding 20 min, which however showed limited performance. The short-term predictive capability of these models can be partially justified by the fact that the auto-correlation function of the subcutaneous glucose measurements vanishes at about 30 min [91].

A predictive model that is able to represent and infer the response of the blood glucose metabolism to the exogenous inputs (e.g. carbohydrates intake, subcutaneous insulin administration, exercise) may allow predictions for longer horizons compared with AR models. Because of the intrinsic nonlinearity and nonstationarity of the glucose regulatory system [142], nonlinear regression techniques of machine learning, such as FFNNs and RNNs, and GP, have been efficiently used for predicting the subcutaneous glucose concentration in type 1 diabetes [114, 150, 151]. The results of these studies are highly dependent on the input which is used, which, in all cases, includes the past continuous measurements of the subcutaneous glucose concentration and quantitative information concerning the carbohydrates intake and the exogenous insulin administration. A more comprehensive feature set has been considered in [114] which encompassed qualitative descriptors of the lifestyle and the emotional status of the patient. Furthermore, in [151] the physical activity was taken into account by using real data recorded continuously throughout the observation days.

In this study, the problem of subcutaneous glucose prediction in patients with type 1 diabetes is addressed in the context of the SVR technique based on a multivariate dataset acquired under free-living conditions. SVR performs nonlinear regression based on the computation of a linear regression function in a high dimensional feature space where the input variables are mapped to with the aid of a kernel function. Considering that both exogenous and endogenous factors have been shown to be critical for the regulation of blood glucose, we examine 6 input cases. First, the predictions are made using only past continuous measurements of the subcutaneous glucose concentration (Case 1). In order to model the glucose dynamics

resulting from the insulin injections and the daily meals, the predictive model is enhanced with information regarding the plasma insulin concentration and, either the rate of appearance of meal-derived glucose in plasma alone (Case 2) or in combination with the total amount of exogenous glucose entering the systemic circulation (Case 3). The time of the day is additionally used as a predictor of the 24-hour variations of glucose (Case 4). In addition to the inputs of the two previous cases, the energy consumed during daily physical activities is utilized in Case 3 (to form Case 5) and in Case 4 (to form Case 6). We evaluate and compare the predictive accuracy of the SVR technique for each input case in relation to the prediction horizon. To our knowledge, this is the first systematic work which examines the effect of a number of factors on subcutaneous glucose prediction in people with type 1 diabetes with the aid of the SVR technique.

4.1.2 Subjects

Data from 27 type 1 diabetic subjects following multiple-dose insulin therapy were collected in the framework of an EU research project called METABO [152] from the participating clinical partners. The observation period of the study ranged from 5 to 22 days (average 13.42±3.69). The baseline characteristics of the patients and the daily average number of hypo/hyperglycaemic events as well as the average duration of them, as calculated for all patients together, are given in *Table 4.1*. Hypoglycaemia was defined as the event in which at least two consecutive subcutaneous glucose values are less than 60 $mg \cdot dL^{-1}$, whereas hyperglycaemia as the event in which at least two consecutive subcutaneous glucose values are larger than 180 $mg \cdot dL^{-1}$. Calculations were made with a 5-min measurement sampling which is that of the CGM system used in this study.

Each patient wore the Guardian® Real-Time CGM system (Medtronic Minimed Inc.), which records an average glucose value every 5 min. The patients were also equipped with the SenseWear® Armband (BodyMedia Inc.), which is a wearable body monitoring system acquiring body physiological signals from multiple-sensors. This system reports the EE of daily physical activities or exercise events every 1 min. Furthermore, information regarding the food intake (i.e. type of food, serving sizes and time) was recorded on a daily basis by the patients using a specially designed paper diary. The carbohydrate content of each meal was post-analysed by a dietician. Similarly, the daily insulin doses, types of insulin and injection times were recorded.

We split the 27 patients in 3 groups according to the type of information that was recorded since some patients either were not wearing the activity body monitoring system for a long period of time or were not systematically recording the meal/insulin intakes. In particular, group A includes 15 patients for whom we have all the information required, group B includes 5 patients for whom it was not possible to exploit activity data and, group C includes the remaining 7 patients for whom only the CGM signal was available.

Table 4.1 Dataset Characteristics

Patient Baseline Characteristics		**Descriptive Statistics of the Glucose Dataset**	
Gender		Average Hypoglycaemic Events Per Day	0.40 (0-2)
No. Female	12		
No. Male	15		
Age (y/o)		Average Duration of Hypoglycaemic Events (min)	43.10 (0-88.33)
Mean ± SD	43.5±13.4		
Range	19-72		
BMI (kg·m^{-2})		Average Hyperglycaemic Events Per Day	1.64 (0-3.36)
Mean ± SD	25±3.70		
Range	18.75–35.80		
HbA1c (%)		Average Duration of Hyperglycaemic Events (min)	129.30 (0-283.75)
Mean ± SD	7.07±1.11		
Range	5.20 – 8.50		

SD: Standard deviation
The values in parenthesis indicate min and max average values per patient.

4.1.3 The Proposed Method

The proposed method relies on the combination of compartmental models of the glucose-insulin regulatory system and a patient-specific predictive model of subcutaneous glucose concentration. The compartmental models are used to simulate (i) the absorption and, the kinetics and dynamics of subcutaneous administered insulin and (ii) the absorption of ingested carbohydrates. To learn the glucose metabolism of each specific patient and, consequently, to provide individualized predictions of the subcutaneous glucose concentration, we employ the SVR technique. The principal input variables of the glucose predictive model include: (1) the subcutaneous glucose measurements (*gl*), (2) the plasma insulin concentration (I_p), (3) the rate of exogenous glucose appearance in plasma (*Ra*), (4) the cumulative amount of exogenous glucose that appeared in the systemic circulation (*SRa*), (5) the hour of day from 1 to 24 (*h*) and, (6) the cumulative amount of the energy expended during physical activities or exercise (*SEE*).

The predicted subcutaneous glucose concentration at time $t+l$ assuming that t is the

current time and *l* is the prediction horizon, is expressed as a function $f : R^d \to R$ as follows:

$$f(x) = f(v_1, \ldots, v_n), \tag{4.1}$$

where each individual constituent v_i is associated with one of the input variables (i.e. *gl*, I_p, *Ra*, *SRa*, *h*, *SEE*) and the n $(1 \le n \le 6)$ denotes the number of the input variables used in the predictive model.

We model the time delays in glucose regulation process by considering the history of the input variables with respect to the time at which the prediction is made (i.e. *t*). More specifically, each input variable v_i in (4.1), except when $v_i = h$, is described by a finite length vector containing successive values within the time window $\left[t_{v_i} - \left(n_{v_i} - 1\right)\Delta t_{v_i}, t_{v_i}\right]$:

$$v_i = \left[v_i\left(t_{v_i} - \left(n_{v_i} - 1\right)\Delta t_{v_i}\right), \ldots, v_i\left(t_{v_i} - \Delta t_{v_i}\right), v_i\left(t_{v_i}\right)\right], \tag{4.2}$$

where t_{v_i} is the upper limit of the time window, Δt_{v_i} is the sampling period and the parameter n_{v_i} determines the length of the time window. Thus, the total size *d* (number of features) of the input x of the glucose predictive model is:

$$d = \sum_{i=1}^{n} n_{v_i}. \tag{4.3}$$

The value of t_{v_i} is equal to t or $t + l$ depending on whether the input variable v_i derives from the monitoring devices or the compartmental models, respectively. Furthermore, the parameter n_{v_i}, which physically shows the temporal effect of the input v_i on glucose, and the sampling period Δt_{v_i} are determined based on some observations as well as on theoretical and clinical results found in literature [70, 71, 90, 91, 105]. A detailed description of the different components of our method is given in the following subsections.

4.1.3.1 Insulin Model

We model the absorption kinetics of subcutaneous administered insulin according to a mechanical approach [153], which is able to describe the absorption of different insulin

formulations including rapid-acting (lispro, aspart), short-acting (regular), intermediate-acting (NPH) and long-acting (glargine) analogues of insulin. In this model the diffusion of insulin in the subcutaneous tissue was considered to be isotropic i.e. homogeneous and with rotational symmetry with respect to the injection site. In addition to the chemical relationship between insulin dimers and hexamers, a virtual insulin association state was introduced to explain the kinetics of long–acting insulin analogs. By assuming that only the dimeric form of insulin can be absorbed into the plasma with a rate proportional to its concentration, the exogenous insulin flow at time t, $I_{ex}(t)$ (U·min^{-1}), into the bloodstream is given by:

$$I_{ex}(t) = B_d \int_{V_{sc}} c_d(t,r)\, dV, \tag{4.4}$$

where B_d is the absorption rate constant, c_d is the dimeric insulin concentration in the subcutaneous tissue, V_{sc} is the complete subcutaneous volume and r is the distance from the injection site. The computation of the dimeric insulin concentration, c_d, requires the solution of a system of partial differential equations describing the overall insulin infusion process.

A compartmental model is used to simulate the dynamics of plasma insulin after a subcutaneous injection [154]. This model estimates the plasma insulin concentration, I_p, (uU·mL^{-1}), as follows:

$$\dot{I}_p = \frac{I_{ex}(t)}{V_d} - k_1 I_p(t) + k_2 I_h(t) + k_3 I_i(t), \tag{4.5}$$

where I_h and I_i are the insulin concentrations in the liver and the interstitial tissue, respectively, V_d is the plasma insulin distribution volume, and k_1, k_2 and k_3 are the rate constants of plasma, hepatic and interstitial insulin elimination, respectively. Given the lack of insulin production in pancreas on type 1 diabetes, the only input to this physiological model is the exogenous insulin flow, $I_{ex}(t)$, obtained by (4.4).

4.1.3.2 Meal Model

The rate of appearance of meal-derived glucose into the systemic circulation (Ra) is described by the model of Lehmann *et al.* [155]. Ra is determined by assuming a trapezoidal gastric emptying function, a single compartment for the intestine and a constant rate of intestinal

glucose absorption. The time interval for which the rate of gastric emptying function is constant and maximal is a function of the carbohydrate content of the meal, while the time intervals corresponding to the increase and the decrease of this trapezoidal function have a default value of 30 min. Thus, the amount of glucose in the gut at time t, q_{gut} (mg), following the ingestion of a meal, which contains D grams of glucose equivalent carbohydrates, and the rate of appearance of exogenous glucose in plasma are given as:

$$\dot{q}_{gut} = -k_{abs} q_{gut}(t) + G_{empt}(t, D), \tag{4.6}$$

$$Ra(t) = k_{abs} q_{gut}(t), \tag{4.7}$$

where k_{abs} is the intestinal absorption rate constant and G_{empt} (mg·min^{-1}) is the rate of gastric emptying.

4.1.3.3 Support Vector Regression

According to the SVR technique [156], the prediction function f in (4.1) is given by the following linear form:

$$f(x) = w^T \varphi(x) + b, \tag{4.8}$$

where $\varphi(x)$ denotes a fixed feature-space transformation, and *w* and *b* are the weight and bias parameters, respectively. A key feature of the SVR algorithm is solving nonlinear regression problems by mapping the training data x^j, with $j = 1, \ldots, N$ denoting the size of the training dataset, into a feature space φ where the relation between x^j and the target output y_j becomes linear. To obtain sparse solutions, an ε-insensitive loss function is utilized in which the error increases linearly with distance beyond the insensitive region. However, errors larger than $\pm\varepsilon$ are treated by introducing the slack variables ξ_j and ξ_j^* for each data point x^j. The optimization problem is defined as:

$$\text{Minimize} \quad C\sum_{j=1}^{N}\left(\xi_j+\xi_j^*\right)+\frac{1}{2}\|w\|^2,$$
$$\text{subject to} \quad \begin{cases} y_j \le f\left(x^j\right)+\varepsilon+\xi_j \\ y_j \ge f\left(x^j\right)-\varepsilon-\xi_j^*. \\ \xi_j,\xi_j^* \ge 0 \end{cases} \tag{4.9}$$

The constant C determines the trade-off between the flatness of the SVR function f (i.e. small *w*) and the amount up to which deviations larger than ε are tolerated. Solving the optimization problem, it is found that the prediction for a new point *x* can be made using:

$$f\left(x\right)=\sum_{j=1}^{N}\left(a_j-a_j^*\right)\kappa\left(x,x^j\right)+b, \tag{4.10}$$

where a_j, a_j^* are the Lagrange multipliers and the kernel function κ is used for computing the similarity between two input vectors x and x^j in the transformed space.

4.1.4 Impact of Input Variables on Glucose Prediction

One of the most crucial issues in machine learning techniques, as they apply to real problems, is the evaluation of the significance of the input variables. In the present work, 6 different cases are investigated in order to elucidate the predictive capability of each input variable regarding the prediction of subcutaneous glucose concentration in type 1 diabetes.

In the first case, denoted herein as Case 1, the prediction of subcutaneous glucose is made based only upon the past interstitial glucose profile (i.e. $n=1$). This implies that the effect of the external inputs has been already incorporated into the glucose concentration, and thus it is assumed that this information is sufficient to predict the future glucose values. More specifically, we simply utilize the measurements of the *gl* variable in the last 30 min with respect to the current time t and, therefore, the corresponding time window in (4.2) becomes $\left[t-\left(n_{gl}-1\right)\Delta t_{gl}, t\right]$ with $n_{gl}=7$ and $\Delta t_{gl}=5\,\text{min}$. This is in accordance with previous studies in diabetes demonstrating the existence of a strong dependency between glucose samples which are 30 or fewer minutes apart [70, 71, 90, 91, 105].

In the second case, denoted as Case 2, the I_p and the Ra variables are also added in

the input of the model (i.e. $n=3$). Since both variables reflect the human's body response to insulin and food intake, respectively, it is more efficient to use their values that expand up to the time for which the prediction is to be made i.e. $t+l$. The upcoming values of these variables within the time interval $[t,t+l]$ are computed by the compartmental models using the insulin and meal recordings until the current time t, provided that no future event (i.e. meal, insulin injection) will occur during the period $[t,t+l]$ which could alter the time course of these two signals. The latter assumption is valid since otherwise the prediction of subcutaneous glucose for the time $t+l$ would not be sensible. The time window for the I_p and the Ra variables is defined with respect to $t+l$ as $\left[t+l-\left(n_{v_i}-1\right)\Delta t_{v_i}, t+l\right]$ with $v_i = I_p$ or $v_i = Ra$, $n_{I_p} = n_{Ra} = 7$ and $\Delta t_{I_p} = \Delta t_{Ra} = 5\,\text{min}$, which means that we exploit their values within the last 30 min with respect to the time of prediction $t+l$.

In the third case, Case 3, a new variable, called SRa, providing information on the cumulative amount of exogenous glucose appeared in plasma during the last 90 min with respect to the time of prediction $t+l$, is additionally included in the input of the predictive model (i.e. $n=4$). Similar to the previous cases, the subcutaneous glucose concentration at time $t+l$ is assumed to depend on SRa values within the window $\left[t+l-\left(n_{SRa}-1\right)\Delta t_{SRa}, t+l\right]$ with $n_{SRa}=6$ and $\Delta t_{SRa}=15\,\text{min}$. Each value, SRa_i, for $i=0,\ldots,5$, in this vector expresses the amount of exogenous glucose absorbed during the time period $\left[t+l-90, t+l-\left(75-i\Delta t_{SRa}\right)\right]$ and is given by:

$$SRa_i = \sum_{\tau=t+l-90}^{t+l-\left(75-i\Delta t_{SRa}\right)} Ra(\tau). \tag{4.11}$$

There is experimental evidence from *in vivo* and *in vitro* studies on type 1 diabetes that the absorption time of meal-derived glucose into the systemic circulation lasts approximately 3 hrs after meal ingestion . In this study, we utilize the last 90 min of Ra assuming that the effect of its previous values is already reflected in the glucose signal.

The fourth case, Case 4, accounts for the circadian control of the daily glucose metabolism. The circadian clock has been reported to generate daily rhythms in plasma glucose concentrations by mediating cellular and physiological functions related to glucose

homeostasis (e.g. endocrine control, peripheral glucose uptake, hepatic glucose production) [137, 138]. On this basis, the h variable identifying the 24 hourly intervals in a day is added in the input of Case 3 in an attempt to capture the daily rhythms of blood glucose concentration (i.e. $n=5$ and $n_h=0$).

The last two cases, namely Case 5 and Case 6, result from the addition of information about physical activity to the input of Case 3 (i.e. $n=5$) and Case 4 (i.e. $n=6$), respectively. The moderate-intensity physical activities as well as more intense exercise events have been shown to stimulate the peripheral glucose uptake, thus being a potential risk factor for hypoglycaemia especially in subjects with type 1 diabetes [132, 136]. Using the same rationale as in Case 3, the physical activity is described by a vector, SEE, whose values (SEE_i) denote the EE during $\left[t-180,\ t-\left(170-i\Delta t_{SEE}\right)\right]$:

$$SEE_i = \sum_{\tau=t-180}^{t-\left(170-i\Delta t_{SEE}\right)} EE\left(\tau\right), \tag{4.12}$$

for $i=0,\ldots,17$ ($n_{SEE}=18$) and for $\Delta t_{SEE}=10\,\text{min}$. EE expresses the instantaneous EE provided by the SenseWear® Armband. Thus, the short-term effect of physical activities performed during the last 3 hrs on the subsequent glucose concentration levels is investigated.

4.1.5 Model Training and Evaluation

The proposed method is intended to build patient-specific glucose predictive models and, therefore, it is evaluated individually for each patient using the dataset acquired during the observation period. The dataset of each patient is transformed to a $N\times\left(d+1\right)$ matrix containing the whole set of features (i.e. $d=49$) and the predicted value of the subcutaneous glucose concentration. More specifically, each row in the matrix concerns a specific time instance t and provides the values within the time window $\left[t_{v_i}-n_{v_i}\Delta t_{v_i},\ t_{v_i}\right]$ for each input variable v_i, $i=1,\ldots,6$, as well as the subcutaneous glucose concentration at time $t+l$. Predictions are performed for four different values of prediction horizon l, i.e. 15, 30, 60 and 120 min. The dataset for each one of the 6 different cases is formed by keeping the columns they are associated with. It should be noted that Case 1 may be applied to all groups of patients, Cases 2-4 may be applied to groups A and B, whereas Cases 5-6 only to group A.

The total number of instances in the dataset, N, depends mainly on the length of observation period for each patient but also on the number of gaps in the sensor data. Ideally, the time difference between two consecutive rows in the dataset is 5 min, i.e. equal to the sampling time of subcutaneous glucose concentration. However, since our method requires a defined set of input features, when (i) some values of the *gl* variable within the time window $[t-30, t]$ are not available, or (ii) some sums SEE_i, for $i = 0,\ldots,17$, cannot be calculated due to gaps in the SenseWear Armband data, then the corresponding row is removed from the dataset (Condition A). The same also applies when the glucose concentration at time $t+l$ is not available (Condition B). In addition, if an event (i.e. food intake, insulin intake, moderate or intense exercise) occurs at the time interval $[t, t+l]$ then the corresponding row into the dataset is also deleted, because that training instance does not represent a rational mapping between the input and the output (Condition C). Actually, in this case, the subcutaneous glucose concentration at time $t+l$ depends not only on the configured input but also on these future events, which cannot be known in advance in real conditions so as to be incorporated in the model. The average percentages of data remaining in group A for 15, 30, 60 and 120 min prediction horizon are 81%, 74%, 61% and 43%, respectively. The corresponding percentages in group B are 90%, 84%, 72% and 52%, and in group C 96%, 94%, 92% and 86%. It is essential to notice that Conditions A and B are applied to all patient groups, while the Condition C is applied only to groups A and B and actually, for the latter, partially, due to the lack of physical activity data by the SenseWear® Armband. This justifies the greater reduction of the dataset in these groups compared with group C, which becomes more significant as the prediction horizon increases.

A 10-fold cross validation procedure is employed to evaluate the predictive performance of the SVR technique. It should be noted that all input data x^j, with $j = 1,\ldots,N$, were normalized between 0 and 1 prior to validation. The SVR is built with a Gaussian kernel and the hyper parameters *C*, ε and the kernel parameter γ are optimized using the differential evolution algorithm [157]. The fitness function for differential evolution algorithm is defined as the average RMSE of the 10-fold cross validation process as it is shown in (13):

$$RMSE_{10-fold} = \frac{1}{10}\sum_{k=1}^{10}\sqrt{\frac{1}{N_k}\sum_{j=1}^{N_k}\left(y_j - f\left(x^j\right)\right)^2}, \tag{4.13}$$

where N_k represents the size of k^{th} fold, y_j is the actual value of subcutaneous glucose

concentration associated with the input x^j and $f\left(x^j\right)$ is the glucose value computed by the SVR. In addition, the three dimensional search space of the parameters is set as $C \in [0.001, 1024]$, $\varepsilon \in [0.0001, 1]$ and $\gamma \in [0.00001, 8]$.

The assessment of the predictive accuracy of the proposed method is based on the $RMSE_{10\text{-}fold}$ and on the correlation coefficient ($r_{10\text{-}fold}$) resulting from the 10-fold cross validation:

$$r_{10-fold} = \frac{1}{10}\sum_{k=1}^{10} r_k, \tag{4.14}$$

where r_k is the correlation coefficient regarding the k^{th} fold. The percentage of the successful hypoglycaemic (≤70 mg·dL^{-1}) and hyperglycaemic (≥180 mg·dL^{-1}) predictions [158] is also used to evaluate the proposed method. Besides differences in the values between the predicted and actual signals, another aspect of the prediction capability is the TL observed between them. This is estimated by using the approach proposed in [70] in which the TL is equal to the lag that yields the peak cross-correlation. We calculate the cross-correlation over segments of the two signals that are at least 120-min long. The TL between the two signals is calculated as the average of each segment's lag.

In addition, the CG-EGA [93, 149, 159] is used aiming to evaluate the clinical impact of the predictions in terms of both location and rate of change. This analysis defines three types of prediction errors (i.e. Accurate Readings, Benign Errors and Erroneous Readings) which are computed separately for each glucose range, namely for hypoglycaemia (≤70 mg·dL^{-1}), euglycaemia (71-180 mg·dL^{-1}) and hyperglycaemia (>180 mg·dL^{-1}).

4.1.6 Model Evaluation over the whole Glucose Range

4.1.6.1 Optimized SVR Parameters

The average value and the standard deviation of the parameters of SVR model (i.e. C, ε and γ) concerning group A, as derived from the differential evolution optimization algorithm, are given in *Table 4.2*. We observe that the three parameters are found in specific regions of the search space for each input case and prediction horizon; however, there exist considerable

inter-patient deviations. More specifically, it can be seen that the average values of parameter *C* in Cases 2-6 are significantly higher compared to Case 1 for both short-term (i.e. for 15 min and 30 min) and medium- to long-term (i.e. for 60 min and 120 min) predictions, which means that we obtain smoother predictions at the expense of increasing model's complexity. However, the values of *C* vary slightly among different prediction horizons. Regarding parameter ε, its average values show no prevalence trend with respect to the different input cases ranging between 0.32 and 0.57, except in Cases 1 and 2 for predictions of 15 min and 60 min, respectively, where ε is ≈0.7. Furthermore, we observe a substantial decrease in the average values of parameter γ in Cases 5 and 6, which also implies a better generalization ability of the SVR model in these cases. However, parameter γ increases with increasing prediction horizon showing that the SVR function becomes less smooth for longer predictions. Finally, the optimization results for groups B and C revealed no significant inter-group differences regarding Cases 1-4.

4.1.6.2 Assessment of Predictions

The average value of $RMSE_{10\text{-}fold}$ and $r_{10\text{-}fold}$ for the respective patient groups of each input case, and the corresponding standard deviation, are reported in *Table 4.3*. Regarding group A, it can be seen that the short-term predictions (i.e. for 15 min and 30 min) of the subcutaneous glucose concentration in Case 1 exhibit low error and a high degree of correlation with the observed ones. However, as expected, the prediction accuracy becomes considerably lower for medium- to long-term predictions (i.e. for 60 min and 120 min). The corresponding average time TLs were: 2.8, 7.8, 16.4, 25.8 min, respectively, which shows that the long-term predictions are not reliable. In Case 2, the SVR model yields 15-min and 30-min glucose concentration predictions with an average $RMSE_{10\text{-}fold}$ less than 10 mg·dL^{-1}, while, as the prediction horizon increases, it tends to be comparable with that of 30 min in Case 1. The inclusion of the *SRa* variable in

Table 4.2 Optimized Parameters of the SVR Glucose Predictive Model for Group A

	Prediction Horizon											
	15 min			30 min			60 min			120 min		
	C	e	γ	C	e	γ	C	e	γ	C	e	γ
Case 1	557.82 (255.96)	0.68 (0.24)	6.07 (2.45)	593.33 (326.57)	0.46 (0.33)	6.48 (1.54)	516.96 (274.67)	0.45 (0.29)	7.08 (2.02)	622.39 (346.46)	0.57 (0.33)	7.69 (0.70)
Case 2	801.27 (166.08)	0.33 (0.24)	4.48 (1.58)	986.58 (66.05)	0.47 (0.34)	7.50 (0.70)	953.05 (112.33)	0.69 (0.26)	7.91 (0.22)	983.41 (65.73)	0.39 (0.37)	7.93 (0.14)
Case 3	863.94 (186.85)	0.51 (0.32)	3.71 (1.68)	875.72 (197.68)	0.35 (0.21)	6.48 (1.28)	947.15 (114.77)	0.47 (0.35)	7.83 (0.38)	938.27 (124.89)	0.52 (0.35)	7.89 (0.24)
Case 4	861.07 (182.47)	0.42 (0.28)	3.26 (1.14)	839.81 (194.82)	0.50 (0.37)	6.22 (1.58)	880.29 (125.73)	0.51 (0.29)	7.28 (0.81)	954.92 (132.61)	0.46 (0.32)	7.87 (0.50)
Case 5	707.07 (217.32)	0.49 (0.25)	1.68 (0.63)	791.40 (157.37)	0.37 (0.25)	2.74 (0.91)	873.90 (169.41)	0.40 (0.31)	3.75 (1.73)	867.76 (211.22)	0.33 (0.30)	4.73 (2.48)
Case 6	801.49 (176.96)	0.51 (0.32)	1.53 (0.66)	875.63 (130.78)	0.32 (0.24)	2.58 (0.94)	791.80 (208.67)	0.47 (0.36)	3.34 (1.65)	850.48 (179.60)	0.48 (0.29)	4.74 (2.48)

Data are mean (standard deviation) values.

Table 4.3 Average Prediction Accuracy of the SVR Glucose Predictive Model for all Input Cases and for Different Patient Groups

	Prediction Horizon							
	15 min		30 min		60 min		120 min	
Case#	*RMSE*	*r*	*RMSE*	*r*	*RMSE*	*r*	*RMSE*	*r*
	Group A							
Case 1	9.05 (2.24)	0.98 (0.01)	15.29 (2.76)	0.95 (0.01)	24.19 (3.78)	0.87 (0.05)	33.04 (6.49)	0.72 (0.12)
Case 2	7.31 (1.74)	0.99 (0.00)	9.15 (1.88)	0.98 (0.01)	12.24 (2.89)	0.97 (0.02)	15.31 (4.27)	0.94 (0.04)
Case 3	6.55 (1.74)	0.99 (0.00)	8.24 (2.25)	0.99 (0.01)	10.55 (2.85)	0.97 (0.02)	13.43 (4.20)	0.95 (0.03)
Case 4	6.10 (1.83)	0.99 (0.00)	7.16 (2.01)	0.99 (0.01)	8.56 (2.23)	0.98 (0.01)	10.33 (2.99)	0.97 (0.02)
Case 5	5.35 (1.63)	0.99 (0.00)	6.38 (1.57)	0.99 (0.00)	7.82 (2.01)	0.99 (0.01)	8.57 (1.75)	0.98 (0.01)
Case 6	5.21 (1.58)	0.99 (0.00)	6.03 (1.67)	0.99 (0.00)	7.14 (1.84)	0.99 (0.01)	7.62 (1.81)	0.99 (0.01)
	Group B							
Case 1	9.56 (0.67)	0.98 (0.00)	16.60 (1.94)	0.95 (0.01)	27.51 (5.07)	0.86 (0.04)	37.56 (7.34)	0.72 (0.07)
Case 2	7.45 (1.21)	0.99 (0.00)	9.83 (1.39)	0.98 (0.01)	13.65 (2.48)	0.96 (0.02)	16.26 (3.33)	0.95 (0.03)
Case 3	6.92 (1.23)	0.99 (0.00)	8.66 (1.65)	0.99 (0.01)	11.90 (1.84)	0.97 (0.01)	14.28 (2.50)	0.96 (0.01)
Case 4	6.03 (0.94)	0.99 (0.00)	6.96 (1.04)	0.99 (0.00)	7.77 (1.57)	0.99 (0.00)	10.00 (2.01)	0.98 (0.01)
	Group C							
Case 1	10.44 (2.26)	0.97 (0.02)	17.30 (2.58)	0.92 (0.05)	26.73 (3.53)	0.81 (0.06)	37.45 (6.82)	0.57 (0.10)

Data are mean (standard deviation) values.

Case 3 contributes to a further reduction of the average $RMSE_{10\text{-}fold}$ by 14% for 60 min and 12% for 120 min, compared with Case 2. The results obtained for Case 4 show that the time alone, expressed through the *h* variable, is also a significant predictor of the subcutaneous glucose concentration. Nevertheless, the best predictions are obtained when introducing the *SEE* variable (Cases 5 and 6), with Case 6 resulting in an average prediction error less than 8 $mg \cdot dL^{-1}$ for all horizons. For Cases 2-6, the average $r_{10\text{-}fold}$, is close to 1 for all horizons. Regarding the TLs, the ranges were 1.6 – 6.5 min and 1.0 - 3.4 min for Case 2 and 3, respectively, with the lags increasing with the horizon, whereas for Cases 4-6, all TLs were shorter than 1 min. The actual vs. predicted glucose signals for Cases 1, 3 and 6 for 30-min and 60-min horizons can be seen in Figure 4.1 and Figure 4.2, respectively, for a patient during a day.

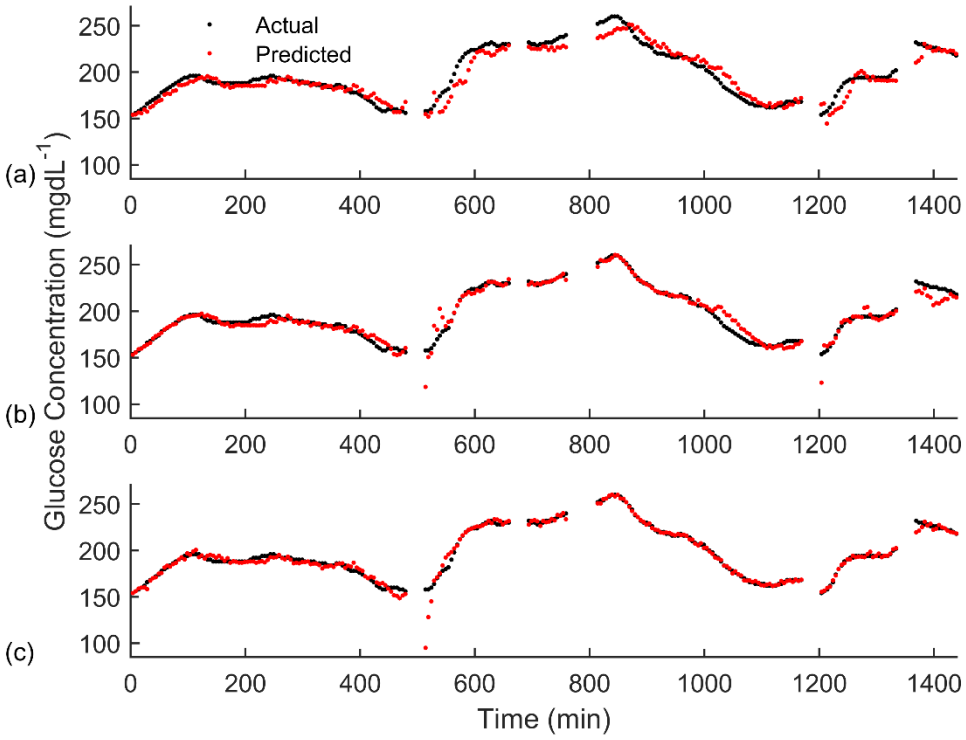

Figure 4.1 Predicted vs measured subcutaneous glucose concentration of a typical subject during one day for 30-min prediction horizon based on (a) Case 1, (b) Case 3 and (c) Case 6.

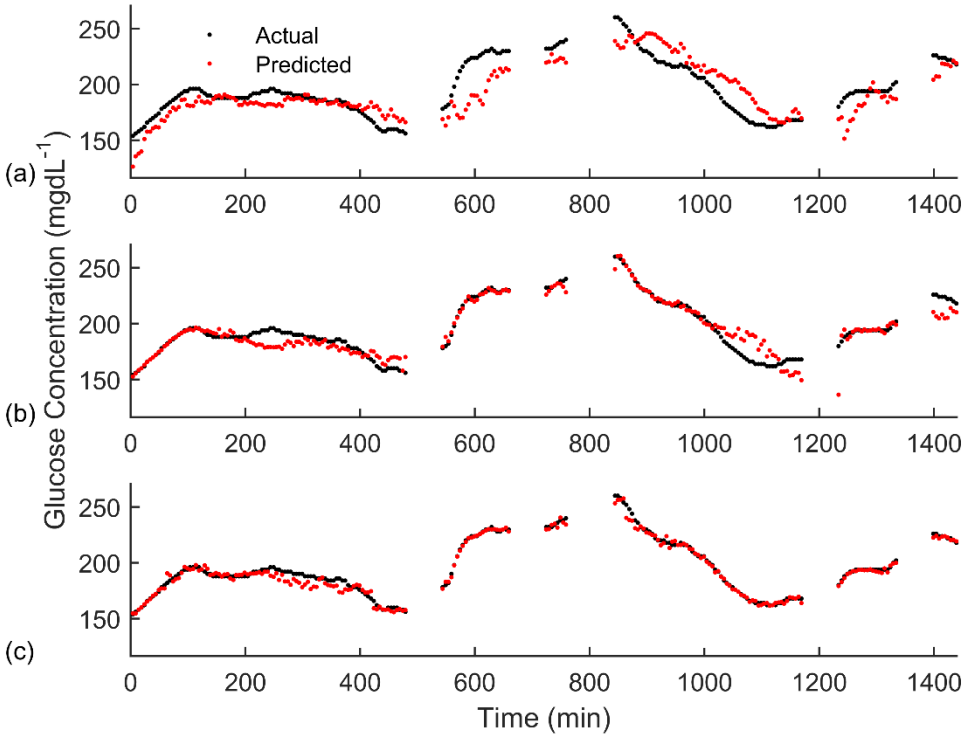

Figure 4.2 Predicted vs measured subcutaneous glucose concentration of a typical subject during one day for 60-min prediction horizon based on (a) Case 1, (b) Case 3 and (c) Case 6.

In critical glucose value regions, the percentage of successful predictions is gradually improved from Case 1 to 3. Particularly for Case 3, 89%, 85%, 76% and 70% of the values of group A are successfully predicted as hypoglycaemic, whereas 96%, 95%, 91% and 89% are successfully predicted as hyperglycaemic for each horizon, respectively. For Cases 4-6 the performance is further improved, although there are no systematic differences among them. Case 6 produces 91%, 87%, 83% and 85% successful hypoglycaemic predictions and 96%, 96%, 94% and 92% hyperglycaemic ones. In general, the percentages are higher when the glucose values are greater than 180 mg/dl, which is probably attributed to the existence of more hyperglycaemic instances in the dataset.

Table 4.4 contains the results of the CG-EGA concerning group A only for Cases 4 and 6. It can be observed that in both cases for all horizons more than 90% of the predictions are classified as clinically accurate or with benign errors (i.e. unlikely to lead to a negative outcome). The short-term predictions are more accurate in the hypoglycaemic range compared to the hyperglycaemic one, whereas the accuracy is decreased for hypoglycaemia as the horizon increases. Overall, Cases 4, 5 and 6 perform equally as regards this type of analysis, while Cases 1-3 are associated with higher erroneous predictions (CG-EGA results are not shown herein). The predictive behaviour of the model is also confirmed for groups B and C. Nevertheless, the results obtained for these groups should be interpreted with caution because of the free parameters (future meal/insulin intakes and physical activities) existing during the training-validation phase.

Table 4.4 CG-EGA of Predictions for Group A

	Prediction Horizon											
	15 min			30 min			60 min			120 min		
	AR	BE	ER	AR	BE	ER	AR	BE	ER	AR	BE	ER
Hypoglycaemia												
Case 4	96.76	2.00	1.24	94.56	2.56	2.88	92.16	2.74	5.09	87.63	4.50	7.88
Case 6	96.75	2.37	0.89	94.05	2.93	3.02	90.59	3.91	5.50	90.05	6.32	3.63
Euglycaemia												
Case 4	95.84	3.79	0.37	95.51	4.20	0.28	94.35	5.33	0.33	93.03	6.65	0.32
Case 6	96.56	3.16	0.29	95.80	3.91	0.29	94.93	4.81	0.25	93.57	6.24	0.20
Hyperglycaemia												
Case 4	89.68	6.09	4.23	88.20	7.76	4.04	86.45	9.53	4.02	84.85	11.03	4.12
Case 6	90.00	5.82	4.19	89.28	6.57	4.15	87.45	8.75	3.81	83.29	12.98	3.73

AR = Accurate readings, BE = Benign errors, ER = Erroneous readings.

4.1.7 Discussion and Conclusions

In this paper, a study on the prediction of subcutaneous glucose concentration in patients with type 1 diabetes under free-living conditions was presented. The innovative elements of the study are that (a) we experimented with different inputs corresponding to combinations of several variables associated with both the endogenous and the exogenous regulation of glucose in order to elucidate their effect on the prediction capability of a regression technique, and (b) the SVR technique was proposed for modelling the dynamic behaviour of blood glucose metabolism. Comparisons of the numerical accuracy of the generated predictions were made for six input cases.

This prediction problem was addressed for the first time in the literature with the aid of the SVR technique. SVR may approximate non-linear functions of the input variables, such as the blood glucose concentration, with a given accuracy, while controlling model's complexity to avoid over-fitting. Despite the fact that SVR accounts for non-linearity by mapping the input space to a higher dimensional feature space, the use of kernel functions enables the computations to be made in the original one. This is very important considering the great number of features already introduced to represent the temporal dependencies between the input variables and the glucose concentration. Furthermore, the utilization of the ε-insensitive loss function and of the slack variables not only further enhance the generalization performance of SVR but also lead to a sparse solution rendering SVR advantageous over other kernel-based approaches for the manipulation of large datasets, which is the case in glucose prediction problems. In addition to these, the fact that the regularized error function is characterized from the absence of local minima, as opposed to other machine learning techniques such as neural networks, is an especially important feature. However, capacity control in SVR requires the fine tuning of the hyper parameters C, ε, and the kernel parameters, which increases the computational cost involved in solving the convex optimization problem.

It becomes apparent that the determination of the input variables is essential for making reasonable and accurate predictions of glucose. The findings of the current and other studies [70, 71, 90, 95, 105, 149] showed that the subcutaneous glucose signal itself (gl) contains a sufficient amount of the information needed to make accurate short-term (up to 30 min) predictions, however, the auto-correlation of the signal attenuates rapidly after that time point. To this end, previous studies [150, 151] have also used the past values of the I_p and the Ra simulated signals to improve the capabilities of their predictive models. In order to exploit the

most of the compartmental models, in the present work we further proposed to expand the simulation time from the current time up to the time for which the prediction is to be made and use those additional future values as input to the SVR. Although comparative results were not provided herein, those future values contributed to more accurate predictions than when using only the time history up the current time. Furthermore, we moved one step forward by exploiting the area under the Ra curve, through the introduction of the variable SRa, which represents the cumulative amount of exogenous glucose inserted in the plasma over time (calculated every 10 min). Similarly, the effects of physical activities and exercise on type 1 diabetes were treated by introducing the variable SEE, which expresses the EE over the last 3 hrs in the form of a vector calculated cumulatively every 10 min. The only study [151] which used information from an activity monitor for making predictions was based only on the METs recorded every 5 min, which is, however, an instantaneous value of the activity intensity not showing the history of the activity. Our preliminary results reported in [160] showed that METs were less significant than SEE for SVR. Furthermore, an attempt was made to capture the effect of the circadian rhythms on glucose variability by using as input the hour of day which was proved to contribute to significantly better predictions. The six input cases that were considered in this study were employed so as to address different practical conditions, namely: (i) Case 1 is concerned with patients wearing only the CGM device, (ii) Cases 2-4 additionally require the patients to systematically record the food and insulin intake, and (iii) Cases 5-6 require the patients to wear an activity monitoring system for long-time periods within the day.

The evaluation of the proposed method was based on a representative dataset from 27 people with type 1 diabetes, whose subcutaneous glucose concentration profile included a sufficient amount of hypo/hyperglycaemic events. *Table 4.3* revealed that the short-term subcutaneous glucose concentration can be predicted with a sufficient numerical accuracy in all patient groups in all cases. However, when we exploited the full set of input variables (Case 6), a significant improvement was achieved in the average $RMSE_{10\text{-}fold}$, compared with Case 1, which was 42% and 61% for 15-min and 30-min predictions, respectively. As expected, the increase in the prediction horizon led to lower accuracy in the predictions for all cases. For Case 1, the predictions that were made in the medium- and long-term (60 and 120 min) had not only low accuracy but can also lead to potentially erroneous treatment. By introducing additional inputs, the prediction accuracy was greatly improved and became clinically acceptable in both normal and critical glucose ranges. More specifically, for Case 4 the accuracy for 60-min and 120-min predictions was 8.56 $mg \cdot dL^{-1}$ and 10.33 $mg \cdot dL^{-1}$ (i.e.

improved by 65% and 69% compared to Case 1), whereas for Case 6 was 7.14 mg·dL^{-1} and 7.62 mg·dL^{-1} (i.e. improved by 70% and 77%), respectively. Besides improved accuracy, equally important is the fact that we achieved a strong positive linear correlation as well as a very short TLs (<1 min) in Cases 4-6, regardless of the prediction horizon. Comparison of Cases 4 and 6 reveals the important role of the information about physical activity on the whole prediction process. Nevertheless, the results obtained from Case 4 indicate that predictions can be sufficiently accurate and clinically acceptable even if the patient does not use an activity monitor, which renders the proposed predictor effective in less intrusive and thus more practical conditions.

A comparison of the proposed method with those reported in the literature is shown in *Table 4.5*. The results indicate that the proposed method outperforms all the other methods except for that of Gani *et al.* [70] for 30-min predictions; however, the results of that method were computed based only on CGM data segments that were described by a stationary process. On the other hand the proposed method may as well perform in the presence of external inputs, when the stationarity hypothesis is no more valid, by timely modelling the data obtained from the patients. We should also mention that the performance of the predictive model in [114] is assessed on data from patients not included in the training set.

Table 4.5 Comparison with other Methods Reported in the Literature

Study	**Method**	**Dataset**	**Prediction Horizon (min) / RMSE (mg·dL^{-1})**			
Sparacino *et al.* [24]	AR	CGM Data	30 /18.78	45 / 34.64		
Eren-Oruklu *et al.*[26]	AR, ARMA	CGM Data	30 / 3.83[a]			
Gani *et al.* [27]	AR	CGM Data	30 / 1.8	60 / 12.6	90 / 28.8	
Perez - Gandia *et al.* [29]	FFNN	CGM Data	15 / 9.7	30 / 17.5	45 / 27.1	
Mougiakakou *et al.* [31]	NN	CGM Data, Insulin, CHO	5 / 13.65			
Pappada *et al.* [33]	FFNN	CGM Data, Insulin, Nutrition, Lifestyle/Emotional Factors, Time	75 / 43.9			
This work	SVR (Case 6)	CGM Data, Insulin, CHO, Exercise Data, Time	15 / 5.21 (2.06[a])	30 / 6.03 (2.41[a])	60 / 7.14 (2.79[a])	120 / 7.62 (3.02[a])

[a]This value refers to mean absolute percentage error (MAPE).

Although the present study treats the blood glucose metabolism in type 1 diabetes as a multi-parametric, dynamic system, there are still factors that have not been taken into consideration. Firstly, the model of the subcutaneous insulin kinetics [153] relies solely on the physicochemical properties, concentration and dose of insulin, without taking into account the effect of the injection conditions (e.g. site of injection, skin temperature) on the diffusion and absorption of insulin in the subcutaneous tissue [140]. Similarly, the meal simulation model [155] does not consider the influence of meal's composition (e.g. fats, fibres, glycaemic index) on the dynamics of the digestive and absorptive processes of carbohydrates [135]. In addition, these models are applied using population parameters and, thus, do not describe the inter- and intra-patient variability [79, 139-141]. A challenging prospective could be to additionally use as input to the model further information such as lifestyle details (e.g. working night shifts, frequent traveling), the psychological status (e.g. stress), patient's profile (e.g. age, HbA1c, BMI).

The advantages offered by a glucose prediction method are extremely useful for personal diabetes advisory systems intended for daily use. The proposed method has already been integrated in the METABO diabetes monitoring and management system as part of a mobile decision support subsystem. The architecture of the proposed method requires the data to be first collected from each patient for a period and thereafter to train and test the personalized predictor based on these data. However, additional technical issues need to be examined, such as what is the optimal observation period required for data collection, the rate of model updating etc. Besides these issues, an extensive clinical validation of the prediction system is ongoing which is essential for the potential real life application of the system.

4.2 A Glucose Model Based on Support Vector Regression for the Prediction of Hypoglycaemic Events under Free-Living Conditions

4.2.1 Introduction

The most vital and challenging issue for people with type 1 or advanced type 2 diabetes is the achievement and maintenance of euglycaemia over time in a safe manner. The long-term benefits of IIT along with the increased frequency of hypoglycaemic events were first demonstrated by the Diabetes Control and Complications Trial [29]. Since then, despite the significant improvements in insulin analogues, hypoglycaemia has been recognized as the

major barrier to the management of diabetes [3]. The unpleasant symptoms that accompany the impermanent brain dysfunction, as well as the fact that prolonged and untreated hypoglycaemia may directly or indirectly be fatal, discourage those with diabetes from more intensive glycaemic control.

Hypoglycaemia in insulin-dependent diabetes patients is the aggregate of therapeutic hyperinsulinemia and an attenuated sympathoadrenal response to falling plasma glucose concentrations [161]. Recent antecedent hypoglycaemia, prior exercise, and sleep further impair the physiological and behavioural defences against a potential subsequent hypoglycaemia (i.e., HAAF) and therefore cause a vicious cycle of recurrent hypoglycaemia [3, 162]. The awareness of all these factors by patients with diabetes may contribute to the prevention of hypoglycaemia on a daily basis. Nevertheless, those with diabetes could take advantage of computational solutions that alert them for an upcoming hypoglycaemia and thus enable its prevention.

The last advances in CGM technologies have promoted the research in predictive modelling of glucose metabolism both in type 1 and in type 2 diabetes. AR and ARMA models of the CGM time series [70, 71, 95, 105, 149] as well as FFNNs [90] based only on recent CGM data were found to have short-term (up to 30 min) predictive capacity of the subcutaneous glucose concentration. More accurate predictions were achieved by applying a RNN on a wider (200-min) CGM history [163]. The fact that (1) the autocorrelation function of the subcutaneous glucose measurements vanishes at about 30 min [91] and (2) several exogenous inputs play a vital role in glucose regulation have led to predictive models incorporating more comprehensive information [92-94, 114, 130, 164]. More specifically, multivariate nonlinear regression techniques of machine learning, such as FFNNs [94, 114] and RNNs [92, 93, 164], and SVR [130] were efficiently used for this purpose, demonstrating the effect of additional inputs on short- and long-term predictions.

Although hypoglycaemia is the limiting factor in the glycaemic management of insulin-treated diabetes, there have been only a few studies that went one step further by addressing the problem of hypoglycaemic event prediction. This problem involves the successful prediction of the beginning of the event and therefore differs from predicting single hypoglycaemic values [106, 120, 158]. On this basis, only statistical and time-series methods [121-123] were evaluated for prediction horizons up to 55 min using hypoglycaemic thresholds ranging from 60 $mg \cdot dL^{-1}$ to 90 $mg \cdot dL^{-1}$. The results obtained are promising with sensitivity

reaching 100% in a study [122] with lead times close to the examined prediction horizons. However, these methods were evaluated on CGM recordings of patients with type 1 diabetes who underwent an insulin-induced hypoglycaemia test during their admission in clinical research centres. With the view to embedding these new models eventually into CGM systems or into diabetes advisory mobile systems, the need to test them under free-living conditions in daily life is evident.

We have previously proposed an individualized approach to predicting the subcutaneous glucose concentration that relies on the SVR technique, which was evaluated on a multivariate dataset of 27 type 1 diabetes patients in free-living conditions [130]. One of the innovations of our work was the experimentation with different inputs corresponding to combinations of variables associated with the subcutaneous glucose profile, the plasma insulin concentration, the rate of appearance of meal-derived glucose in the system circulation, the EE during physical activities, and the time of the day. Besides high performance over the full range of glucose values, more than 94% of both short-term (i.e., for 15 min and 30 min) and medium- to long-term (i.e., for 60 min and 120 min) hypoglycaemic predictions were classified as clinically accurate or with benign errors according to the continuous glucose-error grid analysis [159].

In this study, we extend our method to predict hypoglycaemic events 30 min and 60 min in advance and provide a comparison of SVR with other well-established machine learning techniques. Considering that in type 1 diabetes hypoglycaemia occurs most frequently at night during sleep and is potentially fatal if untreated [165], we separated the hypoglycaemic events into nocturnal and diurnal ones. In particular, for nocturnal events, we introduce new input variables in addition to those defined in our previous work [130] with the aim of capturing the effect of HAAF on the incidence of a future hypoglycaemic event. To our knowledge, this is the first work that deals with the problem of hypoglycaemia prediction as an event in free-living patients using SVR.

4.2.2 Subjects

Fifteen type 1 diabetes patients, following multiple-dose insulin therapy, were monitored for from 5 to 22 days (average, 12.5 ± 4.6 days) in free-living conditions within the European Union co-funded research project METABO [152]. The dataset consisted of three women and 12 men whose ages ranged from 19 to 65 years (average, 40.3 ± 13.5 y/o) with a body mass

index from 21.4 to 30.0 kg·m^{-2} (average, 25.2 ± 2.9 kg·m^{-2}) and hemoglobinA1c level from 5.2% to 8.5% (average, 7.1 ± 1.2%). Patients wore the Guardian® Real-Time CGM system (Medtronic Minimed Inc., Northridge, CA), which reports an average subcutaneous glucose value every 5 min. They were also recording information on food intake (i.e., type, amount, and time) and insulin regimen (i.e., type, dose, and time) on a daily basis, while a dietician calculated the amount of carbohydrates for each meal. In addition, the SenseWear® Armband (BodyMedia® Inc., Pittsburgh, PA) physical activity monitor was used, which computes a range of relative variables (e.g., EE, metabolic equivalents [MET], sleep detection) every 1 min. The descriptive characteristics of the subcutaneous glucose dataset are given in *Table 4.6*.

Table 4.6 Statistics of the Glucose Dataset per Patient

	Time Interval	
	Diurnal	*Nocturnal*
Subcutaneous glucose concentration (mg·dL^{-1})		
Mean	148.85 ± 23.41	140.75 ± 29.89
Minimum	52.92 ± 11.96	60.79 ± 18.06
Maximum	332.44 ± 47.81	281.12 ± 49.38
% of values		
Hypoglycaemic	0.04 ± 0.04	0.05 ± 0.05
Hyperglycaemic	0.27 ± 0.15	0.22 ± 0.18
Hypoglycaemic events per day/night	0.68 ± 0.48	0.35 ± 0.15
Duration per hypoglycaemic event (min)	56.78 ± 28.31	75.98 ± 42.97

Data are mean ± standard deviation values. A glucose concentration value of ≤70 mg·dL^{-1} is defined as hypoglycaemic; a glucose concentration value of ≥180 mg·dL^{-1} is defined as hyperglycaemic.

4.2.3 Glucose Predictive Model

The prediction of the subcutaneous glucose concentration at time $t+l$, assuming that t is the time at which the prediction is made and l is the prediction horizon, is given by the SVR function [156] of the input $x \in R^d$ until time t. SVR function is of the form $f(x) = w^T \varphi(x) + b$, where w and b are the weight and bias parameters, respectively, and φ is a fixed mapping to a high-dimensional feature space introduced for the approximation of nonlinear functions of the input variables, such as the blood glucose concentration. However, the use of a kernel function enables the computations to be made in the original space of fewer dimensions while, through an ε-insensitive loss function, a sparse solution is also obtained. Moreover, SVR achieves very good generalization performance by controlling, with the use of the constant C, the amount up to which deviations larger than $\pm\varepsilon$ are tolerated as well as the

model's complexity (i.e., small w).

In our study, the SVR model was built with a Gaussian kernel, and the hyperparameters C, ε, and the kernel parameter γ were optimized using the differential evolution algorithm [157], in which the objective function was defined as the average root mean square error of the 10-fold cross-validation procedure. The three-dimensional search space was set as $C \in [0.001, 1024]$, $\varepsilon \in [0.0001, 1]$, and $\gamma \in [0.00001, 8]$. The overall evaluation of the glucose predictive model was performed individually for each patient's dataset by 10-fold cross-validation.

For comparison purposes, the problem of hypoglycaemic event prediction is also addressed by two other widely known machine learning techniques: the FFNN [166] and GP [167] regression techniques. The FFNN is composed of one hidden layer with *H* neurons having a tangent sigmoid activation function and one output layer with one neuron having a linear function. The weights and bias parameters of the network are trained based on the Levenberg–Marquardt back-propagation algorithm applied in a batch mode and with early-stopping (i.e., validation set). The number of hidden neurons *H* is optimized individually for each patient based on 10-fold cross-validation. The GP model is built with an exponential quadratic kernel, while its hyperparameters (i.e., kernel parameters and noise precision) are learned for each patient separately through the maximization of the log likelihood function. Both MLP and GP are evaluated separately for each patient by 10-fold cross-validation.

4.2.4 Hypoglycaemic Event Prediction

In accordance with the American Diabetes Association recommendations [165], we use the threshold of 70 mg·dL^{-1} to identify a subcutaneous glucose concentration value, measured by the CGM system, as hypoglycaemic. To this end, we define that: (1) a hypoglycaemic event starts when at least two consecutive subcutaneous glucose concentration values (i.e., 10 min or more) are ≤70 mg·dL^{-1}, and (2) it ends when the glucose value rise above 70 mg·dL^{-1} [36]. To treat potential oscillations either in the predicted or in the actual time-series, consecutive hypoglycaemic events that are ≤30 min away are considered as the same event. Predictions are performed for horizons of 30 min and 60 min. Moreover, a new glucose prediction is produced every 5 min, which is the sampling period of the CGM system used in this study.

A prediction of a hypoglycaemic event is considered true-positive (TP) when the start

of the actual hypoglycaemic either precedes the start of the predicted one by $\leq l$ min or follows the start of the predicted one by $\leq l$ min. Otherwise, when a true hypoglycaemic event is not predicted or a false hypoglycaemic event is predicted, then a false-negative (FN) or a false-positive (FP) prediction, respectively, is identified. Note that we do not apply the term true-negative, which in our case would mean to correctly identify a non-hypoglycaemic region (i.e., euglycaemia or hyperglycaemia) as such.

Because hypoglycaemia occurring during nocturnal sleep is important for diabetes patients, we separate hypoglycaemic events into nocturnal and diurnal ones. In particular, nocturnal hypoglycaemia is defined as each hypoglycaemic event occurring at night when the individual is asleep, whereas all the other events are characterized as diurnal. The sleep state is detected using the related information provided by the SenseWear armband activity monitor.

4.2.5 Determination of the Input

The SVR glucose predictive model is fed with three different cases of input. In the first case, denoted herein as Case 1_{hypo} (corresponding to Case 4 in Georga et al. [130]), the input consists of the variables *gl*, I_p, *Ra*, *SRα*, and *h*, whereas in the second case, namely, Case 2_{hypo} (corresponding to Case 6 in Georga et al. [130]), the variable *SEE* is additionally used.

The concept of HAAF led us to introduce an additional input case, denoted herein as Case 3_{hypo}, which would also allow for the inclusion of its causes, namely, recent antecedent hypoglycaemia, prior exercise, and sleep. Variable *SEE*, which concerns the EE during the last 3 h, may only explain hypoglycaemia shortly after exercise. However, exercise-related HAAF is exemplified by hypoglycaemia that typically occurs several hours (6–15 h) after exercise and thus is often nocturnal [162].

HAAF is mainly associated with hypoglycaemic events that occur during sleep. Thus, we define Case 3_{hypo} only for nocturnal events, whereas Case 1_{hypo} and Case 2_{hypo} are applied to both the prediction of nocturnal and diurnal ones. This means that in Case 3_{hypo} the SVR model is trained to predict only the night glucose time series. Thus, in addition to the inputs of Case 1_{hypo}, Case 3_{hypo} includes:

1. The total EE during the day due to physical activities of intensity of <3 METs ($EE_{daily,<3METs}$).
2. The total EE during the day due to physical activities of intensity ≥3 METs

($EE_{daily,\geq 3METs}$).

3. The time passed from the start of the sleep state (t_{sleep}).
4. A Boolean variable describing the incidence or not of a hypoglycaemic event during the previous 24 h (hypo).

Moreover, experimental and clinical observations have indicated that glucose levels change more gradually at night than during the day . Therefore, in the present analysis for each of the previous cases as regards the nocturnal events, we consider one subcase (i.e., Case $1a_{hypo}$, Case $2a_{hypo}$, Case $3a_{hypo}$), where the history of gI is set equal to 60 min.

4.2.6 Evaluation Criteria

The proposed method is evaluated by computing the measures of sensitivity, precision, and TL. Sensitivity, defined as $TP/(TP+FN)$, relates to the method's ability to identify positive hypoglycaemic events. On the other hand, precision, defined as $TP/(TP+FP)$, reflects the probability that a predicted event is true. Finally, TL, defined as the mean absolute temporal error between the start of the actual and the predicted hypoglycaemic event, is a highly crucial measure that reflects the TG in preventing the upcoming event.

4.2.7 Model Evaluation over the Hypoglycaemic Range

The average results obtained in all 15 subjects of the study are reported in *Table 4.7* separately for nocturnal and diurnal hypoglycaemic events. In Case 1_{hypo}, the 30-min and 60-min nocturnal predictions are of satisfactory sensitivity and of high precision, but they are associated with relatively high TLs. Case 2_{hypo}, as expected, does not induce significant changes in the number of TP and FP outcomes. In contrast, Case 3_{hypo} increases sensitivity and precision especially of 60-min predictions (average, 90% and 100%, respectively) and lowers markedly the TL for both prediction horizons (average, 5.00 min and 6.18 min, respectively) compared with the previous cases. In Figure 4.3, we see the actual onset of the nocturnal events of a patient and the predicted onset (with 30-min horizon) denoted by a vertical dotted line. It can be observed that in Case 3_{hypo} the TL is smaller than in Case 1_{hypo}. The sensitivity of Case 1_{hypo} and Case 2_{hypo} is almost unaffected by increasing the gI history from 30 min to 60 min (Case $1a_{hypo}$ and Case $2a_{hypo}$), whereas there is a noticeable improvement in their precision rate. Regarding Case $3a_{hypo}$, it results in predicting correctly 94% of the events with 98% precision

for both prediction horizons. Nevertheless, it is obvious that gl history has a great influence on the TG in the TP events for a 60-min prediction horizon.

Table 4.7 Evaluation Results of the Support Vector for Regression Model for Predicted Nocturnal and Diurnal Hypoglycaemic Events and for all Input Cases

Hypoglycaemic events, case number	**Prediction Horizon**					
	30 min			60 min		
	SNS	*PRC*	*TL*	*SNS*	*PRC*	*TL*
Nocturnal						
Case 1_{hypo}	0.89 ± 0.21	0.95 ± 0.11	9.26 ± 9.78	0.86 ± 0.26	0.93 ± 0.12	14.39 ± 15.04
Case $1a_{hypo}$	0.89 ± 0.21	0.98 ± 0.06	8.68 ± 8.73	0.88 ± 0.20	0.96 ± 0.12	7.81 ± 10.39
Case 2_{hypo}	0.88 ± 0.21	0.97 ± 0.10	7.50 ± 9.23	0.86 ± 0.23	0.90 ± 0.15	12.71 ± 15.07
Case $2a_{hypo}$	0.87 ± 0.20	0.97 ± 0.10	6.91 ± 9.54	0.86 ± 0.20	0.96 ± 0.12	8.13 ± 12.10
Case 3_{hypo}	0.91 ± 0.23	0.98 ± 0.08	5.00 ± 6.85	0.90 ± 0.17	1.00 ± 0.00	6.18 ± 8.35
Case $3a_{hypo}$	0.94 ± 0.10	0.98 ± 0.08	5.43 ± 7.11	0.94 ± 0.10	0.98 ± 0.08	4.57 ± 5.47
Diurnal						
Case 1_{hypo}	0.92 ± 0.12	0.93 ± 0.13	4.53 ± 5.30	0.96 ± 0.14	0.97 ± 0.10	3.64 ± 4.72
Case 2_{hypo}	0.84 ± 0.23	0.94 ± 0.16	3.17 ± 4.65	0.93 ± 0.17	0.96 ± 0.14	4.52 ± 5.97

Data are mean ± standard deviation values.
PRC: Precision, SNS: Sensitivity, TL: Time lag.

Regarding diurnal hypoglycaemic events, Case 1_{hypo} predicts correctly 92% and 96% of the true hypoglycaemic events 30 min and 60 min in advance, respectively, with 93% and 97%, respectively, of the positive predictions being indeed true. The TL for both prediction horizons is less than 5 min. However, the sensitivity of the method is reduced when the variable *SEE* is additionally used in Case 2_{hypo}, reaching 84% for 30-min predictions and 93% for 60-min predictions. In addition, there are no significant changes in precision rate compared with Case 1_{hypo}, while the TL is still less than 5 min. The output of Case 1_{hypo} and Case 2_{hypo} for a patient is illustrated in Figure 4.4, where for the ninth hypoglycaemic event we observe that Case 2_{hypo} generates a FN result contrary to Case 1_{hypo}.

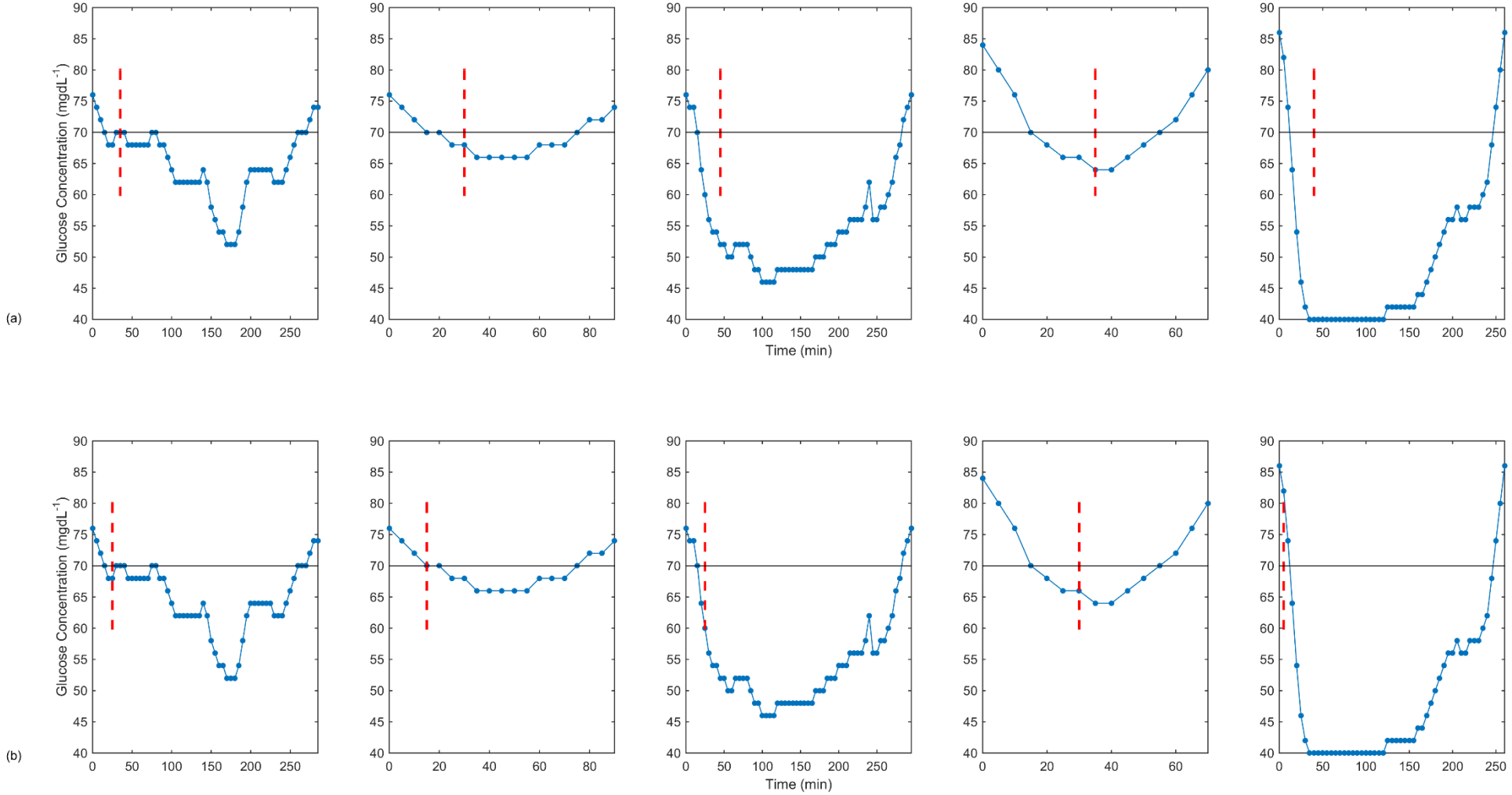

Figure 4.3 The output of (a) Case 1_{hypo} and (b) Case 3_{hypo} for a prediction horizon of 30 min regarding the nocturnal hypoglycaemic events of a typical patient. Each hypoglycaemic event (solid blue line represents glucose values) was predicted to happen at the time indicated by the red dotted line.

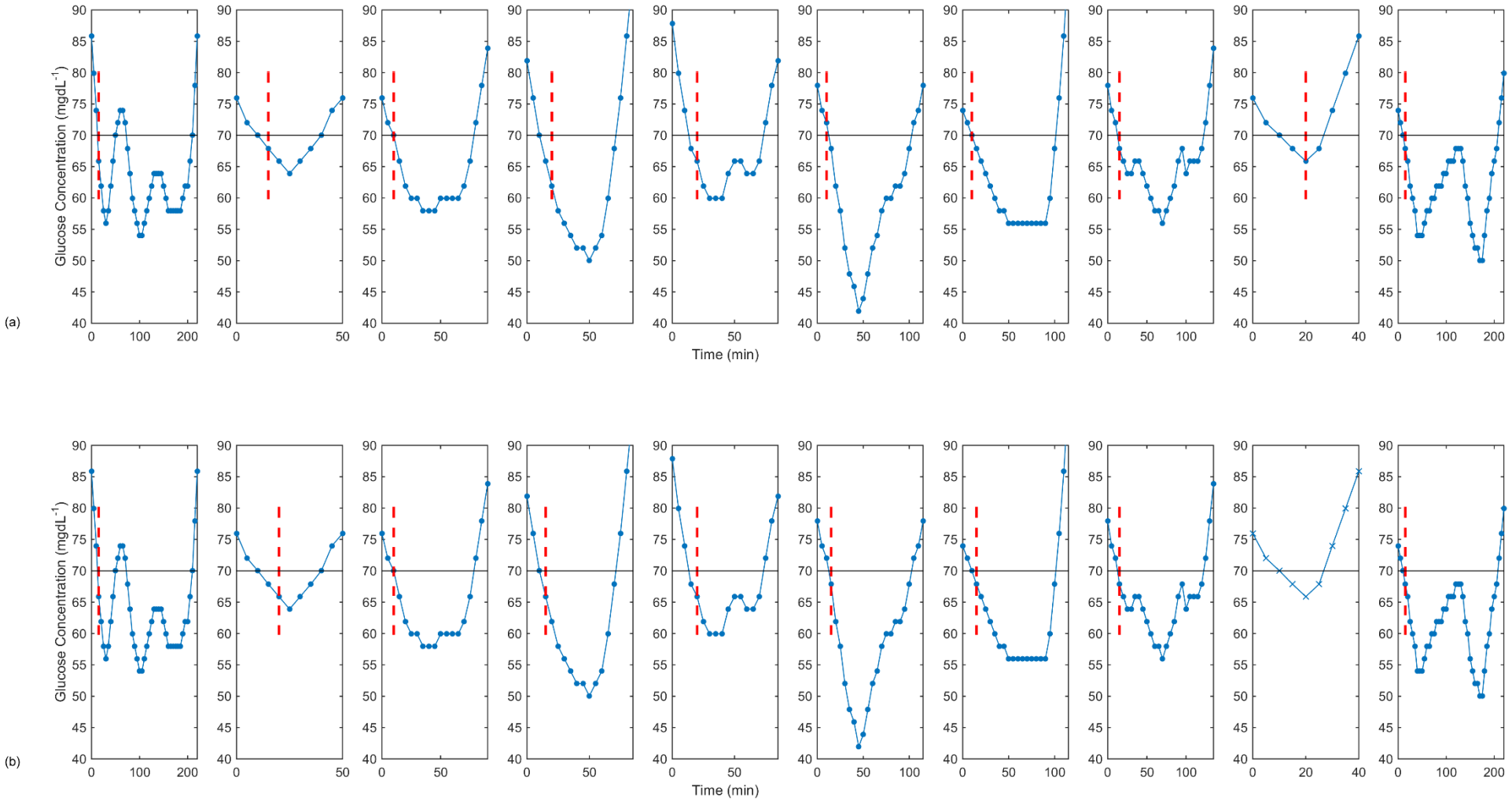

Figure 4.4 The output of (a) Case 1hypo and (b) Case 2hypo for a prediction horizon of 30 min regarding the diurnal hypoglycaemic events of a typical patient. Each hypoglycaemic event (solid blue line represents glucose values) was predicted to happen at the time indicated by the red dotted line.

Table 4.8 and *Table 4.9* present the average results obtained by the MLP and GP prediction techniques, respectively. Regarding the nocturnal events, SVR outperforms MLP in all cases except Case 3_{hypo} for the 30-min prediction horizon and Case $2a_{hypo}$ for 60 min. We observe that Case 3_{hypo} and Case $3a_{hypo}$ improve significantly the performance of MLP, and especially the TL, for both horizons. On the other hand, GP produces smaller TLs than SVR and, consequently, higher sensitivities for most of the input cases, which becomes more apparent in 60-min predictions. More specifically, the sensitivity of GP in Case 3_{hypo} for 30-min and 60-min predictions is 95% and 98%, respectively, reaching 100% in Case $3a_{hypo}$ for both horizons, and all TLs are less than 5 min. However, SVR and GP techniques have similar precision rates. As far as diurnal events are concerned, SVR performs better than both other techniques except for Case 2_{hypo} for the 30-min prediction horizon, where it has a slightly lower sensitivity.

Table 4.10 presents the evaluation results of the three techniques only on diurnal hypoglycaemic events verified by a finger-stick blood glucose measurement. The most significant changes are observed for Case 1_{hypo}, where the 30-min sensitivity of SVR and GP is reduced to 82% and 71%, respectively, whereas the 60-min sensitivity of MLP and GP is reduced to 48% and 57%, respectively. However, it should be noted that blood glucose measurements were not available for all hypoglycaemic events.

Table 4.8 Evaluation Results of the FFNN Regression Model

Hypoglycemic events, case number	**Prediction Horizon**					
	30 min			60 min		
	SNS	*PRC*	*TL*	*SNS*	*PRC*	*TL*
Nocturnal						
Case 1_{hypo}	0.76 ± 0.25	0.89 ± 0.17	14.11 ± 10.63	0.82 ± 0.28	0.91 ± 0.13	22.00 ± 16.69
Case $1a_{hypo}$	0.67 ± 0.38	0.78 ± 0.39	15.19 ± 11.05	0.84 ± 0.26	0.93 ± 0.13	18.67 ± 16.81
Case 2_{hypo}	0.86 ± 0.21	0.88 ± 0.20	10.88 ± 9.08	0.80 ± 0.22	0.94 ± 0.12	12.50 ± 13.68
Case $2a_{hypo}$	0.86 ± 0.21	0.88 ± 0.21	11.47 ± 9.01	0.94 ± 0.15	0.91 ± 0.15	10.29 ± 12.36
Case 3_{hypo}	0.93 ± 0.16	0.95 ± 0.12	4.72 ± 4.62	0.83 ± 0.27	0.95 ± 0.12	6.00 ± 6.87
Case $3a_{hypo}$	0.91 ± 0.23	1.00 ± 0.00	5.71 ± 6.08	0.92 ± 0.16	0.95 ± 0.12	3.48 ± 3.85
Diurnal						
Case1_{hypo}	0.76 ± 0.20	0.89 ± 0.19	8.51 ± 9.08	0.73 ± 0.39	0.95 ± 0.16	10.86 ± 9.55
Case2_{hypo}	0.86 ± 0.17	0.90 ± 0.17	5.85 ± 6.56	0.89 ± 0.21	0.97 ± 0.10	10.48 ± 12.74

Data are mean ± standard deviation values.
PRC: Precision, SNS: Sensitivity, TL: Time lag.

Table 4.9 Evaluation Results of the GP Regression Model

Hypoglycemic events, case number	**Prediction Horizon**					
	30 min			60 min		
	SNS	*PRC*	*TL*	*SNS*	*PRC*	*TL*
Nocturnal						
Case 1_{hypo}	0.81 ± 0.33	0.98 ± 0.06	6.29 ± 5.91	0.82 ± 0.25	0.96 ± 0.09	8.06 ± 8.53
Case $1a_{hypo}$	0.87 ± 0.26	0.98 ± 0.06	5.61 ± 6.22	0.93 ± 0.12	0.95 ± 0.10	6.67± 8.45
Case 2_{hypo}	0.84 ± 0.28	0.94 ± 0.13	6.06 ± 8.08	0.93 ± 0.16	0.95 ± 0.12	6.89 ± 8.02
Case $2a_{hypo}$	0.86 ± 0.26	0.92 ± 0.17	6.62 ± 8.41	0.95 ± 0.15	0.94 ± 0.16	4.17 ± 4.39
Case 3_{hypo}	0.95 ± 0.10	0.98 ± 0.08	4.31 ± 4.95	0.98 ± 0.08	1.00 ± 0.00	4.34 ± 5.60
Case $3a_{hypo}$	1.00 ± 0.00	0.98 ± 0.06	4.08 ± 5.31	1.00 ± 0.00	0.98 ± 0.08	2.84 ± 2.77
Diurnal						
Case1_{hypo}	0.83 ± 0.24	0.96 ± 0.14	3.88 ± 4.92	0.73 ± 0.39	0.95 ± 0.16	3.93 ± 5.67
Case2_{hypo}	0.86 ± 0.18	0.94 ± 0.16	2.55 ± 3.20	0.72 ± 0.44	0.90 ± 0.32	4.04 ± 4.00

Data are mean ± standard deviation values.
PRC: Precision, SNS: Sensitivity, TL: Time lag.

Table 4.10 Evaluation Results of the Support Vector for Regression, FFNN, and GP Regression Techniques on Diurnal Hypoglycaemic Events verified by Blood Glucose Measurements

Regression technique, case number	**Prediction Horizon**			
	30 min		**60 min**	
	SNS	*TL*	*SNS*	*TL*
Support vector for regression				
Case 1_{hypo}	0.82 ± 0.32	4.44 ± 6.84	0.94 ± 0.18	3.33 ± 5.69
Case 2_{hypo}	0.78 ± 0.37	2.59 ± 4.14	0.93 ± 0.19	4.12 ± 5.37
Multiplayer perceptron				
Case 1_{hypo}	0.78 ± 0.33	6.73 ± 7.99	0.48 ± 0.45	8.33 ± 9.85
Case 2_{hypo}	0.90 ± 0.18	6.21 ± 7.52	0.83 ± 0.26	9.67 ± 12.17
Gaussian processes				
Case 1_{hypo}	0.71 ± 0.40	3.54 ± 6.51	0.57 ± 0.45	3.46 ± 5.91
Case 2_{hypo}	0.82 ± 0.34	2.50 ± 3.41	0.70 ± 0.48	3.08 ± 3.84

Data are mean ± standard deviation values.
PRC: Precision, SNS: Sensitivity, TL: Time lag.

4.2.8 Discussion and Conclusions

The objective of this study was to evaluate the ability of the SVR glucose predictive model, which was presented in a previous study [130], to predict hypoglycaemic events over 30-min and 60-min time horizons. The novelty of our work consists in that (1) this problem is addressed with the SVR technique based on a multivariate dataset acquired in free-living conditions from multiple patients and (2) new inputs are introduced for treating hypoglycaemia during nocturnal sleep.

This specific problem was dealt only through linear mathematical approaches that exploit solely the recent CGM profile [123]. The CGM signal itself is indeed the most

important feature but mainly explains its subsequent behaviour for up to 30 min [91] and thus allows only for short-term predictions of low accuracy [70, 71, 90, 95, 105, 149]. We demonstrated herein the implicit or explicit influence of the exogenous inputs on the glucose dynamics. This is actually the main advantage of the proposed method over the ones presented in the literature [121-123]; it has the ability to learn the effect of patient's contextual information (e.g., meals, insulin, exercise, sleep) on the subcutaneous glucose concentration, without requiring any a priori knowledge about their physiological relationships. Moreover, the SVR technique may accurately explain both linear and nonlinear relationships between the input variables and the glucose dynamics, while exhibiting a very good generalization performance. In addition, for the first time we examined thoroughly additional indicators of hypoglycaemia concerning (1) those related to the HAAF concept mechanisms triggering nocturnal hypoglycaemia and (2) the slow change of glucose time series during night, which were proved to contribute to significantly better predictions.

Results for 15 type 1 diabetes patients suggest that our SVR method performs adequately well in all cases for both prediction horizons. One important finding is that the method's sensitivity to nocturnal hypoglycaemic events increases in Case 3_{hypo} , whereas it shows no significant change in Case 2_{hypo}, compared with Case 1_{hypo}, which means that even a summary of the daily physical activities affects nocturnal hypoglycaemia. This is also reflected in reduced TLs. The comparative assessment of SVR with MLP and GP regarding nocturnal events has demonstrated that GP and SVR have comparable performance for the 30-min horizon, whereas GP shows better sensitivity as well as improved TLs for the 60-min horizon compared with SVR. The improvement of predictions in Case 3_{hypo} and Case $3a_{hypo}$ is systematically observed for all techniques, which verifies the observations.

Regarding diurnal predictions, the SVR performs generally better compared with the MLP and GP techniques. There is one exception in Case 2_{hypo}, which concerns the introduction of information on physical activity, where for the 30-min horizon the sensitivity of SVR is lower than the other techniques. Unexpectedly, this sensitivity is even smaller than in Case 1_{hypo}, as opposed to the corresponding MLP and GP cases. This leads us to conclude that the poorer SVR prediction in Case 2_{hypo} should be possibly attributed to the technique itself and not to the introduction of this extra information. Diurnal predictions over 60-min horizons are better than those over 30-min horizons for SVR and MLP; however, a direct comparison of the results for 30 min and 60 min should not be made because the set of hypoglycaemic events on which the methods are evaluated are different (i.e., the events for 60 min is a subset of the ones

for 30 min). This stems from the fact that different datasets have been constructed for each horizon (e.g., instances at which meal or insulin events occurred in the meantime were excluded) [130].

The methods presented in the literature for hypoglycaemic event prediction [121-123] have been all assessed in datasets acquired from short-term (usually 24-h) studies conducted under controlled conditions in clinical settings. This enables fairly accurate predictions despite the fact that they apply time series or statistical analysis of the continuous glucose concentration values without using any exogenous inputs. In particular, Eren-Oroklu et al. [123] have reported a sensitivity of 89%, a precision rate of 78%, and a lead time of 27.7 min, having set the hypoglycaemic threshold to 60 $mg \cdot dL^{-1}$ and the prediction horizon to 30 min. Moreover, the method by Dassau et al. [122] predicted 91% and 100% of the hypoglycaemic events 35 min and 55 min ahead, respectively, with a threshold of 80 $mg \cdot dL^{-1}$. Although our method is evaluated under free-living conditions, it compares favourably with them regarding sensitivity and lead times for both horizons, while showing a much better precision.

The proposed method has the potential to be applied in everyday life conditions given that it is adequately accurate, achieves rapid response times, and is not intrusive. Moreover, it has been designed to be fully automatic for potential use in smart mobile devices, but this could only be feasible should we have access to the CGM data in real time. To ensure its proper and reliable operation, the patient should record systematically the food and insulin intakes and wear the physical activity monitor. An activity monitor does not constraint the usability of the method because today there are light, comfortable, and discreet devices that accurately track daily physical activities. Moreover, the number and timing of the CGM sensor calibrations inevitably affect the quality of the predictions. Therefore, such predictions are only reliable if the CGM device is suitably calibrated, whereas nocturnal predictions should be interpreted with caution.

One crucial issue in machine learning techniques, when applied to real and dynamic problems, is that they need frequent retraining so as to reflect the most recent state of the examined system. Thus, the rate of the SVR model updating and the optimal observation period required for data collection constitute some issues under examination. An improvement of the proposed approach could be the use of fuzzy logic for the definition of hypoglycaemic events in place of the sharp threshold of 70 $mg \cdot dL^{-1}$. Moreover, additional descriptive characteristics could be devised for summarizing the daily physical activity (e.g., number, intensity, and

duration of exercise events, etc.) for nocturnal hypoglycaemic event prediction considering that even a simplified input had a significant effect. Nevertheless, the potential incorporation of the proposed method either into a CGM system or into a smartphone as a personal diabetes management system necessitates an extensive clinical validation.

CHAPTER 5. EVALUATION OF SHORT-TERM PREDICTORS OF GLUCOSE CONCENTRATION IN TYPE 1 DIABETES COMBINING FEATURE RANKING AND REGRESSION MODELS

5.1 Introduction

Daily management of type 1 diabetes at its core can be viewed as a feedback loop where patients adjust the insulin regime based primarily on their real-time blood glucose measurements and secondarily on their overall lifestyle context (e.g. meals, physical activities, stress) [32, 168, 169]. Patients on multiple insulin injection therapy could maintain complete glycaemic control, if it were not for the increased risk of hypoglycaemia [3]. The technological progress in CGM and in CSII has contributed to a more practical and safe therapy scheme [51, 66, 170]. In particular, SAP therapy has been shown to reduce glycaemic variability. Until researchers close the loop in insulin delivery, the patient, as the main actor in this process, should continually reason the effect of insulin intake and lifestyle on his/her glucose metabolism.

Prediction algorithms of subcutaneous glucose concentration have the potential to further advance insulin-treated diabetes management either in open or in semi-closed loop conditions [12-15]. Initial approaches to this problem, which were based on AR or ARMA models of the CGM time series either with constant [70, 89] or with recursively identified [95,

123] parameters, had sufficiently accurate short-term (15 min and 30 min) predictive capacity. The combination of a RNN with compartmental models of plasma insulin concentration and carbohydrates absorption was proposed in [92, 93]. Zecchin *et al.* demonstrated that feed-forward [94] as well as jump neural networks [96] exploiting not only the past CGM data but also meal information allow for improved accuracy when compared to [90, 95] over 30-min horizon. In addition, the inclusion of real physical activity data in glucose predictive models has recently emerged, which is very important considering the prominent effect of exercise on blood glucose concentration. In our previous work [130], we proposed an individualized predictive model relying on SVR of multiple input variables concerning the recent subcutaneous glucose concentration profile, the effect of food and insulin intake, the EE in physical activities and the time of the day. We demonstrated that these additional inputs not only result in better short-term predictions but also make feasible the predictions for longer horizons (60 min and 120 min). Similarly, a patient-specific recursive ARMAX from a multi-sensor body monitor outperformed a univariate model as applied to people with type 2 diabetes [106] and allowed the accurate prediction of hypoglycaemic events in people with type 1 diabetes [107, 108].

The existent inter- and intra-patient variability in type 1 diabetes implies the individualization of the predictive models and their continuous adaptation to both biological and environmental changes as well [112, 171]. For instance, the fusion of real-time adaptive models (RNN and AR) resulted in 100% prediction accuracy of hypoglycaemic events for patients under SAP therapy during everyday living conditions [112]. This need can also be partially met by performing a periodic patient-specific training process. A complementary procedure to adaptive learning can be considered the individualized evaluation of the short-term predictors of glucose concentration and the subsequent refinement of the model's input [172]. In [130], we predefined a high-dimensional feature set in an attempt to represent spatial and temporal input-output dependencies. As expected, we found out considerable inter-patient deviations in the hyper-parameters of the SVR regarding the same input, which means that it can be further customized.

In this study, we propose feature ranking as a pre-processing step in the construction of patient-specific predictive models of the short-term subcutaneous glucose concentration in type 1 diabetes. Two well-established feature ranking algorithms suitable for regression problems, i.e. RF and RReliefF, are employed for assessing the set of features defined in [130] separately for each patient. RF is a prediction technique that incorporates feature ranking as part of the

training process [173], while RRelief is a pure feature filtering algorithm based on the nearest neighbours approach [174]. Their main advantages which render them appropriate for the specific application are: (i) the sensitivity to informative features as well as to the correlations among them, (ii) the absence of assumptions about the (non)linearity of the underlying function and (iii) the low computational complexity [174, 175]. The generality and effectiveness of the result of feature ranking is demonstrated with respect to the performance of a non-linear regression model for the estimation of glucose concentration. Herein, we choose SVR and GP kernel-based methods as prediction tools since they have been shown to perform equally well over the full range of glucose values in our previously developed dataset [131]. In this context, the top-ranked features obtained per individual are examined and a clinical interpretation of the results is attempted. To our knowledge, this is the first work which examines the concurrent and cumulative impact of the most important predictors of the short-term daily glucose dynamics in individuals with type 1 diabetes (i.e. meals, insulin therapy, physical activities and the glucose signal itself) with the aid of feature ranking.

5.2 Materials and Methods

5.2.1 Subjects

A short-term observational study was carried out in two centres (Parma University Hospital, Parma and University Hospital Motol, Prague) as part of a European-Union co-funded research project named METABO [152]. The study was approved by the Ethics Committees of each hospital**.** Fifteen type 1 diabetic patients, following multiple-dose insulin therapy and without significant micro- and macro-vascular complications, were monitored from 5 to 22 days (average 12.5±4.6) in free-living conditions. All subjects provided written informed consent before enrolment. Patients wore the Guardian® Real-Time CGM system (Medtronic Minimed Inc.) which reports an average subcutaneous glucose value every 5 min. In addition, they were equipped with the SenseWear® Armband (BodyMedia Inc.) physical activity monitor which computes E every 1 min. Information on food intake (i.e. type of food, serving sizes and time) and insulin regime (i.e. type of insulin, injection dosage and time) was also recorded on a daily basis using a specially designed paper diary. The amount of carbohydrates for each meal was post-analysed by a dietician. *Table 5.1* presents the baseline characteristics of the patients and some descriptive statistics of their CGM data.

Table 5.1 Description of the Dataset

Patient Baseline Characteristics	
Gender	3 F / 12 M
Age (y/o)	40.3±13.5
BMI (kg·m^{-2})	25.2±2.9
HbA1C (%)	7.1±1.2
Descriptive Statistics of the Glucose Dataset	
Average Subcutaneous Glucose Concentration (mg·dL^{-1})	145.9±22.8
Min Subcutaneous Glucose Concentration (mg·dL^{-1})	49.7±10.1
Max Subcutaneous Glucose Concentration (mg·dL^{-1})	333.8±48.7
% of Hypoglycaemic Values	0.05±0.04
% of Hyperglycaemic Values	0.25±0.14

Data are mean±standard deviation values.
A glucose concentration value ≤70 mg·dL^{-1} is defined as hypoglycaemic.
A glucose concentration value ≥180 mg·dL^{-1} is defined as hyperglycaemic.

5.2.2 Dataset Construction

A separate dataset $Z^{(s)} = \left\{ \left(x^i, y_i \right) \middle| i = 1, \ldots, N_s \right\}$ is constructed for each subject s. Each sample associates the input vector $x^i \in R^d$ at time t_i with the observed subcutaneous glucose concentration y_i at time $t_i + l$, where l is the prediction horizon. The feature set $F = \{F_1, \ldots, F_d\}$ is defined with respect to the present time (i.e. t) and the horizon l as follows:

- $F_1 = h$: the hour of the day associated with time t.
- $F_{2-8} = \{gl(t-30), ..., gl(t-5), gl(t)\}$: Subcutaneous glucose measurements within the last 30 min.
- $F_{9-15} = \{Ra(t+l-30), ..., Ra(t+l-5), Ra(t+l)\}$: Rate of appearance of meal-derived glucose into plasma within the time interval $[t+l-30, t+l]$ [155].
- $F_{16-21} = \{SRa(t+l-75), ..., SRa(t+l-15), SRa(t+l)\}$: Total glucose inserted into plasma calculated cumulatively every 15 min over the last 90 min with respect to $t+l$, where $SRa(t+l-(5-i)15) = \sum_{\tau=t+l-90}^{t+l-(75-15i)} Ra(\tau)$ for $i = 0, \ldots, 5$.
- $F_{22-28} = \{I_p(t+l-30), ..., I_p(t+l-5), I_p(t+l)\}$: Plasma insulin concentration within the time interval $[t+l-30, t+l]$ [153].
- $F_{29-46} = \{SEE(t-170), ..., SEE(t-10), SEE(t)\}$: Energy expenditure calculated

cumulatively every 10 min over the last three (3) hours where $SEE\left(t-\left(17-i\right)10\right)=\sum_{\tau=t-180}^{t-\left(170-10i\right)} EE\left(\tau\right)$ for $i=0,\ldots,17$. The term EE expresses the instantaneous (i.e. per minute) EE estimated by the physical activity monitor.

In particular, a new sample is added into $Z^{(s)}$ for each time instance in the glucose time series of subject s for which all $d=46$ features can be defined and the value of glucose concentration l min ahead is available. The size of dataset, N_s, depends mainly on the length of the observation period for each patient and, ideally, the time difference between two consecutive samples in $Z^{(s)}$ is equal to the sampling period of the glucose time series i.e. 5 min. Nevertheless, the existence of gaps in the sensor data reduces N_s. In addition, all samples $\left(x^i, y_i\right)$ for which an event (i.e. food intake, insulin intake, moderate or intense exercise) exists within the time interval $\left[t_i, t_i+l\right]$ are excluded from $Z^{(s)}$ since they do not represent a rational mapping between the configured input and the output. This also ensures that for all samples in $Z^{(s)}$ the upcoming values of Ra and I_p within $\left[t_i, t_i+l\right]$ have been computed based only on the insulin and meal recordings until t_i

5.2.3 Feature Ranking

The feature set $F=\left\{F_j\right\}$, with $j=1,\ldots,d$, is evaluated individually for each subject s by applying the RF or RReliefF algorithm on $Z^{(s)}$. In that way, each F_j is assigned an importance score ω_j and a ranked list of features, R, is produced by sorting them in descending order by W_j. More specifically, let $J=\left[1,\ldots,d\right]$ denote the indices of F. Then, the ranked list of features is defined as $R=\left[F_{j'_1},\ldots,F_{j'_d}\right]$ where $J'=\left[j'_1,\ldots,j'_d\right]$, $j'_j\in J$ and $\omega_{j'_j}\geq\omega_{j'_{j+1}}$. For comparison purposes, the average score of each feature F_j over all patients i.e. ϖ_j and the corresponding average feature ranking $\bar{R}$ are also calculated.

5.2.3.1 Random Forests

RF is an ensemble of low correlated regression trees, which output is computed as the average

of the individual predictions [173]. Each tree in the RF is constructed using an independent set of random vectors generated from a fixed probability distribution. Randomness is usually incorporated into the tree growing process by bootstrap resampling the original training set and randomly selecting $mtry$ out of d features to split a node. The value of $mtry$ is usually determined *a priori* equal to $d/3$.

RF provides an internal mechanism for evaluating the importance of each feature according to its contribution to the prediction of the target variable. The prediction error of each tree on its out-of-bag (OOB) data, i.e. the training instances that are not included in the bootstrap sample used to construct that tree, is utilized. Herein, the number of trees, $ntree$, is set to the default value of 500 provided that RF does not overfit as $ntree$ increases.

The importance ω_j of each feature F_j, with $j = 1,\ldots,d$, is calculated as follows:

1. For each tree T_k in the RF with $k = 1,\ldots,ntree$:
    a. Compute the Mean Squared Error (MSE) of T_k on its OOB data, MSE_k.
    b. Permute the values of feature F_j in the OOB data of T_k and compute the new OOB error $MSE_{k,j}$.
2. The raw importance score of feature F_j is given by:

$$\omega_j = \frac{1}{ntree}\sum_{k=1}^{ntree}\left(MSE_{k,j} - MSE_k\right) \tag{5.1}$$

5.2.3.2 RReliefF

RReliefF, a classical feature ranking algorithm for regression problems, is also employed [174]. RReliefF estimates the discriminative power of each feature F_j between adjacent instances by approximating the following difference of probabilities:

$$\omega_j = \frac{P_{diff\,C|diff\,F_j} P_{diff\,F_j}}{P_{diff\,C}} - \frac{\left(1 - P_{diff\,C|diff\,F_j}\right) P_{diff\,F_j}}{1 - P_{diff\,C}}, \tag{5.2}$$

where $P_{diff\,C}$ corresponds to the probability two nearest instances have different predictions,

$P_{diff\ F_j}$ corresponds to the probability that two nearest instances have different values for F_j, and $P_{diff\ C|diff\ F_j}$ corresponds to the probability that two nearest instances have different predictions and different values for F_j.

In particular, RReliefF approximates the above probabilities by iteratively (M times) selecting an instance u_m, finding its K nearest neighbours υ_k and computing the following quantities:

$$Q_{diff\ F_j} = \sum_{m=1}^{M}\sum_{k=1}^{K}\left|x_j^m - x_j^k\right|\alpha_{m,k}, \tag{5.3}$$

$$Q_{diff\ C} = \sum_{m=1}^{M}\sum_{k=1}^{K}\left|y_m - y_k\right|\alpha_{m,k}, \tag{5.4}$$

$$Q_{diff\ C\&\&diff\ F_j} = \sum_{m=1}^{M}\sum_{k=1}^{K}\left|y_m - y_k\right|\left|x_j^m - x_j^k\right|\alpha_{m,k}. \tag{5.5}$$

The city-block distance function (L_1 norm) is used to find the K nearest neighbours of u_m with respect to x_m, while K is set equal to 10. The distance between u_m and υ_k is taken into account through the term $\alpha_{m,k}$ such that closer instances have greater influence:

$$\alpha_{m,k} = \frac{e^{-\left(\frac{rank(u_m,\upsilon_k)}{\sigma'}\right)^2}}{\sum_{k'=1}^{K} e^{-\left(\frac{rank(u_m,\upsilon_{k'})}{\sigma'}\right)^2}}, \tag{5.6}$$

where $rank(u_m,\upsilon_k)$ is the position of υ_k in the list of nearest neighbours of u_m sorted by distance in ascending order and σ' ($\sigma' = 50$ by default) is a user-defined parameter. Moreover, M is set equal to its maximum value i.e. the number of training instances.

Finally, the estimastion of each ω_j is given by:

$$\omega_j = \frac{Q_{diff\ C\&\&diff\ F_j}}{Q_{diff\ C}} - \frac{Q_{diff\ F_j} - Q_{diff\ C\&\&diff\ F_j}}{M - Q_{diff\ C}}. \tag{5.7}$$

5.2.4 Short-Term Predictive Modelling of Glucose Concentration

Predicting glucose concentration in the subcutaneous space is essentially a regression problem that can be described by a linear model of the form:

$$f(x) = w^T \varphi(x) + b, \tag{5.8}$$

in which *w* is a vector of parameters, φ is a vector of fixed non-linear basis functions, and *b* is the bias parameter. The function $f : R^d \to R$ maps the input vector $x \in R^d$ to glucose concentration at time $t+l$, with t being the time at which the prediction is made and l the prediction horizon. In the present study, f is implemented through the SVR [156] and GP [167] methods, both utilizing a kernel function $\kappa(x, x')$ rather than working directly in the transformed feature space ϕ. The parameters of the model are learnt from the training set $\{(x^i, y_i)\}$, with $i = 1, \ldots, N$, of each subject.

5.2.4.1 Support Vector Regression

Given a new input $x \in R^d$, the predicted by SVR glucose concentration at time $t+l$ is expressed in terms of the kernel function as follows:

$$f(x) = \sum_{i=1}^{N} (a_i - a_i^*) \kappa(x, x^i) + b, \tag{5.9}$$

where the Lagrange multipliers a_i, a_i^* ($a_i \geq 0,\ a_i^* \geq 0$) are introduced in the constrained optimization process of w and, in our study, the kernel κ is a Gaussian RBF. The sparseness of SVR solution is ensured by employing an ε-insensitive error function; the corresponding Karush-Kuhn-Tucker conditions imply that $a_i a_i^* = 0$ for $i = 1, \ldots, N$ and that all points lying inside the ε-tube have $a_i = a_i^* = 0$. Moreover, the model's complexity is controlled by the regularization parameter C which is used in the error function.

5.2.4.2 Gaussian Processes

In the case of GP, the glucose for a new point $x \in R^d$ is estimated from a Gaussian distribution with mean and covariance given by:

$$\mu(x)=\sum_{i=1}^{N} a_i \kappa\left(x, x^i\right), \quad \boldsymbol{\sigma}^2(x)=\kappa(x, x)+\beta^{-1}-\mathbf{k}^T K_C{}^{-1}\mathbf{k}, \tag{5.10}$$

where a_i is the i^{th} component of $K_C{}^{-1}y$, with K_C denoting the $N \times N$ covariance matrix and $\mathbf{y}$ the target vector $\mathbf{y}=\left(y_1, y_2, \ldots, y_N\right)^T$, and the vector $\mathbf{k}$ has elements $\kappa\left(x, x^i\right)$ for $i=1, \ldots, N$. The squared exponential kernel is the default one for GP regression. The noise on the observed values y is considered and it is further assumed to be Gaussian distributed with zero mean and constant variance β for all x^i. The latter contributes to the total variance of the predictive distribution given by Eq. 10. In contrast to SVR, the kernel function κ must be evaluated for all possible pairs x^i and x^j resulting in a non-sparse model.

5.2.5 Evaluation of Feature Ranking

The effectiveness of feature ranking for a specific subject S is examined with respect to the predictive performance of SVR and GP. A forward selection procedure is employed where features are sequentially added in decreasing order of importance based on RF or RReliefF ranking. To estimate the error rate of the prediction method, an external 10-fold cross-validation is applied on the dataset $Z^{(s)}$ with feature ranking following the resampling procedure itself. The latter ensures that the dataset used in the ranking process does not overlap with the test set and, therefore, reduces the selection bias in the estimates of the prediction error [176-179]. The procedure used is described as follows:

1. Randomly partition $Z^{(s)}$ into 10 disjoint folds $Z_k^{(s)}$, with $k=1, \ldots, 10$, of equal size (i.e. $N_s/10$).
2. For $k=1, \ldots, 10$:
    a. Let $Z^{(s)}-Z_k^{(s)}$ be the training set and $Z_k^{(s)}$ the test set.
    b. Apply the RF or RReliefF algorithm to $Z^{(s)}-Z_k^{(s)}$ so as to produce a ranked list of features R_k.
    c. For $n=1, \ldots, d$:
        i. Let $Z_{k,n}^{tr}$ and $Z_{k,n}^{test}$ be produced from $Z^{(s)}-Z_k^{(s)}$ and $Z_k^{(s)}$, respectively, by

retaining the first n most important features according to R_k.

ii. Train SVR or GP glucose predictive model $\mathbf{M}_{k,n}$ on $Z_{k,n}^{tr}$.

iii. Test $\mathbf{M}_{k,n}$ on $Z_{k,n}^{test}$ and compute the related $RMSE_{k,n}$.

3. For $n = 1, \ldots, d$:

a. Compute the average RMSE for all 10 folds i.e. $RMSE_n = \frac{1}{10}\sum_{k=1}^{10} RMSE_{k,n}$.

As the notation implies, the ranked list of features R_k can be different for each k ($k = 1, \ldots, 10$). Moreover, it should be mentioned that the hyper-parameters of SVR and GP are optimized for each $Z_{k,n}^{tr}$. More specifically, the values of C, ε and γ minimizing the 4-fold cross-validation RMSE of SVR in $Z_{k,n}^{tr}$ are chosen by the Differential Evolution algorithm [157]. Regarding GP, the parameters of the squared exponential kernel along with the noise variance β are also learned for each $Z_{k,n}^{tr}$. In fact, they are internally optimized by the GP algorithm through the minimization of the negative log likelihood function, while multiple restarts are used to alleviate the local-minimum problem.

The performance of the average feature ranking (i.e. $\bar{R}$) is assessed in an unbiased way by precisely averaging, for each feature F_j, the scores obtained from the same fold of each 10-fold cross-validation across all patients as follows:

1. For $s = 1, \ldots, 15$:

a. Randomly partition $Z^{(s)}$ into 10 disjoint folds $Z_k^{(s)}$, with $k = 1, \ldots, 10$, of equal size (i.e. $N_s/10$).

2. For $k = 1, \ldots, 10$:

a. For $s = 1, \ldots, 15$:

i. Compute the importance scores of F by applying the RF or RReliefF algorithm to $Z^{(s)} - Z_k^{(s)}$. Let $\omega_k^{(s)} = \left[\omega_{k,1}^{(s)}, \ldots, \omega_{k,d}^{(s)}\right]$ where $\omega_{k,n}^{(s)}$, with

$n = 1, \ldots, d$, is the importance score of feature F_n based on $Z^{(s)} - Z_k^{(s)}$.

b. Compute $\varpi_k = \left[\varpi_{k,1}, \ldots, \varpi_{k,d} \right]$ by averaging $\omega_{k,n}^{(s)}$, with $n = 1, \ldots, d$, over S.

c. Compute the ranked list $\bar{R}_k$ by sorting ϖ_k in descending order.

Then, the same procedure is followed as for individualized ranking, with the difference that the dataset of each patient is not resampled and the list $\bar{R}_k$ is used in place of R_k. In this case, the average RMSE is denoted by $RMSE'_n$.

5.3 Results

Figure 5.1 shows the average value and the standard deviation of the importance scores W_j, with $j = 1, \ldots, 46$, over all 15 patients according to RF. The importance scores of features F_{1-8} and F_{9-46} are plotted separately to aid visualization. The predominance of the features corresponding to glucose concentration (i.e. F_{2-8}) is evident in both 30-min and 60-min horizons, with most recent values conveying more information. The contribution of the other features to the prediction of glucose by RF is comparatively lower but not insignificant, as will be demonstrated later. In particular, their importance increases and becomes apparent for a prediction horizon of 60 min, which can be attributed to the increase of the problem complexity. Regarding gl and SEE features, which are defined with respect to the time t, their most recent values are clearly found to explain better the glucose concentration in the short-term. This is the case only for Ra among the features representing the effect of meal and insulin intake (i.e Ra, SRa and I_p) and which have been defined with respect to the time $t + l$. More specifically, it was observed that for a few patients the values of SRa and I_p closer to the time $t + l$ are less associated with the glucose at that time. The evaluation of features by RReliefF exhibits similar patterns as it is shown in *Figure 5.2*. However, the difference in importance between gl and the other features is much less prominent and h is found to discriminate adjacent samples equally well as gl. We also observe a smooth change in importance score over time for each type of features and, in contrast to RF, the alterations between prediction horizons are not so notable.

The image plots in *Figure 5.3* and *Figure 5.4* illustrate the ranking of features obtained by RF and RReliefF, respectively, for each individual patient. Dark shades of grey correspond to high positions in the ranking, while light shades of grey represent low positions. It is obvious that h and the full I_p vector, in addition to gl, are ranked in the first positions for the majority of patients. On the other hand, there exist larger deviations in the ranking of the remaining features across patients, and especially of Ra and SRa. In particular for SEE, its most recent values (i.e. $SEE(t-20)$, $SEE(t-10)$ and $SEE(t)$) belong to the highly ranked features in more than 50% of the patients.

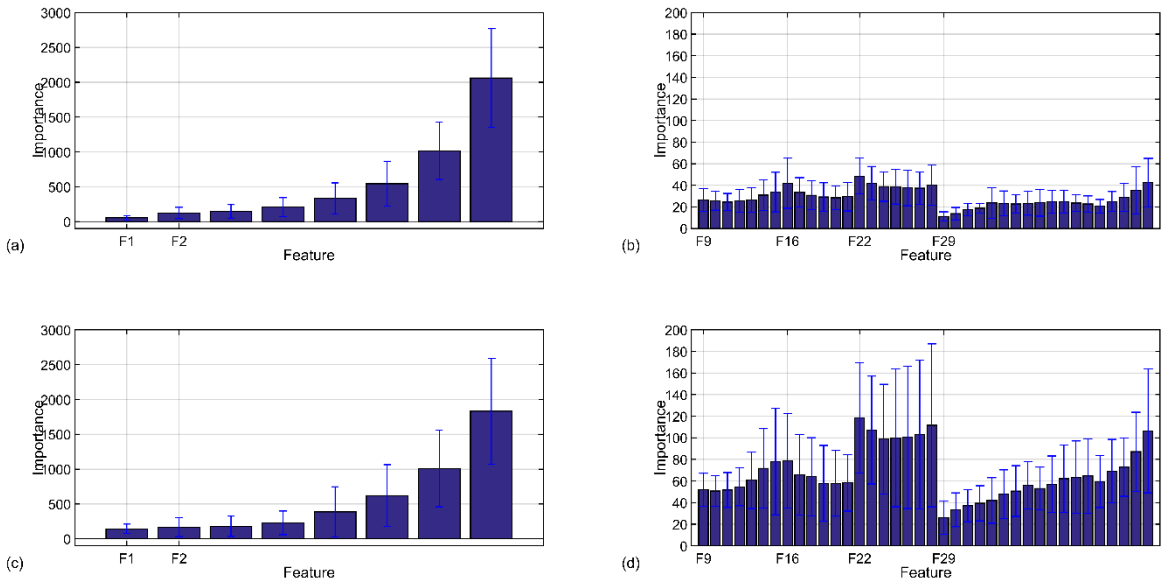

Figure 5.1 Average value and standard deviation of the importance of features based on RF algorithm for (a, b) 30-min and (c, d) 60-min predictions and for all patients. The x-axis labels correspond to the first feature of each type i.e. $F_1 = h$, $F_2 = gl(t-30)$, $F_9 = Ra(t+l-30)$, , $F_{22} = I_p(t+l-30)$ and $F_{29} = SEE(t-170)$.

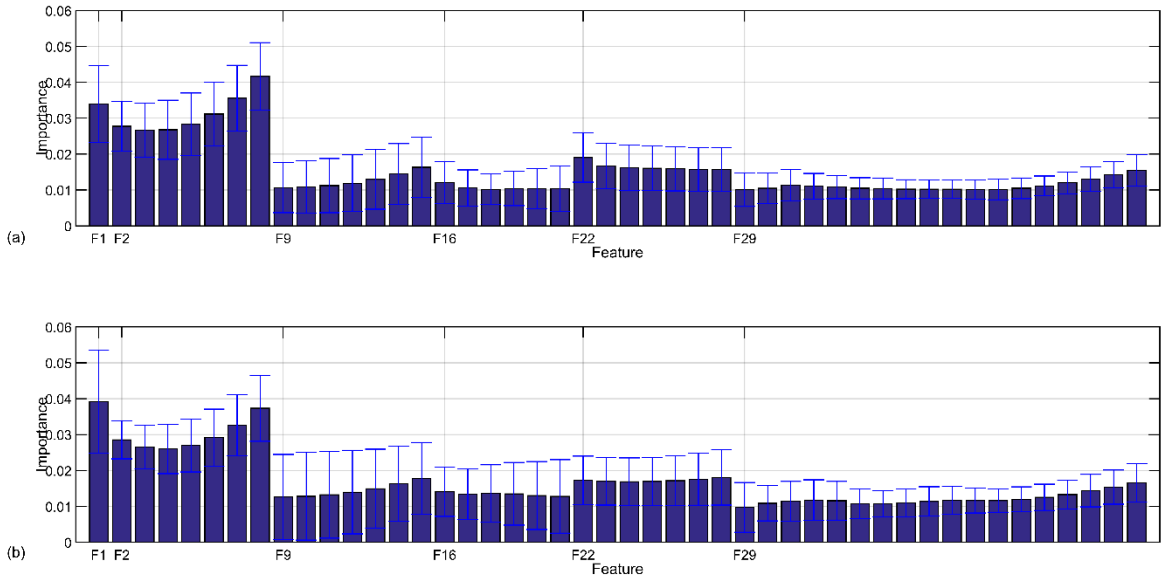

Figure 5.2 Average value and standard deviation of the importance of features based on RReliefF algorithm for (a) 30-min and (b) 60-min predictions and for all patients. The x-axis labels correspond to the first feature of each type i.e. $F_1 = h$, $F_2 = gl(t-30)$, $F_9 = Ra(t+l-30)$, $F_{16} = SRa(t+l-75)$, $F_{22} = I_p(t+l-30)$ and $F_{29} = SEE(t-170)$.

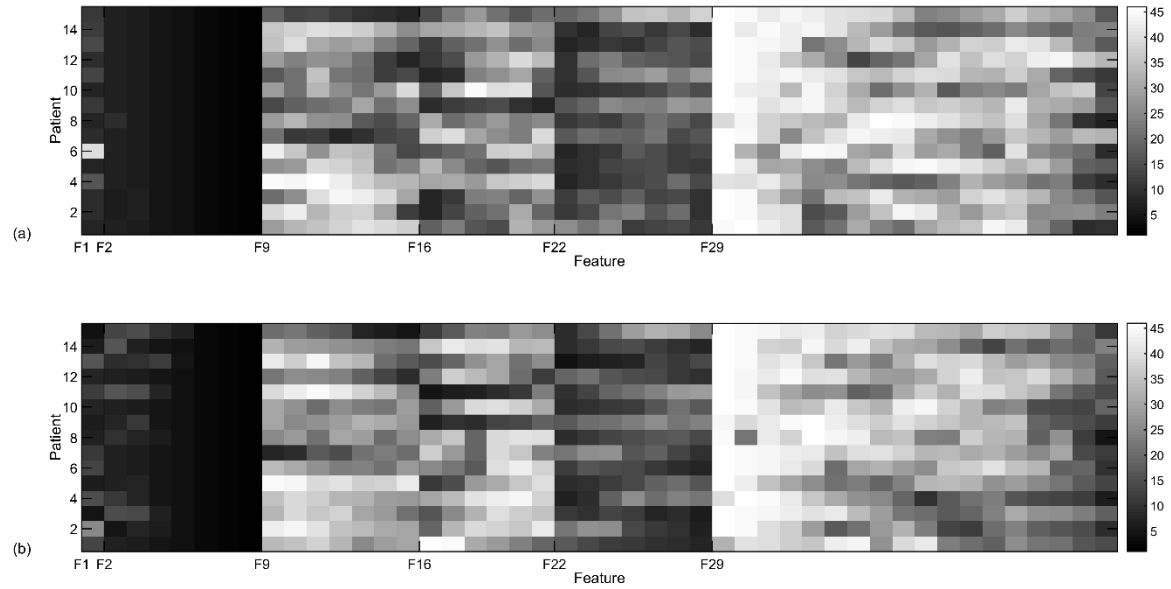

Figure 5.3 Image plot of RF-ranking for each patient for (a) 30-min and (b) 60-min prediction horizon. Darker shades of gray indicate a higher ranking position and lighter shades of gray represent a lower one. The x-axis labels correspond to the first feature of each type i.e. $F_1 = h$, $F_2 = gl(t-30)$, $F_9 = Ra(t+l-30)$, $F_{16} = SRa(t+l-75)$, $F_{22} = I_p(t+l-30)$ and $F_{29} = SEE(t-170)$.

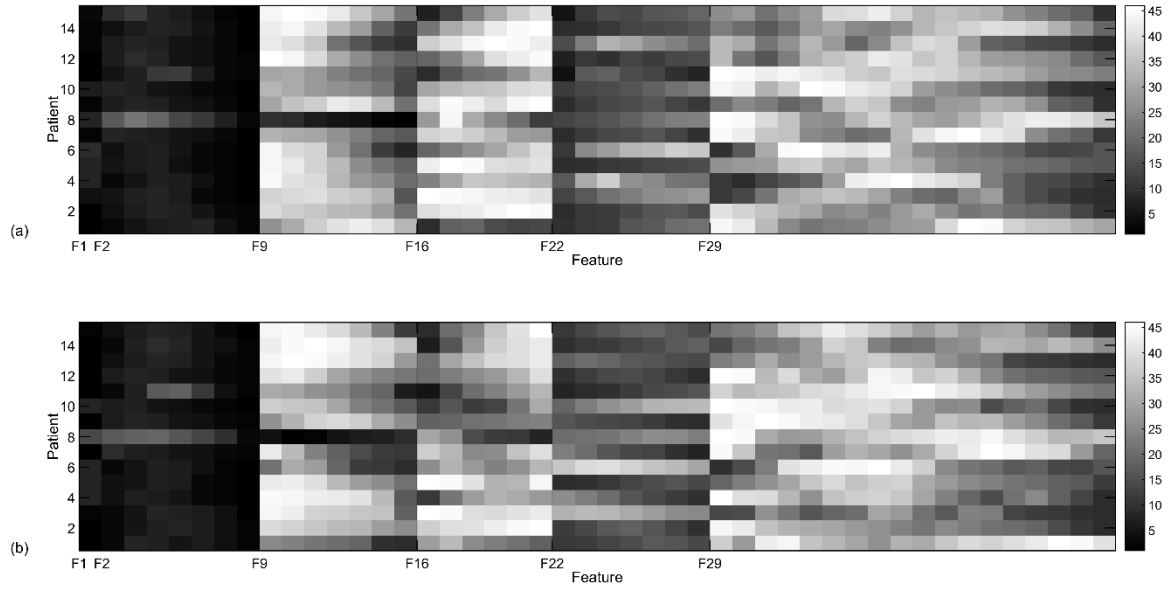

Figure 5.4 Image plot of RReliefF-ranking for each patient for (a) 30-min and (b) 60-min prediction horizon. Darker shades of gray indicate a higher ranking position and lighter shades of gray represent a lower one. The x-axis labels correspond to the first feature of each type i.e. $F_1 = h$, $F_2 = gl(t-30)$, $F_9 = Ra(t+l-30)$, $F_{16} = SRa(t+l-75)$, $F_{22} = I_p(t+l-30)$ and $F_{29} = SEE(t-170)$.

In *Figure 5.5* and *Figure 5.6* the average $RMSE_n$ and $RMSE'_n$ of SVR and GP, respectively, over all 15 patients are plotted against the top-ranked ($n = 1,\ldots,46$) features for a prediction horizon of 30 min. *Figure 5.7* and *Figure 5.8* illustrate the same information for 60-min horizon. We observe that the average $RMSE_n$ curve shows a sigmoidal behaviour after the first iteration. Its convergence for almost $d/2$ features implies that both feature ranking algorithms properly locate high in hierarchy the most predictive features of glucose concentration. It is obvious that RReliefF outperforms RF in the first few iterations ($n \approx 7$), which is more evident in the case of GP (with the exception of $n = 1$ where RF yields to a significantly smaller error). This could be explained by considering that RReliefF, for the majority of the patients, locates the feature h in the first positions along with the gl values. For greater values of n, both algorithms lead to comparable average errors, although RF has systematically a slightly better performance for $n > 15$.

Similar observations hold for the $RMSE'_n$ where the average ranking of the features has been used. As it can be observed for 30-min horizon (*Figure 5.5* and *Figure 5.6*) the predictive capability of the features ranked by RF in the first $n \leq 8$ positions, according to the

individualized scores, is comparable with that of the average scores. After this point and until convergence is achieved, the average RF-ranking, especially for SVR, yields to smaller 30-min errors compared with the individualized one. The opposite behaviour is observed for RReliefF, in which the 30-min predictions with $n > 8$ best features are slightly better when the individualized scores are considered. As it is shown in *Figure 5.7* and *Figure 5.8*, when the horizon increases to 60-min, the individualized RF-ranking becomes superior to the average one for $n \leq 8$. This can be attributed to the fact that the average RF-ranking includes the full gl vector and the h in the first positions, whereas in the individualized case the Ra, SRa, I_p, and SEE features are occasionally included. Then, for both RF and RReliefF, the individualized ranking is clearly better than the average one for $n > 12$ and until convergence.

Figure 5.5, *Figure 5.6*, *Figure 5.7*, *Figure 5.7* and *Figure 5.8* are also annotated with the average RMSE concerning three of the input cases which were defined in our previous study [130], namely Case1 (gl), Case4 (h, gl, Ra, SRa, I_p) and Case 6 (h, gl, Ra, SRa, I_p, SEE). We can see that the average error of Case 4, in which the number of features is 28, can be obtained with much less features. Moreover, a better solution can be also achieved even when the 7 best features are used instead of Case 1.

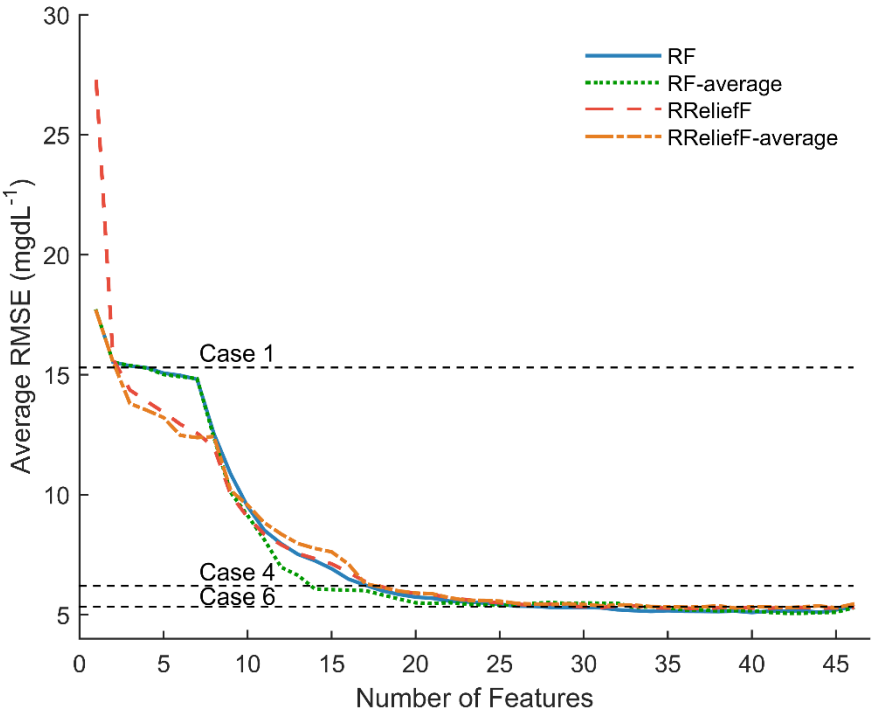

Figure 5.5 Average 10-fold cross-validation RMSE rate of SVR regression models over all 15 patients against the top-ranked features identified by RF and RReliefF for prediction horizon of 30 min.

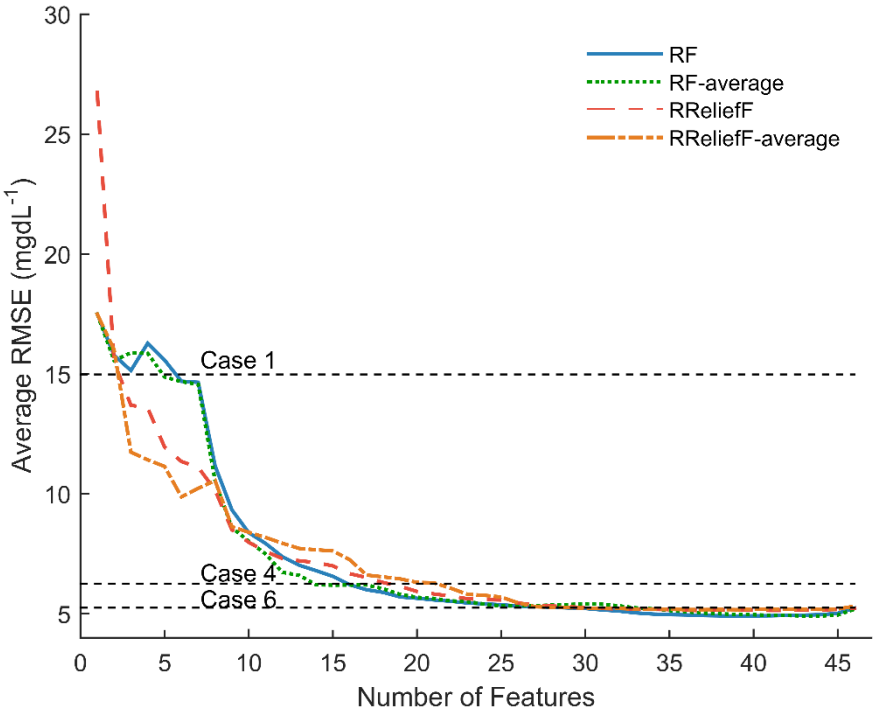

Figure 5.6 Average 10-fold cross-validation RMSE rate of GP regression models over all 15 patients against the top-ranked features identified by RF and RReliefF for prediction horizon of 30 min.

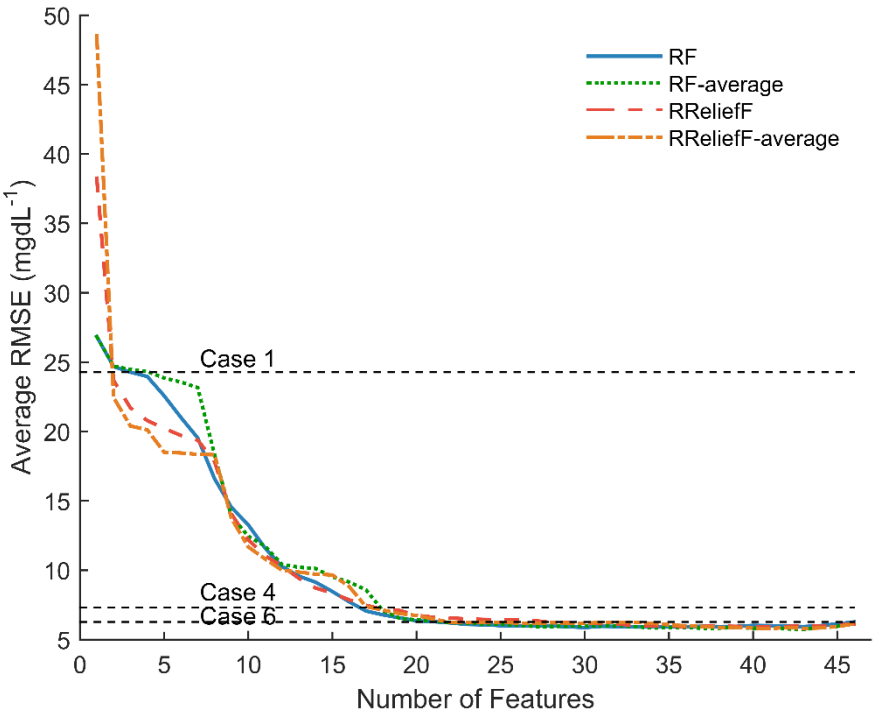

Figure 5.7 Average 10-fold cross-validation RMSE rate of SVR regression models over all 15 patients against the top-ranked features identified by RF and RReliefF for prediction horizon of 60 min.

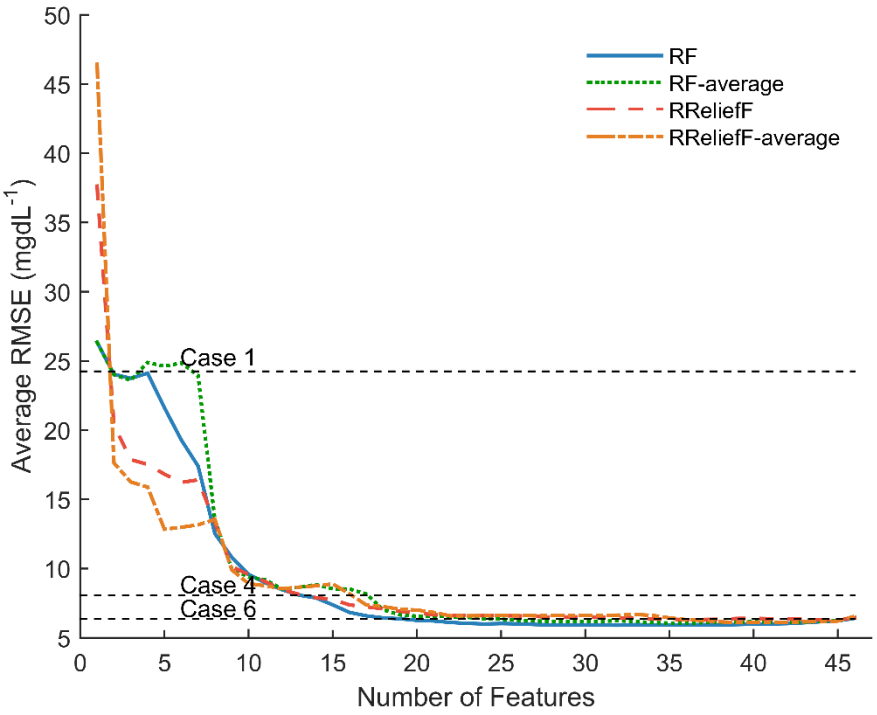

Figure 5.8 Average 10-fold cross-validation RMSE rate of GP regression models over all 15 patients against the top-ranked features identified by RF and RReliefF for prediction horizon of 60 min.

The number of best features to which the average $RMSE_n$ and $RMSE'_n$ converge within 5% of the value obtained with $n = 46$ features (i.e. n_c and n'_c, respectively) was calculated. *Table 5.2* presents the average value of n_c and n'_c over all patients and the corresponding standard deviation. We can see that SVR and GP generally converge a little faster in the case of RF than in the case of RReliefF. The average values of n_c and n'_c concerning the 30-min predictions are close to each other. Nevertheless, in most of the cases the 60-min error curves converge considerably faster when features are ranked individually for each subject.

5.4 Discussion and Conclusions

A study on the evaluation of short-term predictors of subcutaneous glucose concentration in type 1 diabetes was presented. This problem was addressed for the first time in the literature with the aid of RF and RReliefF algorithms, which were applied to self-monitoring data. Their efficacy was verified with respect to the predictive performance of two machine-learning regression models.

Table 5.2 Number of Features to which the RMSE Rate Converges for all 15 Subjects

	Prediction Horizon			
	30 min		60 min	
	SVR	GP	SVR	GP
Individualized Ranking				
RF	22.3±7.0	22.5±7.7	21.5±6.8	18.1±8.9
RReliefF	24.5±8.0	24.8±9.2	24.7±10.2	22.3±10.6
Average Ranking				
RF	21.4±7.5	22.9±9.7	26.5±9.5	24.6±12.6
RReliefF	24.9±5.9	25.6±7.4	23.5±7.6	26.4±11.6

Data are mean±standard deviation values.

The need to augment the input of predictive models with features able to reveal the daily dynamics of glucose concentration is critical. The utilization of information on meals, insulin therapy and physical activities, besides glucose time series, has been shown to lower the prediction error [83, 94, 96, 106, 107, 112, 130, 172]. The proposed dataset, in addition to the glucose signal and the time of the day, includes some novel features highly connected to glucose dynamics. First, the future values of the Ra and I_p simulated signals were used by expanding the simulation time from the present time up to the time for which the prediction is to be made and provided that that no future event (i.e. meal, insulin injection) will occur during that period. This approach was also followed in [94] for the Ra signal with the difference that meal information should be announced by the patient l min in advance. Nevertheless, the area under the Ra curve has not been introduced elsewhere as a predictor variable. Similarly, the variable SEE, which represents the cumulative EE over time, was first introduced in [130]. Actually, the few studies using information from a physical activity monitor for making predictions are based only on the past instantaneous values of physiological signals (e.g. EE, GSR, heat flux) [106, 107]. However, the effect of all these variables on glucose metabolism varies considerably among type 1 diabetes patients due to a combination of environmental and biological factors. In addition, the efficient representation of the temporal dependencies between the input variables and the glucose concentration can be challenging. On this basis, we attempted to evaluate separately for each patient the proposed feature set, whose predictive capacity has already been validated as a whole. This is the main novelty of this work, since to the authors' knowledge, there has been no other attempt to determine and assess the importance of such a multivariate feature set for predicting glucose at the individual level.

RF and RReliefF are two entirely different feature ranking algorithms but both are well-suited for regression problems [174, 175]. The importance score computed for each feature by RF expresses the increase in the OOB prediction error when its values are randomly permuted (to mimic its absence in the prediction). It should be mentioned that the OOB error is an unbiased estimation of the generalization error of RF, which converges as the number of trees increases [173]. On the other hand, RReliefF is a statistical approach that approximates the probabilities of (non)separation of near instances by a given feature across the problem space. An appealing property of both algorithms is that they are context sensitive i.e. they take into account all attributes when estimating their importance. More specifically, RF can efficiently learn the relationships hidden in the dataset, while RReliefF detects existing dependencies in the feature space by exploiting the distance between instances. As a result, both algorithms behave well in the presence of groups of highly-correlated features, which is the case in our problem. Moreover, as opposed to shrinkage methods for linear regression [180], RF and RRelief do not assume a linear and sparse (with many zero regression coefficients) model. This is of particular importance in glucose predictive modelling where linear and nonlinear components of glucose dynamics should be described. Another important class of embedded methods use the change in the objective function when one feature is removed or added as a ranking criterion and, in combination with a greedy search strategy, they yield nested subsets of features e.g. Recursive Feature Elimination [181]. However, in this approach the prediction technique should be retrained for each new subset of features (i.e. d times in stepwise feature selection); whereas, RF needs to be fitted to the training set only once. Note that the computational complexity of RF (i.e. $\mathrm{O}\left(ntree \cdot mtry \cdot N \cdot \log N\right)$ with $mtry = d/3$) can be considered comparable to that of RReliefF (i.e. $\mathrm{O}\left(d \cdot N \cdot \log N\right)$, despite being an embedded method.

The way the two feature ranking algorithms operate is definitely reflected in their output. In particular, RF's output reveals: (i) the infeasibility of predicting the subcutaneous glucose concentration without exploiting its recent values (e.g. the average OOB MSE increases by ≈2000 mg·dL^{-1} when $gl\left(t\right)$ is randomly permuted) and (ii) the more pronounced effect of the other features with increasing prediction horizon. On the other hand, the fact that RReliefF computes the discriminative (and not the predictive) ability of each feature being, however, aware of the context of other features can explain: (i) the lack of great differences in features' scores, (ii) the similarity of the output between prediction horizons and (iii) the

smooth transition in scores over time for features of the same type.

Both RF and RRelief highlighted how essential is the subcutaneous glucose signal itself for both prediction horizons and for all 15 patients. Of great interest is that the time at which the predictions are made (i.e. h) is systematically located in the first positions and its score is comparable to that of glucose. This reflects the existence of daily (24 h) patterns in glucose time series which are imposed either by each patient's lifestyle or by circadian rhythms related to glucose homeostasis [137, 138]. The contribution of the other features was also well demonstrated, with I_p features outweighing on average Ra, SRa and SEE ones. In addition, both algorithms, and especially RF, revealed some rational attenuation trends over time in average scores of gl, Ra, and SEE [91, 155, 182, 183]. The effect of I_p seems to be less immediate (since its scores tend to decrease as getting closer to the time of prediction $t+l$), which can be considered consistent with clinical evidence indicating inherent delays in peripheral and hepatic insulin action [184]. Moreover, the results support the existence of substantial inter-patient differences.

Short-term predictive modelling of the subcutaneous glucose concentration using SVR and GP further verified the quality of the resulting feature ranking. The behaviour of the average $RMSE_n$ curve did confirm that the top-ranked features constitute the best predictors of glucose in the examined feature set. The fact that the prediction performance did not degenerate by applying the average feature ranking reveals the generalizability and robustness of the results. In particular, individualized feature ranking was found to be more appropriate for 60-min predictions, which may suggest personalized glucose predictive approaches are preferable as prediction horizon increases. Regarding the short-term glucose dynamics (i.e. 30-min horizon), the convergence rate of the average $RMSE'_n$ error curve was similar with that of the average $RMSE_n$ curve. Moreover, the convergence of both error curves for a considerably smaller than $d=46$ number of features, and the consequent reduction of the input size, is indeed of paramount importance for regression analysis. Nevertheless, we did not find a certain point after which the average error starts to increase, which is mainly due to the fact that all features are relevant to the studied problem. We should mention at this point that the two kernel-based techniques were chosen due to their high prediction accuracy in both normal and critical glucose value regions [131]. However, other well-established machine-learning regression techniques could be also applied.

Table 5.3 presents a comparison of the proposed work with other literature studies utilizing a multivariate dataset. Note that the prediction error provided for SVR and GP corresponds to the first $n = 20$ best features. A direct comparison of the presented results is not fair since they have been derived by different training/testing approaches. In [94, 96], the predictive models are tested on patients not included in the training set, while those in [106, 107, 112] are recursively trained on each patient dataset. Our results indicate that multivariate non-linear regression models can provide predictions of high accuracy, which is also in agreement with previous findings. Moreover, we can see that the inclusion of information on physical activities is able to improve performance even when a linear model is adopted. The main difference of our work is that the input is not predefined but it is selected separately for each patient from a high-dimensional feature set which may result in much simpler models.

Table 5.3 Comparison with other Methods reported in the Literature

Study	**Method**	**Feature set (number of features)**	**Dataset**	**Prediction Horizon (min) / RMSE ($mg \cdot dL^{-1}$)**
Zecchin et al. (2012) [94]	Feed-forward neural network and first-order polynomial model	CGM data, glucose rate of appearance after a meal (8)	15 Type 1 diabetic subjects	30 / 14.0±4.1
Eren-Oruklu et al. (2012) [106]	Recursive ARMAX model	CGM data, EE, average longitudinal acceleration, near-body temperature, heat flux, GSR (15)	5 Type 2 diabetic subjects	30 / 4.2±5.1[1]
Turksoy et al. (2013) [107]	Recursive ARMAX model	CGM data, insulin on board, EE, GSR (20)	14 Type 1 diabetic subjects	30 / 11.7 60 / 34.7
Daskalaki et al. (2013) [112]	Online adaptive RNN	CGM data and insulin pump infusion rate (N/A, patient-specific)	23 Type 1 diabetic subjects	15 / 11.9 30 / 18.9 45 / 26.1
Zecchin et al. (2014) [96]	Jump neural network model	CGM data, glucose rate of appearance after a meal (4)	20 Type 1 diabetic subjects	30 / 16.6±3.1
This work	SVR – RF	CGM data, glucose rate of appearance after a meal, plasma insulin concentration, EE, time of the day (20)	15 Type 1 diabetic subjects	30 / 5.7±1.5 60 / 6.4±2.1
	SVR - RRF			30 / 5.9±1.4 60 / 6.8±2.0
	GP – RF			30 / 5.6±1.7 60 / 6.3±2.6
	GP - RRF			30 / 5.9±1.6 60 / 6.8±2.9

Data are mean±standard deviation values.
[1]This value refers to RAD (%).

The fact that RF and RReliefF algorithms yield consistent results across multiple subjects for both 30-min and 60-min prediction horizons implies their potential for use as an exploratory tool in the predictive analysis of type 1 diabetes data. Given the monitoring data of a new unseen patient, these algorithms can be applied to obtain a first reliable estimate of the predictive capability of the input variables. Certainly, the low computational complexity of feature ranking allows one to investigate longer latency time intervals than those examined in this study as well as to examine the impact of new descriptive features. The specification of the dimension of the input with respect to a regression technique requires employing the forward selection procedure, not necessarily in an exhaustive way, but for some subsets of features until the error converges. Similarly, the average ranking of the features could be utilized in the construction of "generalized" predictive models from the entire patients' set. Again, the precise merging of the same folds of each 10-fold cross-validation across all patients would be needed to ensure unbiased estimates of the prediction error. As a future work, RF and RReliefF need to be evaluated in a large number of patients over a long period of time. To this end, both algorithms could be also tested on patients who are monitored during different time periods to investigate how consistent are the results for a patient and what is the effect of lifestyle or physiological changes. In any case, the clinicians should interpret the calculated set of best features together with other clinical information.

CHAPTER 6. SHORT-TERM PREDICTION OF GLUCOSE IN TYPE 1 DIABETES USING KERNEL ADAPTIVE FILTERS

6.1 Introduction

Well-established representations of $\hat{y}(t|\theta) = f\left(Z^{t-pT}, \theta\right)$ from linear system theory have been applied to glucose predictive modelling by assuming that the underlying system of glucose is linear and time-invariant [70, 87, 185]. Nonlinearity is incorporated into the glucose model by black-box parameterizations and, particularly, neural networks and kernel-based regression models, which, however, rely on batch learning algorithms (e.g. back-propagation, quadratic programming) [90, 96, 97, 102, 114, 130, 131, 185, 186]. Weighted recursive least squares, with an adjustable forgetting factor, has been used in the identification of multivariate ARMAX models of subcutaneous glucose dynamics in both type 1 [107, 108] and type 2 diabetes [105, 106]. Physiological signals related to a subject's physical activity or emotional condition (EE, GSR) as well as information on insulin regime (insulin on-board) complemented the input of the ARMAX models and, in conjunction with physiological constraints imposed to model's parameters, led to stable accurate short-term (30-min ahead) predictions. Nevertheless, the dominance of a discrete-time nonlinear dynamic system of glucose in type 1 diabetes identified by an EKF over a recursively-identified ARX model having a similar configuration indicates a need for nonlinear adaptive learning of the glucose system [109].

Naumova et al. proposed a novel subject-independent approach to iteratively

selecting/adjusting the hyper-parameters of a Tikhonov regularization-learning algorithm (i.e. the regularization parameter and the parameters of the kernel generating the associated reproducing kernel Hilbert space) to each new input, which was evaluated in the context of the blood glucose concentration prediction. [101]. Both 30-min and 60-min predictions of that regularized scheme with input previous, but not-necessarily equi-sampled, CGM measurements were significantly better compared to two state of the art glucose prediction methods [89, 114]. Zhao et al. utilized the concept of model migration; a base ARX model is first built from a representative subject and, then, proper customization of the parameters related to the exogenous inputs (i.e. food and insulin) is performed for a new subject using a small amount of data [86]. Results for *in-silico* subjects show that model migration presents better generalization ability than individualized ARX models when training and testing conditions differ.

The purpose of this work is: (i) to present a recursive multivariable KAF approach to personalized short-term glucose prediction in type 1 diabetes, and (ii) to demonstrate the validation of the proposed predictive model on patients with type 1 diabetes in free-living conditions. The novelty of the proposed glucose prediction model consists in that recursivity is performed in the RKHS such that the number of adjustable parameters is finite and upper bounded. In particular, either the QKLMS-FB [187, 188] and the KRLS-ALD [189] algorithms are employed for comparison purposes. A preliminary version of this work has been reported, which introduced KAF (QKLMS-FB in [190] and KRLS-ALD in [191]) to auto-regression of subcutaneous glucose concentration in type 1 diabetes. Herein, both univariate AR and multivariate input models are constructed and compared aiming at methodically elucidating the predictive potential of the exogenous inputs especially in critical hypoglycaemic and hyperglycaemic regions. Moreover, an extensive evaluation and comparison of QKLMS-FB and KRLS-ALD algorithms is presented aiming at featuring their efficacy in adaptive learning of subcutaneous glucose concentration course, which could advance the major ongoing research in the field.

6.2 Materials and Methods

6.2.1 Subjects

A short-term observational study was carried out as part of the METABO study [152]. The

study was approved by the Ethics Committees of the participating hospitals (i.e. Parma University Hospital, Parma and University Hospital Motol, Prague) and all subjects provided written informed consent before enrolment.

Fifteen people with type 1 diabetes (3F/12M, age: 40.3±13.5 y/o, BMI: 25.2±2.9 kg·m^{-2}, HbA1c: 7.1±1.2%), following multiple-dose insulin therapy and without significant micro- and macro-vascular complications, were monitored from 5 to 22 days (average 12.5±4.6) in free-living conditions. Patients were equipped with the Guardian® Real-Time CGM system (Medtronic Minimed Inc.) and the SenseWear® Armband (BodyMedia Inc.) physical activity monitor. They were also methodically recording information on daily food intake and insulin regime.

6.2.2 Problem Formulation

Consider a sequence of input-output pairs $Z = \left\{\left(x^i, y_i\right)\right\}_{i=1}^{N}$, where $\left(x^i, y_i\right) \in Z = X \times Y$, $X \subseteq R^d$ and $Y \subseteq R$. Each sample $\left(x^i, y_i\right) \equiv \left(x\left(t_i - pT\right), y\left(t_i\right)\right)$ associates the input vector x^i corresponding to observations up to time $t_i - pT$ with the observation of subcutaneous glucose concentration y_i at time t_i, where p is the prediction step and $T = 5\,\text{min}$ is the sampling interval of the subcutaneous glucose concentration. For ease of notation we will assume $t_{i+1} - t_i = T$. Our objective is to incrementally learn a sparse regularized kernel-based approximation $f : R^d \to R$ of the true mapping such that f_i (the estimate of f at time t_i) is updated on the basis of the previous model f_{i-1} and the instantaneous prediction error $e_i = y_i - f_{i-1}\left(x^i\right)$ on the current sample $\left(x^i, y_i\right)$ (*Figure 6.1*a) [192].

The input $x\left(t\right) \in R^d$ is formed by past sequences of 5 variables $\left\{v_i\right\}_{i=1}^{5}$, which are defined by an embedding dimension n_{v_i} and a delay time Δt_{v_i}:

1. $\left[gl\left(t - \left(n_{gl} - 1\right)\Delta t_{gl}\right), \ldots, gl\left(t - \Delta t_{gl}\right), gl\left(t\right)\right]$: The subcutaneous glucose concentration within the last 30 min with respect to t given a delay time equal to its sampling period $\Delta t_{gl} = T = 5\,\text{min}$ and $n_{gl} = 7$. This is in accordance with previous studies in diabetes

showing a strong autocorrelation and short-term predictive capacity of glucose samples which are 30 or fewer minutes apart [71, 90, 91, 106, 186].

2. $\left[Ra\left(t-\left(n_{Ra}-1\right)\Delta t_{Ra}\right),\ldots,Ra\left(t-\Delta t_{Ra}\right),Ra\left(t\right)\right]$: The rate of appearance of exogenous glucose into plasma within the interval $\left[t-30,t\right]$ with $\Delta t_{Ra}=T=5\,\text{min}$ and $n_{Ra}=7$ [155]. It should be mentioned that the computational time step of Ra is 1 min; however, Ra is resampled concurrently with the output y assuming that it is constant between discrete time instants $iT\le t\le\left(i+1\right)T$.

3. $\left[SRa\left(t-\left(n_{SRa}-1\right)\Delta t_{SRa}\right),\ldots,SRa\left(t-\Delta t_{SRa}\right),SRa\left(t\right)\right]$: The exogenous glucose absorbed into plasma calculated cumulatively every $\Delta t_{SRa}=15\,\text{min}$ over the last 90 min with $n_{SRa}=6$ and $SRa\left(t'\right)=\sum_{s=t-90}^{t'}Ra\left(s\right)$. The time interval of 90 min reflects the peak time of Ra following the ingestion of a meal and, it is approximately equal to half the length of the postprandial state [17]. Via the introduction of the variable SRa, we exploit the area under the Ra curve aiming at capturing the cumulative effect of exogenous glucose inserted in the plasma over time.

4. $\left[I_p\left(t-\left(n_{I_p}-1\right)\Delta t_{I_p}\right),\ldots,I_p\left(t-\Delta t_{I_p}\right),I_p\left(t\right)\right]$: The plasma insulin concentration within the time interval $\left[t-30,t\right]$ with $\Delta t_{I_p}=T=5\,\text{min}$ and $n_{I_p}=7$ [153]. The I_p input signal is computed every 1 min, however, similarly to the Ra signal, it is kept constant over the sampling interval $T=5\,\text{min}$.

5. $\left[SEE\left(t-\left(n_{SEE}-1\right)\Delta t_{SEE}\right),\ldots.SEE\left(t-\Delta t_{SEE}\right),SEE\left(t\right)\right]$: The EE calculated cumulatively every $\Delta t_{SEE}=10\,\text{min}$ over the last three hours with $n_{SEE}=18$ and $SEE\left(t'\right)=\sum_{s=t-180}^{t'}EE\left(s\right)$. The term EE expresses the instantaneous EE sampled every 1 min. Thus, we investigate the immediate or short-term effect of physical activities or exercise performed over the last 3 hrs on the glucose-insulin metabolism.

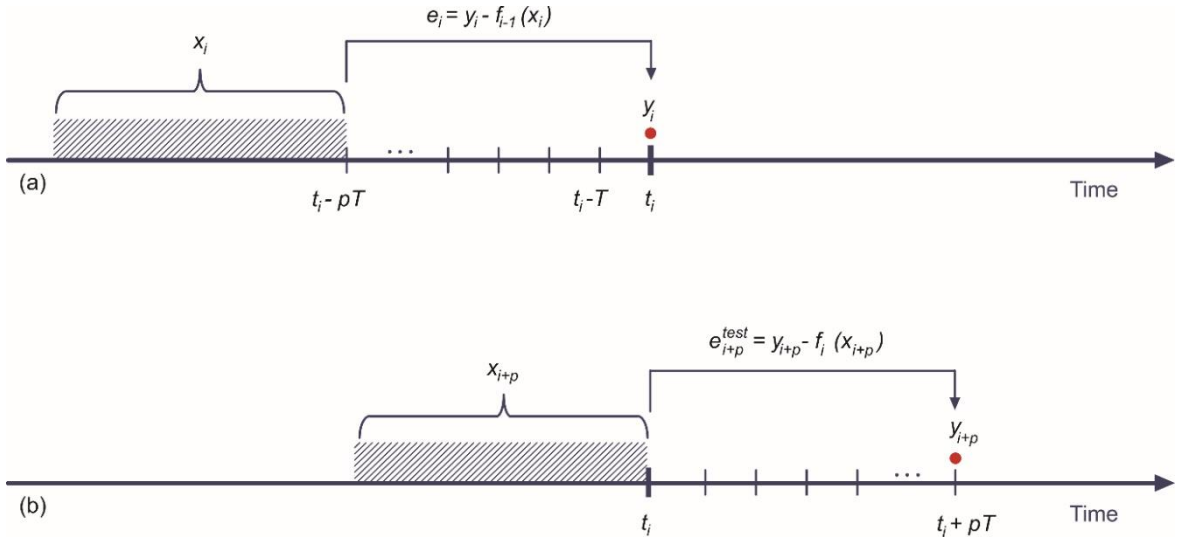

Figure 6.1 Online (a) learning and (b) testing of the glucose prediction model.

We have defined three input cases, namely Case 1 (gl), Case 2 (gl, Ra, SRa, I_p) and Case 3 (gl, Ra, SRa, I_p, SEE), in order to examine the effect of the different input variables on the prediction accuracy.

6.2.3 Kernel Adaptive Filters

According to the reproducing kernel theory, there exists a RKHS H and a mapping $\varphi: \mathrm{X} \to H$ such that $\varphi(x) = \kappa(x, \cdot)$, where $\kappa: X \times X \to R$ is a positive definite kernel, and the minimizer $f_i \in H$ lies in the span of the finite set of kernels centred at the input vectors $x^1, x^2, \ldots, x^i$. Herein, a Gaussian kernel has been applied, with σ denoting its bandwidth. QKLMS-FB [187, 188] and KRLS-ALD [189] attain a sparse solution by sequentially building a dictionary $Q \subset X$, which content at iteration i is denoted by $Q(i) = \left\{q^j(i)\right\}_{j=1}^{m_i}$. Given a new input $x \in R^d$, the output $f_i(x)$ is expressed as follows:

$$f_i(x) = \sum_{j=1}^{m_i} a_j(i) \kappa\left(q^j(i), x\right) \tag{6.1}$$

where $a_j(i)$ denotes the j^{th} component of the coefficient vector $a(i) = \left[a_1(i), \ldots, a_{m_i}(i)\right]^T$ at

iteration i. QKLMS-FB relies on stochastic gradient descent and, similarly to KLMS, at each iteration i, updates only the coefficient of the new centre, i.e. $a_{m_i}(i)$, or quantizes a redundant sample to its nearest centre. KRLS-ALD, at each iteration i, minimizes the sum of squared errors over the current dictionary and, as such, it updates the coefficient associated with the new centre, i.e. $a_{m_i}(i)$, and all previous coefficients, i.e. $a(i-1)$. The latter results in an order of magnitude higher convergence rate than that of QKLMS-FB. Nevertheless, the dependence of KRLS-ALD on the Gram matrix $\tilde{\mathbf{K}}(i-1)$ defined on $Q(i-1)$ increases the time and space complexity from $O(m_i)$ in QKLMS-FB to $O(m_i^2)$. The adaptive learning process is outlined in *Table 6.1*. In the following subsections, we focus on the sparsification process employed in each algorithm.

Table 6.1 Adaptive Learning of Subcutaneous Glucose Concentration

Input: $\left\{\left(x^i, y_i\right) \middle| x^i \in R^d, y_i \in R\right\}, i = 1, 2, \ldots$, kernel κ, algorithms's hyperparameters

Computation:

while $\left(x^i, \mathrm{y}_i\right)$ is available

A. Adaptive Learning Phase

1. Predict the output $\hat{y}_i = f_{i-1}\left(x^i\right)$ according to (6.1).
2. Compute the error $e_i = y_i - \hat{y}_i$.
3. Evaluate the sparsification criterion (QKLMS-FB: (6.2); KRLS-ALD: (6.9)) and update accordingly the dictionary $Q(i)$.
4. Update the parameters' vector $a(i)$ (equivalently the solution f_i) based on e_i and according to the applied algorithm.

B. Prediction and Testing Phase

1. Predict the output $\hat{y}_{i+p} = f_i\left(x^{i+p}\right)$.
2. Evaluate the test error $e_i^{test} = y_i - f_{i-p}\left(x^i\right)$

end while

Output: $a(i), Q(i)$

6.2.3.1 Fixed Budget Quantized Kernel Least Mean Square Algorithm

QKLMS-FB controls the growth of the dictionary by using a quantization parameter ε_x and a maximum size M. A new input vector x_i is included into $Q(i-1)$ if their distance is greater than ε_x [188]:

$$dis\left(x^i, Q(i-1)\right) = \min_{1\le j\le m_{i-1}} \left\| x^i - q^j(i-1) \right\| > \varepsilon_x \tag{6.2}$$

whereas the less significant centre is first eliminated from $Q(i-1)$ when $m_{i-1} = M$. The significance of a centre q_k at iteration i is denoted by $E_k(i)$ and represents the average error induced in the prediction of all observations up to time t_i, $\left\{x^j\right\}_{j=1}^{i}$, by removing q_k [187]:

$$E_k(i) = \frac{\eta\left|a_k(i)\right|}{i} \sum_{j=1}^{i} \kappa\left(x^j, q^k\right) \tag{6.3}$$

with η denoting the step size parameter and $\eta\left|a_k(i)\right|\kappa\left(x^j, q^k\right)$ the error injected in the prediction of the sample $\left(x^j, y_j\right)$. To reduce the computational complexity of (6.3) (i.e. $O(i)$), the probability density function of X (i.e. $p(x)$) is exploited:

$$\lim_{i\to\infty} E_k(i) = \eta\left|a_k(i)\right| \int_X \kappa\left(x, q^k\right) p(x)\, dx \tag{6.4}$$

where $p(x)$ is estimated by the Parzen window method considering a Gaussian kernel κ_p such that:

$$\hat{p}(x) = \frac{1}{i} \sum_{j=1}^{i} \kappa_P\left(x, x^j\right) \tag{6.5}$$

Thus, (6.4) is written as:

$$E_k(i) = \frac{\eta\left|a_k(i)\right|}{i} \sum_{j=1}^{i} \int_X \kappa\left(x, q^k\right) \kappa_P\left(x, x^j\right) dx \tag{6.6}$$

Input data quantization is likewise applied at this step such that the contribution of each $\left\{x^j\right\}_{j=1}^{i}$

to $p(x)$ is approximated by its nearest centre:

$$E_k(i) = \frac{\eta|a_k(i)|}{i}\sum_{j=1}^{M}\int_X \lambda_j(i)\kappa(x,q^k)\kappa_P(x,q^j)dx \sim |a_k(i)|\sum_{j=1}^{M}\int_X \lambda_j(i)\kappa(x,q^k)\kappa_P(x,q^j)dx \quad (6.7)$$

The function $\lambda_j(i)$ quantifies the number of input vectors being quantized to q^j:

$$\lambda_j(i) = \begin{cases} \beta\lambda_j(i-1)+1, & \text{if } x^i \text{ is quantized to } q^j \\ \beta\lambda_j(i-1), & \text{otherwise} \end{cases} \quad (6.8)$$

with $0 << \beta \le 1$ being the forgetting factor. A recursive method is applied for the computation of (6.7) reducing its time complexity to $O(M)$.

6.2.3.2 Approximate Linear Dependency Kernel Recursive Least-Squares Algorithm

KRLS-ALD ensures that the centres of the dictionary at each iteration i are approximately linearly independent in the RKHS H:

$$\delta_i = \min_b \left\| \sum_{j=1}^{m_{i-1}} c_j \varphi(q^j) - \varphi(x^i) \right\|^2 \le \nu \quad (6.9)$$

with parameter $\nu > 0$ determining the level of sparsity; Equation (6.9) represents the approximate linear dependency (ALD) condition. Assuming that the $m_{i-1} \times m_{i-1}$ Gram matrix $\tilde{\mathbf{K}}(i-1)$ is invertible, the optimal $c(i)$ is the solution of $\tilde{\mathbf{K}}(i-1)c(i) = \mathbf{k}(i)$, where $\mathbf{k}(i) = \left[\kappa(x^i,q^1),\ldots,\kappa(x^i,q^{m_{i-1}})\right]^T$, and, correspondingly, the ALD condition becomes:

$$\delta_i = \kappa(x^i,x^i) - \mathbf{k}^T(i)c(i) = \kappa(x^i,x^i) - \mathbf{k}^T(i)\tilde{\mathbf{K}}^{-1}(i-1)\mathbf{k}(i) \le \nu \quad (6.10)$$

In the case where $\delta_i > \nu$ then the dictionary is expanded such that $Q(i) = Q(i-1) \cup \{x^i\}$. The time and memory complexity of (6.10) is $O(m_i^2)$.

6.2.4 Model Evaluation

Each algorithm is evaluated for each patient individually for multiple prediction horizons of 5, 15, 30, 45 and 60 min, which correspond to 1, 3, 6, 9, 12 samples ahead. All simulations were performed using the Kernel Adaptive Filtering MATLAB Toolbox [193]. *Table 6.2* presents the range of the free parameters' values for which the QKLMS-FB and the KRLS-ALD algorithms are tested (i.e. σ, ε_x, η, β in the case of QKLMS-FB or σ, ν in the case of KRLS-ALD). Their values have been selected for each patient individually by grid search minimizing an empirical function of the RMSE and TG of the predictions (i.e. $RMSE^3/TG$), over the period starting from the third day of monitoring. TG is defined as in [96]. The objective function $RMSE^3/TG$ provided a rational balance between these performance metrics, eliminating time-delayed replications of the actual glucose time series.

Table 6.2 Range of the Hyperparameters of QKLMS-FB and KRLS-ALD Algorithms

QKLMS-FB	$\sigma:[0.01,\ 0.05,\ 0.1,\ 0.2,\ldots,5]$
	$\varepsilon_x:[0.01,\ 0.02,\ldots,0.5]$
	$\eta = 0.99$
	$\beta = 0.99$
	$M = 50$
KRLS-ALD	$\sigma:[0.01,\ 0.05,\ 0.1,\ 0.2,\ldots,5]$
	$\nu:[0.0001,\ 0.001,\ 0.003,\ 0.01,\ 0.02,\ 0.05,\ 0.1,\ 0.2,\ 0.3,\ 0.5]$

As it is shown in *Figure 6.1b*, at each time instant t_i, the updated model f_i is tested on the prediction of the sample $\left(x(t_i), y(t_i + pT)\right) \equiv \left(x^{i+p}, y^{i+p}\right)$. The associated prediction error is denoted by $e_{i+p}^{test} = y_{i+p} - f_i\left(x^{i+p}\right)$, with $e_j^{test} = 0$ for $1 \le j \le p$. The goodness of fit of $\hat{y}\left(t|\theta\right)$ is assessed over the period starting from the third day of monitoring by the following performance metrics:

(1) The RMSE.

(2) The MAPE.

(3) The TG defined as $TG = PH - delay$, where *delay* is estimated by two different methods which define accordingly the TG_1 and TG_2 metrics:

   a. the temporal shift minimizing the square of the L^2 distance between the

predicted time series and the actual one [96]:

$$delay = \arg\min_{j\in[0,p]} \left\{ \frac{1}{N-p+1} \sum_{i=1}^{N-p} \left(y_i - \hat{y}_{i+j} \right)^2 \right\} T \tag{6.11}$$

b. the lag maximizing their cross-correlation function.

(4) The normalized ESOD ($ESOD_{norm}$) defined as the ESOD of the predicted time series $\hat{y}$ (i.e. the sum of the squared second-order differences), normalized by the ESOD of the target time series y [96]:

$$ESOD_{norm} = \frac{ESOD(\hat{y})}{ESOD(y)} \tag{6.12}$$

(5) The index J defined as:

$$\mathbf{J} = \frac{ESOD_{norm}}{\left(TG_{norm}\right)^2} \tag{6.13}$$

with lower values of J indicating better predictions. TG_{norm} is the TG of the predicted time series divided by the prediction horizon [94, 133].

(6) The sensitivity and specificity of predictions in the hypoglycaemic range, considering hypoglycaemic instances (subcutaneous glucose concentration values $\leq$70 mg·dL^{-1}) as positive and non-hypoglycaemic instances as negative. An individual glucose prediction is characterized as true positive (TP) with regard to the corresponding actual glucose concentration value if both fall in the hypoglycaemic region.

For comparison purposes, SVR is also applied to the same data and task. The dataset of each patient is split up, at a ratio of 0.7 to 0.3, into two consecutive parts constituting the training and test set, respectively. The hyperparameters C, ε and the Gaussian kernel parameter γ are optimized using the Differential Evolution algorithm which fitness function is defined as the RMSE over a held-out validation set, consisting of the last 30% samples of the training set. In particular, the search space of the hyperparameters is set to $C \in [0.001, 1024]$, $\varepsilon \in [0.0001, 1]$ and $\gamma \in [0.00001, 8]$.

6.3 Results

6.3.1 The Effect of Hyperparameters

The average value and the standard deviation of the hyperparameters and dictionary size, over all patients, are given in *Table 6.3*. Case 1, for both QKLMS-FB and KRLS-ALD algorithms, leads to a lower average σ compared to Case 2 and Case 3, with a less pronounced variation of σ values between the two latter cases. Case 2 and Case 3 induce an additional systematic increase in ε_x values, exploiting, in parallel, the maximum network size of QKLMS-FB (i.e. $m_i = 50$). The network size of KRLS-ALD increases with increasing input size without, however, a consistent variation in ν values among the three input cases for the examined prediction horizons. We can also observe a substantial increment in σ in the transition from 1- to 6-step-ahead predictions for KRLS-ALD in Case 1. In addition, longer prediction horizons are associated with a decreasing trend in ε_x and, contrarily, an increasing trend in ν, with the latter yielding sparser solutions.

6.3.2 Assessment of Predictions

The mean value and the standard deviation, over all patients, of the evaluation metrics for QKLMS-FB and KRLS-ALD are given in *Table 6.4* and *Table 6.5*, respectively. We commence with the description of the results concerning QKLMS-FB. We can observe that the RMSE and MAPE metrics in the case of 1- and 3-step ahead predictions are comparable among the 3 input cases. In addition, Case 1 yields slightly higher TGs, which counterbalance the associated higher $\text{ESOD}_{\text{norm}}$ values and lead to lower J indices for $p = 1$. Adequately accurate predictions are also achieved for p=6, where Case 2 and Case 3 outperform Case 1 yielding comparable RMSEs (22.2±3.9 mg·dL^{-1} and 22.6±4.9 mg·dL^{-1}, respectively) and both attaining an average MAPE of the order of 12.0 % (11.5±2.9 % and 11.9±3.3 %, respectively). We can also observe that both cases balance well the TG (Case 2: TG_1: 8.4±4.3 min, TG_2: 13.4±4.7 min; Case 3: TG_1: 8.4±3.8 min, TG_2: 12.7±4.5 min) and $\text{ESOD}_{\text{norm}}$ (Case 2: 1.1±0.3; Case 3: 1.3±0.4) metrics. The RMSE increases considerably for p>6, where the associated with the multivariate input cases MAPE values reach ~17.0 % and ~21.0 % for p=9 and p=12, respectively. Case 2 and Case 3 lead to less erroneous predictions as compared with Case 1, featuring better *J* indices, particularly due to lower $\text{ESOD}_{\text{norm}}$ values; the contribution of extra

inputs to TG_1 and TG_2 becomes noticeable for p=12.

The prediction error of KRLS-ALD is significantly better than that of QKLMS-FB. Case 2 and Case 3, as compared with Case 1, lead constantly to a higher RMSE (as well as MAPE) even for longer prediction horizons. Nevertheless, as we can see in *Figure 6.2*, they result in a less delayed and, concurrently, smoother output. The full case (Case 3) improves the average RMSE of 1- and 3-step-ahead predictions, as compared with QKLMS-FB, by 33.2 % (4.0±1.2 mg·dL^{-1}) and 20.0 % (10.5±2.4 mg·dL^{-1}), respectively. The latter is also translated into better average TGs (TG_1: 3.0±1.3 min, TG_2:4.3±0.7 min for p=1; TG_1: 7.1±2.0 min, TG_2:10.2±2.7 min for p=3) as well as J indices. Similarly, the average RMSE of 30-min predictions in Case 3 is reduced by 16.9 % (18.8±3.5 mg·dL^{-1}), attaining an average MAPE of 10.0±1.8 % and proactive time of 11.3±.3.0 min with respect to TG_1 and of 16.4±4.4 min with respect to TG_2. The RMSE associated with Case 3 increases to 25.8±3.9 mg·dL^{-1} and 31.8±6.3 mg·dL^{-1} for p=9 and p=12, respectively. Nevertheless, the respective MAPE values are of the order of ~14.0 % and ~18.0 %. It should be mentioned that KRLS-ALD is inferior to QKLMS-FB in terms of $ESOD_{norm}$ values across all input cases and prediction horizons, which is also reflected into higher J indices $\forall p$ concerning Case 1 and for $p \geq 6$ concerning Cases 2 and 3. *Figure 6.3* shows the prediction error curves (a plot of the $\sqrt{E\left(\left(e_i^{test}\right)^2\right)}$ versus the number of iterations i, over a running window of $N/10$ samples and starting from $i = 0$) of QKLMS-FB vs KRLS-ALD in Case 3 for an indicative subject. As expected, KRLS-ALD is predominantly associated with lower errors in the majority of patients. In addition, we observed that the error curves of both algorithms exhibit noticeable fluctuations during the learning phase.

Table 6.3 Optimal Values of the Hyperparameters of QKLMS-FB and KRLS-ALD averaged over all Patients

		PH 5 min			PH 15 min			PH 30 min			PH 45 min			PH 60 min		
		Case 1	*Case 2*	*Case 3*	*Case 1*	*Case 2*	*Case 3*	*Case 1*	*Case 2*	*Case 3*	*Case 1*	*Case 2*	*Case 3*	*Case 1*	*Case 2*	*Case 3*
OKLMS-FB	σ	0.79 (0.19)	1.73 (0.70)	1.77 (0.74)	0.77 (0.21)	2.23 (0.74)	2.37 (0.75)	0.69 (0.23)	2.19 (0.77)	2.37 (0.99)	0.65 (0.36)	2.09 (1.02)	2.23 (1.01)	0.71 (0.30)	2.13 (1.05)	2.05 (0.87)
	ε_x	0.13 (0.11)	0.31 (0.11)	0.35 (0.12)	0.12 (0.13)	0.29 (0.07)	0.34 (0.10)	0.09 (0.09)	0.23 (0.10)	0.34 (0.11)	0.11 (0.08)	0.24 (0.11)	0.26 (0.13)	0.08 (0.08)	0.24 (0.12)	0.25 (0.16)
	m_1	41.93 (14.98)	50.00 (0.00)	50.00 (0.00)	42.40 (16.01)	50.00 (0.00)	50.00 (0.00)	45.20 (11.94)	50.00 (0.00)	50.00 (0.00)	43.27 (12.37)	50.00 (0.00)	50.00 (0.00)	47.07 (11.09)	50.00 (0.00)	50.00 (0.00)
KRLS-ALD	σ	1.65 (1.13)	3.05 (1.18)	3.77 (1.04)	2.35 (1.34)	3.57 (1.14)	4.15 (1.00)	2.79 (1.64)	3.78 (1.08)	3.87 (1.14)	2.56 (1.67)	3.77 (1.13)	3.62 (0.93)	2.53 (1.31)	3.40 (1.23)	3.73 (1.32)
	γ	0.0013 (0.0026)	0.0002 (0.0002)	0.0003 (0.0004)	0.0014 (0.0026)	0.0007 (0.0008)	0.0011 (0.0025)	0.0010 (0.0026)	0.0011 (0.0009)	0.0017 (0.0024)	0.0018 (0.0034)	0.0097 (0.0255)	0.0065 (0.0125)	0.0691 (0.1750)	0.0298 (0.0581)	0.0201 (0.0513)
	m_1	43.13 (34.42)	174.87 (129.68)	197.07 (121.99)	23.47 (19.65)	86.73 (34.65)	123.80 (55.43)	25.67 (18.26)	62.40 (34.92)	96.13 (59.89)	32.60 (47.11)	46.00 (25.80)	73.87 (43.66)	21.00 (21.96)	49.93 (35.67)	60.87 (47.57)

PH: Prediction horizon
Data are mean (standard deviation) values.

Table 6.4 Evaluation of Goodness-of-fit of QKLMS-FB averaged over all Patients

	PH 5 min			**PH 15 min**			**PH 30 min**			**PH 45 min**			**PH 60 min**		
	Case 1	*Case 2*	*Case 3*	*Case 1*	*Case 2*	*Case 3*	*Case 1*	*Case 2*	*Case 3*	*Case 1*	*Case 2*	*Case 3*	*Case 1*	*Case 2*	*Case 3*
RMSE ($mg \cdot dL^{-1}$)	5.1±1.8	5.6±1.7	6.0±2.5	13.6±5.1	12.8±3.3	13.1±3.0	25.5±6.8	22.2±3.9	22.6±4.9	37.9±7.9	31.8±7.9	30.9±5.6	43.2±7.6	37.9±8.7	37.7±8.3
MAPE (%)	2.2±0.5	2.6±0.7	2.7±0.9	6.4±1.8	6.4±1.9	6.6±1.7	13.1±3.6	11.5±2.9	11.9±3.3	19.7±4.1	17.1±5.6	16.5±4.3	22.5±5.3	20.8±6.9	20.8±6.1
TG_1 (min)	2.2±0.9	1.6±1.1	1.6±1.1	4.4±1.7	3.5±1.4	3.7±1.7	8.6±4.6	8.4±4.3	8.4±3.8	16.7±8.0	15.6±6.4	14.9±5.4	20.7±9.8	24.8±9.3	25.1±7.1
TG_2 (min)	4.0±0.9	3.2±1.4	3.4±1.2	8.1±2.6	7.5±2.6	7.4±2.7	13.8±6.2	13.4±4.7	12.7±4.5	18.5±10.1	21.3±6.1	19.5±6.8	22.6±13.1	25.2±8.0	29.4±8.8
$ESOD_{norm}$ (-)	1.9±0.6	1.2±0.2	1.3±0.3	2.0±1.0	1.2±0.4	1.2±0.3	2.1±0.9	1.1±0.3	1.3±0.4	2.3±1.0	1.4±0.5	1.4±0.5	2.0±1.2	1.4±0.5	1.2±0.6
J (-)	10.6 (6.8, 18.3)	24.6 (11.4, 28.3)	24.1 (12.2, 32.0)	22.6 (15.4, 35.8)	26.2 (18.8, 35.4)	21.5 (13.7, 51.6)	36.0 (15.5, 42.8)	20.3 (9.2, 42.4)	15.8 (9.5, 39.9)	20.9 (13.7, 29.2)	12.1 (6.3, 22.4)	11.4 (7.2, 24.3)	18.3 (11.5, 27.0)	7.9 (5.2, 15.4)	5.5 (4.1, 13.3)

Data are mean±standard deviation or median (25^{th} percentile, 75^{th} percentile) values.
PH: Prediction horizon

Table 6.5 Evaluation of Goodness-of-fit of KRLS-ALD averaged over all Patients

	PH 5 min			**PH 15 min**			**PH 30 min**			**PH 45 min**			**PH 60 min**		
	Case 1	*Case 2*	*Case 3*	*Case 1*	*Case 2*	*Case 3*	*Case 1*	*Case 2*	*Case 3*	*Case 1*	*Case 2*	*Case 3*	*Case 1*	*Case 2*	*Case 3*
RMSE ($mg \cdot dL^{-1}$)	3.8±1.1	4.1±1.4	4.0±1.2	9.4±2.2	10.2±2.5	10.5±2.4	17.0±3.1	18.2±3.4	18.8±3.5	23.7±4.4	24.7±4.7	25.8±3.9	30.9±7.6	32.1±6.6	31.8±6.3
MAPE (%)	1.6±0.3	1.7±0.3	1.8±0.3	4.5±0.8	5.0±0.9	5.2±0.9	8.8±1.5	9.5±1.7	10.0±1.8	12.8±2.2	13.5±2.9	14.3±2.6	17.9±5.1	17.8±3.6	18.0±4.3
TG_1 (min)	2.4±1.1	3.0±1.1	3.0±1.3	5.9±1.6	7.1±2.1	7.1±2.0	9.3±3.0	11.4±4.4	11.3±3.0	12.1±3.8	15.3±5.7	16.8±4.6	20.2±14.7	25.9±6.5	22.7±6.4
TG_2 (min)	4.2±0.8	4.4±0.6	4.3±0.7	9.3±2.8	10.0±2.6	10.2±2.7	14.9±5.0	17.0±4.3	16.4±4.4	17.7±6.6	21.8±4.8	22.9±5.3	28.2±12.5	30.5±8.0	30.7±6.4
$ESOD_{norm}$ (-)	3.1±0.9	4.4±2.0	3.7±1.1	6.3±2.7	4.9±1.4	5.0±2.2	10.3±4.4	6.3±3.0	5.1±3.5	15.6±9.0	6.1±4.4	4.6±3.2	13.6±9.8	5.6±4.6	3.3±2.8
J (-)	15.3 (6.1, 29.2)	13.3 (7.8, 23.9)	10.3 (5.2, 25.7)	43.7 (34.4, 49.3)	25.9 (15.7, 36.2)	19.7 (16.0, 36.3)	113.5 (66.1, 160.4)	38.3 (25.3, 64.9)	35.6 (17.9, 54.5)	228.9 (127.6, 308.7)	45.0 (31.2, 69.0)	22.5 (17.4, 60.3)	213.1 (87.3, 498.6)	27.5 (10.1, 67.9)	15.8 (12.5, 37.7)

Data are mean±standard deviation or median (25^{th} percentile, 75^{th} percentile) values.
PH: Prediction horizon

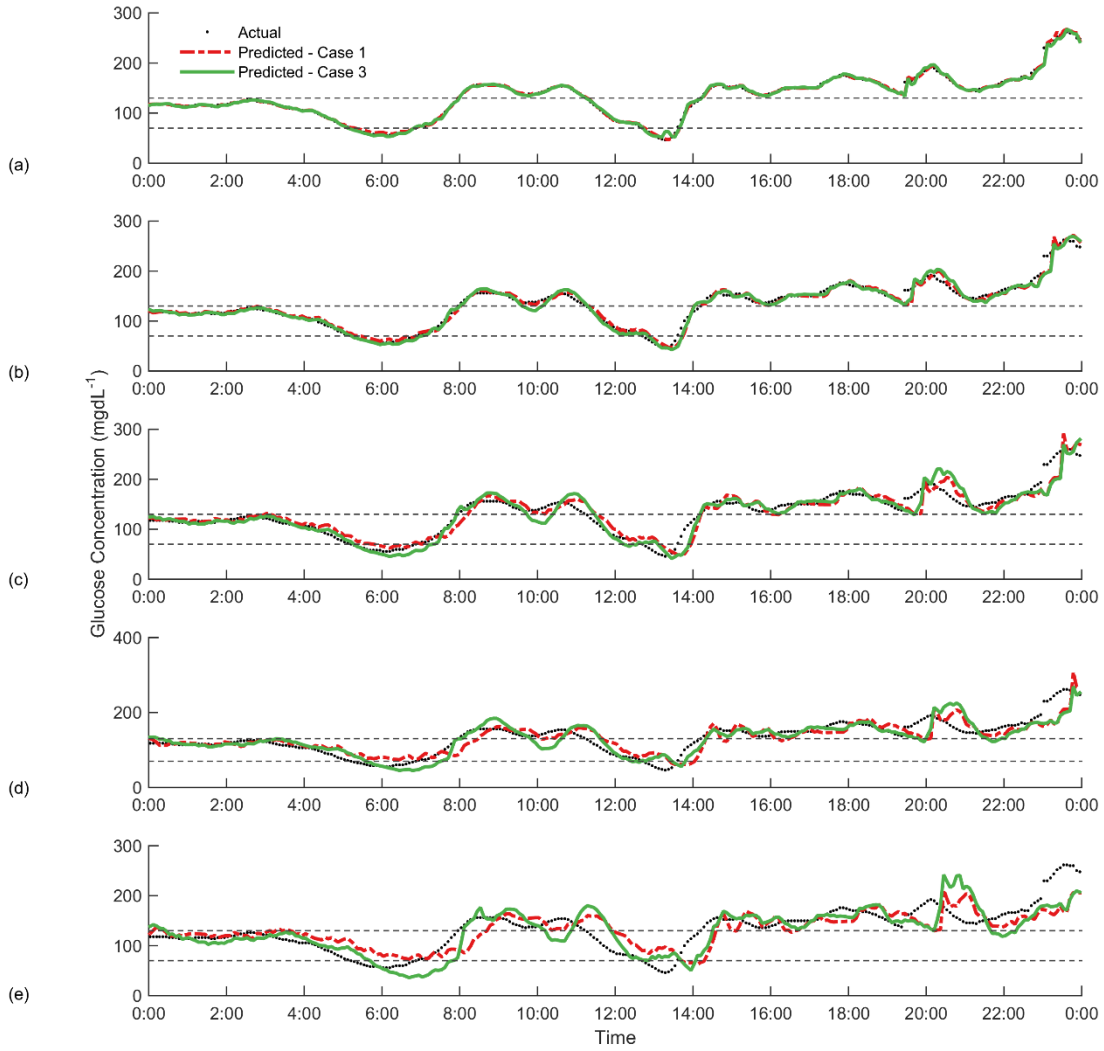

Figure 6.2 Predicted vs measured glucose concentration concerning Patient 6 by KRLS-ALD for multiple prediction horizons of 5, 15, 30, 45 and 60 min (a-e). The horizontal lines indicate the glycaemic range [70, 130] mg·dL^{-1}.

Figure 6.4 portrays the distribution of RMSEs in the hypoglycaemic range (≤70 mg·dL^{-1}) for each input case and prediction horizon. Both QKLMS-FB and KRLS-ALD produce highly accurate 3-step ahead predictions with Case 2 yielding a median (25th percentile, 75th percentile) error equal to 7.2 (6.2, 10.0) mg·dL^{-1} and 5.8 (5.0, 8.1) mg·dL^{-1}, respectively. The median and 75th percentile values of the RMSE of QKLMS-FB indicate that Case 2 and Case 3 lead to more accurate predictions in the hypoglycaemic range for p=6 [Case 1: 19.9 (15.1, 23.1) mg·dL^{-1}; Case2: 16.1 (13.5, 16.9) mg·dL^{-1}; Case 3: 17.0 (15.5, 19.1) mg·dL^{-1}] and p=9 [Case 1: 28.3 (20.2, 34.6) mg·dL^{-1}; Case 2: 23.9 (21.9, 32.4) mg·dL^{-1}; Case 3: 24.0 (21.3, 29.4) mg·dL^{-1}], whereas Case 3 considerably improves the 75th percentile values (Case1: 45.4 mg·dL^{-1}; Case2: 46.3 mg·dL^{-1}; Case 3: 38.7 mg·dL^{-1}) as well as the overall interquartile range

(IQR) (Case 1: 21.1 mg·dL^{-1}; Case 2: 20.3 mg·dL^{-1}; Case 3: 9.2 mg·dL^{-1}) of the RMSE associated with 12-step-ahead predictions of hypoglycaemic values. In the case of KRLS-ALD, the median RMSE of 6- and 9-step ahead predictions is of the order of 15.0 mg·dL^{-1} and 24.0 mg·dL^{-1}. The effect of the multivariate input cases becomes apparent for p=12, with Case 3 yielding a median RMSE 30.3 mg·dL^{-1}. As it is shown in *Figure 6.5*, the QKLMS-FB prediction error in the hyperglycaemic region (≥180 mg·dL^{-1}) is also improved in Case 2 and Case 3, particularly for $p \geq 6$, being, however, inferior to that of KRLS-ALD (median RMSE in Case 3: 29.7 vs. 24.5 mg·dL^{-1} for p=6; 40.1 vs 33.8 mg·dL^{-1} for p=9; 47.3 vs 39.8 mg·dL^{-1} for p=12).

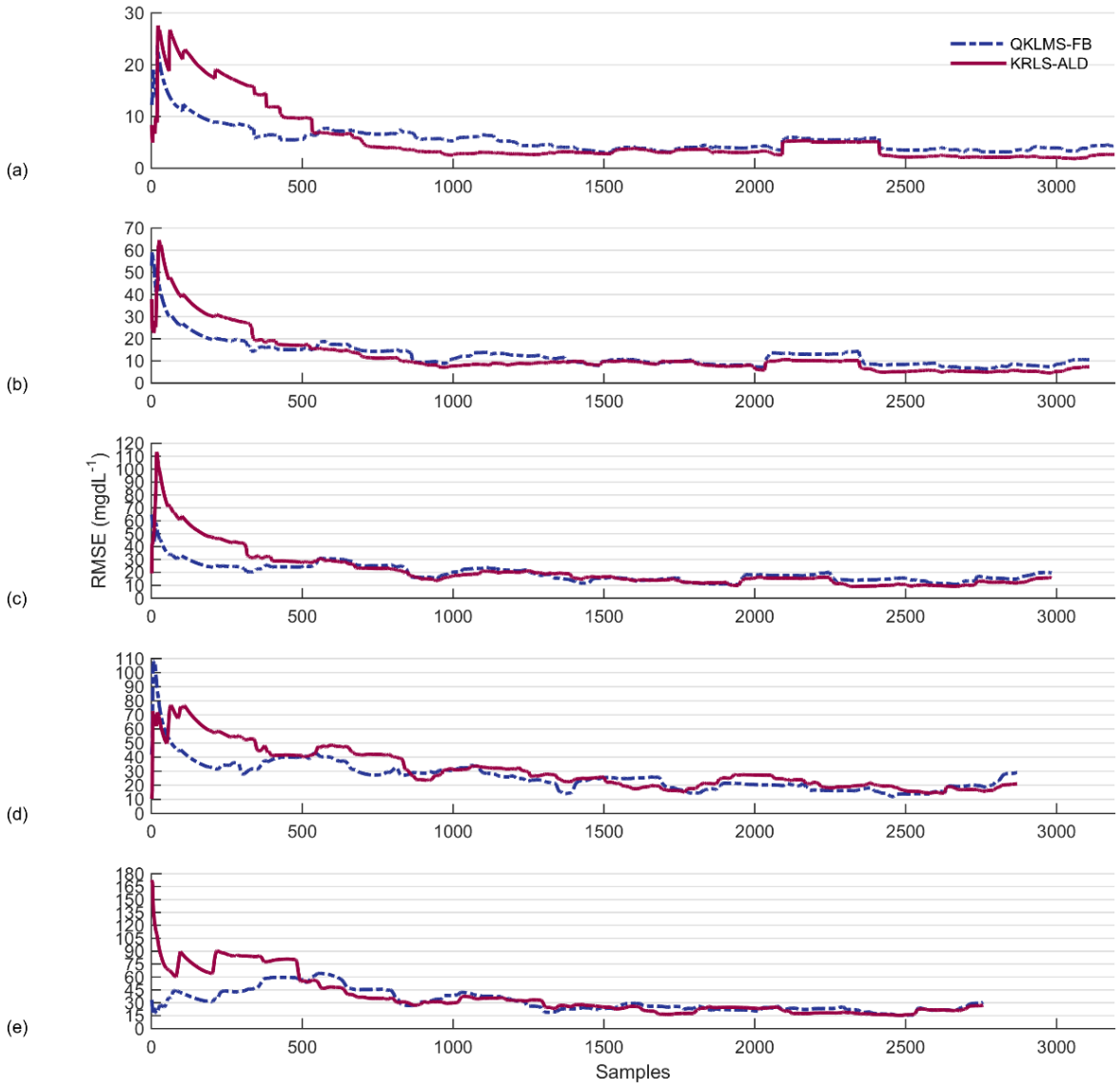

Figure 6.3 Convergence curves of QKLMS-FB and KRLS-ALD in Case 3 regarding Patient 12 for each prediction horizon i.e. 5, 15, 30, 45 and 60 min (a-e).

Figure 6.6 depicts the ROC curve with respect to the prediction of single hypoglycaemic values (≤70.0 mg·dL^{-1}), which is formed by increasing the hypoglycaemic threshold from 70.0 to 90.0 mg·dL^{-1} by 5.0 mg·dL^{-1}. In the case of QKLMS-FB, it is confirmed that Case 2 and Case 3 increase the sensitivity and specificity of predictions in the hypoglycaemic region for p=6 and p=9, with the effect of SEE becoming more apparent for p=9. For p=12, Case 2 exhibits a higher sensitivity as well as specificity as compared with Case 1, whereas Case 3 does increase TN predictions and slightly improves TP ones as compared with Case 1. The contribution of the exogenous inputs to hypoglycaemia prediction is also evident in the case of KRLS-ALD for $p \geq 6$. In particular for Case 3, we can observe that it leads systematically to a lesser specificity. Moreover, QKLMS-FB tends to be more sensitive than KRLS-ALD with respect to the identification of true positive hypoglycaemic values for $p \geq 6$, despite producing higher RMSEs.

In order to determine the clinical accuracy of the treatment decisions, we verified the aforementioned behaviour by the CG-EGA, whose classification of the errors is based both on spatial (i.e. the proximity between y and $\hat{y}$) and temporal characteristics (i.e. the rate and direction of glucose change) of the reference and predicted glucose values [194]. CG-EGA demonstrated (i) the better behaviour of both algorithms in Case 2 and Case 3 as compared to Case 1 in both hypoglycaemic and hyperglycaemic value regions for $p \geq 6$, (ii) the better performance of QKLMS-FB in the hypoglycaemic region for $p \geq 6$, and (iii) the less clinically erroneous behaviour of KRLS-ALD in the hyperglycaemic region for $p = 9$ and $p = 12$.

Table 6.6 summarizes QKLMS-FB, KRLS-ALD and SVR models' performance on the last $3N/10$ samples of the dataset of each patient. KRLS-ALD tends to produce on average lower errors than SVR for all prediction horizons, as it is denoted by the RMSE and MAPE metrics. We can observe that KRLS-ALD's predictions are associated with higher $ESOD_{norm}$ values, which is balanced with higher TGs (TG_1, TG_2), particularly in Case 2 and Case 3 as prediction horizon increases. The latter could explain the lower 75th percentile values of Jin Case 2 and Case 3. On the other hand, QKLMS-FB does not improve on the SVR's error. Nevertheless, QKLMS-FB when fed with Case 2 or Case 3 outperforms SVR with respect to TG_1 for all horizons as well as TG_2 for $p \geq 6$, attaining comparable predictions to those of SVR in relation to the $ESOD_{norm}$ metric and, in turn, considerably lower J values concerning the multivariate input cases for $p \geq 6$.

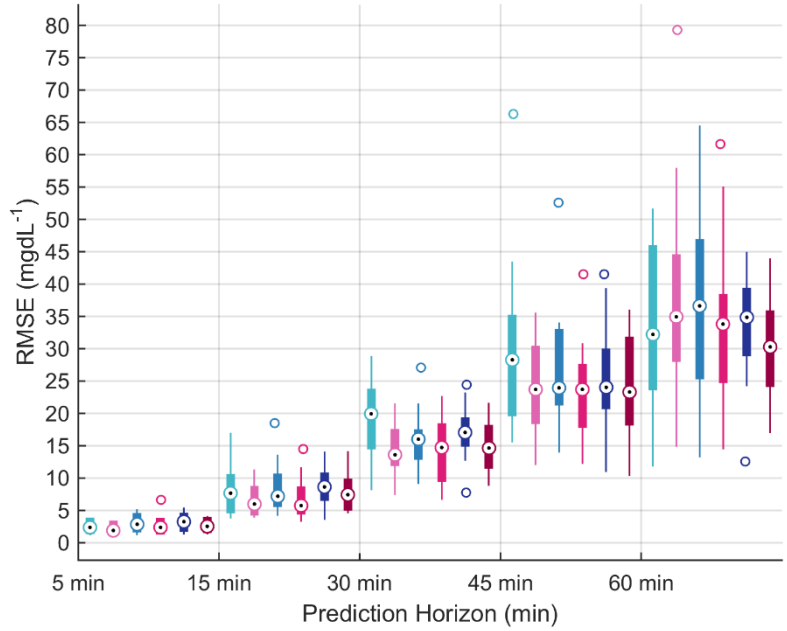

Figure 6.4 Boxplot of the RMSE of QKLMS-FB (blue hues corresponding to Case 1, 2 and 3) and KRLS-ALD (red-purple hues corresponding to Case 1, 2 and 3) algorithms in the hypoglycaemic region (≤70 mgdL^{-1}). On each box, the central mark corresponds to the median, the edges of the box are the 25th and 75th percentiles, the whiskers extend to the most extreme RMSE values not considered outliers, and outliers are plotted individually

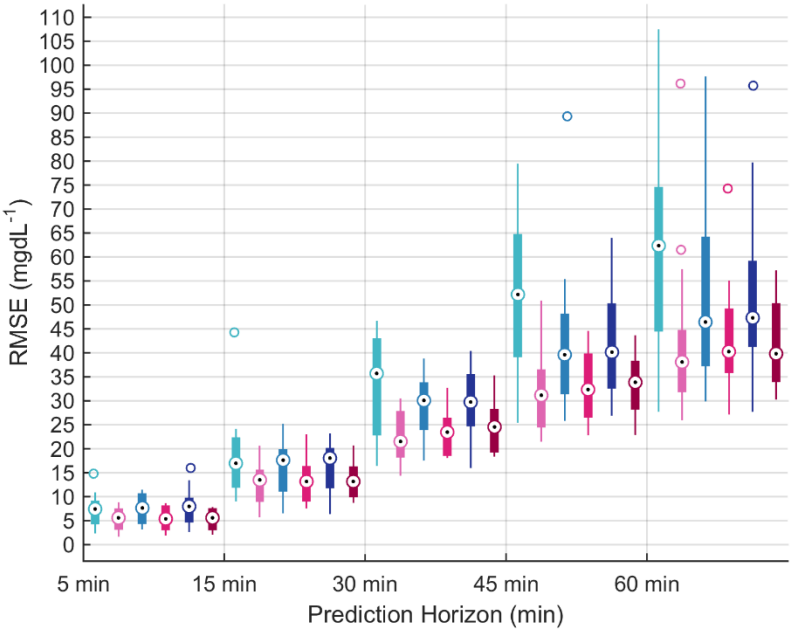

Figure 6.5 Boxplot of the RMSE of QKLMS-FB (blue hues corresponding to Case 1, 2 and 3) and KRLS-ALD (red-purple hues corresponding to Case 1, 2 and 3) algorithms in the hyperglycaemic region (≥180 mgdL^{-1}). On each box, the central mark corresponds to the median, the edges of the box are the 25th and 75th percentiles, the whiskers extend to the most extreme RMSE values not considered outliers, and outliers are plotted individually.

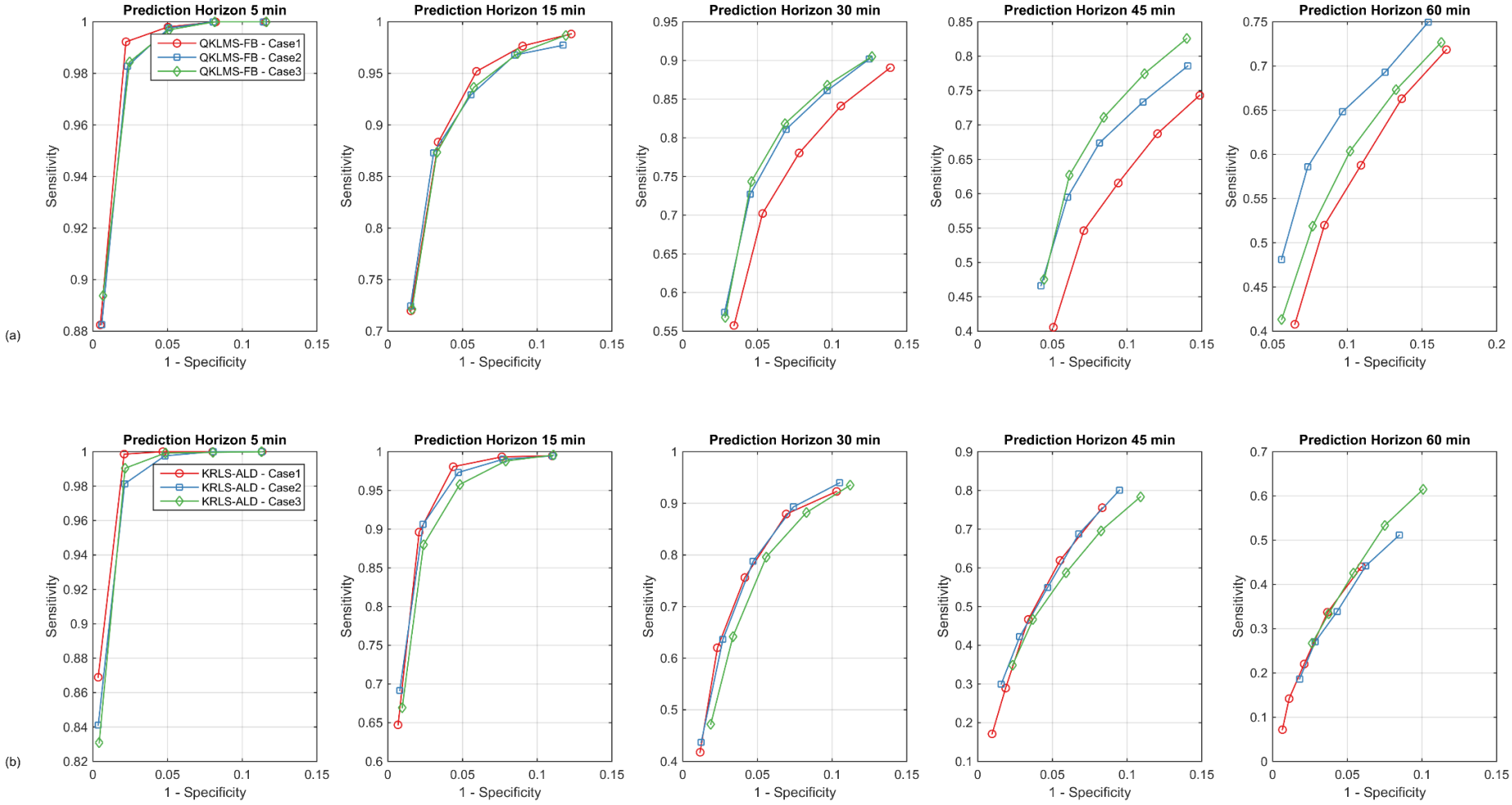

Figure 6.6 The ROC curves corresponding to the prediction of single hypoglycaemic values with the hypoglycaemic threshold being increased from 70 to 90 mg·dL^{-1} by 5 mg·dL^{-1}. (a) QKLMS-FB and (b) KRLS-ALD algorithms.

Table 6.6 Comparative Evaluation of Goodness-of-fit of QKLMS-FB, KRLS-ALD and SVR Models over the last 3N/10 samples of each Patient's Dataset

		PH 5 min			PH 15 min			PH 30 min			PH 45 min			PH 60 min		
		Case 1	**Case 2**	**Case 3**	**Case 1**	**Case 2**	**Case 3**	**Case 1**	**Case 2**	**Case 3**	**Case 1**	**Case 2**	**Case 3**	**Case 1**	**Case 2**	**Case 3**
QKLMS-FB	RMSE ($mgdL^{-1}$)	4.5±2.4	5.4±2.2	5.6±2.6	13.4±7.7	12.4±4.7	12.8±4.1	23.9±8.6	21.0±4.9	21.5±6.3	34.2±10.3	30.4±10.6	29.5±7.9	39.6±11.2	37.6±12.4	35.9±11.6
	MAPE (%)	2.0±0.8	2.6±0.9	2.7±1.1	6.3±2.4	6.3±2.4	6.5±2.0	12.5±4.5	11.2±3.3	11.5±3.8	18.1±4.9	16.7±7.0	15.9±5.3	20.9±5.4	21.1±8.3	19.8±7.7
	TG_1 (min)	2.3±1.6	1.6±1.0	1.4±1.1	4.5±2.9	4.3±1.9	4.4±3.1	7.9±4.4	10.1±6.0	10.7±6.1	13.1±11.0	19.9±10.8	19.3±9.9	16.9±14.5	30.0±14.1	28.3±13.2
	TG_2 (min)	4.3±1.1	3.3±1.4	3.6±1.6	8.5±3.0	8.4±2.8	7.3±3.7	12.8±4.4	13.9±7.3	14.3±8.0	16.9±9.3	22.4±11.1	20.3±13.3	18.4±17.3	25.0±11.7	31.1±13.9
	$ESOD_{norm}$ (-)	2.0±0.4	1.3±0.3	1.4±0.4	2.1±1.1	1.2±0.5	1.3±0.3	2.5±1.5	1.2±0.3	1.5±0.7	2.6±1.1	1.9±1.7	1.8±1.3	2.1±1.2	1.9±1.9	1.6±1.5
	J (-)	9.4 (5.2, 17.4)	11.1 (6.6, 47.3)	19.7 (6.1, ∞)	25.2 (14.8, 38.2)	22.5 (7.7, 29.7)	15.8 (8.8, 52.1)	38.6 (22.7, 70.1)	11.1 (4.7, 50.2)	10.9 (5.1, 55.1)	49.0 (10.2, 252.7)	8.2 (2.8, 69.5)	10.0 (3.2, 43.9)	53.4 (13.5, 98.3)	8.2 (2.4, 26.9)	5.6 (3.2, 14.7)
KRLS-ALD	RMSE ($mgdL^{-1}$)	3.4±1.5	3.9±1.9	3.7±1.6	9.3±3.7	9.7±4.1	9.9±3.9	16.3±5.0	16.7±5.5	17.8±5.9	22.9±6.8	22.7±7.0	23.0±5.4	29.4±9.3	28.0±7.9	28.2±7.8
	MAPE (%)	1.6±0.5	1.7±0.5	1.7±0.5	4.6±1.4	4.9±1.6	5.1±1.7	8.7±2.4	9.0±2.7	9.6±2.5	12.9±3.6	12.8±3.9	13.0±3.0	17.6±6.5	16.3±4.6	16.2±4.5
	TG_1 (min)	2.5±1.8	2.5±1.7	2.8±1.6	5.7±1.9	6.6±2.7	6.7±2.2	8.7±3.7	11.6±5.5	11.1±5.4	9.9±4.7	16.3±8.5	16.8±7.0	19.0±17.9	27.4±13.5	24.9±12.0
	TG_2 (min)	4.5±0.7	4.5±0.8	4.5±0.7	9.3±2.6	10.3±3.1	10.6±3.3	14.8±4.7	18.1±6.6	16.1±6.8	15.9±5.4	22.4±11.1	22.6±9.7	28.7±15.6	34.1±14.7	31.5±15.1
	$ESOD_{norm}$ (-)	3.1±0.5	4.2±2.2	3.1±0.7	6.5±2.9	4.7±1.6	4.3±1.4	9.9±5.3	5.9±2.7	4.7±3.2	14.4±10.9	5.6±4.3	4.4±3.5	11.7±10.0	5.4±4.3	3.5±3.1
	J (-)	15.0 (4.3, 75.6)	19.6 (7.4, 66.4)	11.6 (4.4, 21.6)	47.8 (30.9, 70.7)	29.6 (14.6, 51.1)	18.2 (12.7, 39.3)	125.3 (79.2, 195.6)	44.4 (22.8, 78.7)	44.1 (19.4, 80.3)	328.0 (127.6, 597.3)	36.2 (24.4, 124.5)	35.4 (8.3, 91.8)	225.0 (73.7, 818.4)	30.2 (5.6, 104.0)	24.3 (5.6, 51.2)
SVR	RMSE ($mgdL^{-1}$)	3.8±2.3	4.1±1.8	4.5±2.2	11.3±9.0	10.5±4.7	10.4±4.1	18.5±9.1	18.3±7.2	19.3±7.1	24.7±8.4	25.8±10.6	25.8±10.9	29.5±8.4	30.1±12.2	31.9±11.5
	MAPE (%)	1.8±1.2	1.9±0.7	2.3±1.4	5.8±5.5	5.3±2.3	5.4±2.0	10.1±5.7	9.9±4.0	10.5±4.1	14.0±5.7	14.2±5.8	14.6±6.9	17.2±6.1	17.0±6.5	18.5±7.0
	TG_1 (min)	1.8±1.7	1.0±1.5	1.3±1.6	4.9±2.6	4.3±2.9	4.1±3.2	8.1±4.8	7.8±5.5	7.3±5.9	10.9±7.3	13.4±12.4	11.6±9.0	11.6±8.9	16.8±15.1	17.0±10.2
	TG_2 (min)	4.4±0.7	4.3±0.9	3.7±1.5	9.4±2.5	8.8±3.1	8.2±3.2	14.0±3.7	13.5±5.8	14.0±7.1	17.5±7.5	19.7±12.6	16.2±9.5	18.2±7.3	22.7±16.0	24.2±12.8
	$ESOD_{norm}$ (-)	2.5±0.7	1.4±0.5	1.2±0.5	4.4±2.4	1.8±1.0	1.6±1.0	5.2±3.3	1.7±1.3	1.5±1.3	5.5±5.0	1.6±1.4	1.2±1.1	5.8±5.6	1.5±1.3	0.9±0.7
	J (-)	20.1 (8.5, ∞)	∞ (13.3, ∞)	34.2 (11.0, ∞))	49.1 (31.5, 70.6)	15.1 (11.0, 104.8)	18.6 (9.2, 122.4)	95.0 (42.1, 181.9)	38.9 (10.0, 87.6)	33.4 (12.6, 223.6)	112.5 (45.3, 252.0)	21.1 (7.8, 151.2)	39.9 (7.3, 146.0)	219.4 (65.1, 355.4)	29.8 (9.8, 138.3)	11.5 (3.7, 65.0)

Data are mean±standard deviation or median (25^{th} percentile, 75^{th} percentile) values.
PH: Prediction horizon

6.4 Discussion and Conclusions

The QKLSM-FB and KRLS-ALD algorithms were applied and contrasted, for the first time in the literature, with respect to the identification and prediction of the dynamic glucose system in type 1 diabetes. Their effectiveness was verified using a multivariate dataset obtained during everyday living conditions.

KAF combine the universal approximation property of neural networks (for universal kernels) with the convexity of least squares problems [192]. QKLSM-FB and KRLS-ALD algorithms are capable of solving recursively nonlinear system identification and prediction problems by: (i) expressing all operations in terms of inner products in the RKHS and, (ii) sparsifying the solution online to confine the structure of the underlying RBF network and, consequently, accomplish regularization. A distinct feature of QKLMS-FB sparsification measure is that it incorporates information not only on the distance in the input space but also on the prediction error, which gives QKLMS-FB the capability of better tracking time-varying input-output relationships. ALD is an effective sparsification approach, with proven its relationship to kernel principal components analysis, which also improves the numerical stability of KRLS-ALD provided that no regularization is employed [195]. In SVR, a sparse solution is also attained, but the time complexity of SVR, which scales super-linearly with the size of the training set, discourages its online operation. Yu et al., concurrently with our work, looked at non-sparse KRLS [195] and extended KRLS algorithms [196], which were integrated into an adaptive linear fusion scheme of RLS-based models of subcutaneous glucose concentration for people with type 1 diabetes [197]. However, non-sparse KAF, by retaining the $i \times i$ Gram matrix (i.e. $O\left(i^2\right)$ time and space complexity), poses significant scalability issues during continuous online operation, whilst regularization is needed to alleviate overfitting. The results of the present study indicated the superiority of KRLS-ALD over QKLMS-FB and SVR algorithms with respect to the RMSE, MAPE, and TG metrics. The reliance of QKLMS-FB on stochastic gradient descent and the subsequent update of one model parameter per iteration, besides leading to a slower convergence rate, may also explain its improved $ESOD_{norm}$ values as compared with the KRLS-ALD. It should be mentioned that QKLMS-FB achieves comparable $ESOD_{norm}$ values to SVR and, in parallel, better TGs. Regarding the critical blood glucose ranges, QKLMS-FB demonstrates a higher sensitivity and clinical accuracy (according to CG-EGA) with respect to the prediction of hypoglycaemia

despite the fact that those predictions are associated with higher prediction errors. On the other hand, KRLS-ALD's predictions are less erroneous in the hyperglycaemic region $\forall p$ and, CG-EGA shows that they become more clinically acceptable for $p=9$ and $p=12$.

The subcutaneous glucose signal shows a strong positive auto-correlation at lags ≤ 6, which can explain its high predictive capacity for horizons up to 30 min [91]. Herein, we additionally exploited the recent profile (within the last 30 min) of the Ra and I_p discrete signals, together with the SRa vector representing the cumulative amount of exogenous glucose inserted into plasma over the last 90 min. In addition, we utilized the cumulative EE during the last 3 h (*SEE*) to explain potential hypoglycaemic or hyperglycaemic excursions during or shortly after exercise. In our previous work, by using appropriate feature ranking algorithms, we had demonstrated that the full I_p vector and the most recent values of SEE (i.e. $SEE(t-20)$, $SEE(t-10)$ and $SEE(t)$), in addition to gl, are located high in hierarchy for the majority of patients, whereas there existed larger deviations in the ranking of the remaining features (Ra, SRa) across patients [186]. At this point we should mention that the degree of a linear dependency between Ra and Ip, primarily, due to the concurrent and in a specified ratio (ICR) delivery of insulin dosages and meal carbohydrate content, respectively has been shown to be negatively correlated with the performance of linear dynamical systems [81]. An attempt to address input collinearity and, in turn, increase the input excitation into the system, was made by Zhao et al. via the use of latent variables [83]. As it has been also discussed in [101], the *gl* vector certainly conveys information on the glycaemic effect of previous meals, insulin injections and physical activities up to the time t at which the prediction is made, which can act synergistically with the information conveyed by the discrete signals of *Ra*, I_p, *SRa*, and *SEE*. For instance, exercise-related HAAF is exemplified by hypoglycaemia that typically occurs several hours (6-15 h) after exercise, thus, the specified effect of exercise can be seen in the glucose signal [162]. However, we expect that actions performed very close to the time *t*, whose influence has not been seen yet in the glucose data, would lower the prediction error with increasing horizon. Our reasoning is corroborated by the findings by Zecchin et al. [103] showing that the carbohydrate and insulin information improves only postprandial (up to 2h following a meal) and, presumably, hyperglycaemic predictions for p≥6. To this end, our results support that Case 2 and Case 3: (i) make QKLMS-FB's overall output less erroneous and smoother for $p \geq 6$ as well as less delayed for $p=12$,

as compared with Case 1, (ii) drive KRLS-ALD to significantly lower TGs and $ESOD_{norm}$ values slightly increasing, however, its total error, (iii) improve the sensitivity and clinical accuracy of both algorithms in the hypoglycaemic region for $p \geq 6$, and (iv) improve the clinical accuracy of both algorithms in the hyperglycaemic region, which in the case of QKLMS-FM is also mirrored in clearly lower RMSEs. By evaluating the RMSE in the glycaemic region of <54 $mg \cdot dL^{-1}$, which was recently recommended by the International Hypoglycaemia Study Group as clinically significant biochemical hypoglycaemia which should be reported in clinical trials, Case 2 and Case 3, as regards KRLS-ALD, contributed to more accurate predictions for $p \geq 6$, whereas their effect on the performance of QKLMS-FB with respect to hypoglycaemia is more apparent in the interval $[54, 70]$ $mg \cdot dL^{-1}$ [198]. The latter observation may give prominence to QKLMS-FB's higher sensitivity in the hypoglycaemic region, which along with the smoother predictions produced by QKLMS-FB may explain its higher clinical accuracy in that region.

Table 6.7 presents a comparison of the proposed work with other literature studies utilizing a recursively identified individualized prediction model, which has been evaluated on real patient data and under free-living conditions. The results reported in each study ought to be considered with caution provided that they refer to different datasets, particular input modelling approaches, and various training/testing conditions. A recursively-identified multivariate ARMAX model [107] performs better, in terms of the average RMSE, for 5- and 15-min prediction horizons as compared to nonlinear solutions (i.e. RNN [118] and our work), whereas the latter are more robust to the increase of the prediction horizon. RNN are universal approximators of dynamical systems; however, their non-convex objective function and the high complexity of the training algorithm impede their use in online applications. In addition, an EKF-identified state-space model, as a non-optimal solution to nonlinear problems, is associated with a higher MAPE regarding 30-min predictions [109]. It is noteworthy that a recursive ARMAX model applied to patients with Type 2 diabetes achieves a MAPE less than 5% for a prediction horizon of 30 min [106], which is an indicator of the lower system's complexity in type 2 diabetes. Literature studies relying on batch nonlinear learning approaches have reported similar or better results; however, one should consider (i) the differentials in training/testing conditions (10-fold cross-validation vs training/test sets vs online assessment of the errors), and (ii) the fact that the need for recursivity may become evident in longitudinal observations where different modes of the system can be excited and a time-varying behaviour may be captured; note that the generalization performance of glucose models is now being

demonstrated in small-scale observational studies (ranging from 48h to 2 weeks in the case of type 1 diabetes). Herein, as well as in our preliminary work [191], we demonstrated the benefit of an adaptive non-linear glucose predictive modelling scheme over a time-invariant one, during everyday living conditions through the direct comparison of KAF-based recursive models with an SVR-based model trained in a batch mode.

Table 6.7 Comparative Results with other Methods in the Literature

Study	**Method**	**Feature Set**	**Dataset**	**Prediction Horizon (min) / RMSE (mg·dL^{-1})**
Oruklu et al. 2012, [106]	ARMAX Weighted recursive least squares with adaptive forgetting factor	CGM data Physiological Data: Energy expenditure, average longitudinal acceleration, heat flux, GSR, near-body temperature	Five people with type 2 diabetes Monitoring Period: 23.8±2.4 days	30 / 4.24±5.14%[a]
Turksoy et al., 2013 [107]	ARMAX in state-space form Constrained recursive least squares Real-time Kalman filtering	CGM data Insulin on board Energy expenditure and GSR	Fourteen people with type 1 diabetes	5 / 1.86 15 / 7.18 30 / 18.55 45 / 32.86 60 / 48.93
Wang et al., 2014 [109]	Time-varying state-space model Extended Kalman Filter	CGM data FIR modelling of subcutaneous insulin absorption and meal absorption	Five people with type 1 diabetes using insulin pump Monitoring Period: 60.4±10.6 hours	30 / 20.31±10.44%[a]
Daskalaki et al., 2012 [118]	RNN with real-time recurrent learning	CGM data Insulin infusion rate data	Twenty three people with type 1 diabetes under SAP therapy Monitoring Period: - Training Set 5.30±1.40 days Evaluation Set 4.83±1.80 days	15 / 11.9 (7.7, 22.7)[b] 30 / 18.9 (12.8, 32.3)[b] 45 / 26.1 (17.2, 39.8)[b]
This work	QKLMS-FB	Case 3	Fifteen people with type 1 diabetes Monitoring Period: 12.5±4.6 days	5 / 6.0±2.5 (2.7±0.9 %[a]) 15 / 13.1±3.0 (6.6±1.7 %[a]) 30 / 22.6±4.9 (11.9±3.3 %[a]) 45 / 30.9±5.6 (16.5±4.3 %[a]) 60 / 37.7±8.3 (20.8±6.1 %[a])
This work	KRLS-ALD	Case 3	Fifteen people with type 1 diabetes Monitoring Period: 12.5±4.6 days	5 / 4.0±1.2 (1.8±0.3 %[a]) 15 / 10.5±2.4 (5.2±0.9 %[a]) 30 / 18.8±3.5 (10.0±1.8 %[a]) 45 / 25.8±3.9 (14.3±2.6 %[a]) 60 / 31.8±6.3 (18.0±4.3 %[a])

Data are mean±standard deviation values.
[a]This value refers to MAPE (%).
[b]This value refers to median (5th percentile, 95th percentile).

A few issues need further study. First, the complexity of the predictive model and, consequently, its generalization ability largely depend on the values of the hyperparameters. Model selection through cross-validation is the most widely employed approach, but it is most applicable for stationary learning. Adaptive learning of kernel bandwidth is an alternative solution, which has been shown to improve the prediction accuracy of KLMS significantly [199]. For a nonstationary system, sparsification parameters should be adaptive too. In addition, in the context of a patient-specific glucose model, the use of compartmental models of Ra and I_p, constitutes a limitation that needs to be addressed. An interesting approach is that proposed by Wang et al. [109] which is based on real-time identified finite impulse response functions. Moreover, KAF methods are best suited for learning *a priori* defined and fixed memory mappings of input-output data [200]. For instance, herein we explicitly defined the embedding dimension for each input in order to model the glucose dynamics and, additionally, we introduced specific variables, i.e. SRa and SEE, to model the temporal effect of meals and physical activities constraining, in parallel, the input size. However, state-space models in the RKHS may learn the different modes of the glucose signal more efficiently [200]. Finally, innovative online adaptive sparsification and vector quantization methods are currently studied aiming at better exploiting the potential of kernel recursive algorithms [201, 202].

CHAPTER 7. CONCLUSIONS AND FUTURE WORK

7.1 Conclusions

The problem of identification and prediction of short-term glycaemic dynamics in type 1 diabetes has been largely studied on the basis of time series and machine learning principles, with glucose models' generalization performance now being demonstrated in small-scale observational studies conducted in real-life conditions. On the one hand, parameterized models from linear systems theory assume that the examined glucose system is linear and time-invariant and, on the other hand, non-linearity is treated by machine-learning models (neural networks, kernel-based methods, ensemble models). In addition, dynamic adaptive learning of the glucose system is considered an integral component of modern modelling schemes. In this context, both univariate and multivariate input models have been studied, whereas the input level is where the synergy between physiological models and data-driven glucose predictive models lies in. The generalization capability of existing approaches, as it has been estimated on real and in-silico data, is promising; however more methodical approaches to feature learning and model identification and validation are still required.

In this thesis, we studied systematically and thoroughly the problem of subcutaneous glucose concentration prediction in patients with type 1 diabetes. Considering the ability of SVR to produce smooth, global and sparse solutions to non-linear regression problems, we examined their capability to model the subcutaneous glucose dynamics, making a step beyond the state of the art at the time. By utilizing different input cases, we quantified first the effect of each of the examined inputs (subcutaneous glucose concentration, plasma insulin concentration, exogenous glucose appearance rate, EE, time of the day) to the prediction accuracy, coming to the conclusion that both short-term (≤30 min) and mostly long-term

(>30min) predictions over the full glucose range, as well as, over the hypoglycaemic and hyperglycaemic regions, become significantly more accurate and safe when all the available information is used.

Our subsequent study on the prediction of hypoglycaemic events in type 1 diabetes, revealed that the prediction of nocturnal hypoglycaemic events by the SVR model becomes more accurate when hypoglycaemia associated autonomic failure-related factors are additionally considered. In addition, by increasing the glucose history at night, we obtained considerably lower delays between the predicted and the actual glucose signal. The fact that the introduction of information on physical activity reduces the sensitivity of 30-min predictions of diurnal events, as opposed to a FFNN and a GP model which were trained on the same data and task, indicates that further evaluation is needed to encode the immediate effect of exercise on glucose within the overall patient's context. We concluded that the problem of hypoglycaemia prediction should be handled differently for nocturnal and diurnal periods as regards input variables and interpretation of the results.

The utility of RF or RReliefF feature evaluation algorithms towards the exploration of the dynamics of the subcutaneous glucose concentration in type 1 diabetes and, the subsequent refinement of the glucose predictive model's input was also shown. The subcutaneous glucose profile along with time of the day and plasma insulin concentration were systematically highly ranked, while the effect of food intake and physical activity varied considerably among patients. A very interesting finding was that the plasma insulin concentration is systematically found to outweigh the rate of appearance as well as the cumulative amount of meal-derived glucose inserted in the plasma over time. In addition, the possibility of obtaining equally accurate predictions using on average less than half of the original number of features was demonstrated by utilizing the derived feature ranking in the development of SVR and GP predictive models. It was shown that RF and RReliefF result in equally predictive feature ranking, but our foremost conclusion is that both show a consistent behaviour across all patients.

In the final part of this thesis, KAF-based algorithms were proposed to the recursive nonlinear identification and prediction of the subcutaneous glucose concentration system. Their efficiency consists in the expressive power of the RKHS and the convexity of linear adaptive LMS and RLS models. In particular, QKLMS-FB and KRLS-ALD algorithms, provided sufficiently accurate predictions over the full glucose range for prediction horizons up to 30

min and maintained an average MAPE for 45-min and 60-min predictions below 20%. The theoretically proven higher convergence rate of KRLS-ALD rendered its predictions less erroneous and lagged than those of QKLMS-FB; however, QKLMS-FB provided a more regularized solution and a competitive performance in the hypoglycaemic region as horizon increased. Nevertheless, the much higher computational complexity of KRLS-ALD should be also considered when designing a real-time identified prediction model. Most importantly, the examination of model errors in critical glucose value regions revealed that multivariate models are more advantageous than the univariate ones with respect to the prediction of hypoglycaemic excursions for prediction horizons equal to or greater than 30 min, in return of a higher network. In addition, the benefit of these kernel-based recursive models over a time-invariant predictive scheme, during everyday living conditions, was demonstrated through their direct comparison with a multivariate SVR-based model trained in a batch mode. Nevertheless, in a non-stationary context, consideration should be given to the specification of their hyper-parameters which largely affect the generalization ability of KAF. For instance, adaptive learning of kernel bandwidth has been shown to improve the prediction accuracy of KLMS significantly [21].

7.2 Future Work

Based on the findings of this thesis, the observations we made throughout our research and the latest research findings on subcutaneous glucose concentration predictive modelling, we are going to advance our method with respect to: (i) the specification of the input, (ii) the adaptive learning algorithms, and (iii) the validation of the method.

We identified the need for non-linear dynamical functions which may learn the time-varying behaviour of the glucose regulatory system since our first study. Today, we identify also the need to locate and, accordingly, treat separately the linear and non-linear daily glycaemic dynamics. Our current research activity consists of: (i) efficient learning of the effect of insulin therapy and overall patient's context (e.g. meals, physical activities, stress) on subsequent glucose dynamics under normal daily life conditions and, (ii) producing an adaptive solution that explain the intra-patient and inter-patient variability, as well as, linear and non-linear input-output relationships. The modes of the glucose system which can actually be represented as a linear function of the subcutaneous glucose concentration profile, presumably the low-frequency glycaemic dynamics associated with circadian or ultradian rhythms, will be treated through linear adaptive approaches (e.g. ARIMA models [203, 204]), whereas those

modes related to more challenging conditions (e.g. during exercise or stress) will be treated via contemporary system identification and prediction approaches (e.g. state-space models in the RKHS [200]). To this end, we are going to separately assess the predictive capacity and tracking capability of the model in steady-state (e.g. overnight) and dynamic (e.g. postprandially, during exercise) free-living conditions.

Moreover, the precise prediction of hypoglycaemia, treated either as a regression or a classification problem, is going to be based upon a more comprehensive feature set encompassing physiological parameters predictive or reflective of hypoglycaemia (i.e. GSR, heat flux, skin temperature and heart rate) along with behavioural data (i.e. medication, meals and physical activities). Our aim is to perform a more methodical study on how exogenous factors (e.g. exercise) may yield to hypoglycaemia development as well as the physiological changes triggered by hypoglycaemia. The evaluation of the model will be based on a well-designed observational clinical trial, which has been recently completed and provides a higher input-output excitation level as compared to the current dataset.

Looking at the global picture of precision diabetes medicine, advancements in big data technologies and cognitive computing shift continually the research towards more precise predictive, potentially preventive, solutions [205-209]. Provided the chronic and progressive nature of diabetes, contemporary computational prediction models of short-term glycaemic dynamics in the context of type 1 diabetes should be evaluated on longitudinal self-monitoring and multi-omics data from large population cohorts and, as such, they should integrate different information analysis levels [210]. For instance, unsupervised exploratory cluster analysis can provide a finer stratification of people with type 1 diabetes, which, in turn, can augment the glucose system identification and prediction process. Predictive modelling, as a dynamic component, has to be built upon well-defined machine-learning solutions representing the different time-scales and forms of nonlinearities characterizing the input-output dynamics of the blood glucose system without, however, neglecting the knowledge the mechanistic models of diabetes can bring in.

REFERENCES

[1] ADA, "Diagnosis and classification of diabetes mellitus", *Diabetes Care,* vol. 37 Suppl 1, pp. S81-90, Jan 2014.

[2] A. American Diabetes, "Standards of Medical Care in Diabetes-2016 Abridged for Primary Care Providers", *Clin Diabetes,* vol. 34, pp. 3-21, Jan 2016.

[3] P. E. Cryer, "The barrier of hypoglycemia in diabetes", *Diabetes,* vol. 57, pp. 3169-76, Dec 2008.

[4] K. Norgaard, A. Scaramuzza, N. Bratina, N. M. Lalic, P. Jarosz-Chobot, G. Kocsis, *et al.,* "Routine sensor-augmented pump therapy in type 1 diabetes: the INTERPRET study", *Diabetes Technol Ther,* vol. 15, pp. 273-80, Apr 2013.

[5] R. M. Bergenstal, W. V. Tamborlane, A. Ahmann, J. B. Buse, G. Dailey, S. N. Davis, *et al.,* "Effectiveness of sensor-augmented insulin-pump therapy in type 1 diabetes", *N Engl J Med,* vol. 363, pp. 311-20, Jul 22 2010.

[6] D. Rodbard, "Continuous Glucose Monitoring: A Review of Successes, Challenges, and Opportunities", *Diabetes Technol Ther,* vol. 18 Suppl 2, pp. S3-S13, Feb 2016.

[7] A. Facchinetti, "Continuous Glucose Monitoring Sensors: Past, Present and Future Algorithmic Challenges", *Sensors (Basel),* vol. 16, Dec 09 2016.

[8] H. Thabit and R. Hovorka, "Coming of age: the artificial pancreas for type 1 diabetes", *Diabetologia,* vol. 59, pp. 1795-805, Sep 2016.

[9] J. Kropff and J. H. DeVries, "Continuous Glucose Monitoring, Future Products, and Update on Worldwide Artificial Pancreas Projects", *Diabetes Technol Ther,* vol. 18 Suppl 2, pp. S253-63, Feb 2016.

[10] B. W. Bequette, "Hypoglycemia Prevention Using Low Glucose Suspend Systems", in *Data-driven Modeling for Diabetes: Diagnosis and Treatment,* V. Marmarelis and G. Mitsis, Eds., ed Berlin, Heidelberg: Springer Berlin Heidelberg, 2014, pp. 73-89.

[11] D. Howsmon and B. W. Bequette, "Hypo- and Hyperglycemic Alarms: Devices and Algorithms", *J Diabetes Sci Technol,* vol. 9, pp. 1126-37, Apr 30 2015.

[12] C. Zecchin, A. Facchinetti, G. Sparacino, and C. Cobelli, "Reduction of number and duration of hypoglycemic events by glucose prediction methods: a proof-of-concept in silico study", *Diabetes Technol Ther,* vol. 15, pp. 66-77, Jan 2013.

[13] B. Buckingham, F. Cameron, P. Calhoun, D. M. Maahs, D. M. Wilson, H. P. Chase, *et al.,* "Outpatient safety assessment of an in-home predictive low-glucose suspend system with type 1 diabetes subjects at elevated risk of nocturnal hypoglycemia", *Diabetes Technol Ther,* vol. 15, pp. 622-7, Aug 2013.

[14] C. S. Hughes, S. D. Patek, M. D. Breton, and B. P. Kovatchev, "Hypoglycemia prevention via pump attenuation and red-yellow-green "traffic" lights using continuous glucose monitoring and insulin pump data", *J Diabetes Sci Technol,* vol. 4, pp. 1146-55, Sep 2010.

[15] P. Dua, F. J. Doyle, 3rd, and E. N. Pistikopoulos, "Multi-objective blood glucose control for type 1 diabetes", *Med Biol Eng Comput,* vol. 47, pp. 343-52, Mar 2009.

[16] H. J. Woerle, C. Meyer, J. M. Dostou, N. R. Gosmanov, N. Islam, E. Popa, *et al.,* "Pathways for glucose disposal after meal ingestion in humans", *Am J Physiol*

Endocrinol Metab, vol. 284, pp. E716-25, Apr 2003.
[17] M. Z. Shrayyef and J. E. Gerich, "Normal Glucose Homeostasis", in *Principles of Diabetes Mellitus*, L. Poretsky, Ed., ed Boston, MA: Springer US, 2010, pp. 19-35.
[18] P. E. Cryer, "Chapter 34 - Hypoglycemia A2 - Melmed, Shlomo", in *Williams Textbook of Endocrinology (Thirteenth Edition)*, K. S. Polonsky, P. R. Larsen, and H. M. Kronenberg, Eds., ed Philadelphia: Content Repository Only!, 2016, pp. 1582-1607.
[19] S. L. Aronoff, K. Berkowitz, B. Shreiner, and L. Want, "Glucose Metabolism and Regulation: Beyond Insulin and Glucagon", *Diabetes Spectrum*, vol. 17, pp. 183-190, 2004.
[20] J. E. Gerich, "Control of glycaemia", *Baillieres Clin Endocrinol Metab*, vol. 7, pp. 551-86, Jul 1993.
[21] K. N. Frayn, *Metabolic Regulation: A Human Perspective, 3rd Edition*: Wiley-Blackwell, 2019.
[22] P. E. Cryer, "The Prevention and Correction of Hypoglycemia", in *Comprehensive Physiology*, ed: John Wiley & Sons, Inc., 2010.
[23] B. R. Landau, J. Wahren, V. Chandramouli, W. C. Schumann, K. Ekberg, and S. C. Kalhan, "Contributions of gluconeogenesis to glucose production in the fasted state", *J Clin Invest*, vol. 98, pp. 378-85, Jul 15 1996.
[24] M. Stumvoll, C. Meyer, A. Mitrakou, V. Nadkarni, and J. E. Gerich, "Renal glucose production and utilization: new aspects in humans", *Diabetologia*, vol. 40, pp. 749-57, Jul 1997.
[25] G. Perriello, R. Jorde, N. Nurjhan, M. Stumvoll, G. Dailey, T. Jenssen, *et al.*, "Estimation of glucose-alanine-lactate-glutamine cycles in postabsorptive humans: role of skeletal muscle", *Am J Physiol*, vol. 269, pp. E443-50, Sep 1995.
[26] "2. Classification and Diagnosis of Diabetes: Standards of Medical Care in Diabetes—2018", *Diabetes Care*, vol. 41, pp. S13-S27, 2018.
[27] M. A. Atkinson, "Chapter 32 - Type 1 Diabetes Mellitus A2 - Melmed, Shlomo", in *Williams Textbook of Endocrinology (Thirteenth Edition)*, K. S. Polonsky, P. R. Larsen, and H. M. Kronenberg, Eds., ed Philadelphia: Content Repository Only!, 2016, pp. 1451-1483.
[28] D. M. Nathan, J. Kuenen, R. Borg, H. Zheng, D. Schoenfeld, and R. J. Heine, "Translating the A1C Assay Into Estimated Average Glucose Values", *Diabetes Care*, vol. 31, pp. 1473-1478, 2008.
[29] DCCT, "The effect of intensive treatment of diabetes on the development and progression of long-term complications in insulin-dependent diabetes mellitus. The Diabetes Control and Complications Trial Research Group", *N Engl J Med*, vol. 329, pp. 977-86, Sep 30 1993.
[30] "Effect of intensive blood-glucose control with metformin on complications in overweight patients with type 2 diabetes (UKPDS 34). UK Prospective Diabetes Study (UKPDS) Group", *Lancet*, vol. 352, pp. 854-65, Sep 12 1998.
[31] J. S. Skyler, R. Bergenstal, R. O. Bonow, J. Buse, P. Deedwania, E. A. Gale, *et al.*, "Intensive glycemic control and the prevention of cardiovascular events: implications of the ACCORD, ADVANCE, and VA diabetes trials: a position statement of the American Diabetes Association and a scientific statement of the American College of Cardiology Foundation and the American Heart Association", *Diabetes Care*, vol. 32, pp. 187-92, Jan 2009.
[32] "6. Glycemic Targets: Standards of Medical Care in Diabetes—2018", *Diabetes Care*, vol. 41, pp. S55-S64, 2018.
[33] K. M. Miller, R. W. Beck, R. M. Bergenstal, R. S. Goland, M. J. Haller, J. B. McGill, *et al.*, "Evidence of a strong association between frequency of self-monitoring of blood

glucose and hemoglobin A1c levels in T1D exchange clinic registry participants", *Diabetes Care,* vol. 36, pp. 2009-14, Jul 2013.

[34] R. Ziegler, B. Heidtmann, D. Hilgard, S. Hofer, J. Rosenbauer, R. Holl, *et al.*, "Frequency of SMBG correlates with HbA1c and acute complications in children and adolescents with type 1 diabetes", *Pediatr Diabetes,* vol. 12, pp. 11-7, Feb 2011.

[35] M. Phillip, T. Danne, S. Shalitin, B. Buckingham, L. Laffel, W. Tamborlane, *et al.*, "Use of continuous glucose monitoring in children and adolescents (*)", *Pediatr Diabetes,* vol. 13, pp. 215-28, May 2012.

[36] R. M. Bergenstal, A. J. Ahmann, T. Bailey, R. W. Beck, J. Bissen, B. Buckingham, *et al.*, "Recommendations for standardizing glucose reporting and analysis to optimize clinical decision making in diabetes: the Ambulatory Glucose Profile (AGP)", *Diabetes Technol Ther,* vol. 15, pp. 198-211, Mar 2013.

[37] V. A. Fonseca, G. Grunberger, H. Anhalt, T. S. Bailey, T. Blevins, S. K. Garg, *et al.*, "CONTINUOUS GLUCOSE MONITORING: A CONSENSUS CONFERENCE OF THE AMERICAN ASSOCIATION OF CLINICAL ENDOCRINOLOGISTS AND AMERICAN COLLEGE OF ENDOCRINOLOGY", *Endocrine Practice,* vol. 22, pp. 1008-1021, 2016.

[38] E. R. Damiano, K. McKeon, F. H. El-Khatib, H. Zheng, D. M. Nathan, and S. J. Russell, "A comparative effectiveness analysis of three continuous glucose monitors: the Navigator, G4 Platinum, and Enlite", *J Diabetes Sci Technol,* vol. 8, pp. 699-708, Jul 2014.

[39] Juvenile Diabetes Research Foundation Continuous Glucose Monitoring Study Group, W. V. Tamborlane, R. W. Beck, B. W. Bode, B. Buckingham, H. P. Chase, *et al.*, "Continuous glucose monitoring and intensive treatment of type 1 diabetes", *N Engl J Med,* vol. 359, pp. 1464-76, Oct 2 2008.

[40] J. C. Pickup, S. C. Freeman, and A. J. Sutton, "Glycaemic control in type 1 diabetes during real time continuous glucose monitoring compared with self monitoring of blood glucose: meta-analysis of randomised controlled trials using individual patient data", *Bmj,* vol. 343, p. d3805, 2011.

[41] M. Lind, W. Polonsky, I. B. Hirsch, T. Heise, J. Bolinder, S. Dahlqvist, *et al.*, "Continuous Glucose Monitoring vs Conventional Therapy for Glycemic Control in Adults With Type 1 Diabetes Treated With Multiple Daily Insulin Injections: The GOLD Randomized Clinical Trial", *JAMA,* vol. 317, pp. 379-387, Jan 24 2017.

[42] R. W. Beck, T. Riddlesworth, K. Ruedy, A. Ahmann, R. Bergenstal, S. Haller, *et al.*, "Effect of Continuous Glucose Monitoring on Glycemic Control in Adults With Type 1 Diabetes Using Insulin Injections: The DIAMOND Randomized Clinical Trial", *Jama,* vol. 317, pp. 371-378, Jan 24 2017.

[43] P. Choudhary, S. Ramasamy, L. Green, G. Gallen, S. Pender, A. Brackenridge, *et al.*, "Real-Time Continuous Glucose Monitoring Significantly Reduces Severe Hypoglycemia in Hypoglycemia-Unaware Patients With Type 1 Diabetes", *Diabetes Care,* vol. 36, pp. 4160-4162, 2013.

[44] P. Choudhary, M. R. Rickels, P. A. Senior, M.-C. Vantyghem, P. Maffi, T. W. Kay, *et al.*, "Evidence-Informed Clinical Practice Recommendations for Treatment of Type 1 Diabetes Complicated by Problematic Hypoglycemia", *Diabetes Care,* vol. 38, pp. 1016-1029, 2015.

[45] H. C. Yeh, T. T. Brown, N. Maruthur, P. Ranasinghe, Z. Berger, Y. D. Suh, *et al.*, "Comparative effectiveness and safety of methods of insulin delivery and glucose monitoring for diabetes mellitus: a systematic review and meta-analysis", *Ann Intern Med,* vol. 157, pp. 336-47, Sep 4 2012.

[46] T. Battelino, M. Phillip, N. Bratina, R. Nimri, P. Oskarsson, and J. Bolinder, "Effect of

continuous glucose monitoring on hypoglycemia in type 1 diabetes", *Diabetes Care,* vol. 34, pp. 795-800, Apr 2011.

[47] Juvenile Diabetes Research Foundation Continuous Glucose Monitoring Study Group, R. W. Beck, I. B. Hirsch, L. Laffel, W. V. Tamborlane, B. W. Bode, *et al.*, "The effect of continuous glucose monitoring in well-controlled type 1 diabetes", *Diabetes Care,* vol. 32, pp. 1378-83, Aug 2009.

[48] T. Donner, "Insulin - Pharmacology, Therapeutic Regimens and Principles of Intensive Insulin Therapy", in *Endotext*, L. J. De Groot, P. Beck-Peccoz, G. Chrousos, K. Dungan, A. Grossman, J. M. Hershman, *et al.*, Eds., ed South Dartmouth (MA), 2000.

[49] I. B. Hirsch and J. S. Skyler, "The Management of Type 1 Diabetes", in *Endotext*, L. J. De Groot, P. Beck-Peccoz, G. Chrousos, K. Dungan, A. Grossman, J. M. Hershman, *et al.*, Eds., ed South Dartmouth (MA), 2000.

[50] J. C. Pickup and A. J. Sutton, "Severe hypoglycaemia and glycaemic control in Type 1 diabetes: meta-analysis of multiple daily insulin injections compared with continuous subcutaneous insulin infusion", *Diabet Med,* vol. 25, pp. 765-74, Jul 2008.

[51] R. M. Bergenstal, D. C. Klonoff, S. K. Garg, B. W. Bode, M. Meredith, R. H. Slover, *et al.*, "Threshold-based insulin-pump interruption for reduction of hypoglycemia", *N Engl J Med,* vol. 369, pp. 224-32, Jul 18 2013.

[52] T. T. Ly, J. A. Nicholas, A. Retterath, E. M. Lim, E. A. Davis, and T. W. Jones, "Effect of sensor-augmented insulin pump therapy and automated insulin suspension vs standard insulin pump therapy on hypoglycemia in patients with type 1 diabetes: a randomized clinical trial", *JAMA,* vol. 310, pp. 1240-7, Sep 25 2013.

[53] B. A. Buckingham, D. Raghinaru, F. Cameron, B. W. Bequette, H. P. Chase, D. M. Maahs, *et al.*, "Predictive Low-Glucose Insulin Suspension Reduces Duration of Nocturnal Hypoglycemia in Children Without Increasing Ketosis", *Diabetes Care,* vol. 38, pp. 1197-204, Jul 2015.

[54] D. Rodbard, "Continuous Glucose Monitoring: A Review of Recent Studies Demonstrating Improved Glycemic Outcomes", *Diabetes Technol Ther,* vol. 19, pp. S25-s37, Jun 2017.

[55] F. J. Doyle, 3rd, L. M. Huyett, J. B. Lee, H. C. Zisser, and E. Dassau, "Closed-loop artificial pancreas systems: engineering the algorithms", *Diabetes Care,* vol. 37, pp. 1191-7, 2014.

[56] M. Breton, A. Farret, D. Bruttomesso, S. Anderson, L. Magni, S. Patek, *et al.*, "Fully integrated artificial pancreas in type 1 diabetes: modular closed-loop glucose control maintains near normoglycemia", *Diabetes,* vol. 61, pp. 2230-7, Sep 2012.

[57] S. D. Patek, L. Magni, E. Dassau, C. Karvetski, C. Toffanin, G. De Nicolao, *et al.*, "Modular closed-loop control of diabetes", *IEEE Trans Biomed Eng,* vol. 59, pp. 2986-99, Nov 2012.

[58] R. M. Bergenstal, S. Garg, S. A. Weinzimer, B. A. Buckingham, B. W. Bode, W. V. Tamborlane, *et al.*, "Safety of a Hybrid Closed-Loop Insulin Delivery System in Patients With Type 1 Diabetes", *JAMA,* vol. 316, pp. 1407-1408, Oct 04 2016.

[59] A. Weisman, J. W. Bai, M. Cardinez, C. K. Kramer, and B. A. Perkins, "Effect of artificial pancreas systems on glycaemic control in patients with type 1 diabetes: a systematic review and meta-analysis of outpatient randomised controlled trials", *Lancet Diabetes Endocrinol,* vol. 5, pp. 501-512, Jul 2017.

[60] F. H. El-Khatib, C. Balliro, M. A. Hillard, K. L. Magyar, L. Ekhlaspour, M. Sinha, *et al.*, "Home use of a bihormonal bionic pancreas versus insulin pump therapy in adults with type 1 diabetes: a multicentre randomised crossover trial", *Lancet,* vol. 389, pp. 369-380, Jan 28 2017.

[61] E. Atlas, R. Nimri, S. Miller, E. A. Grunberg, and M. Phillip, "MD-logic artificial

pancreas system: a pilot study in adults with type 1 diabetes", *Diabetes Care,* vol. 33, pp. 1072-6, May 2010.
[62] R. Hovorka, J. M. Allen, D. Elleri, L. J. Chassin, J. Harris, D. Xing, *et al.*, "Manual closed-loop insulin delivery in children and adolescents with type 1 diabetes: a phase 2 randomised crossover trial", *Lancet,* vol. 375, pp. 743-51, Feb 27 2010.
[63] R. Hovorka, K. Kumareswaran, J. Harris, J. M. Allen, D. Elleri, D. Xing, *et al.*, "Overnight closed loop insulin delivery (artificial pancreas) in adults with type 1 diabetes: crossover randomised controlled studies", *BMJ,* vol. 342, p. d1855, 2011.
[64] B. Kovatchev, C. Cobelli, E. Renard, S. Anderson, M. Breton, S. Patek, *et al.*, "Multinational study of subcutaneous model-predictive closed-loop control in type 1 diabetes mellitus: summary of the results", *J Diabetes Sci Technol,* vol. 4, pp. 1374-81, Nov 2010.
[65] S. A. Weinzimer, G. M. Steil, K. L. Swan, J. Dziura, N. Kurtz, and W. V. Tamborlane, "Fully automated closed-loop insulin delivery versus semiautomated hybrid control in pediatric patients with type 1 diabetes using an artificial pancreas", *Diabetes Care,* vol. 31, pp. 934-9, May 2008.
[66] M. Phillip, T. Battelino, E. Atlas, O. Kordonouri, N. Bratina, S. Miller, *et al.*, "Nocturnal Glucose Control with an Artificial Pancreas at a Diabetes Camp", *New England Journal of Medicine,* vol. 368, pp. 824-833, 2013.
[67] R. Nimri, N. Murray, A. Ochs, J. E. Pinsker, and E. Dassau, "Closing the Loop", *Diabetes Technol Ther,* vol. 19, pp. S27-s41, Feb 2017.
[68] L. Bally, H. Thabit, and R. Hovorka, "Closed-loop for type 1 diabetes – an introduction and appraisal for the generalist", *BMC Medicine,* vol. 15, p. 14, 2017.
[69] S. C. Christiansen, A. L. Fougner, O. Stavdahl, K. Kolle, R. Ellingsen, and S. M. Carlsen, "A Review of the Current Challenges Associated with the Development of an Artificial Pancreas by a Double Subcutaneous Approach", *Diabetes Ther,* vol. 8, pp. 489-506, Jun 2017.
[70] A. Gani, A. V. Gribok, S. Rajaraman, W. K. Ward, and J. Reifman, "Predicting subcutaneous glucose concentration in humans: data-driven glucose modeling", *IEEE Trans Biomed Eng,* vol. 56, pp. 246-54, Feb 2009.
[71] A. Gani, A. V. Gribok, Y. Lu, W. K. Ward, R. A. Vigersky, and J. Reifman, "Universal glucose models for predicting subcutaneous glucose concentration in humans", *IEEE Trans Inf Technol Biomed,* vol. 14, pp. 157-65, Jan 2010.
[72] Y. Lu, A. V. Gribok, W. K. Ward, and J. Reifman, "The Importance of Different Frequency Bands in Predicting Subcutaneous Glucose Concentration in Type 1 Diabetic Patients", *IEEE Transactions on Biomedical Engineering,* vol. 57, pp. 1839-1846, 2010.
[73] C. Zhao, Y. Sun, and L. Zhao, "Interindividual glucose dynamics in different frequency bands for online prediction of subcutaneous glucose concentration in type 1 diabetic subjects", *AIChE Journal,* vol. 59, pp. 4228-4240, 2013.
[74] F. N. Rahaghi and D. A. Gough, "Blood glucose dynamics", *Diabetes Technol Ther,* vol. 10, pp. 81-94, Apr 2008.
[75] D. A. Gough, K. Kreutz-Delgado, and T. M. Bremer, "Frequency characterization of blood glucose dynamics", *Ann Biomed Eng,* vol. 31, pp. 91-7, Jan 2003.
[76] M. D. Breton, D. P. Shields, and B. P. Kovatchev, "Optimum Subcutaneous Glucose Sampling and Fourier Analysis of Continuous Glucose Monitors", *Journal of diabetes science and technology (Online),* vol. 2, pp. 495-500, 05/ 2008.
[77] F. Stahl and R. Johansson, "Diabetes mellitus modeling and short-term prediction based on blood glucose measurements", *Math Biosci,* vol. 217, pp. 101-17, Feb 2009.
[78] M. Cescon and R. Johansson, "Linear Modeling and Prediction in Diabetes

Physiology", in *Data-driven Modeling for Diabetes*, V. Marmarelis and G. Mitsis, Eds., ed: Springer Berlin Heidelberg, 2014, pp. 187-222.

[79] C. Dalla Man, M. Camilleri, and C. Cobelli, "A system model of oral glucose absorption: validation on gold standard data", *IEEE Trans Biomed Eng,* vol. 53, pp. 2472-8, Dec 2006.

[80] J. U. Poulsen, A. Avogaro, F. Chauchard, C. Cobelli, R. Johansson, L. Nita, *et al.*, "A diabetes management system empowering patients to reach optimised glucose control: from monitor to advisor", *Conf Proc IEEE Eng Med Biol Soc,* vol. 2010, pp. 5270-1, 2010.

[81] D. A. Finan, C. C. Palerm, F. J. Doyle, D. E. Seborg, H. Zisser, W. C. Bevier, *et al.*, "Effect of input excitation on the quality of empirical dynamic models for type 1 diabetes", *AIChE Journal,* vol. 55, pp. 1135-1146, 2009.

[82] R. Hovorka, V. Canonico, L. J. Chassin, U. Haueter, M. Massi-Benedetti, M. Orsini Federici, *et al.*, "Nonlinear model predictive control of glucose concentration in subjects with type 1 diabetes", *Physiol Meas,* vol. 25, pp. 905-20, Aug 2004.

[83] C. Zhao, E. Dassau, L. Jovanovic, H. C. Zisser, F. J. Doyle, 3rd, and D. E. Seborg, "Predicting subcutaneous glucose concentration using a latent-variable-based statistical method for type 1 diabetes mellitus", *J Diabetes Sci Technol,* vol. 6, pp. 617-33, May 2012.

[84] B. Grosman, E. Dassau, H. C. Zisser, L. Jovanovic, and F. J. Doyle, 3rd, "Zone model predictive control: a strategy to minimize hyper- and hypoglycemic events", *J Diabetes Sci Technol,* vol. 4, pp. 961-75, Jul 01 2010.

[85] B. P. Kovatchev, M. Breton, C. D. Man, and C. Cobelli, "In silico preclinical trials: a proof of concept in closed-loop control of type 1 diabetes", *J Diabetes Sci Technol,* vol. 3, pp. 44-55, Jan 2009.

[86] C. Zhao and C. Yu, "Rapid model identification for online subcutaneous glucose concentration prediction for new subjects with type I diabetes", *IEEE Trans Biomed Eng,* vol. 62, pp. 1333-44, May 2015.

[87] M. Cescon, R. Johansson, and E. Renard, "Subspace-based linear multi-step predictors in type 1 diabetes mellitus", *Biomedical Signal Processing and Control,* vol. 22, pp. 99-110, 2015.

[88] M. Verhaegen, "Identification of the deterministic part of MIMO state space models given in innovations form from input-output data", *Automatica,* vol. 30, pp. 61-74, 1994/01/01 1994.

[89] J. Reifman, S. Rajaraman, A. Gribok, and W. K. Ward, "Predictive monitoring for improved management of glucose levels", *J Diabetes Sci Technol,* vol. 1, pp. 478-86, Jul 2007.

[90] C. Perez-Gandia, A. Facchinetti, G. Sparacino, C. Cobelli, E. J. Gomez, M. Rigla, *et al.*, "Artificial neural network algorithm for online glucose prediction from continuous glucose monitoring", *Diabetes Technol Ther,* vol. 12, pp. 81-8, Jan 2010.

[91] B. Kovatchev and W. Clarke, "Peculiarities of the continuous glucose monitoring data stream and their impact on developing closed-loop control technology", *J Diabetes Sci Technol,* vol. 2, pp. 158-63, Jan 2008.

[92] S. G. Mougiakakou, C. S. Bartsocas, E. Bozas, N. Chaniotakis, D. Iliopoulou, I. Kouris, *et al.*, "SMARTDIAB: a communication and information technology approach for the intelligent monitoring, management and follow-up of type 1 diabetes patients", *IEEE Trans Inf Technol Biomed,* vol. 14, pp. 622-33, May 2010.

[93] K. Zarkogianni, A. Vazeou, S. G. Mougiakakou, A. Prountzou, and K. S. Nikita, "An insulin infusion advisory system based on autotuning nonlinear model-predictive control", *IEEE Trans Biomed Eng,* vol. 58, pp. 2467-77, Sep 2011.

[94] C. Zecchin, A. Facchinetti, G. Sparacino, G. De Nicolao, and C. Cobelli, "Neural network incorporating meal information improves accuracy of short-time prediction of glucose concentration", *IEEE Trans Biomed Eng*, vol. 59, pp. 1550-60, Jun 2012.
[95] G. Sparacino, F. Zanderigo, S. Corazza, A. Maran, A. Facchinetti, and C. Cobelli, "Glucose concentration can be predicted ahead in time from continuous glucose monitoring sensior time-series", *IEEE Transactions on Biomedical Engineering*, vol. 54, pp. 931-937, May 2007.
[96] C. Zecchin, A. Facchinetti, G. Sparacino, and C. Cobelli, "Jump neural network for online short-time prediction of blood glucose from continuous monitoring sensors and meal information", *Comput Methods Programs Biomed*, vol. 113, pp. 144-52, Jan 2014.
[97] K. Zarkogianni, K. Mitsis, E. Litsa, M. T. Arredondo, G. Ficomicron, A. Fioravanti, *et al.*, "Comparative assessment of glucose prediction models for patients with type 1 diabetes mellitus applying sensors for glucose and physical activity monitoring", *Med Biol Eng Comput*, vol. 53, pp. 1333-43, Dec 2015.
[98] F. Ståhl, R. Johansson, and E. Renard, "Ensemble Glucose Prediction in Insulin-Dependent Diabetes", in *Data-driven Modeling for Diabetes: Diagnosis and Treatment*, V. Marmarelis and G. Mitsis, Eds., ed Berlin, Heidelberg: Springer Berlin Heidelberg, 2014, pp. 37-71.
[99] F. Ståhl, "Diabetes mellitus glucose prediction by linear and Bayesian ensemble modeling", Department of Automatic Control, Lund University Sweden, 2012.
[100] G. C. Estrada, H. Kirchsteiger, L. d. Re, and E. Renard, "Innovative approach for online prediction of blood glucose profile in type 1 diabetes patients", in *Proceedings of the 2010 American Control Conference*, 2010, pp. 2015-2020.
[101] V. Naumova, S. V. Pereverzyev, and S. Sivananthan, "A meta-learning approach to the regularized learning-case study: blood glucose prediction", *Neural Netw*, vol. 33, pp. 181-93, Sep 2012.
[102] Y. Wang, X. Wu, and X. Mo, "A novel adaptive-weighted-average framework for blood glucose prediction", *Diabetes Technol Ther*, vol. 15, pp. 792-801, Oct 2013.
[103] C. Zecchin, A. Facchinetti, G. Sparacino, and C. Cobelli, "How Much Is Short-Term Glucose Prediction in Type 1 Diabetes Improved by Adding Insulin Delivery and Meal Content Information to CGM Data? A Proof-of-Concept Study", *J Diabetes Sci Technol*, vol. 10, pp. 1149-60, Sep 2016.
[104] T. Bremer and D. A. Gough, "Is blood glucose predictable from previous values? A solicitation for data", *Diabetes*, vol. 48, pp. 445-51, Mar 1999.
[105] M. Eren-Oruklu, A. Cinar, L. Quinn, and D. Smith, "Estimation of future glucose concentrations with subject-specific recursive linear models", *Diabetes Technol Ther*, vol. 11, pp. 243-53, Apr 2009.
[106] M. Eren-Oruklu, A. Cinar, D. K. Rollins, and L. Quinn, "Adaptive System Identification for Estimating Future Glucose Concentrations and Hypoglycemia Alarms", *Automatica (Oxf)*, vol. 48, pp. 1892-1897, Aug 2012.
[107] K. Turksoy, E. S. Bayrak, L. Quinn, E. Littlejohn, D. Rollins, and A. Cinar, "Hypoglycemia Early Alarm Systems Based On Multivariable Models", *Ind Eng Chem Res*, vol. 52, Sep 4 2013.
[108] K. Turksoy, L. Quinn, E. Littlejohn, and A. Cinar, "Multivariable adaptive identification and control for artificial pancreas systems", *IEEE Trans Biomed Eng*, vol. 61, pp. 883-91, Mar 2014.
[109] Q. Wang, P. Molenaar, S. Harsh, K. Freeman, J. Xie, C. Gold, *et al.*, "Personalized State-space Modeling of Glucose Dynamics for Type 1 Diabetes Using Continuously Monitored Glucose, Insulin Dose, and Meal Intake: An Extended Kalman Filter Approach", *J Diabetes Sci Technol*, vol. 8, pp. 331-345, Mar 24 2014.

[110] J. Picard, "Efficiency of the Extended Kalman Filter for Nonlinear Systems with Small Noise", *SIAM Journal on Applied Mathematics,* vol. 51, pp. 843-885, 1991.
[111] E. A. Wan and R. V. D. Merwe, "The unscented Kalman filter for nonlinear estimation", in *Proceedings of the IEEE 2000 Adaptive Systems for Signal Processing, Communications, and Control Symposium (Cat. No.00EX373)*, 2000, pp. 153-158.
[112] E. Daskalaki, K. Norgaard, T. Zuger, A. Prountzou, P. Diem, and S. Mougiakakou, "An early warning system for hypoglycemic/hyperglycemic events based on fusion of adaptive prediction models", *J Diabetes Sci Technol,* vol. 7, pp. 689-98, May 2013.
[113] E. Daskalaki, P. Diem, and S. Mougiakakou, "Adaptive Algorithms for Personalized Diabetes Treatment", in *Data-driven Modeling for Diabetes: Diagnosis and Treatment*, V. Marmarelis and G. Mitsis, Eds., ed Berlin, Heidelberg: Springer Berlin Heidelberg, 2014, pp. 91-116.
[114] S. M. Pappada, B. D. Cameron, P. M. Rosman, R. E. Bourey, T. J. Papadimos, W. Olorunto, *et al.*, "Neural network-based real-time prediction of glucose in patients with insulin-dependent diabetes", *Diabetes Technol Ther,* vol. 13, pp. 135-41, Feb 2011.
[115] D. A. Finan, F. J. Doyle, 3rd, C. C. Palerm, W. C. Bevier, H. C. Zisser, L. Jovanovic, *et al.*, "Experimental evaluation of a recursive model identification technique for type 1 diabetes", *J Diabetes Sci Technol,* vol. 3, pp. 1192-202, Sep 2009.
[116] K. Turksoy, E. S. Bayrak, L. Quinn, E. Littlejohn, and A. Cinar, "Multivariable Adaptive Closed-Loop Control of an Artificial Pancreas Without Meal and Activity Announcement", *Diabetes Technology & Therapeutics,* vol. 15, pp. 386-400, May 2013.
[117] E. S. Bayrak, K. Turksoy, A. Cinar, L. Quinn, E. Littlejohn, and D. Rollins, "Hypoglycemia early alarm systems based on recursive autoregressive partial least squares models", *J Diabetes Sci Technol,* vol. 7, pp. 206-14, Jan 01 2013.
[118] E. Daskalaki, A. Prountzou, P. Diem, and S. G. Mougiakakou, "Real-time adaptive models for the personalized prediction of glycemic profile in type 1 diabetes patients", *Diabetes Technol Ther,* vol. 14, pp. 168-74, Feb 2012.
[119] S. L. Cichosz, M. D. Johansen, and O. Hejlesen, "Toward Big Data Analytics: Review of Predictive Models in Management of Diabetes and Its Complications", *J Diabetes Sci Technol,* vol. 10, pp. 27-34, Oct 14 2015.
[120] C. C. Palerm and B. W. Bequette, "Hypoglycemia Detection and Prediction Using Continuous Glucose Monitoring—A Study on Hypoglycemic Clamp Data", *Journal of diabetes science and technology (Online),* vol. 1, pp. 624-629, 09/ 2007.
[121] F. Cameron, G. Niemeyer, K. Gundy-Burlet, and B. Buckingham, "Statistical hypoglycemia prediction", *J Diabetes Sci Technol,* vol. 2, pp. 612-21, Jul 2008.
[122] E. Dassau, F. Cameron, H. Lee, B. W. Bequette, H. Zisser, L. Jovanovic, *et al.*, "Real-Time hypoglycemia prediction suite using continuous glucose monitoring: a safety net for the artificial pancreas", *Diabetes Care,* vol. 33, pp. 1249-54, Jun 2010.
[123] M. Eren-Oruklu, A. Cinar, and L. Quinn, "Hypoglycemia prediction with subject-specific recursive time-series models", *J Diabetes Sci Technol,* vol. 4, pp. 25-33, Jan 2010.
[124] M. H. Jensen, T. F. Christensen, L. Tarnow, Z. Mahmoudi, M. D. Johansen, and O. K. Hejlesen, "Professional continuous glucose monitoring in subjects with type 1 diabetes: retrospective hypoglycemia detection", *J Diabetes Sci Technol,* vol. 7, pp. 135-43, Jan 01 2013.
[125] M. H. Jensen, Z. Mahmoudi, T. F. Christensen, L. Tarnow, E. Seto, M. D. Johansen, *et al.*, "Evaluation of an Algorithm for Retrospective Hypoglycemia Detection Using Professional Continuous Glucose Monitoring Data", *J Diabetes Sci Technol,* vol. 8, pp. 117-122, Jan 2014.

[126] S. L. Cichosz, J. Frystyk, O. K. Hejlesen, L. Tarnow, and J. Fleischer, "A novel algorithm for prediction and detection of hypoglycemia based on continuous glucose monitoring and heart rate variability in patients with type 1 diabetes", *J Diabetes Sci Technol,* vol. 8, pp. 731-7, Jul 2014.
[127] S. L. Cichosz, J. Frystyk, L. Tarnow, and J. Fleischer, "Combining information of autonomic modulation and CGM measurements enables prediction and improves detection of spontaneous hypoglycemic events", *J Diabetes Sci Technol,* vol. 9, pp. 132-7, Jan 2015.
[128] "Accuracy of the GlucoWatch G2 Biographer and the continuous glucose monitoring system during hypoglycemia: experience of the Diabetes Research in Children Network", *Diabetes Care,* vol. 27, pp. 722-6, Mar 2004.
[129] E. Tsalikian, C. Kollman, N. Mauras, S. Weinzimer, B. Buckingham, D. Xing, *et al.*, "GlucoWatch G2 Biographer alarm reliability during hypoglycemia in children", *Diabetes Technol Ther,* vol. 6, pp. 559-66, Oct 2004.
[130] E. I. Georga, V. C. Protopappas, D. Ardigò, M. Marina, I. Zavaroni, D. Polyzos, *et al.*, "Multivariate Prediction of Subcutaneous Glucose Concentration in Type 1 Diabetes Patients Based on Support Vector Regression", *IEEE Journal of Biomedical and Health Informatics,* vol. 17, pp. 71-81, 2013.
[131] E. I. Georga, V. C. Protopappas, D. Ardigo, D. Polyzos, and D. I. Fotiadis, "A glucose model based on support vector regression for the prediction of hypoglycemic events under free-living conditions", *Diabetes Technol Ther,* vol. 15, pp. 634-43, Aug 2013.
[132] E. I. Georga, J. C. Príncipe, and D. I. Fotiadis, "Short-term prediction of glucose in type 1 diabetes using kernel adaptive filters", *Medical & Biological Engineering & Computing,* July 02 2018.
[133] A. Facchinetti, G. Sparacino, E. Trifoglio, and C. Cobelli, "A new index to optimally design and compare continuous glucose monitoring glucose prediction algorithms", *Diabetes Technol Ther,* vol. 13, pp. 111-9, Feb 2011.
[134] D. C. Klonoff, "Continuous glucose monitoring: roadmap for 21st century diabetes therapy", *Diabetes Care,* vol. 28, pp. 1231-9, May 2005.
[135] ADA, J. P. Bantle, J. Wylie-Rosett, A. L. Albright, C. M. Apovian, N. G. Clark, *et al.*, "Nutrition recommendations and interventions for diabetes: a position statement of the American Diabetes Association", *Diabetes Care,* vol. 31 Suppl 1, pp. S61-78, Jan 2008.
[136] ADA, "Physical activity/exercise and diabetes", *Diabetes Care,* vol. 27 Suppl 1, pp. S58-62, Jan 2004.
[137] W. Huang, K. M. Ramsey, B. Marcheva, and J. Bass, "Circadian rhythms, sleep, and metabolism", *J Clin Invest,* vol. 121, pp. 2133-41, Jun 2011.
[138] O. Froy, "Metabolism and circadian rhythms--implications for obesity", *Endocr Rev,* vol. 31, pp. 1-24, Feb 2010.
[139] T. Soeborg, C. H. Rasmussen, E. Mosekilde, and M. Colding-Jorgensen, "Absorption kinetics of insulin after subcutaneous administration", *Eur J Pharm Sci,* vol. 36, pp. 78-90, Jan 31 2009.
[140] B. Guerci and J. P. Sauvanet, "Subcutaneous insulin: pharmacokinetic variability and glycemic variability", *Diabetes Metab,* vol. 31, pp. 4S7-4S24, Sep 2005.
[141] L. Heinemann, "Variability of insulin absorption and insulin action", *Diabetes Technol Ther,* vol. 4, pp. 673-82, 2002.
[142] A. Caumo, M. Simeoni, and C. Cobelli, "Chapter 12 - Glucose Modelling", in *Modeling Methodology for Physiology and Medicine*, ed San Diego: Academic Press, 2001, pp. 337-372.
[143] A. Makroglou, J. Li, and Y. Kuang, "Mathematical models and software tools for the glucose-insulin regulatory system and diabetes: an overview", *Applied Numerical*

Mathematics, vol. 56, pp. 559-573, 2006.
[144] C. Dalla Man, R. A. Rizza, and C. Cobelli, "Meal simulation model of the glucose-insulin system", *IEEE Trans Biomed Eng*, vol. 54, pp. 1740-9, Oct 2007.
[145] G. D. Mitsis, M. G. Markakis, and V. Z. Marmarelis, "Nonlinear modeling of the dynamic effects of infused insulin on glucose: comparison of compartmental with Volterra models", *IEEE Trans Biomed Eng*, vol. 56, pp. 2347-58, Oct 2009.
[146] G. Robertson, E. D. Lehmann, W. Sandham, and D. Hamilton, "Blood glucose prediction using artificial neural networks trained with the AIDA diabetes simulator: a proof-of-concept pilot study", *JECE*, vol. 2011, pp. 2-2, 2011.
[147] V. Tresp, T. Briegel, and J. Moody, "Neural-network models for the blood glucose metabolism of a diabetic", *IEEE Trans Neural Netw*, vol. 10, pp. 1204-13, 1999.
[148] B. P. Kovatchev, D. Shields, and M. Breton, "Graphical and numerical evaluation of continuous glucose sensing time lag", *Diabetes Technol Ther*, vol. 11, pp. 139-43, Mar 2009.
[149] F. Zanderigo, G. Sparacino, B. Kovatchev, and C. Cobelli, "Glucose Prediction Algorithms from Continuous Monitoring Data: Assessment of Accuracy via Continuous Glucose Error-Grid Analysis", *J Diabetes Sci Technol*, vol. 1, pp. 645-51, Sep 2007.
[150] S. G. Mougiakakou, A. Prountzou, D. Iliopoulou, K. S. Nikita, A. Vazeou, and C. S. Bartsocas, "Neural network based glucose - insulin metabolism models for children with Type 1 diabetes", *Conf Proc IEEE Eng Med Biol Soc*, vol. 1, pp. 3545-8, 2006.
[151] J. J. Valletta, A. J. Chipperfield, and C. D. Byrne, "Gaussian Process modelling of blood glucose response to free-living physical activity data in people with type 1 diabetes", *Conf Proc IEEE Eng Med Biol Soc*, vol. 2009, pp. 4913-6, 2009.
[152] E. Georga, V. Protopappas, A. Guillen, G. Fico, D. Ardigo, M. T. Arredondo, *et al.*, "Data mining for blood glucose prediction and knowledge discovery in diabetic patients: the METABO diabetes modeling and management system", *Conf Proc IEEE Eng Med Biol Soc*, vol. 2009, pp. 5633-6, 2009.
[153] C. Tarin, E. Teufel, J. Pico, J. Bondia, and H. J. Pfleiderer, "Comprehensive pharmacokinetic model of insulin Glargine and other insulin formulations", *IEEE Trans Biomed Eng*, vol. 52, pp. 1994-2005, Dec 2005.
[154] C. Cobelli, G. Federspil, G. Pacini, A. Salvan, and C. Scandellari, "An Integrated Mathematical-Model of the Dynamics of Blood-Glucose and Its Hormonal-Control", *Mathematical Biosciences*, vol. 58, pp. 27-60, 1982.
[155] E. D. Lehmann and T. Deutsch, "A physiological model of glucose-insulin interaction in type 1 diabetes mellitus", *J Biomed Eng*, vol. 14, pp. 235-42, May 1992.
[156] A. J. Smola and B. Scholkopf, "A tutorial on support vector regression", *Statistics and Computing*, vol. 14, pp. 199-222, Aug 2004.
[157] R. Storn and K. Price, "Differential evolution - A simple and efficient heuristic for global optimization over continuous spaces", *Journal of Global Optimization*, vol. 11, pp. 341-359, Dec 1997.
[158] S. M. Pappada, B. D. Cameron, and P. M. Rosman, "Development of a neural network for prediction of glucose concentration in type 1 diabetes patients", *J Diabetes Sci Technol*, vol. 2, pp. 792-801, Sep 2008.
[159] W. L. Clarke, S. Anderson, and B. Kovatchev, "Evaluating clinical accuracy of continuous glucose monitoring systems: Continuous Glucose-Error Grid Analysis (CG-EGA)", *Curr Diabetes Rev*, vol. 4, pp. 193-9, Aug 2008.
[160] E. I. Georga, V. C. Protopappas, D. Polyzos, and D. I. Fotiadis, "A predictive model of subcutaneous glucose concentration in type 1 diabetes based on Random Forests", in *2012 Annual International Conference of the IEEE Engineering in Medicine and*

Biology Society, 2012, pp. 2889-2892.
[161] P. E. Cryer, S. N. Davis, and H. Shamoon, "Hypoglycemia in diabetes", *Diabetes Care,* vol. 26, pp. 1902-12, Jun 2003.
[162] P. E. Cryer, "Exercise-related hypoglycemia-associated autonomic failure in diabetes", *Diabetes,* vol. 58, pp. 1951-2, Sep 2009.
[163] F. Allam, Z. Nossai, H. Gomma, I. Ibrahim, and M. Abdelsalam, "A Recurrent Neural Network Approach for Predicting Glucose Concentration in Type-1 Diabetic Patients", in *Engineering Applications of Neural Networks: 12th INNS EANN-SIG International Conference, EANN 2011 and 7th IFIP WG 12.5 International Conference, AIAI 2011, Corfu, Greece, September 15-18, 2011, Proceedings Part I*, L. Iliadis and C. Jayne, Eds., ed Berlin, Heidelberg: Springer Berlin Heidelberg, 2011, pp. 254-259.
[164] A. Y. Alanis, B. S. Leon, E. N. Sanchez, and E. Ruiz-Velazquez, "Blood glucose level neural model for type 1 diabetes mellitus patients", *Int J Neural Syst,* vol. 21, pp. 491-504, Dec 2011.
[165] ADA, "Defining and reporting hypoglycemia in diabetes: a report from the American Diabetes Association Workgroup on Hypoglycemia", *Diabetes Care,* vol. 28, pp. 1245-9, May 2005.
[166] C. M. Bishop, *Pattern Recognition and Machine Learning (Information Science and Statistics)*: Springer-Verlag New York, Inc., 2006.
[167] C. E. Rasmussen and H. Nickisch, "Gaussian Processes for Machine Learning (GPML) Toolbox", *Journal of Machine Learning Research,* vol. 11, pp. 3011-3015, Nov 2010.
[168] "4. Lifestyle Management: Standards of Medical Care in Diabetes—2018", *Diabetes Care,* vol. 41, pp. S38-S50, 2018.
[169] "8. Pharmacologic Approaches to Glycemic Treatment: Standards of Medical Care in Diabetes—2018", *Diabetes Care,* vol. 41, pp. S73-S85, 2018.
[170] J. C. Pickup, "Insulin-pump therapy for type 1 diabetes mellitus", *N Engl J Med,* vol. 366, pp. 1616-24, Apr 26 2012.
[171] A. Abu-Rmileh, W. Garcia-Gabin, and D. Zambrano, "A robust sliding mode controller with internal model for closed-loop artificial pancreas", *Med Biol Eng Comput,* vol. 48, pp. 1191-201, Dec 2010.
[172] M. Yamaguchi, C. Kaseda, K. Yamazaki, and M. Kobayashi, "Prediction of blood glucose level of type 1 diabetics using response surface methodology and data mining", *Med Biol Eng Comput,* vol. 44, pp. 451-7, Jun 2006.
[173] L. Breiman, "Random forests", *Machine Learning,* vol. 45, pp. 5-32, Oct 2001.
[174] M. Robnik-Sikonja and I. Kononenko, "Theoretical and empirical analysis of ReliefF and RReliefF", *Machine Learning,* vol. 53, pp. 23-69, Oct-Nov 2003.
[175] C. Strobl, J. Malley, and G. Tutz, "An introduction to recursive partitioning: rationale, application, and characteristics of classification and regression trees, bagging, and random forests", *Psychol Methods,* vol. 14, pp. 323-48, Dec 2009.
[176] C. Ambroise and G. J. McLachlan, "Selection bias in gene extraction on the basis of microarray gene-expression data", *Proc Natl Acad Sci U S A,* vol. 99, pp. 6562-6, May 14 2002.
[177] W. J. Krzanowski, "Discriminant-Analysis and Statistical Pattern-Recognition - Mclachlan,Gj", *Journal of Classification,* vol. 10, pp. 128-130, 1993.
[178] B. Di Camillo, T. Sanavia, M. Martini, G. Jurman, F. Sambo, A. Barla, *et al.*, "Effect of Size and Heterogeneity of Samples on Biomarker Discovery: Synthetic and Real Data Assessment", *Plos One,* vol. 7, Mar 5 2012.
[179] C. Furlanello, M. Serafini, S. Merler, and G. Jurman, "Entropy-based gene ranking without selection bias for the predictive classification of microarray data", *BMC Bioinformatics,* vol. 4, Nov 6 2003.

[180] M. A. Rasmussen and R. Bro, "A tutorial on the Lasso approach to sparse modeling", *Chemometrics and Intelligent Laboratory Systems*, vol. 119, pp. 21-31, Oct 1 2012.
[181] I. Guyon, J. Weston, S. Barnhill, and V. Vapnik, "Gene selection for cancer classification using support vector machines", *Machine Learning*, vol. 46, pp. 389-422, 2002.
[182] A. Roy and R. S. Parker, "Dynamic modeling of exercise effects on plasma glucose and insulin levels", *J Diabetes Sci Technol*, vol. 1, pp. 338-47, May 2007.
[183] M. Derouich and A. Boutayeb, "The effect of physical exercise on the dynamics of glucose and insulin", *J Biomech*, vol. 35, pp. 911-7, Jul 2002.
[184] P. D. Miles, M. Levisetti, D. Reichart, M. Khoursheed, A. R. Moossa, and J. M. Olefsky, "Kinetics of insulin action in vivo. Identification of rate-limiting steps", *Diabetes*, vol. 44, pp. 947-53, Aug 1995.
[185] S. Oviedo, J. Vehí, R. Calm, and J. Armengol, "A review of personalized blood glucose prediction strategies for T1DM patients", *International Journal for Numerical Methods in Biomedical Engineering*, vol. 33, p. e2833, 2017.
[186] E. I. Georga, V. C. Protopappas, D. Polyzos, and D. I. Fotiadis, "Evaluation of short-term predictors of glucose concentration in type 1 diabetes combining feature ranking with regression models", *Med Biol Eng Comput*, Mar 15 2015.
[187] S. L. Zhao, B. D. Chen, P. P. Zhu, and J. C. Principe, "Fixed budget quantized kernel least-mean-square algorithm", *Signal Processing*, vol. 93, pp. 2759-2770, Sep 2013.
[188] B. D. Chen, S. L. Zhao, P. P. Zhu, and J. C. Principe, "Quantized Kernel Least Mean Square Algorithm", *Ieee Transactions on Neural Networks and Learning Systems*, vol. 23, pp. 22-32, Jan 2012.
[189] Y. Engel, S. Mannor, and R. Meir, "The kernel recursive least-squares algorithm", *Ieee Transactions on Signal Processing*, vol. 52, pp. 2275-2285, Aug 2004.
[190] E. I. Georga, J. C. Principe, D. Polyzos, and D. I. Fotiadis, "Non-linear dynamic modeling of glucose in type 1 diabetes with kernel adaptive filters", in *2016 38th Annual International Conference of the IEEE Engineering in Medicine and Biology Society (EMBC)*, 2016, pp. 5897-5900.
[191] E. I. Georga, J. C. Príncipe, E. C. Rizos, and D. I. Fotiadis, "Kernel-based adaptive learning improves accuracy of glucose predictive modelling in type 1 diabetes: A proof-of-concept study", in *2017 39th Annual International Conference of the IEEE Engineering in Medicine and Biology Society (EMBC)*, 2017, pp. 2765-2768.
[192] W. Liu, J. C. Príncipe, and S. Haykin, "Background and Preview", in *Kernel Adaptive Filtering*, ed: John Wiley & Sons, Inc., 2010, pp. 1-26.
[193] S. V. Vaerenbergh and I. Santamaría, "A comparative study of kernel adaptive filtering algorithms", in *2013 IEEE Digital Signal Processing and Signal Processing Education Meeting (DSP/SPE)*, 2013, pp. 181-186.
[194] B. P. Kovatchev, L. A. Gonder-Frederick, D. J. Cox, and W. L. Clarke, "Evaluating the accuracy of continuous glucose-monitoring sensors: continuous glucose-error grid analysis illustrated by TheraSense Freestyle Navigator data", *Diabetes Care*, vol. 27, pp. 1922-8, Aug 2004.
[195] W. Liu, J. C. Príncipe, and S. Haykin, "Kernel Recursive Least-Squares Algorithm", in *Kernel Adaptive Filtering*, ed: John Wiley & Sons, Inc., 2010, pp. 94-123.
[196] W. Liu, J. C. Príncipe, and S. Haykin, "Extended Kernel Recursive Least-Squares Algorithm", in *Kernel Adaptive Filtering*, ed: John Wiley & Sons, Inc., 2010, pp. 124-151.
[197] X. Yu, K. Turksoy, M. Rashid, J. Feng, N. Hobbs, I. Hajizadeh, *et al.*, "Model-fusion-based online glucose concentration predictions in people with type 1 diabetes", *Control Engineering Practice*, vol. 71, pp. 129-141, 2018/02/01/ 2018.

[198] "Glucose Concentrations of Less Than 3.0 mmol/L (54 mg/dL) Should Be Reported in Clinical Trials: A Joint Position Statement of the American Diabetes Association and the European Association for the Study of Diabetes", *Diabetes Care,* vol. 40, pp. 155-157, 2017.
[199] R. Pokharel, S. Seth, and J. C. Principe, "Mixture kernel least mean square", in *The 2013 International Joint Conference on Neural Networks (IJCNN)*, 2013, pp. 1-7.
[200] K. Li and J. C. Principe, "The Kernel Adaptive Autoregressive-Moving-Average Algorithm", *IEEE Trans Neural Netw Learn Syst,* vol. 27, pp. 334-46, Feb 2016.
[201] K. Li and J. C. Príncipe, "Transfer Learning in Adaptive Filters: The Nearest Instance Centroid-Estimation Kernel Least-Mean-Square Algorithm", *IEEE Transactions on Signal Processing,* vol. 65, pp. 6520-6535, 2017.
[202] W. Liu, I. Park, and J. C. Principe, "An information theoretic approach of designing sparse kernel adaptive filters", *IEEE Trans Neural Netw,* vol. 20, pp. 1950-61, Dec 2009.
[203] E. Montaser, J. L. Diez, and J. Bondia, "Stochastic Seasonal Models for Glucose Prediction in the Artificial Pancreas", *J Diabetes Sci Technol,* vol. 11, pp. 1124-1131, Nov 2017.
[204] J. Yang, L. Li, Y. Shi, and X. Xie, "An ARIMA Model with Adaptive Orders for Predicting Blood Glucose Concentrations and Hypoglycemia", *IEEE Journal of Biomedical and Health Informatics*, pp. 1-1, 2018.
[205] Q. Sun, M. Jankovic, L. Bally, and S. Mougiakakou, *Predicting Blood Glucose with an LSTM and Bi-LSTM Based Deep Neural Network*, 2018.
[206] I. Fox, L. Ang, M. Jaiswal, R. Pop-Busui, and J. Wiens, "Deep Multi-Output Forecasting: Learning to Accurately Predict Blood Glucose Trajectories", presented at the Proceedings of the 24th ACM SIGKDD International Conference on Knowledge Discovery & Data Mining, London, United Kingdom, 2018.
[207] I. Contreras and J. Vehi, "Artificial Intelligence for Diabetes Management and Decision Support: Literature Review", *J Med Internet Res,* vol. 20, p. e10775, 2018.
[208] T. Kamuran, H. Iman, H. Nicole, K. Jennifer, L. Elizabeth, S. Sediqeh, *et al.*, "Multivariable Artificial Pancreas for Various Exercise Types and Intensities", *Diabetes Technology & Therapeutics*, vol. 20, pp. 662-671, 2018.
[209] I. Hajizadeh, M. Rashid, K. Turksoy, S. Samadi, J. Feng, M. Sevil, *et al.*, "Incorporating Unannounced Meals and Exercise in Adaptive Learning of Personalized Models for Multivariable Artificial Pancreas Systems", *J Diabetes Sci Technol,* vol. 12, pp. 953-966, Sep 2018.
[210] D. Zeevi, T. Korem, N. Zmora, D. Israeli, D. Rothschild, A. Weinberger, *et al.*, "Personalized Nutrition by Prediction of Glycemic Responses", *Cell,* vol. 163, pp. 1079-94, Nov 19 2015.

AUTHOR'S PUBLICATIONS

PUBLICATIONS RELATED TO THIS THESIS

Journal Articles

1. E. I. Georga, J. C. Príncipe, and D. I. Fotiadis, "Short-term prediction of glucose in type 1 diabetes using kernel adaptive filters", *Med Biol Eng Comput*, July 02 2018.
2. E. I. Georga, V. C. Protopappas, D. Polyzos, and D. I. Fotiadis, "Evaluation of short-term predictors of glucose concentration in type 1 diabetes combining feature ranking with regression models", *Med Biol Eng Comput*, vol. 53, pp. 1305-18, Dec 2015.
3. E. I. Georga, V. C. Protopappas, D. Ardigo, D. Polyzos, and D. I. Fotiadis, "A glucose model based on support vector regression for the prediction of hypoglycemic events under free-living conditions", *Diabetes Technol Ther*, vol. 15, pp. 634-43, Aug 2013.
4. E. I. Georga, V. C. Protopappas, D. Ardigò, M. Marina, I. Zavaroni, D. Polyzos, *et al.*, "Multivariate Prediction of Subcutaneous Glucose Concentration in Type 1 Diabetes Patients Based on Support Vector Regression", *IEEE J Biomed Health Inform*, vol. 17, pp. 71-81, 2013.
5. E. Georga, V. Protopappas, C. Bellos, and D. Fotiadis, "Wearable systems and mobile applications for diabetes disease management", *Health and Technology*, pp. 1-12, 2014.

Conference Papers

1. E. I. Georga, J. C. Príncipe, E. C. Rizos, and D. I. Fotiadis, "Kernel-based adaptive learning improves accuracy of glucose predictive modelling in type 1 diabetes: A proof-of-concept study", in *2017 39th Annual International Conference of the IEEE Engineering in Medicine and Biology Society (EMBC)*, 2017, pp. 2765-2768.
2. E. I. Georga, J. C. Principe, D. Polyzos, and D. I. Fotiadis, "Non-linear dynamic modeling of glucose in type 1 diabetes with kernel adaptive filters", in *2016 38th Annual International Conference of the IEEE Engineering in Medicine and Biology Society (EMBC)*, 2016, pp. 5897-5900.
3. E. I. Georga, V. C. Protopappas, D. Polyzos, and D. I. Fotiadis, "Online prediction of glucose concentration in type 1 diabetes using extreme learning machines", in *2015 37th Annual International Conference of the IEEE Engineering in Medicine and Biology Society (EMBC)*, 2015, pp. 3262-3265.
4. E. I. Georga, V. C. Protopappas, D. Polyzos, and D. I. Fotiadis, "A predictive model of subcutaneous glucose concentration in type 1 diabetes based on Random Forests", in

2012 Annual International Conference of the IEEE Engineering in Medicine and Biology Society, 2012, pp. 2889-2892.

5. E. I. Georga, V. C. Protopappas, and D. I. Fotiadis, "Predictive Metabolic Modeling for Type 1 Diabetes Using Free-Living Data on Mobile Devices", in *2010 Wireless Mobile Communication and Healthcare International Conference (MobiHealth)*, Berlin, Heidelberg, 2011, pp. 187-193.
6. E. I. Georga, V. C. Protopappas, and D. Polyzos, "Prediction of glucose concentration in type 1 diabetic patients using support vector regression", in *Proceedings of the 10th IEEE International Conference on Information Technology and Applications in Biomedicine*, 2010, pp. 1-4.
7. E. I. Georga, V. C. Protopappas, D. Polyzos, and D. I. Fotiadis, "Predictive modeling of glucose metabolism using free-living data of type 1 diabetic patients", in *2010 Annual International Conference of the IEEE Engineering in Medicine and Biology*, 2010, pp. 589-592.
8. E. Georga, V. Protopappas, A. Guillen, G. Fico, D. Ardigo, M. T. Arredondo, *et al.*, "Data mining for blood glucose prediction and knowledge discovery in diabetic patients: The METABO diabetes modeling and management system", in *2009 Annual International Conference of the IEEE Engineering in Medicine and Biology Society*, 2009, pp. 5633-5636.
9. V. C. Protopappas, E. I. Georga, A. Guillen, G. Fico, D. Ardigo, J. Colas, "Diabetes Metabolic Model and Personalised Treatment Based On A Multi-parametric Monitoring Platform", in *2009 Annual International Conference in Advanced Technologies and Treatments for Diabetes*, 2009.
10. S. Sotiriadis, E. G. M. Petrakis, S. Covaci, P. Zampognaro, E. Georga, and C. Thuemmler, "An architecture for designing Future Internet (FI) applications in sensitive domains: Expressing the software to data paradigm by utilizing hybrid cloud technology", in *13th IEEE International Conference on BioInformatics and BioEngineering*, 2013, pp. 1-6.
11. G. I. Gogolos, E. I. Georga, E. C. Rizos, and D. I. Fotiadis, "An mhealth Platform to Evaluate Glycaemic Variability in Type 1 Diabetes", in *2017 IEEE 17th International Conference on Bioinformatics and Bioengineering (BIBE)*, 2017, pp. 273-278.
12. E. I. Georga, V. C. Protopappas, E. Arvaniti, and D. I. Fotiadis, "The Diabino System: Temporal Pattern Mining from Diabetes Healthcare and Daily Self-Monitoring Data", *in 2015 International Conference on Biomedical and Health Informatics (ICBHI)*, 2015.
13. E. I. Georga, V. C. Protopappas, C. Bellos, D. Makriyiannis, and D. I. Fotiadis, "Interpretation of Long-Term Clinical Diabetes Data and Prediction of Glycemic Control Based on Data Mining Techniques", in *2014 International Conference on Health Informatics*, 2014, pp. 315-318.
14. E. I. Georga, V. C. Protopappas, S. G. Mougiakakou, and D. I. Fotiadis, "Short-term vs. long-term analysis of diabetes data: Application of machine learning and data mining techniques", in *13th IEEE International Conference on BioInformatics and BioEngineering*, 2013, pp. 1-4.

Book Chapters

1. E. I. Georga, A. N. Papadopoulos, and D. I. Fotiadis. "mHealth Environments for Chronic Disease Management", *in Handbook of Research on Trends in the Diagnosis and Treatment of Chronic Conditions*, D. I. Fotiadis, IGI Global, 2016, pp. 518-535.
2. E. I. Georga, V. C. Protopappas, and D. I. Fotiadis, "Glucose Prediction in Type 1 and Type 2 Diabetic Patients Using Data - Driven Techniques", *Knowledge - Oriented Applications in Data Mining*, InTech, 2011, ISBN: 978-953-307-154-1.

Books

1. E.I. Georga, D.I. Fotiadis, and S.K. Tigkas, Personalised Predictive Modelling in Type 1 Diabetes, Academic Press, 2018.

OTHER PUBLICATIONS

Journal Articles

1. K. Kourou, V. C. Pezoulas, E. I. Georga, T. Exarchos, P. Tsanakas, M. Tsiknakis, *et al.*, "Cohort Harmonization and Integrative Analysis from a Biomedical Engineering Perspective", *IEEE Rev Biomed Eng*, Jul 11 2018.

Conference Papers

1. E. I. Georga, N. S. Tachos, A. I. Sakellarios, G. Pelosi, S. Rocchiccioli, O. Parodi, *et al.*, "A Multimodal Machine Learning Approach to Omics-Based Risk Stratification in Coronary Artery Disease", in *World Congress on Medical Physics and Biomedical Engineering 2018*, Springer Singapore, 2019, pp. 879-882.
2. A. I. Sakellarios, N. Tachos, E. Georga, G. Rigas, V. Kigka, P. Siogkas, *et al.*, "A Novel Concept of the Management of Coronary Artery Disease Patients Based on Machine Learning Risk Stratification and Computational Biomechanics: Preliminary Results of SMARTool Project", in *World Congress on Medical Physics and Biomedical Engineering 2018*, Springer Singapore, 2019, pp. 629-633.
3. V. I. Kigka, E. I. Georga, A. I. Sakellarios, N. S. Tachos, I. Andrikos, P. Tsompou, *et al.*, "A Machine Learning Approach for the Prediction of the Progression of Cardiovascular Disease based on Clinical and Non-Invasive Imaging Data", in *2018 Annual International Conference of the IEEE Engineering in Medicine and Biology Society*, 2018, pp. 6108-6111.

4. A. Sakellarios, P. Siogkas, E. Georga, N. Tachos, V. Kigka, P. Tsompou, *et al.*, "A Clinical Decision Support Platform for the Risk Stratification, Diagnosis, and Prediction of Coronary Artery Disease Evolution", in *2018 Annual International Conference of the IEEE Engineering in Medicine and Biology Society*, 2018, pp. 4556-4559.

Book Chapters

1. E. I. Georga, N. S. Tachos, A. I. Sakellarios, V. I. Kigka, T. P. Exarchos, G. Pelosi, *et al.*, "Artificial Intelligence and Data Mining Methods for Cardiovascular Risk Prediction", in *Cardiovascular Computing — Methodologies and Clinical Applications*, S. Golemati and K. S. Nikita, Springer Singapore, 2019.
2. E. Vlachopapadopoulou, E. I. Georga, and D. I. Fotiadis, "Management of Obese Pediatric Patients in the Digital Era", in *Mobile Health Applications for Quality Healthcare Delivery*, A. Moumtzoglou, IGI Global, 2019

SHORT CV

Eleni I. Georga received the B.Sc. and M.Sc. degrees from the Department of Computer Science, University of Ioannina, Greece, in 2005 and 2008, respectively. She is currently a Ph.D. candidate at the Department of Materials Science and Engineering, University of Ioannina, Greece. Her PhD research is focused on the non-linear identification and prediction of short-term glycaemic dynamics in type 1 diabetes. Since 2004, she has been a member of Unit of Medical Technology and Intelligent Information Systems, Department of Materials Science and Engineering, University of Ioannina. Her research interests include medical data mining, biomedical informatics, mobile computing and IoT software system development.